Identification of novel mechanisms controlling cell cycle progression in *S. cerevisiae*

Inaugural-Dissertation
to obtain the academic degree
Doctor rerum naturalium (Dr. rer. nat.)
submitted to the Department of Biology, Chemistry and Pharmacy
of Freie Universität Berlin

by

Christian Linke

from Oranienburg

2012

„Wissenschaft ist die Voraussicht von Wiederholungen.“

Antoine de Saint-Exupéry (1900-44)

Diese Arbeit wurde am Max Planck Institut für molekulare Genetik im Zeitraum vom 4. 04. 2008 bis 31. 03. 2012 angefertigt.

1. Gutachter : Prof. Dr. Hans Lehrach
2. Gutachter : Prof. Dr. Rupert Mutzel

Disputation am 11.07.2012

Index

1. Introduction

In eukaryotes cell cycle progression is a tightly controlled set of events that regulate cell duplication. Intensive research on this field during the last decades revealed that the molecular basis for cell cycle control is highly conserved among all eukaryotic cells.

The eukaryotic cell cycle generally consists of four distinct phases: G1 (gap 1), S (synthesis) and G2 (gap 2) that are collectively known as interphase and the M (mitosis) phase, during which the cell devides into two distinct cells, often called "daughter cells".

The progression through cell cycle is controlled by heterodimeric protein complexes called cyclin-dependent kinases (Cdks). The activity of these serine and threonine kinases is dependent on its binding to regulatory subunits called cyclins. Multiple cyclins are probably advantageous because they allow for flexible control of the cell cycle. The sequential synthesis and activation as well as the degradation of cyclins gives directionality to the cell cycle events. A phase-specific appearance of multiple cyclins in turn is required for the phosphorylation of Cdk-specific substrates, for example transcription factors, which drive definite stages of the cell cycle in a timely manner. Thus, cyclin-dependent activities promote critical events such as spindle pole body duplication, DNA replication, spindle formation, initiation and exit of mitosis and cell division.

The dysregulation of cell cycle components are known to be involved in the decline of multiple cellular functions raising suspicions to cause cancer, senescence, aging and age-related diseases such as neurodegenerative disorders. The aging of western societies renders understanding of cell cycle regulation and its interconnection with environmental stimuli to be a promising goal to potentially delay the onset of age-related pathologies in the future perspective.

For researchers the yeast *Saccharomyces cerevisiae* becomes an important eukaryotic model organism due to conserved protein functions including cell cycle components, protein-processing enzymes and age-related effectors. Furthermore, it scores favorably on a number of positive characteristics: The requirement of simple

equipment for culturing, a short generation time, easy genetic manipulation and comparability of complex internal cell structures with plants and animals. In addition, the genome of *S. cerevisiae,* which comprises a low percentage of non-coding DNA, was the first eukaryotic genome completely sequenced.

1.1 Cell cycle regulation in budding yeast *S. cerevisiae*

1.1.1 Cyclin cascades regulate cell cycle-specific gene epression

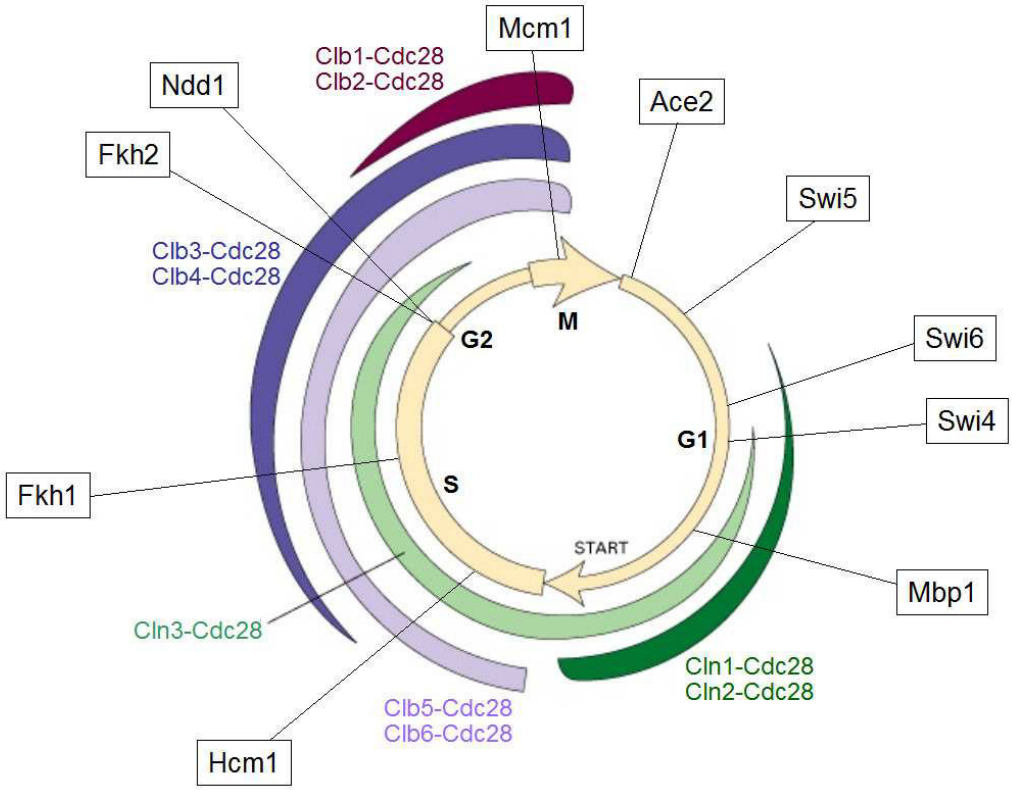

Figure 1-1. Regulation of the yeast cell cycle. Different length of colored arrows represents timing of distinct cyclin/Cdk complex activities. Size of arrows indicates the assumed enzyme activity of respective complexes (taken from Lodish H., Berk A. et al., *Molecular Cell Biology*, *Sixth Edition*, 2008, pp. 973).The nine major transcriptional activators of cell cycle-specific gene expression are shown in small boxes. The location of transcrpitional activities of these factors bases on genome-wide promoter binding analysis [1].

In the budding yeast *Saccharomyces cerevisiae* a single Cdk named Cdc28 coordinates cell cycle regulation in association with G1-specific cyclins Cln1-3 and mitotic B-type cyclins Clb1-6 (Figure 1-1). *CLN3* transcripts peak during late M and early G1 phase [2]. Transcription of *CLN1* and *CLN2* genes as well as *CLB5* and

CLB6 transcripts peak at G1/S phase [3, 4, 5]. During S/G2 phase *CLB3* and *CLB4* transcript levels rises, followed by expression of *CLB1* and *CLB2* in G2/M [6, 7].

Cln1, Cln2 and Cln3 are important for the coordination of a subset of regulatory events known as Start [8]. Progression through Start sets the timing of bud emergence, spindle pole body duplication and initiation of DNA replication and requires at least one of the G1-specific cyclins [8, 9, 10]. Cln3 is mainly monitoring cell size dependent on the growth conditions. When cells reach a critical size, Cln3 activates the heterodimeric transcription factor complex SBF consisting of Swi4 and Swi6, and MBF a complex formed by Mbp1 and Swi6 [10]. Activation of SBF initiates the transcription of *CLN1* and *CLN2* [11,12], whereas MBF promotes the expression of *CLB5* and *CLB6* [5]. However, there is a high functional overlap between the activities of both transcription factor complexes [13]. Clb5 and Clb6 are mainly responsible for initiation of the S phase but they have significant overlapping functions with Cln1 and Cln2 in G1, and with Clb3 and Clb4 in G2/M phase [5]. Clb3 and Clb4 are mainly responsible for early mitotic events, such as formation of the short mitotic spindle, whereas Clb1 and Clb2 mainly regulate late mitotic events, particularly spindle elongation and cell division [4, 6].

The differential regulation of G1 and B-type cyclins and their substrate-specific functions are crucial for the proper order and timing of cell cycle events. Consistently, the waves of cyclins are thought to be autoregulatory: Cln3-Cdc28 complex phosporylates the repressor Whi5, which in turn leads to its dissociation from SBF allowing expression of *CLN1* and *CLN2* [14, 15]. Cln1-, Cln2- and Clb5-Cdc28 complexes phosporylate SBF, thus stimulating its own expression [16, 17]. Furthermore, Clb6-Cdc28 phosphorylates Swi6 promoting its nuclear export and inactivation of the transcription factor [18]. An additional mechanism for inhibiting SBF complex activity has been reported as well for Clb2-Cdc28 through phosphorylation of Swi4 [19, 20]. Importantly, also Clb2 has been demonstrated to activate its own transcription. While efficient expression of *CLB2* cluster requires the formation of a ternary complex composed of Mcm1, Fkh2 and the transcriptional coactivator Ndd1, the complex formation in turn requires the phosphorylation of Ndd1 and Fkh2 by Clb2-Cdc28 [21, 22, 23].

The *CLB2* cluster contains about 35 genes and includes *CLB1*, *CLB2*, *CDC5* (yeast polo-like kinase homolog), *CDC20* (a mitotic specificity factor for the APC protein-

ubiquitin ligase), *SWI5* and *ACE2* (transcription factors required for late M- early G1 phase-specific gene expression). The classification bases on the presence of promoter binding elements, known as SFF (Swi5 factor), which are occupied by Fkh1 and Mcm1/Fkh2 [23, 24].

The MADS box transcription factor Mcm1 is not only a key regulator for transcriptional activation at G2/M but also for repression of target genes at M/G1 phase [25]. Therefore, Mcm1 forms complexes with the homedomain repressors Yox1p and Yhp1 [26, 27]. In addition, Mcm1 binds to early cell cycle box (ECB) elements at promoters of M/G1 genes such as *CLN3* [28]. In contrast to *CLB2* cluster, no positively acting partner for Mcm1 has yet been identified to activate gene expression in M/G1 phase.

1.1.2 Degradation of cyclins and inhibition of Cdk-cyclin activity

Another important mechanism to control cell cycle progression is represented by the regulation of cyclins at their protein level. Different cyclins are substrates of different ubiquitin ligases, which mark proteins for degradation by the 26 S proteasome. It has been demonstrated that Cln1 and Cln2 are degraded by an SCF (Skp1/Cullin/F-box) complex, whereby substrate specificity is mediated by the F-box protein Grr1 (SCF^{Grr1}) [29, 30]. The ubiquitination and degradation of Clb6 is mediated by an SCF complex that contains the F-box protein Cdc4 (SCF^{Cdc4}) [31]. During metaphase, Clb5 and other B-type cyclins are targeted for degradation by the F-box protein Cdc20, an adaptor protein of the Anaphase Promoting Complex (APC^{Cdc20}) [32, 33]. Later in mitosis, degradation of B-type cyclins, including the main mitotic cyclin Clb2, is completed by the APC^{Cdh1} complex [34]. Differential degradation of cyclins limits Clb-Cdc28 activity at different phases of the cell cycle and may help to fine-tune the proper order of events.

The activity of Clb-Cdc28 complexes are negatively regulated by the association with stoichiometric inhibitors. One of this, named Sic1, is well characterized according to its function in the regulation of cell cycle events. Clb-Cdc28 but not Cln-Cdc28 complexes are blocked in their activity, if bound to Sic1 [35]. Sic1 level rises at the end of mitosis and the protein is largely degraded at the onset of S phase [36]. Phosphorylation of Sic1 by cyclin-Cdc28 complexes results in an ubiquitin-mediated

degradation by the SCF^{Cdc4} complex [30, 37, 38]. As soon as Sic1 is diminished, Clb5/6-Cdc28 activity is relieved, which allows cells to enter into S phase [35].

Another cyclin-Cdk inhibitor named Far1 controls cell cycle in the presence of mating pheromones, such as α-factor, and ultimately causes an arrest of yeast cells in G1 phase [39]. The pheromone binds to the Ste2 receptor to induce a MAPK (mitogen-activated protein kinase) cascade that phosphorylates Fus3. Phosphorylated Fus3 subsequently activates Far1 to bind G1-specific cyclins thus inhibiting Cln-Cdc28 complex activity [40, 41]. In the absence of α-factor Far1 levels are regulated during the cell cycle by phosphorylation of Cln2-Cdc28 followed by its SCF-dependent degradation [42, 43]. Despite the observation that Far1 peaks during G1 it is not clear whether this inhibitor plays a fundamental functional role in the regulation of cell cycle events.

1.1.3 Cell cycle checkpoints delay cell division and growth

In cells that have not formed a bud Cdc28 activity is inhibited when binding to Swe1 [44, 45]. This pathway, known as the morphogenesis checkpoint, delays G2/M phase and nuclear division [46]. In turn, Cdc28 phosphorylates Swe1 to mark it for APC-mediated degradation [47, 48]. Clb2-Cdc28 phosphorylates Swe1 in vivo, which is important for its inhibitory function. Later, when Swe1 becomes hyperphosphorylated and dissociates from the Clb-Cdc28 complex, kinase activity becomes fully activated [46].

Exit from mitosis is promoted by Cdc14 and ultimately leads to the degradation of the B-type cyclins and the accumulation of Sic1 [49, 50]. Cdc14 dephosphorylates Cdh1 to activate APC^{Cdh1}-mediated ubiquitination of B-type cyclins and Swi5, a transcription factor that drives Sic1 expression [51, 52]. Additionally, dephosphorylation of Sic1 by Cdc14 prevents the inhibitor of kinase activity for proteolysis, thus stabilizing Clb-Cdc28 complex inhibitor [51].

When bound to the nucleolar protein Net1, Cdc14 activity is blocked during most of the cell cycle but is released in anaphase. Two signaling pathways are responsible for the release of Cdc14 from the nucleolus: MEN (mitotic exit network) and FEAR (Cdc14 early anaphase release network). Components of the MEN, which are restricted to the daughter SPB (spindle pole body) and the bud cortex, remain

inactive until the nucleus has entered the bud [53]. In response to defects in spindle alignment (spindle-position checkpoint) MEN is inhibited through Bub2 [54].

The activation of MEN is promoted by Clb-Cdc28 and FEAR network. Clb1- and Clb2-Cdc28 phosphorylate Net1 to dissociate from Cdc14 [55]. Cdc14 dephosphorylates Cdc15, a component of MEN, to promote Clb1 and Clb2-Cdc28 activity [56, 57]. Cells expressing Net1 with mutated Cdc28 consensus phosphorylation sites or lack of Clb2 are defective for the Cdc14 release [58].

1.2 Forkhead box transcription factors

Forkhead (FKH) box (Fox) proteins are present throughout the animal kingdom and their functional conservation ranges from yeast to humans [59]. They regulate a wide variety of critical biological processes including cell cycle, cell proliferation, development, stress resistance, apoptosis, immunity, metabolism and aging [60-62]. The classification of these proteins bases on the presence of a DNA-binding FKH box or winged helix domain that contains around 100 amino acids and shows structural homology with the linker histones [63-65].

The differential functionality of Fox proteins in gene regulation is determined, despite the similarity in their FKH domains, by a divergent protein structure in the remaining amino acids. The ability of Fox proteins to activate or repress genes corresponds to recruitment of numerous coregulators [66-68].

Up to now, four Fox proteins have been identified in the budding yeast: Hcm1 (high copy suppressor of calmodulin), Fkh1 (Forhead homolog 1), Fkh2 (Forhead homolog 2) and Fhl1 (Forkhead-like 1).

1.2.1 Forkhead transcription factor Fhl1

The forkhead transcription factor Fhl1 regulates the expression of genes encoding ribosomal proteins hence controlling cell proliferation [69]. It was originally discovered as a multi-copy suppressor of a *pol3* deletion and recruits the cofactor Ifh1 (Interacts with forkhead 1) to activate gene expression [70-72]. In response to stress, Ifh1 dissociates from FHA domain of Fhl1 and the corepressor Crf1 (Corepressor with Fhl1) binds to inhibit transcription of ribosomal genes [73].

1.2.2 Forkhead transcription factor Hcm1

Hcm1 was originally discovered as a high-copy suppressor of a temperature-sensitive calmodulin mutant that is defective in chromosome segregation [74]. *HCM1* is periodical transcribed and peaks at late G1 and early S phase. Target genes of *HCM1* are expressed during late S phase and encode proteins involved in chromosome organization, spindle dynamics and budding [75]. The transcription factor is also required for periodic expression of Fkh1, Fkh2, coactivator Ndd1 as well as the repressors Whi5 and Yhp1 [75]. The deletion mutant of *hcm1* partially shows a loss of chromosomes, suggesting a putative role in spindle assembly checkpoint [75].

1.2.3 Forkhead transcription factors Fkh1 and Fkh2

The transcription factors Fkh1 and Fkh2 share 47 % identity and 82 % similarity across the amino acid sequence of Fkh1 [76]. The DNA-binding domains (FKH) of both proteins show an identity of 72 %. Consistently, both proteins strongly overlap in promoter occupancy of target genes *in vivo*, indicating redundant functions [77]. Compared to Fkh1, Fkh2 contains a Carboxy (C)-terminal extension of approximately 280 amino acids (see Figure 1-2 for details).

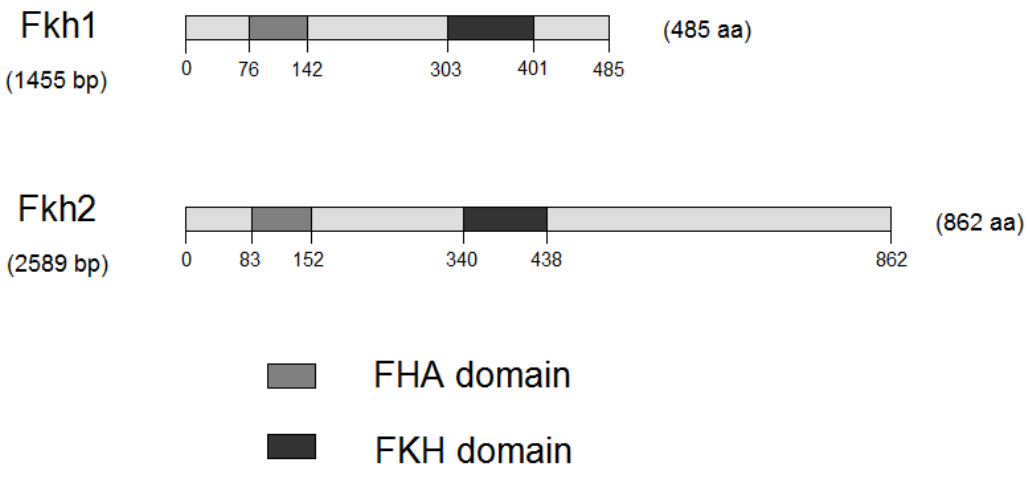

Figure 1-2. Schematic illustration of forkhead transcription factors Fkh1 and Fkh2. The locations of the FHA (forkhead associated) and FKH (forkhead) domains are indicated. Since the FKH domain mediates DNA-binding the FHA domain is important to provide protein-protein interactions.

According to gene deletion analysis, Fkh1 and Fkh2 have both activating and repressive functions [78]. Simultaneous disruption of *FKH1* and *FKH2* results in a

strong reduction of *CLB2* cluster expression leading to a highly abnormal pseudohyphal cell phenotype [76]. Furthermore, mutations in *FKH1* and *FKH2* lead to defects in transcriptional elongation of the large subunit of RNA polymerase II and in transcriptional termination [78]. However, both transcription factors have been shown to play also distinct roles in the regulation of the cell cycle. Specifically, Fkh2 but not Fkh1 binds cooperatively to Mcm1 (minichromosome maintenance 1) [24, 79]. Mcm1, a member of the MADS box protein family, is involved in transcription, minichromosome maintenance, cell cycle control, mating and stress response [80].

Since DNA-binding of Fkh1, Fkh2 and Mcm1 is not cell cycle-dependent and does not explain periodic expression of phase-specific genes, the key cofactor is Ndd1 (nuclear division defective 1) [24, 81]. Ndd1 is periodically expressed and peaks during S phase [81]. Timing of Ndd1-dependent gene transactivation depends on binding to the FHA (forkhead associated) domain of Fkh2 [79] and correlates with transcription of the *CLB2* cluster [21]. When Ndd1 degrades during late mitosis transcription of *CLB2* cluster is terminated [81]. Ndd1 protein function is essential and cells that fail to express this coactivator becomes inviable. Interestingly, a deletion of the C-terminus of Fkh2 has been shown to be sufficient for rendering Ndd1 nonessential [21]. How the C-terminal region of Fkh2 establishes repression of the *CLB2* cluster and how Ndd1 antagonizes this process remains to be determined. In addition, the mechanism by which Fkh1 mediates cell cycle-regulated expression of Clb2 cluster genes in the absence of Fkh2 and Ndd1 is not understood [21]. Another coregulator that drives cell cycle regulation has been predicted to be involved [78].

1.2.4 Phosphorylation of Fkh proteins regulates *CLB2* cluster

Cell cycle regulation requires the activation of Fkh proteins through phosphorylation by Cdk1 (Cdc28 in yeast) and polo like kinases (Plks). In budding yeast Clb5-Cdc28 complex phosphorylates Fkh2 during S phase and Clb2-Cdc28 activates Fkh2 and Ndd1 in G2/M phase [1, 23]. As mentioned above, simultaneous deletion of Ndd1 and Fkh2 (or C-terminus of Fkh2) rescues the lethality of *ndd1* cells [79, 82, 83]. In addition, cells lacking both transcription factors show hyperexpression of *CLB2* cluster genes in G1 and reduced transcript levels in G2/M [79]. Moreover, activation

of *CLB2* transcription is enhanced by the phosphorylation of Ndd1 via the yeast polo like kinase homolog Cdc5, generating a positive-feedback loop [84].

Despite the data available for Fkh-dependent transcriptional activation little is known about how genes are regulated in a repressive way. Previous findings suggested a simple competition between the recruitment of activators and repressors to Fox proteins like it was shown for Fkh2. Yox1 has been suggested to displace the coactivator Ndd1 deactivating *CLB2* cluster transcription [27]. Later, it has been shown that DNA-binding sites of Yox1 and Fkh2 are positioned next to each other to allow both proteins to bind the same binding pocket of Mcm1. Since the recruitment of Fkh2 to Mcm1 is essential for activation of G2/M genes constitutive expression of Yox1 inhibits binding of Ndd1 to the *SPO12* promoter [25].

1.2.5 Mammalian homologues of forkhead transcription factors

Up to now, 18 subfamilies of mammalian forkhead transcription factors have been identified [60, 61] and two of them, Fox class O and M (FOXO and FOXM), have been suggested to be the closest homologs of yeast Hcm1, Fkh1 and Fkh2 proteins. The FOXOs integrate signals from energy, growth factors and stress signaling cascades to regulate cell cycle progression, apoptosis, autophagy, DNA-damage repair, metabolism and stress response [85-92]. Particularly, nutrient (insulin) and growth factors, internal reactive oxygen species (ROS) generation, DNA damage sensing and starvation signals influence transcription factor activity through posttranslational modifications [85, 86, 91, 92]. Mammalian FoxO3 is structurally similar to yeast Hcm1 and has been demonstrated to be involved in cell cycle, aging and cancer [93].

A functional human homolog of Fkh1 and Fkh2 named FoxM1 has been shown to play a role in the regulation of cyclin B1, the human homolog of yeast Clb2 [93, 94]. FoxM1 is expressed in proliferating, not in terminally-differentiated cells, potentially presenting a novel therapeutic target in cancer [95-99]. During G1/S phase the protein accumulates in the cytoplasm, while it becomes nuclear at G2/M [100]. Cells deficient in FoxM1-expression show a slight delay in G1/S and a severe delay in G2 phase. Moreover, these cells fail to undergo cytokinesis correctly and show missegregated chromosomes [101-104]. Additionally, knock-out mouse studies

revealed a regulatory role for FoxM1 in organogenesis during late embryogenesis [105].

A partial rescue in G2/M transition of mammalian cells lacking FoxM1 can be achieved by overexpression of cyclin B. Consistently, this mitotic subunit of Cdk1 has been demonstrated to interact with this oncogenic forkhead transcription factor [101]. Strikingly, both yeast Fkh and mammalian FoxM1 control G2/M transition by activating Cdc25, a membrane bound guanine nucleotide exchange factor (GTP/GDP exchange factor), indicating that Fox protein mediated gene expression is highly conserved from yeast to human [101, 106].

Activation of FoxM1-dependent transcription of mitotic genes requires multiple phosphorylation events. During S phase the cyclin E-Cdk2 complex phospho-rylates FoxM1, subsequently followed by cyclin A-Cdk2 kinase activity [107]. Phosphorylation levels increase during G2 phase due to the kinase activity of cyclin A and B complexed with Cdk1. A transactivition domain that contains a cyclin-binding motif (LXL) is thought to be responsible for recruitment of cyclin/kinase complexes and phosphorylation is needed for the association of polo like kinase 1 (Plk1) with FoxM1 [108]. Plk1 kinase activity fully activates FoxM1-dependent transcription in G2/M, thus allowing expression of mitotic regulators like *PLK1* itself [108].

1.3 Interplay between Fkh transcription factors and histone deacetylases

In higher eukaryotes homologs of the yeast histone deacetylase (HDAC) Sir2 are important cofactors of forkhead transcription factors. Mammalian SIRT1 associates with FOXO1, 3 and 4 in a stress dependent manner [109-112]. It has been reported that this interaction promotes deacetylation of forkhead transcription factors resulting in a nuclear import and transactivation of genes involved in oxidative stress resistance [109, 113]. However, the exact mechanism whereby SIRT1/Sir2 affects expression of forkhead protein-dependent genes is not well understood.

Interestingly, yeast Hcm1, which is believed to be the closest homolog of mammalian FoxOs, interacts with Sir2 to enter the nucleus under stress conditions [114]. Transcriptome analysis for *HCM1* revealed its involvement in mitochondria

biogenesis, stress response and derepression of respiratory genes necessary for entering diauxic shift and early stationary phase [114].

In yeast, histone deacetylases are known to play important roles in cell cycle regulation. A crucial player in the negative regulation of G2/M genes is the histone deacetylase Sin3 and its catalytic subunit Rdp3 [115]. Sin3 binds directly to FHA domain of Fkh2 at the end of M-phase until the onset of S-phase and has been shown to counteract on histone H4-acetylating-dependent chromatin decondensation and Ndd1 recruitment [115].

Yeast Rpd3, a class one HDAC, deacetylates lysine 5 or 12 of histone H4 [116] and is required for timing of origin firing in DNA replication including those of rDNA repeats [117, 118]. Furthermore, it appears to be involved in transcriptional regulation of critical targets like DNA damage response genes and G2/M cluster genes [115, 119]. Deletion of *RPD3* enhances chromatin silencing at mating type loci, telomeres and rDNA similar to overexpression of *SIR2* [116, 119, 120, 121]. The opposing effect between Rpd3 and Sir2 is confirmed by the observation that cells lacking Rpd3 live significantly longer than wild type cells [120]. In addition, simultaneous deletion of *RPD3* and *SIR2* (or *SIR4*) restores the expression of reporter genes to wild type levels [122].

Recently, it has been shown that Rpd3 is a boundary element for Sir2-dependent heterochromatin formation, thus antagonizing the spread of nucleosome condensation at telomeres and mating loci [123]. Sir2 and Rdp3 target different histone residues on H3 and H4 leading to the proposal that both factors are required to determine silencing at chromosomal loci and expression of genes [119, 124].

In *Drosophila melanogaster* a *RPD3*-knockout is lethal but loss-of-function mutations extends life span of adult flies [125]. Moreover, Rpd3 level is decreased under starvation conditions suggesting a potential role in the calorie restriction pathway [125, 126].

1.3.1 Sir2 a NAD-dependent histone deacetylase

In eukaryotes three classes of HDACs (I, II and III) have a variety of targets and biological functions. Members of class III are functional dependent on NAD^+ and are

known as sirtuins [127-131]. The Sir2 (silent information regulator 2) family deacetylases are highly conserved accross all kingdoms of life and their functional diversity in cellular processes has been generated through gene duplications [132]. The deacetylases retain a well-conserved catalytic core, including a zinc-bindinding module critical for the structural integrity of the protein [132].

Sir2, one of the first described HDAC in yeast, is involved in silencing of telomeres and rDNA, genome stability maintaining and aging [133]. Sir2 removes acetyl groups from lysines of nucleosomal histone tails and promotes the direct binding of Sir3 and Sir4 to N-terminal tails of histone H3 and H4. The Sir protein complex deacetylates histone residues H3K9, H3K14 and H4K16, thus being essential for chromatin silencing and further histone deacetylation events [127].

As mentioned above Sir2-dependent deacetylation requires the presence of the cofactor NAD^+. It has been proposed that this dependency may allow cells to sense metabolic state and thus nutrient availability to trigger transcriptional regulation accordingly [134]. In addition, Sir2-dependent hydrolysis of the glycosidic bond between the ribose and nicotinamide moieties of NAD^+ may allow a negative feedback loop. Sir2 can trigger its own activity due to a decrease in availability of the cosubstrate [134, 135].

Importantly, it has been demonstrated that the product of the Sir2-dependent hydrolysis of NAD+ called nicotinamide inhibits Sir2 activity. In the presence of this compound life span of yeast cells is equal to that of *sir2* deletion mutants. Interestingly, inhibitory effects of nicotinamide can be observed as well in mammalian cell cultures both *in vitro* and *in vivo* [135, 137]. It has been proposed that nicotinamide fluctuations may be responsible for Sir2-dependent silencing and provide an additional mechanism by which NAD-dependent HDACs limit their own activity [137]. This assumption implies the involvement of factors that regulates nicotinamide concentrations *in vivo*. A key regulator gene has been identified with *PNC1* that encodes a nicotinamidase converting nicotinamide into nicotinamide acid [137]. The enzyme is part of the NAD^+ salvage pathway and may reduce the level of nicotinamide in the cell and controls Sir2 activity directly [137]. In support of this model, silencing at telomeres and rDNA is greatly abolished when *PNC1* is deleted and can not be restored by calorie restriction [138, 139]. Furthermore,

overexpression of *PNC1* extends replicative life span by 70 % in an nutrient starvation independent manner [138]. Interestingly, *PNC1* expression is altered in response to various stimuli that are known to extend replicative life span, including low concentrations of glucose and amino acids, heat stress and osmotic stress [138, 140, 141].

1.3.2 Sir2 activity in metabolism and aging of yeast

In mammals it has been proposed that aging of mitotic cells may differ from those remaining in a postmitotic state. This distinction is made as well in *S. cerevisiae* between replicative life span and chronological life span.

Replicative life span of yeast cells is defined as the number of divisions of an individual mother cell before dying [133]. One key feature in replication of yeast is the asymmetry of cell division: The progenitor cell, the mother cell, can easily be distinguished from its smaller descendant, the daughter cell. The average replicative life span of virgin mother cells in laboratory strains differ substantially but was determined as approximately 22 divisions before dying [133].

The chronological life span, also known as postdiauxic survival, is the length of time a population of yeast cells remains viable in a nondividing state following nutrient deprivation [142]. Yeast cells grown in nutrient-rich medium divide until nutrients are exhausted before entering a postdiauxic hypometabolic state named stationary phase. At this point, yeast cells remain viable for several months. In contrast to rich medium, yeast cells have a relative short chronological life span if grown to stationary phase in synthetic medium [142]. Although, cells stop dividing they retain higher metabolic rates and this status is thought to reflect metabolic rate of postmitotic cells in multicellular organisms more closely [143].

Budding yeast is a facultative anaerobe organism. When glucose is available at high levels cells prefer to generate energy by fermentation. When nutrients become limited, the metabolic status changes and cells prefer to generate energy more efficiently by respiration. Flux of carbon source to tricarboxylic acid (TCA) cycle in mitochondria leads to an increased electron transport, resulting in the production of 16 ATPs per glucose molecule compared to 2 ATPs obtained from fermentation [144].

Yeast cultured in media with low glucose concentrations (0.2 %) shows a threefold higher rate of respiration. It has been assumed that an increase in oxidation of NADH to NAD^+ in TCA cycle may result in a higher Sir2-dependent chromatin silencing activity due to the increased availability of cofactor [145].

Chronological aging in yeast can be analyzed under laboratory conditions when cells reach stationary phase and remain in G0. Haploid cells pregrown in nutrient-rich medium to stationary phase accumulate glycogen and trehalose and develop thick cell walls [146]. At this point, protein synthesis is severely decreased and cells are significantly more resistant to oxidative stress [146-148]. Similar to other metazoans in the diapause state, unbudded yeast cells utilize stored nutrients like glycogen [142]. Furthermore, limited energy, as a product of almost exclusively respiration, is primary used to resist cellular damage and stress [142]. At stationary phase, diploid cells generates stress-resistant spores, which remain viable for years [142].

Many other yeast genes that are involved in chronological aging play a role in free radical damage protection, for example mitochondrial enzymes Sod1 and Sod2 [143, 149]. The results of previous studies have given support to the free-radical theory that proposes chronological aging as a consequence of oxidative damage [150].

In addition, components of signaling pathways involved in glucose/nutrient sensing have been found to influence chronological life span to a great extend. These components include the adenylate cyclase Cyr1, that is required for cyclic AMP (cAMP)-dependent protein kinase (PKA) activity, and the GTP-binding protein Ras2, an upstream regulator of Cyr1 [151, 152]. Interestingly, *cyr1* and *ras2* deletion strains extend life span roughly two or three fold relative to wild type arguing that PKA pathway-mediated up-regulation of growth and glycolysis in turn down-regulates stress resistance, glycogen accumulation and gluconeogenesis [142, 153]. Mutations in PKA pathway stimulate extension of replicative life span in yeast [154].

1.3.3 Sirtuins and chromatin silencing in yeast

Genetic screens for deletion mutants in *S. cerevisiae* that prolonged longevity in response to starvation led to the discovery of genes involved in the formation of silent heterochromatin at repeated DNA sequences [155].

In the budding yeast heterochromatin formation occurs at telomeres, the two mating type loci (Hidden MAT Left, *HML* and Hidden MAT Right, *HMR*), and the rDNA locus *RDN1* [156, 157]. Transcriptional silencing at telomeres is dependent on the formation of a complex composed of Sir2, Sir3, Sir4 and Ku [158, 159]. In contrast, the establishment of heterochromatin at rDNA locus requires Sir2 but not other sirtuins [142, 160].

A function of Sir2 in DNA repair by nonhomologues end-joining has been proposed due to the observation that the Sir complex relocalizes from silent loci (telomeres, rDNA, mating cassettes) to DNA breaks [159, 161, 162]. Interestingly, this process can lead to cell sterility equal to a marker characteristic, which have been observed in old grown cells [163, 164]. In fact, a reliable marker for aged cells is the loss of silencing at mating-type loci resulting in expression of both a and α information [164]. In addition, old cells become insufficient in silencing other repetitive loci like telomeres and rDNA, resulting in the fragmentation of the nucleolus [165, 166, 167]. Yeast rDNA is located on chromosome XII and contains 100 to 200 tandem repeats of 9.1 kb length that encodes the rDNA genes required for ribosome assembly [168, 169]. In old cells the usual highly packaged nuclear structure becomes enlarged followed by its fragmentation into multiple chromosomal rDNA structures. However, rDNA remains intact due to a relocalization of sirtuin complexes [167, 170]. In addition, a senescence factor that accumulates when cells divide has been proposed to limit life span in yeast [171]. This factor, first discovered in 1997, is a product of recombination between adjacent rDNA repeats known as extrachromosomal rDNA circle (ERC) [167]. ERCs are generated during DNA replication in S phase and segregate mostly to the mother cell. ERCs replicate in each cell division and accumulate exponentially in mother cells, resulting in cellular senescence [167, 172]. It is not known how accumulation of ERCs causes cell death but recent studies give rise to the evidence that ERC generation causes aging. Overexpression of Sir2 prevents formation of ERCs by reduction of rDNA recombination, thus leading to an extended life span of approximately 40 % [173-175]. Deletion of Sir2 accelerates ERC abundance and significantly reduces yeast life span [174]. A transfer of ERCs from old mothers to virgin daughter cells has been demonstrated to cause premature aging resulting in a reduction of daughter cell life span [167].

1.3.4 Conservation of Sir2 activity

Since first discoveries have been made in rats it is well known that calorie restriction extends live span in a wide variety of organisms [176, 117]. The insulin like growth factor type 1 (IGF-1) signaling pathway in *Caenorhabditis elegans* down-regulates, similar to yeast Ras-Cyr1-PKA pathway, genes involved in stress resistance and storage of nutrient reserves [178- 180]. Knock-out mutations in the IGF-1 pathway cause worms to enter diapause state, which is normally initiated when nutrients become limited, and weak mutations extend life span of adult worms to 50 % [178, 179].

In addition, mutations in the IGF-1 pathway of *Drosophila* extend life span by 85 % [181, 182]. Down-regulation of IGF-1 pathway in human cells stimulates the storage of fat, the primary carbon source during starvation, similar to yeast glycogen [142, 153]. These findings suggest a common conserved pathway that regulates genes in organisms, ultimately resulting in an increased chance to survive a period of nutrient limitation [183].

Strikingly, Sir2-dependent live span extension appears to be conserved from bacteria to humans. Sir2 homologues have been found in *Salmonella*, although this eubacterial organism lack histones [184]. An increased dosage of the *C. elegans* homologue sir2.1 extends life span of adult worms [185]. There are seven mammalien Sir2 homologs (Sirt1-7); Sirt1, the most similar to Sir2, deacatylates the tumor suppressor protein p53, which is required for apoptosis and DNA repair [136, 186]. Sirt1 activity can be inhibited by addition of nicotinamide *in vitro* and *in vivo* [136, 187]. Moreover, nicotinamide inhibits PARP1 (Polyadenosine diphosphate-ribose polymerase 1), an enzyme involved in DNA break repair, telomere length regulation, histone modification and transcription [188].

Interestingly, overexpression of Sir2 homologs in worms, yeast and flies extends lifespan [129, 185, 189, 190], emphasizing an evolutionarily conserved role of Sir2 in longevity determination.

1.3.5 Role of sirtuins in Huntington's disease (HD)

Next to its effect on longevity, mammalian SIRT1 attracted the interest of researchers because it targets many of the same cellular pathways that have specifically been implicated in the HD pathogenesis. One important issue researchers in aging share with neurologists in neurodegenerative disorders arise from the fact, that age is a risk factor in many human diseases. A promising goal to effectively delay the onset and progression of age-related diseases like HD may be to focus on molecular mechanisms involving sirtuins and effectors in pathogenesis of such diseases.

Patients with HD are characterized by degeneration of neurons in the striatum and cerebral cortex, leading to various clinical symptoms: Psychiatric and cognitive abnormalities, involuntary movements (chorea), dementia and finally death [191, 192]. The dominantly inherited disease is caused by an expansion of CAG repeats in exon 1 of the *IT15* gene [193, 194]. If the polyglutamine stretch reaches a critical length, usually beyond 40 CAGs, HD develops. The onset and severity of the disease correlates with the age of patients and length of this expansion [195]. It has been demonstrated in transgenic HD models that mutant huntingtin (HTT) oligomerizes and forms large macromolecular inclusions equal to that detected in neurons of HD patients [196, 197]. Although, aggregation correlates with cell toxicity mutant htt monomers and oligomers are supposed to be primary responsible for cytotoxic effects rather than marcromolecular inclusions [198-200]. Importantly, expression of mutant HTT is sufficient to promote protein aggregation and cell lethality in several models including yeast, worm, fly, cell culture and mouse [201, 202].

As a consequence of unusual protein aggregation several cellular pathways are effected. Pathogenic HTT fragments impair the ubiquitin-proteasome system and are substrates for direct ubiquitination [203]. Moreover, effects on vesicular and organelle trafficking, the kynurenine pathway and transcriptional regulation have been reported amongst others [204, 205, 206].

Interestingly, the kynurenine pathway catalyzes *de novo* synthesis of NAD^+ from tryptophan in organisms ranging from yeast to humans. However, the pathway does

not appear to be essential for Sir2-dependent silencing and life span extension in yeast [139].

In addition, patient studies revealed functional defects in mitochondrial complexes, leading to ATP depletion [207, 208, 209]. Yeast cells, expressing mutant polyQ fragments, show dysfunction of complex I and III in the electron transport chain [210]. In fact, mitochondrial dysfunction is a hallmark of HD and might be the consequence of depolarisation events at mitochondrial membranes, leading to alterations in its voltage gradient [204]. Interestingly, an enhanced mitochondrial biogenesis in yeast and mammals suppresses HD-dependent toxicity [211].

1.3.6 Oxidative stress and Sir2 in HD

A mayor hallmark of neurodegenative disorders, such as HD, is oxidative cell damage [192, 198, 212]. Since mutant polyQ aggregation increases reactive oxygen species (ROS) production in cells by mitochondrial impairment and alteration of the kynurenine pathway [210, 213], conformational changes of proteins as a result from oxidative stress has been demonstrated in mouse and humans [212, 214, 215, 216, 217]. Consistently, some of them have been identified as mitochondrial enzymes involved in energy metabolism [209].

In this context, important neuroprotective properties of Sir2/SIRT1 was originally discovered in experiments made with resveratrol [218]. This polyphenolic compound, naturally found in red wine and the skin of red grapes, reduces mutant polyQ toxicity in several organisms including worms, flies, mouse and mammalian neurons [219, 220]. In mammals, resveratrol indirectly activates SIRT1 thus promoting deacetylation and activation of PCG-1α (peroxisome proliferator activated receptor-gamma co-activator-1α) [221, 222]. PCG-1α has been shown to play a key role in modulation of cell metabolism, implicating energy homeostasis, adaptive thermogenesis, ß-oxidation of fatty acids, repression of glycolysis and mitochondrial biogenesis [222]. Activation of PGC-1α by SIRT1-activator reseveratrol promotes also protection from reactive oxygen species (ROS) production [223]. Interestingly, equal to HD patients, striatal degeneration was observed in PGC-1α knockout mice [210].

In yeast cells, it has been demonstrated that expression of mutant HTT fragments increases ROS accumulation, thus resulting in elevated Sir2 levels [224]. These findings led to the assumption that expanded polyQ expression in yeast cells generates an oxidative stress condition and mimics the situation when glucose becomes limited. As a consequence of cellular adaption, genes involved in mitochondrial metabolism and stress resistance becomes activated [224].

Although, a PGC-1α ortholog in yeast has not been identified yet, another Sir2-dependent ROS detoxification mechanism seems to play an important role in HD. In fact, SIRT1-mediated oxidative stress protection of neurons, caused by mutant polyQ expression, requires both FoxO3 and PGC-1α [219, 225]. Recently it has been reported that mutant HTT directly interacts with Sirt1, resulting in a reduced deacetylase activity and hyperacetylation of FoxO3 [219, 226]. Overexpression of SIRT1 counteracts deacetylation deficits and restores pro-survival function of the transcription factor [226].

1.4 Objectives of this study

Molecular mechanisms controlling DNA replication and cell division depend on cell cycle regulators that are highly conserved among different species. Some of these proteins are believed to play diverse rolls in cancer, stress response, longevity determination and neurodegenerative disorders. A vast amount of functional data concerning cell cycle components have been accumulated using *Saccharomyces cerevisiae* as a model organism which is often utilized to elucidate regulation of fundamental eukaryotic mechanisms.

The main aim of this thesis was to validate protein-protein interactions based on a computational model to analyze cell cycle regulation on a more system-wide level. Therefore, a major focus was to investigate the regulatory interactions of Sic1, an inhibitor of Cdc28-Clb complexes, with the B-type cyclins Clb1-6. For this, yeast-two-hybrid and GST pull-down studies were perfomed.

In a next step, the role of Forkhead transcription factors Fkh1 and Fkh2 in the regulation of the cell cycle was examined. In particular, the specificity of B-type cyclins to interact with Fkh1, Fkh2 and Ndd1 and a potential association between Fkh1 and Ndd1 was analyzed using yeast-two-hybrid and GST pull-down studies. In

addition, it was aimed to investigate whether the Forkhead proteins Fkh1 and Fkh2 and the transcriptional coactivator Ndd1 alters cell cycle-regulated expression of *CLB3, 4*. For this, promoter binding studies and transcriptional analyses were performed.

Since an involvement of chromatin remodeling factors as crucial targets for forkhead transcription factors has been suggested, a direct association between histone deacetylase Sir2 and Fkh1, 2 was further analyzed using a fluorescence-based approach called Bimolecular Fluorescence Complemen-tation (BiFC). To identify a potential involvement of Sir2 in a timely regulation of *CLB2* gene, functional analyses including promoter binding studies, transcriptional analyses and western blots should additionally be performed.

Another interesting aspect of this work was to examine a potential relevance for a functional link between histone deacetylase Sir2 and Fkh1, 2 on the cellular stress response. In this light, it was aimed to examine the influence of oxidative stress on the physical interactions between Fkh proteins and Ndd1 or Sir2, respectively.

The final goal of this thesis was to shed light on the interconnection between Fkh-dependent cell cycle regulation and Sir2 and its relevance for Huntington's disease. To investigate whether Fkh1 and Fkh2 play a role in mutant Huntingtin-mediated protein aggregation, fluorescence microscopy and FACS analyses were performed.

2. Material and methods

2.1 Material

2.1.1 *Escherichia coli* strains

Table 2-1. *E. coli* strains used in this study.

Strain	Genotype	Source
XL1-Blue	endA1 gyrA96(nal^R) thi-1 recA1 relA1 lac glnV44 F'[::Tn10 proAB$^+$ lacI^q Δ(lacZ)M15] hsdR17(r_K^- m_K^+)	Stratagene
DH5α	F$^-$ endA1 glnV44 thi-1 recA1 relA1 gyrA96 deoR nupG Φ80d*lacZ*ΔM15 Δ(*lacZYA-argF*)U169, hsdR17(r_K^- m_K^+), λ–	Invitrogen
BL21(DE3)	F$^-$ ompT gal dcm lon hsdS_B(r_B^- m_B^-) λ(DE3 [lacI lacUV5-T7 gene 1 ind1 sam7 nin5])	Novagene

2.1.2 Yeast strains

Table 2-2. Yeast strains used in this study.

Strain	Genotype	Source
L40ccua	*MAT***a** *his3*_200 *trp1*-901 *leu2*-3,112 *LYS2*::(lexAop)4-*HIS3 ura3*::(lexAop)8-lacZ *ADE2*::(lexAop)8-*URA3 gal80* canR cyh2R	[227, 228]
L40ccua Δsir2	*MAT***a** *sir2*::*kanMX6*	This study
BY4741	*MAT***a** *his3Δ1 leu2Δ0 met15Δ0 ura3Δ0*	Euroscarf
Sic1-Myc	*MAT***a** *SIC1-MYC9*::*kanMX6*	This study
Fkh1-Myc	*MAT***a** *FKH1-MYC9*::*kanMX6*	This study
Fkh2-Myc	*MAT***a** *FKH2-MYC9*::*natNT2*	This study
Hcm1-Myc	*MAT***a** *HCM1-MYC9*::*kanMX6*	This study
Sir2-Myc	*MAT***a** *SIR2-MYC9*::*kanMX6*	This study
Δfkh1 Sir2-Myc	*MAT***a** *fkh1*:: *SIR2-MYC9*::*kanMX6*	This study
Δfkh2 Sir2-Myc	*MAT***a** *fkh2*:: *SIR2-MYC9*::*kanMX6*	This study

Δfkh1	*MAT***a** *fkh1*::	This study
Δfkh2	*MAT***a** *fkh2*::	This study
Δfkh1Δfkh2	*MAT***a** *fkh1*:: *fkh2*::	This study
Δsir2	*MAT***a** *sir2*::*kanMX6*	This study
Δfkh1Δsir2	*MAT***a** *fkh1*:: *sir2*::*kanMX6*	This study
Δfkh2Δsir2	*MAT***a** *fkh2*:: *sir2*::*kanMX6*	This study
Ndd1-VC/VN	*MAT***a** *NDD1-VC*::*his3MX6* p426GPDpr-*VN*	This study
Ndd1-VC/VN-Fkh1	*MAT***a** *NDD1-VC*::*his3MX6* p426GPDpr-*VN-FKH1*	This study
Ndd1-VC/VN-Fkh2	*MAT***a** *NDD1-VC*::*his3MX6* p426GPDpr-*VN-FKH2*	This study
Ndd1-VC/VN-Clb1	*MAT***a** *NDD1-VC*::*his3MX6* p426GPDpr-*VN-CLB1*	This study
Ndd1-VC/VN-Clb2	*MAT***a** *NDD1-VC*::*his3MX6* p426GPDpr-*VN-CLB2*	This study
Ndd1-VC/VN-Clb3	*MAT***a** *NDD1-VC*::*his3MX6* p426GPDpr-*VN-CLB3*	This study
Ndd1-VC/VN-Clb4	*MAT***a** *NDD1-VC*::*his3MX6* p426GPDpr-*VN-CLB4*	This study
Ndd1-VC/VN-Fkh2-Clb2-CFP	*MAT***a** *NDD1-VC*::*his3MX6* p426GPDpr-*VN-FKH2* *CLB2-CFP*::*kanMX6*	This study
Ndd1-VC/VN-Fkh2-Clb3-CFP	*MAT***a** *NDD1-VC*::*his3MX6* p426GPDpr-*VN-FKH2* *CLB3-CFP*::*kanMX6*	This study
Ndd1-VC/VN-Clb2-Clb3-CFP	*MAT***a** *NDD1-VC*::*his3MX6* p426GPDpr-*VN-CLB2* *CLB3-CFP*::*kanMX6*	This study
Ndd1-VC/VN-Clb3-Clb3-CFP	*MAT***a** *NDD1-VC*::*his3MX6* p426GPDpr-*VN-CLB3* *CLB3-CFP*::*kanMX6*	This study
Sir2-VC/VN-Fkh1	*MAT***a** *SIR2-VC*::*kanMX6* p426GPDpr-*VN-FKH1*	This study
Sir2-VC/VN-Fkh2	*MAT***a** *SIR2-VC*::*kanMX6* p426GPDpr-*VN-FKH2*	This study
Sir2-VC/VN-Hcm1	*MAT***a** *SIR2-VC*::*kanMX6* p426GPDpr-*VN-HCM1*	This study
Sir2-VC/VN-Clb1	*MAT***a** *SIR2-VC*::*kanMX6* p426GPDpr-*VN-CLB1*	This study
Sir2-VC/VN-Ndd1	*MAT***a** *SIR2-VC*::*kanMX6* p426GPDpr-*VN-NDD1*	This study

2.1.3 Plasmids

Table 2-3. Plasmids used in this study.

Plasmid	Description	Source/Accession
pACT41b	N-terminal AD gene fusion vector	[229]
pACT41b-Sic1	AD-Sic1	This study
pACT41b-Clb1	AD-Clb1	This study
pACT41b-Clb2	AD-Clb2	This study
pACT41b-Clb3	AD-Clb3	This study

pACT41b-Clb4	AD-Clb4	This study
pACT41b-Clb5	AD- Clb5	This study
pACT41b-Clb6	AD-Clb6	This study
pACT41b-Fkh1	AD-Fkh1	This study
pACT41b-Fkh2	AD-Fkh2	This study
pACT41b-Ndd1	AD-Ndd1	This study
pBTM117c	N-terminal LexA gene fusion vector	[229]
pBTM117c-Sic1	LexA-Sic1	This study
pBTM117c-Clb1	LexA-Clb1	This study
pBTM117c-Clb2	LexA-Clb2	This study
pBTM117c-Clb3	LexA-Clb3	This study
pBTM117c-Clb4	LexA-Clb4	This study
pBTM117c-Clb5	LexA-Clb5	This study
pBTM117c-Clb6	LexA-Clb6	This study
pBTM117c-Fkh1	LexA-Fkh1	This study
pBTM117c-Fkh1$_{360}$	LexA-Fkh1$_{360}$ (C-terminal fragment)	This study
pBTM117c-Fkh2	LexA and Fkh2	This study
pBTM117c-Fkh2$_{387}$	LexA-Fkh2$_{387}$ (C-terminal fragment)	This study
pBTM117c-Ndd1	LexA-Ndd1	This study
pGEX6p2	N-terminal GST gene fusion vector	Phamarcia Biotech
pGEX6p2-Clb1	GST-Clb1	This study
pGEX6p2-Clb2	GST-Clb2	This study
pGEX6p2-Clb3	GST-Clb3	This study
pGEX6p2-Clb4	GST-Clb4	This study
pGEX6p2-Clb5	GST-Clb5	This study
pGEX6p2-Clb6	GST-Clb6	This study
pGEX6p2-Fkh1	GST-Fkh1	This study
pGEX6p2-Fkh2	GST-Fkh2	This study
p426GPD	yeast vector for constitutive expression	[230, 231]
p426GPD-VN	N-terminal Venus-N gene fusion vector	This study
p426GPD-VN-Fkh1	Venus-N-Fkh1	This study
p426GPD-VN-Fkh2	Venus-N-Fkh2	This study
p426GPD-VN-Clb1	Venus-N-Clb1	This study
p426GPD-VN-Clb2	Venus-N-Clb2	This study
p426GPD-VN-Clb3	Venus-N-Clb3	This study
p426GPD-VN-Clb4	Venus-N-Clb4	This study
p423GALL	yeast vector for galactose inducible expression	[230, 231]
p423GALL-VN-Fkh1	Venus-N-Fkh1	This study
p423GALL-VN-Fkh2	Venus-N-Fkh2	This study
p423GALL-Sir2	galactose inducible expression of Sir2	This study
pFA6a-VN-KanMX6	ORF of Venus-N with KanMX6 marker	[232]

pFA6a-VN-His3MX6	ORF of Venus-N with His3MX6 marker	[232]
pFA6a-VC-KanMX6	ORF of Venus-C with KanMX6 marker	[232]
pFA6a-VC-His3MX6	ORF of Venus-C with His3MX6 marker	[232]
pYM30-ECFP-His3MX6	ORF of ECFP with His3MX6 marker	Euroscarf
pYESGALL-25Q-RFP	galactose inducible expression of HTT-25Q-RFP	[233]
pYESGALL-103Q-RFP	galactose inducible expression of HTT-103Q-RFP)	[233]

2.1.4 Oligonucleotides

Table 2-4. Oligonucleotides used in this study to generate PCR products for cloning. Underlined primer sequences represent target restriction sites.

Primer	Sequence
sic1_Fwd_SalI	5'-TACAGTCGACAATGACTCCTTCCACC-3'
sic1_Rev_NotI	5'-ATTGCGGCCGCTTCAATGCTCTTGATC-3'
pbp1_Fwd_SalI	5'-CATTGTCGACCAATATGAAGGGAAAC-3'
pbp1_Rev_NotI	5'-ATTGCGGCCGCTTCCTTCACTATTTATG-3'
clb1_Fwd_SalI	5'-GCTTGTCGACTAATCTTCTCATAATG-3'
clb1_Rev_NotI	5'-ATTGCGGCCGCTTCACTCATGCAATG-3'
clb2_Fwd_SalI	5'-CAGTCGACATTGATCTTATAGATGTCC-3'
clb2_Rev_NotI	5'-ATTGCGGCCGCTTCTCATTCATGCAAGG-3'
clb3_Fwd_SalI	5'-CTGAGTCGACAATGCATCATAACTCAC-3'
clb3_Rev_NotI	5'-TATGCGGCCGCTTTAGTTAGATCTTTC-3'
clb4_Fwd_SalI	5'-GATAGTCGACACAGATGATGCTTGAAG-3'
clb4_Rev_NotI	5'-GAAGCGGCCGCAAGATGAGTAAGTTAG-3'
clb5_Fwd_SalI	5'-GTAAGTCGACAACAATGGGAGAGAAC-3'
clb5_Rev_NotI	5'-GTAGCGGCCGCATTACTAGTACTAATC-3'
clb6_Fwd_SalI	5'-GCATGTCGACTAAAATGAATTGTATC-3'
clb6_Rev_NotI	5'-TATGCGGCCGCTGATCTATGTTTCAAC-3'
fkh1_Fwd_SalI	5'-GTCAGTCGACTATGTCTGTTACCAGTAG-3'
fkh1_360_Fwd_SalI	5'-TATTGTCGACCTTCGAGAAGGTGCC-3'
fkh1_402_Fwd_SalI	5'-TTATGTCGACCTCTGTGACAAGACAG-3'
fkh1_Rev_NotI	5'-AATGCGGCCGCTGAATTTCAACTCAG-3'
fkh2_Fwd_SalI	5'-TGAAGTCGACAATGTCCAGCAGCAAT-3'
fkh2_387_Fwd_SalI	5'-TACTGTCGACCATTAGGCATAATTTATC-3'

fkh2_458_Fwd_SalI	5'-ATAAGTCGACCATGGAAATGGACTATAG-3'
fkh2_Rev_NotI	5'-ATTGCGGCCGCTTAGTTGTTGATAATAC-3'
hcm1_Fwd_SalI	5'-TTGAGTCGACAATGATGAATGAAG-3'
hcm1_Rev_NotI	5'-TTGCGGCCGCTCAATTCTTTTCATTACC-3'
ndd1_Fwd_SalI	5'-AGATGTCGACTATGGACAGAGATATAAG-3'
ndd1_Rev_NotI	5'-TAAGCGGCCGCAAGTTTGGTTAATATTAC-3'
venus-N_Fwd_BamHI	5'-TAGGATCCATGGTGAGCAAGGGCG-3'
venus-N_Rev_EcoRI	5'-TCGAATTCCTCGATGTTGTGGCGGAT-3'
fkh1_VN_Fwd_EcoR1	5'-AGAATTCTCGACTATGTCTGTTACC-3'
fkh1_VN_Rev_XhoI	5'-CTCTCGAGTCAACTCAGAGAGGAATTG-3'
fkh2_VN_Fwd_EcoR1	5'-AGAATTCTCGACAATGTCCAGCAGC-3'
fkh2_VN_Rev_XhoI	5'-GTCTCGAGTTAGTTGTTGATAATACTG-3'
clb2_Fwd_EcoR1/SalI	5'-AAGAATTCAGGTCGACGATGTCCAACCCAATAG-3'
clb2_Rev_Not1/XhoI	5'-TTCTCGAGTGCGGCCGCTTCTCATTCATGC-3'

Table 2-5. Oligonucleotides used in this study to amplify integration cassettes for chromosomal gene modification. Sequences in italics represent the gene-specific sequences whereas capital letters comprise vector-specific sequences for amplification of cassette.

Primer	Sequence
sic1_Myc_Fwd	5'-*CAAGCCAAAGGCATTGTTTCAATCTAGGGATCAAGAGCAT* GCTAGTGGTGAACAAAAG-3'
sic1_Myc_Rev	5'-*TTAAATATAATCGTTCCAGAAACTTTTTTTTTTCATTTCT* TAGTGGATCTGATATCATCG-3'
fkh1_Myc_Fwd	5'-*CGTAACAACAAACGCAAACGTGAACAATTCCTCTCTGAGT* GCTAGTGGTGAACAAAAG-3'
fkh1_Myc_Rev	5'-*TATTGTTTAATAATACATATGGGTTCGACGACGCTGAATT* TAGTGGATCTGATATCATCG-3'
fkh2_Myc_Fwd	5'-*ACTAGATACGGATGGTGCAAAGATCAGTATTATCAACAAC* GCTAGTGGTGAACAAAAG-3'
fkh2_Myc_Rev	5'-*TTCATTTCTTTAGTCTTAGTGATTCACCTTGTTTCTTGTC* TAGTGGATCTGATATCATCG-3'
ndd1_Myc_Fwd	5'-*CTGTAATTCTAAATCTAATGGAAATTTATTCAATTCACAG* GCTAGTGGTGAACAAAAG-3'
ndd1_Myc_Rev	5'-*TTCCATAAAAAAAAAAGGTGAGATGCAAGTTTGGTTAATA* TAGTGGATCTGATATCATCG-3'

hcm1_Myc_Fwd	5'-TCATAATCACCCTTCCAACGATAGCGGTAATGAAAAGAAT GCTAGTGGTGAACAAAAG-3'
hcm1_Myc_Rev	5'-CAACCGTTTGCGATGAATCCATCAGATTAAGAATAATTAG TAGTGGATCTGATATCATCG-3'
sir2_Myc_Fwd	5'-*CGTGTATGTCGTTACATCAGATGAACATCCCAAAACCCTC* GCTAGTGGTGAACAAAAG-3'
sir2_Myc_Rev	5'-*TATTAATTTGGCACTTTTAAATTATTAAATTGCCTTCTAC* TAGTGGATCTGATATCATCG-3'
fkh1Δ_Fwd	5'-*TGTGCGTTCAATTAGCAAAGAAAGGCTTGGAGAGACACAG* GTACGCTGCAGGTCGACAAC-3'
fkh1Δ_Rev	5'-*TATTGTTTAATAATACATATGGGTTCGACGACGCTGAATT* CTAGTGGATCTGATATCACC-3'
fkh2Δ_Fwd	5'-*GTGCTCCCTCCGTTTCCTTTATTGAAACTTTATCAATGCG* GTACGCTGCAGGTCGACAAC-3'
fkh2Δ_Rev	5'-TTCATTTCTTTAGTCTTAGTGATTCACCTTGTTTCTTGTC CTAGTGGATCTGATATCACC-3'
sir2Δ_Fwd	5'-CATTCAAACCATTTTTCCC TCATCGGCACATTAAAGCTGG GTACGCTGCAGGTCGACAAC-3'
sir2Δ_Rev	5'-TATTAATTTGGCACTTTTAAATTATTAAATTGCCTTCTAC CTAGTGGATCTGATATCACC-3'
ndd1-VN_Fwd	5'-*CTGTAATTCTAAATCTAATGGAAATTTATTCAATTCACAG* GGTCGACGGATCCCCGGGTT-3'
ndd1-VN_Rev	5'-*TCGATTAAAAAAAAAAGGTGAGATGCAAGTTTGGTTAATA* TCGATGAATTCGAGCTCGTT-3'
sir2-VN_Fwd	5'-*CGTGTATGTCGTTACATCAGATGAACATCCCAAAACCCTC* GGTCGACGGATCCCCGGGTT-3'
sir2-VN_Rev	5'-*TATTAATTTGGCACTTTTAAATTATTAAATTGCCTTCTAC* TCGATGAATTCGAGCTCGTT-3'
clb2-CFP_Fwd	5'-*GGTTAGAAAAAACGGCTATGATATAATGACCTTGCATGAA* GGAGCAGGTGCTGGTGCTGG-3'
clb2-CFP_Rev	5'-*CGATTATCGTTTTAGATATTTTAAGCATCTGCCCCTCTT* CTAGTGGATCTGATATCATCG-3'
clb3-CFP_Fwd	5'-*GAAGTGGATAGCATTAGCTGAACACAGAGTAGAAAGATCTAAC* GGAGCAGGTGCTGGTGCTGG-3'
clb3-CFP_Rev	5'-*CTTTTTCCTTTGTTGATGCCATGTCTCGAGCTGAGGCTTT* CTAGTGGATCTGATATCATCG-3'

Table 2-6. Oligonucleotides used in this study to amplify coprecipitated DNA fragments in ChIP experiments or cDNA reverse transcribed from total RNA preparations.

Primer	Sequence
tsa1_Fwd	5'-ATGGTCGCTCAAGTTCAAAAG-3'
tsa1_Rev	5'-CGTACTTACCCTTGTATTTGTCCAA-3'
act1_Fwd	5'-ATGTGTAAAGCCGGTTTTGC-3'
act1_Rev	5'-TGACCCATACCGACCATGATA-3'
clb1_RT_Fwd	5'-CAGTCTAGGACGTTAGC-3'
clb1_RT_Rev	5'-GTCGTGAATAGTAGATCC-3'
clb1_ChIP_Fwd	5'-CAGACGCGCTTCAATTAG-3'
clb1_ChIP_Rev	5'-GTTACCGTTGACGTGAG-3'
clb2_RT_Fwd	5'-GGAATGTACAAGGTTGG-3'
clb2_RT_Rev	5'-CAAATTGCTGACTACTTGG-3'
clb2_ChIP_Fwd	5'-GTGCAAGTTCAAGGCAC-3'
clb2_ChIP_Rev	5'-CATGCTATGAGATGCTAG-3'
clb3_RT_Fwd	5'-GGATCGTCCAAGTACATG-3'
clb3_RT_Rev	5'-CAGCAATGAAGAGTGAG-3'
clb3_ChIP_Fwd	5'-GCAAGAACATGGACAC-3'
clb3_ChIP_Rev	5'-GTGCAACACTATTCGCATC-3'
clb4_RT_Fwd	5'-CTCTTCTACTGATGACGAAC-3'
clb4_RT_Rev	5'-CTGTCCAGCTCAGTCTG-3'
clb4_ChIP_Fwd	5'-CTAGAAGATTAGCAAGAT-3'
clb4_ChIP_Rev	5'-GAGGTTGTACCGTATACC-3'

2.1.4 Antibodies

Table 2-7. Antibodies used in this study to precipitate or detect proteins.

Name/ Source	Host	Clonality/Isotype/ Concentration	Dilution/ Application
Primary antibodies			
α-Myc tag/Millipore	Mouse	Monoclonal/IgG1/1 mg/ml	1:200/ChIP 1:5000/WB
α-Myc tag/Sigma-Aldrich	Rabbit	Polyclonal/IgG/0.6 mg/ml	1:100/ChIP 1:2000/WB

α-Myc tag/Abcam	Goat	Polyclonal/IgG/1 mg/ml	1:200/ChIP 1:2000/WB
α-GST tag/Sigma	Rabbit	Polyclonal/IgG/0.5 mg/ml	1:10000/WB
α-RNA Polymerase II/ Covance	Mouse	Monoclonal/IgG2a/2-3 mg/ml	1:100/ChIP
α-Clb2/Santa Cruz Biotechnology	Goat	Polyclonal/IgG/0.2 mg/ml	1:1000/WB
Secondary antibodies			
α-mouse peroxidase-conjugated/Sigma	Goat	Polyclonal/IgG/0.4 mg/ml	1:10000/WB
α-rabbit peroxidase-conjugated/Sigma	Goat	Polyclonal/IgG/0.4 mg/ml	1:10000/WB
α-goat peroxidase-conjugated/Dianova	Rabbit	Polyclonal/IgG/0.6 mg/ml	1:10000/W

2.2 Methods

Standard methods and techniques performed in this study are based on Sambrook et al., 1989. Protocols and commercially available kits that have been used with some modifications are described in more detail in this chapter.

2.2.1. *Escherichia coli* strains and growth media

Escherichia coli XL1-Blue and DH5α strains were used for cloning and expression of recombinant proteins, whereas BL21(DE3) cells were used exclusively for protein expression (genotypes are listed in Table 2-1). *E. coli* cells were cultured in liquid LB medium (L-Broth powder, MP Biomedicals LLC, 10 g/l Tryptone, 5 g/l Yeast Extract, 0.5 g/l NaCl dissolved in distilled water and sterilized by autoclavation at 121 °C for 15 min). For solid LB-agar plates, 15 g/l agar were added before autoclavation. When needed, ampicillin (stock: 100 mg/ml in sterile water, Sigma Aldrich, Germany) was added to the medium to a final concentrations of 100 µg/ml. *E. coli* cells were grown at 37 °C in an incubator (Innova 44, Incubator Shaker Series, New Brunswick Scientific) under shaking at 220 rpm.

For long-term storage, glycerol stocks were prepared by adding sterile glycerol (Merck, Germany) to the cells to a final concentration of 20 %. Stocks were frozen on dry ice and then stored at -80 °C.

2.2.2. Transformation of *E. coli*

For the preparation of competent *E. coli* cells, a single colony was inoculated in 100 ml of liquid LB medium supplemented with 20 mM $MgSO_4$. The culture was incubated over night at 23 °C. Then, 2 ml of the culture were inoculated in 200 ml of liquid LB medium (20 mM $MgSO_4$) and again incubated over night at 23 °C. When cells reached an OD_{600} of 0.5 - 0.7, the culture was centrifuged at 3000 g for 10 min at 4 °C (Centrifuge 5810R, Eppendorf, Germany) and the cell pellet was resuspended in 32 ml of TB buffer (10 mM $CaCl_2$, 10 mM Pipes-NaOH, 15 mM KCl_2 and 55 mM $MnCl_2$, pH 6.7). After 10 min of incubation on ice, cells were centrifuged at 450 g for 3 min at 4°C and resuspended in 16 ml of TB buffer supplemented with 7 % DMSO (Sigma-Aldrich, Germany). After 10 min of incubation on ice, 100 µl of cell suspension were aliquoted.

For the transformation of *E.coli* cells, 100 µl of competent cells were incubated on ice and plasmid DNA (10-50 ng/µl) or ligation mixture was added. Then, cells were incubated for 30 min on ice and heat-shocked for 90 sec at 42 °C. Tubes were immediately incubated on ice and the cell suspension was mixed with 900 µl of liquid LB medium. Afterwards, cells were incubated for 60 min at 37 °C under vigorous shaking at 500 rpm in a thermomixer (Thermomixer komfort, Eppendorf, Germany). Then, cells were centrifuged at 1500 g for 3 min, resuspended in 50 µl of LB Medium, plated onto selective LB agar plates and incubated over night at 37°C (Heraeus Instruments, USA).

2.2.3. Plasmid DNA isolation

For the small scale isolation of plasmid DNA, the GeneJet Plasmid Miniprep Kit (Fermentas, EU) was used according to the manufacturer's instructions. A single *E. coli* colony was inoculated in 5 ml LB medium and incubated over night. Then, the culture was centrifuged at 4000 g for 10 min and cells were resuspended in 250 µl of resuspension buffer. 250 µl of lysis buffer were added to the cell solution and inverted carefully for 5-7 times. For precipitation of plasmid DNA, 350 µl of

neutralization buffer was added. The cell lysate was then centrifuged at 10000 g for 5 min to separate the insoluble protein/DNA fraction from soluble plasmids, and the supernatant was transferred to a spin column. After centrifugation at 10000 g for 1 min, the flow-through was discarded and the column washed by adding 500 µl of Wash buffer and then centrifuged at 10000 g for 30 sec. Again, the flow-through was discarded and the wash-step repeated. To evaporate the residual wash buffer, the column was placed in a new tube and heated for 3 min at 42 °C. Plasmid DNA was eluted with 50 µl of sterile water pre-warmed at 42 °C, by centrifugation at 10000 g for 2 min and the eluted plasmid DNA was stored at 4°C or at -20 °C.

2.2.4 Cloning of DNA fragments and PCR products

PCR products were first cloned into the blunted linearized pJET1.2 plasmid. If a specific PCR product appeared as one definite band on a gel, it was directly used for the ligation reaction; alternatively, the PCR product was extracted from an agarose gel (see paragraph 2.2.6). PCR products with 3'-overhangs generated by *Taq* DNA polymerase or DNA fragments with 5'- or 3'-overhangs generated by restriction enzyme digestion were used in a 3:1 molar ratio with the pJET1.2/blunt plasmid (50 ng/µl) (Clone JET PCR Cloning Kit, Fermentas). The blunting reaction was performed on ice as described in the following. In a micro tube 10 µl of 2 × reaction buffer were mixed with maximum 3 µl of purified (gel eluate) or non-purified (PCR product) DNA fragment, and nuclease-free water added to a final volume of 17 µl. 1 µl of DNA blunting enzyme (10 U) was then added to the sample and resuspended. The blunting reaction was incubated for 5 min at 70 °C and transferred on ice. For the ligation reaction, 1 µl of pJET1.2/blunt plasmid (50 ng/µl) and 1 µl of T4 DNA ligase (5 U) were added. The ligation was perfomed by incubation for 30 min at 16 °C. Then, the reaction was stored at -20 °C or directly used for transformation of *E. coli* cells.

Verified pJET1.2-derived constructs were subcloned into expression plasmids (listed in Table 2-3) by using appropriate restriction sites coded by primer sequences (listed in Table 2-4). 3 µg of pJET2.1-derived constructs were treated with appropriate restriction enzymes (New England Biolabs, USA) and incubated at 37 °C for 3 h. Subsequently, 6 × DNA loading buffer was added and samples were loaded on an agarose gel. After purification and quantification of DNA fragments, the ligation

reaction was performed with a 3:1 molar ratio of fragment/digested expression plasmid.

A typical ligation reaction contained 1 µl of plasmid DNA (30-60 ng), 1-3 µl of DNA fragment (3:1 molar ratio of insert:vector), 1 µl of 10 x T4 ligase buffer (New England Biolabs, USA), 1 µl of T4 ligase enzyme (400 U, NEB) and nuclease-free water to a final volume of 10 µl. The ligation reaction was incubated for at least 4 h at 16 °C, and 5-10 µl used to transform competent *E. coli* cells. Clones grown on selection plates were verified by colony PCR (see paragraph 2.2.8).

2.2.5 Quantification of DNA or RNA

Concentration of nucleic samples was measured using a NanoDrop ND-1000 UV-Vis Scanning Spectrophotometer according to manufacturer's instructions. Concentrations of DNA or RNA samples obtained from reverse transcription or genomic DNA fragments co-precipitated in ChIP experiments (see paragraph 2.2.19) were determined using the Quant-iT DNA assay kit (Invitrogen). The concentration of the sample was measured in a range from 200 pg/µl to 10 ng/µl by using a fluorescence signal obtained from a dye (PicoGreen) that intercalates into dsDNA or dsRNA. 1 µl of sample was diluted in 199 µl of buffer and measured in a micro tube reader (Invitrogen). Extinction values were compared to those obtained from DNA standards (500 pg, 1 ng, 2 ng and 4 ng).

2.2.6 Agarose gel electrophoresis

Nucleic acid samples were separated on agarose gels by electrophoresis at 40 V for 45 min. Sample migration depends on the size of DNA fragments, therefore agarose concentration in the gel ranged from 0.7 % to 2 %.

In a 1 % agarose gel (0.5 g/50 ml 1 × TAE, 40 mM Tris-acetate pH 8.2, 1 mM EDTA) 0.1 µg/ml Ethidium bromide (Sigma-Aldrich, Germany) was added to pre-heated agarose-TAE mixture to visualize nucleic acids after exposure under UV light (Transilluminator UVT-28M, Herolab). Size of DNA bands was determined using 1 kb ladder (New England Biolabs, USA) as reference.

2.2.7 Isolation of DNA fragments

The extraction of DNA fragments from agarose gels was performed with Wizard SV Gel and PCR Clean-Up System kit (Promega, USA). Excised bands were weighted in and 10 µl of membrane binding buffer per 10 mg of agarose gel slice was added and dissolved at 50 °C for 10 min. Then, DNA solution was transferred onto a silica membrane of a column. The samples were centrifuged at 10000 g for 1 min and the flow through discarded. The column was washed by adding 700 µl of wash solution and centrifugation at 10000 g for 30 sec. The wash step was then repeated and the sample centrifuged at 10000 g for 2 min. The column was placed in a new 1.5 ml micro tube and heated at 42 °C in a thermomixer to evaporate residual ethanol contained in the Wash buffer. 50 µl of nuclease-free water were applied on the center of the column, the sample incubated at 42 °C for 2 min and then centrifuged at 13000 g to collect eluted DNA. Samples were stored at -20 °C or directly used for further experiments.

2.2.8 Polymerase Chain Reaction (PCR)

Colony PCR of *E. coli* clones

To analyze recombinant *E. coli* clones after transformation of ligation mixtures, single colonies were analyzed in a final volume of 25 µl which comprehends:

13.5 µl	nuclease-free water
2 µl	10 × *Taq* polymerase buffer *
4 µl	$MgCl_2$ (25 mM)
4 µl	5 × CES PCR-Enhancer **
0.5 µl	dNTPs (20 mM each)
0.5 µl	Primer mix (25 pmol/µl each)
0.5 µl	*Taq* DNA polymerase (10 U/µl)***

* (650 mM Tris, 166 mM $(NH_4)_2SO_4$, 31 mM $MgCl_2$, 0.1 % Tween-20, pH 8.8)

** (2.7 M betaine, 6.7 mM DTT, 6.7 % DMSO, 55 µg/ml BSA)

*** in-house

PCR reactions were performed in a Thermocycler (PTC-100, Programmable Thermal Controller, MJ Research Inc.) programmed as described in the following:

Step	Temperature	Time	Number of cycles
Initial denaturation	94 °C	5 min	1
Denaturation	94 °C	1 min	34
Annealing	54 °C	30 sec	
Extension	72 °C	1 min/kb	
Final extension	72 °C	5 min	1

Amplification of DNA integration cassettes and DNA fragments

For the amplification of various DNA integration cassettes and gene ORFs, the Phusion Hot Start High-Fidelity DNA Polymerase (Finnzymes, Sweden) was used. A typical PCR reaction is performed in a total volume of 20 µl as described in the following:

13.9 µl	nuclease-free water
4 µl	5 × Phusion buffer *
0.4 µl	dNTPs (200 µM each)
0.5 µl	Primer mix (20 pmol/µl each)
1 µl	template DNA **
0.2 µl	Phusion DNA polymerase (2U/µl)

* 5 × Phusion HF buffer was used for PCR reactions
5 × Phusion GC buffer was used for GC-rich templates

** plasmid DNA was used in a concentration of 10 ng/µl
genomic yeast DNA was used in a concentration of 150 ng/µl

Phusion PCR reactions were performed in a Thermocycler programmed as described in the following:

Step	Temperature	Time	Number of cycles
Initial denaturation	98 °C	30 sec	1
Denaturation	98 °C	10 sec	34
Annealing	55 °C	10 sec	
Extension	72 °C	30 sec/1 kb	
Final extension	72 °C	5 min	1

2.2.9 *Saccharomyces cerevisiae* strains and growth media

S. cerevisiae strains derived from BY4741, BY4742 and L40adeA were used (genotype are listed in Table 2-2). Yeast cells were grown at 30 °C in an incubator (Incubator Shaker Series, New Brunswick Scientific) under shaking at 160 rpm, whereas plates were incubated at 30 °C (B6770, Heraeus Instruments, USA).

YPD medium was prepared mixing 10 g/l yeast extract (Yeast Extract, Difco Laboratories), 20 g/l peptone (Bacto Peptone, Difco Laboratories) and 20 g/l glucose (D-(+)-Glucose, Sigma-Aldrich) or 20 g/l galactose (D-(+)-Galactose, Sigma-Aldrich, Germany). If a medium with agar was required, 15 g/l Bacto Agar (Difco Laboratories) were added. The components were dissolved in distilled water and autoclaved at 121 °C for 15 min. SD medium (YNB-ADE-HIS-LEU-TRP-URA, Difco Laboratories) was prepared by dissolving 0.67 g/l YNB and 20 g/l glucose in distilled water and autoclavation at 121 °C for 15 min. For the preparation of CSM medium, 0.59 g/l Complete Supplement Mixture (CSM-ADE-HIS-LEU-TRP-URA, MPBio) was added to 1 l of YNB and autoclaved at 121 °C for 15 min.

2.2.10 Isolation of yeast genomic DNA

For isolation of genomic DNA, yeast clones were resuspended in 200 µl of yeast Lysis buffer (2 % Triton X-100, Sigma, 1 % SDS, 100 mM NaCl, 10 mM Tris pH 8, 1 mM EDTA). Then, the cell suspension was incubated on dry ice to break the yeast cell wall and 400 µl of chloroform added. For lysis, cells were incubated for 60 sec in a micro tube vortexer with a constant pulse (Vortex Genie 2, Bender & Hobein AG, Swizerland). The cell lysate was then centrifuged at 10000 g for 5 min and the upper aqueous layer transferred to a new tube. An additional centrifugation at 10000 g for 2 min was performed. For precipitation of DNA, 20 µl of 3 M natrium acetat (pH 5.2)

and 500 µl of pre-cooled 100 % ethanol was added to the upper layer. The mixture was then inverted 6 times, incubated for 10 min at -20 °C and centrifuged at 12000 g for 5 min. Afterwards, the supernatant was discarded and the DNA pellet incubated at 42 °C evaporate residual ethanol. Finally, the DNA pellet was resuspended in 25 µl of nuclease free water or optionally digested with RNase A (DNase free). Genomic DNA samples were stored at 4 °C or, for longer times, at - 20 °C.

2.2.11 Isolation of RNA

For the isolation of total RNA from yeast cells, the RiboPure Yeast Kit (Applied Biosystems, Ambion, Inc., USA) was used according to the manufacturer's instructions. 200 µl of yeast culture derived from an over night culture (OD ~ 1.2 - 1.5) were inoculated in 10 ml of appropriate liquid media (YPD, CSM) and incubated until an exponential growth (OD ~ 0.5 - 0.7). Cells were collected by centrifugation at 4000 g for 1 min and the pellet resuspended in 480 µl of lysis buffer, 48 µl of 10 % SDS and 480 µl of Phenol:Chloroform:IAA. The cell lysate was then transferred to a new tube filled with 750 µl of beads, vortexed at maximum speed for 10 min to and the phenol extraction was completed by centrifugation at 10000 g for 5 min. Then, the aqueous phase containing the nucleic acid was transferred to a new tube and mixed with 1.9 ml of binding buffer. 1.25 ml of 100% ethanol was added, mixed by vortexing, and 700 µl of the sample was added to a filter cartridge. The lysate/ethanol mixture was centrifuged at 10000 g for 1 min and the flow-through discarded. Then, the filter cartridge was returned to collection tube and steps repeated until the entire lysate/ethanol mixture passed the glass-fiber filter to immobilize RNA. The filter was then washed with 700 µl of wash solution 1 by centrifugation at 10000 g for 1 min. The flow-through was discarded and the sample washed twice with 500 µl of wash solution 2 by centrifugation at 10000 g for 1 min. The residual wash solution was removed by additional centrifugation at 10000 g for 2 min. The RNA bound to the filter was eluted by adding 40 µl of elution buffer, pre-heated at 95 °C and post-cooled at 42 °C. The RNA was collected by centrifugation at 10000 g for 1 min and the elution step repeated.

To remove genomic DNA, the sample were treated with 4 µl of DNase I (8 U) and 8 µl of DNase I 10 × buffer. Then, the reaction was incubated for 30 min at 37 °C in a thermomixer before adding 10 µl of DNase inactivation reagent. The sample was

finally mixed by vortexing, incubated for 5 min at room temperature and then centrifuged at 10000 g for 2 min. The supernatant (total RNA) was transferred in a new tube and stored at -80 °C or directly used.

2.2.12 Reverse transcription

RNA samples were used to synthesize cDNA with the SuperScript II Double-Stranded cDNA Synthesis Kit (Invitrogen, USA) according to the manufacturer's instructions. 12 µl of RNA (5 µg) were mixed with 100 pmol oligo-dT Primer (Oligo-dT (15)-Primer, Promega), 10 pmol dNTPs. The mixture was then denatured at 65 °C for 5 min and placed on ice. Afterwards, the sample was briefly centrifuged at 10000 g for 1 min and supplemented with 4 µl of 5 × First-Strand Reaction buffer and 2 µl of 0.1 M DTT. The reaction tube was pre-warmed at 42 °C for 2 min before 1 µl of reverse transcriptase (200 U) was added. Finally, the sample were incubated for 50 min at 42 °C and the enzyme was inactivated for 15 min at 70 °C. After centrifugation at 10000 g for 1 min, the sample was frozen and stored at -20 °C.

Real-time PCR

The real-time PCR was used to amplify cDNA obtained after reverse transcription of mRNA or genomic DNA fragments by allowing a simultaneous amplification and quantification of primer-targeted DNA molecules. The non-specific intercalation of a fluorescent dye, SYBR Green, into dsDNA was used to determine the relative amount of a target sequence in a sample. An increase in the PCR product leads to an increase in the fluorescence intensity due to the fact that the dye fluoresces only when bound to dsDNA. A real-time PCR machine (Applied Biosystems, 7900 HT Real-Time PCR System) detected the level of fluorescence after each PCR cycle, thus allowing the quantification of PCR products. Quantification of target DNA fragments was performed 3 times for each primer pair (listed in Table 2-7) in a 96-well plate (Sarsteadt). In each well DNA samples and the following components were added to a final volume of 10 µl:

3.5 µl	nuclease-free water
5 µl	2 × master mix *
0.5 µl	Primer mix (20 pmol/µl each)
1 µl	template DNA **

* SYBR Green PCR Master Mix (Applied Biosystems)

** cDNA was used in a concentration of 7 ng/µl
genomic DNA was concentrated 300 pg/µl

2.2.13 Transformation of *Sacharomyces cerevisiae*

Yeast strains were inoculated in 5 ml of appropriate liquid media and grown to saturation at 30 °C over night. Then, fresh medium was inoculated with over night cultures to an OD_{600} ~ 0.3 and incubated at 30 °C until an OD_{600} ~ 0.6 - 0.8. Cells were centrifuged at 2500 rpm for 3 min and the supernatant removed. Pellets were then resuspended in 1 ml of Mix 1 (mM Tris 5 pH 7.4, 100 mM lithium acetate, 1.0 M Sorbitol, 0.5 mM EDTA) and incubated for 10 min at room temperature. 40 µl of the mixture were then added to a tube containing 12.5 µg of salmon sperm DNA, 500 ng of DNA and 230 µl of Mix 2 (10 mM Tris pH 7.4, 100 mM lithium acetate, 40 % PEG-3350, 1 mM EDTA). The transformation solution was resuspended and incubated at 30 °C for 30 min. 30 µl of DMSO (Sigma-Aldrich) were added to the mixture and a heatshock was perfomed at 42 °C for 7 min. After centrifugation at 2000 g for 3 min, the supernatant was discarded and the cell pellet resuspended in 50 µl of sterile water and transferred onto plates that contained appropriate selection medium. The plates were incubated at 30 °C and the incubation time varied between 3 and 5 days according to the growth rate of yeast cells.

Transformation of yeast cells required the selection on appropriate markers (genotype are listed in Table 2-2), therefore specific synthetic selection media or antibiotics were used. Selection markers were added directly to the media (YNB, CSM) starting from 100 × stock solutions prepared as follows: 0.1 % Adenine (ADE, Sigma-Aldrich) in 10 mM NaOH, 0.2 % uracil (URA, Sigma-Aldrich) in 10 mM NaOH, 2 % histidine (HIS, Sigma-Aldrich) in water, 6 % leucine (LEU, Sigma-Aldrich) in water and 4 % tryptophane (TRP, Sigma-Aldrich) in water. The antibiotics geniticine (G418 sulphate, Gibco) and nourseothricine (Lexy NTC Nourseothricine, Jena Bioscience) were added to YPD medium in a final concentration of 300 µg/ml and 75 µg/ml, respectively.

2.2.14 Chromosomal modification of yeast genes

Deletion and tagging of yeast genes required the amplification of DNA fragments by PCR. For the sequence-specific integration of a desired DNA fragment by homologous recombination, oligonucleotides were designed which contain sequences for target recombination loci of genomic DNA (see Table 2-5 for details). Sense primers encoded 40 bp of upstream recombination locus at the 5' end, whereas antisense primers contained 40 bp of downstream recombination locus at 3' the end. In addition to recombination loci, the oligonucleotides must comprise sequences for amplification of a selection marker cassette encoded by respective plasmids as well. Specifically, the sense primer encodes a sequence (20 bp) that anneals upstream of the respective cassette (promoter, coding sequence and terminator of selection marker) at the 5' end, whereas respective antisense oligonucleotide encoded DNA sequences (20 bp) that anneal downstream of a selection cassette at the 3' end. The choice of a selection marker was limited by the genotype of the available strains (genotypes listed in Table 2-2).

Approximately 300 ng of the amplified DNA cassette were transformed in yeast cells as previously described (see paragraph 2.2.13). After transformation, cells were centrifuged and the cell pellet was resuspended in 2 ml of 1 × YPD with 2% glucose. The tube was incubated at 30 °C for 2.5 h to allow for recombination events. Finally, cell suspension was centrifuged and plated on appropriate selection media. The incubation time of plates varied (2 - 5 days) according to the desired size of yeast colonies.

An excision of integrated selection marker cassette can be obtained using the Cre/loxP (Causes Recombination/locus of X over P1) recombination system. This technique is based on the excision of loxP-flanked genomic DNA sequences in presence of the site-specific Cre recombinase enzyme. In this study, a loxP-flanked G418 cassette (loxP site, promoter, coding sequence of KanMX, terminator and loxP site) amplified from the pUG6 vector was used. To analyze for the site-specific integration after the transformation of respective selection maker cassette, transformants were selected on G418 containing media. Then, single clones were used for the isolation of genomic DNA and the site-specific insertion was verified by PCR. To this purpose, a sense primer that binds upstream of the START codon (5'

end) of the target gene and an antisense primer that anneals downstream the STOP codon (3' end) were used. A correct integration occurs when the size of the amplification product is equal to the one of the loxP-flanked selection cassette. For excision of loxP-flanked cassette, clones were transformed with the pSH47 plasmid encoding Cre-recombinase under control of a galactose inducible promoter. Then, transformants were selected and single clones inoculated in 1 × CSM (without selection markers) supplemented with 2 % galactose and incubated over night. Afterwards, a sample of this culture was transferred to a new micro tube and centrifuged at 3000 g for 3 min. The cell pellet was resuspended in 50 µl of sterile water and plated on 1 × CSM medium (without selection markers) or 1 × YPD medium supplemented with G418. An excision of selection marker cassette can be assumed, if the number of colonies on YPD/G418 plate is significantly reduced compared to CSM plate. Then, single clones were isolated from CSM plate and loxP-specific excision of the selection marker cassette was verified by PCR. To counterselect on the pSH47 plasmids, verified clones were transferred in 1 × CSM medium containing 1 × 5-fluoroorotic acid (5-FOA, 100 mg/ml in DMSO for a 100 × stock solution, Zymo Research, USA). Nontoxic 5-FOA is converted to its toxic form 5-fluorouracil when cells expressed URA3-encoded orotine-5''-monophosphate. 5-fluorouracil affected cells failed to replicate their DNA due to a lack of thymidine. Clones grown on 5'-FOA media were verified for uracil auxotrophy by plating on appropriate selection media.

2.2.15 Yeast two-hybrid (Y2H) assay

The method is employed for investigating physical protein-protein interactions. A candidate *ORF1* was fused to the DNA binding domain of the Gal4 transcription factor and tested for interaction with the putative partner *ORF2*, fused to the activation domain of Gal4 (which is necessary for the recruitment of RNA polymerase II). A functional Gal4 complex is reconstituted when Orf1 and Orf2 bind to each other, thus leading to the activation of reporter genes.

The assays were performed with the L40ccua strain carrying the selection markers histidine (HIS), uracil (URA), adenine (ADE) and the ß-Galactosidase reporter gene (*lacZ*) under control of the GAL4 promoter. Transformation of pBTM-117c (expressing the Gal4-binding domain) and pACT-41b (expressing the Gal4-activation

domain) plasmids in L40ccua cells is required for the growth of yeast cells on SDII media lacking leucin (-LEU) and tryptophan (-TRP). A functional Gal4, reconstituted after expression of the interacting partners, allows the growth of cells on SDIV media, lacking LEU, TRP, HIS, URA and ADE, and to express *lacZ*. Yeast transformants grown on selective media (-LEU, -TRP) were inoculated in 96-well plates containing liquid SDII medium and spotted onto solid SDII and SDIV media. If a ß-Galactosidase test was performed, a nylon membrane covering the surface of solid SDII plates was additionally spotted with the cell suspension. Plates were incubated for 3 - 7 days.

Autoactivation test

Constructs under examination were tested for autoactivation of marker genes in absence of an interacting partner. Autoactivation was inhibited by adding 3-Amino-1,2,4-triazole (3-AT), a competitive inhibitor of the *HIS3* gene product imidazoleglycerol-phosphat dehydratase, to the media. Since the Gal4-mediated expression of *HIS3* is dependent on the relative strength of an interaction, yeast cells transformed with constructs expressing the interacting partner resist to 3-AT treatment accordingly. The final concentration of 3-AT (range 0.25 - 15 mM) varied based on the specific construct tested.

ß-Galactosidase test

For the ß-Galactosidase test, 2 Whatman papers (Whatman AG) were pre-incubated with 10 ml of Z-buffer (10.7 g/l Na_2HPO_4*2 H_2O, 5.5 g/l NaH_2PO_4*1 H_2O, 0.75 g/l KCL, 0.246 g/l $MgSO_4$*7 H2O, pH 7) mixed with 156 µl of 2 % X-Gal (5-bromo-4-chloro-3-indolyl-D-glycoside in N,N-dimethylformamide, Sigma) and 100 µl of 1 M DTT. Residual buffer was removed and the nylon membrane carrying yeast colonies were frozen in liquid nitrogen for 30 sec to brake the yeast cell wall. Finally, the nylon membrane was placed on Whatman papers and incubated for 4 - 6 h at 37 °C.

Liquid ß-Galactosidase test

pBTM-*ORF* constructs (Table 2-3) under examination were transformed into L40ccua strain and single colonies were used to inoculate 5 ml cultures over night. Afterwards, 50 ml of SDII were inocculated with the over night culture to adjust an OD_{600} ~ 0.3. The culture was incubated at 30 °C until exponential growth. Then, cells

were centrifuged at 4000 g for 3 min and residual medium was discarded. Cell pellets were resuspended in 100 µl of 1 × PBS supplemented with protease inhibitor (1 tablet of protease inhibitor per 25 ml 1 × PBS) and transferred to a new tube containing 150 mg of glass beads (Glass beads, acid-washed, 425-600 µm in diameter, Sigma Aldrich). Tubes were then placed in a micro tube vortexer (Vortex Genie 2, Bender & Hobein AG, Swizerland) 3 times for 90 sec with an interval of 60 sec incubation on ice. Samples were centrifuged at 10000 g for 4 min (Centrifuge 5424, Eppendorf, Germany) and placed on ice. The fraction containing the soluble proteins was transferred to a new micro tube and the protein concentrations were determined as previously described. Then, equal amount of proteins were diluted in a total volume of 500 µl of Z buffer mixed with 2% X-Gal and 1M DTT. Finally, samples were incubated for at least 4 h at 37 °C depending on the saturation of the reaction, and the colorimetric assay was performed. Expression of ß-Galactosidase was measured at an OD_{420} in a photometer (6700 Vis. Spectrophotometer, Jenway) relative to a control without proteins.

2.2.16 Yeast viability test

Growth of yeast cells can be influenced due to an ectopic expression of proteins involved in essential cellular pathways. In order to address recovery or reduced cell viability of genes, viability tests were performed.

Strains were inoculated in 5 ml of appropriate selection media and incubated over night at 30 °C. On the following day, cultures were inoculated at an OD_{600} ~ 0.2 and incubated at 30 °C until exponential growth (OD_{600} ~ 0.5 - 0.7). An amount of cell suspension corresponding to an OD ~ 0.3 was then transferred to a fresh micro tube. Then, 200 µl of the sample were transferred in a 96 well plate and serial dilutions performed by adding 50 µl of cell suspension to 200 µl of sterile water. This procedure corresponds to dilution steps of 1:5, 1:25, 1:125, 1:625 and 1:3125. 5 µl of cell suspension for each well were spotted on solid selection media. Finally, plates were incubated 2 - 7 days at 30 °C.

2.2.17 Bimolecular fluorescence complementation (BiFC) assay

The method is employed for investigating protein-protein interactions and it is based on the reconstitution of a fluorescent protein due to association of two putative interacting partners [232]. The genes under examination were fused to N- and C-terminal fragments of the Venus fluorescence reporter, a variant of YFP (Yellow Fluorescent Protein). The one-step PCR technique was used to tag genes in C-terminal, allowing for their expression from native promoters.

The *ORF*s of interest (Table 2-2) were fused to the *ORF*s of Venus-N-terminal or Venus-C-terminal. Therefore, respective integration cassettes were amplified using specific primers (reported in Table 2-5) and plasmids pFA6a-VN-His3MX6 or pFA6a-VN-KanMX6 and pFA6a-VC-His3MX6 or pFA6a-VC-KanMX6 as templates. Amplified integration cassettes (*ORF1*-VN-His3MX6 and *ORF2*-VC-KanMX6) were then transformed into yeast BY4741 (*MAT*a). Clones grown on selective media were verified by PCR.

Since diploid cells are not sensitive to mating pheromones, the BiFC method was performed in haploid cells. Therefore, haploid cells carrying integrated C-terminal Venus-tagged fusion protein was transformed with plasmid p426GPD encoding N-terminal tagged fusion protein of interest (see Table 2-3 for details). Clones were selected by plating on appropriate medium and the presence of a Venus-dependent BiFC signal was analyzed by microscopy.

2.2.18 Synchronization and stress-dependent arrest of yeast cells

In order to measure transcript and protein levels or to determine the relative strength of a protein-protein or protein-DNA interaction in time, cultured yeast cells were synchronized in their growth.

For synchronization of yeast *Mat*a cells in G1 phase, a small signaling peptide called α-factor (H-Trp-His-Trp-Leu-Lys-Pro-Gly-Gln-Pro-Met-Tyr-OH, purity 93 % Universitat Pompeu Fabra, Barcelona, Spain) was added to the media at a final concentration of 15 µg/ml. An increased efficiency in synchronization was achieved by using 1 × YPD or 1 × CSM media at pH 3.9, due to the fact that inhibition of α-

factor degradation by Bar1 protease occurs at low pH. Then, the culture was incubated at 30 °C for 2.5 h. To follow the synchronized cell growth in time, G1-arrested cells were released in a fresh medium. Yeast clones were inoculated in 50 ml of appropriate medium and incubated to reach an OD_{600} ~ 0.6. Cell arrest was performed by addition of α-factor and the culture centrifuged at 2000 g for 3 min. Cells were washed 2 times by resuspension in 50 ml of 1 × PBS and centrifugation at 2000 g for 3 min. Cell pellets were then resuspended in 50 ml of fresh 1 × CSM medium and incubated at 30 °C for 2 h. Samples were transferred to a new micro tube in 10 min time intervals and stored on ice for further analysis or fixed by adding 95% Ethanol for long term storage at 4 °C. Samples were centrifuged at 2000 g for 3 min and cell pellets resuspended in 300 µl of sterile water and 700 µl of 95 % ethanol.

Synchronization in S phase was realized using ribonucleotide reductase inhibitor Hydroxyurea (Sigma-Aldrich). Treatment of cells with Hydroxyurea causes deoxyribo-nucleotide depletion, resulting in inhibition of DNA replication and activation of the S-phase checkpoint. Hydroxyurea was added to the media to a final concentration of 75 mM and cultures incubated at 30 °C for 2 h. Then, the culture was centrifuged at 2000 g for 3 min and cell pellet resuspended in 300 µl of sterile water and 700 µl of 95 % ethanol for further analysis.

Synchronization in M phase was realized using Nocodazole (AppliChem). This chemical interferes with polymerization of microtubles, delaying their attachment to kinetochores and activating spindle assembly checkpoint in metaphase. Nocodazole was added to the media to a final concentration of 5 µg/ml and cultures incubated at 30 °C for 2 h. Then, the culture was centrifuged at 2000 g for 3 min and cell pellet resuspended in 300 µl of sterile water and 700 µl of 95 % ethanol for further analysis.

Arrest of yeast cells by oxidative stress was induced adding Hydrogen peroxide (30% H_2O_2 solution, Sigma-Aldrich) to a final concentration of 2 mM, Menadione (2-Methylnaphthalene-1,4-dione, $C_{11}H_8O_2$, stock solution: 50 mM in DMSO, Sigma-Aldrich) to a final concentartion of 40 µM or Arsenite (Natrium-meta-Arsenit, $NaAsO_2$, stock solution: 200 mM in H_2O, Merck) to a final concentration of 2 mM.

2.2.19 Chromatin immunoprecipitation (ChIP) assay

Each yeast strain was inoculated in 20 ml of appropriate media and incubated at 30°C over night. Then, 250 ml of fresh selection medium was inoculated with the over night culture to adjust an OD_{600} ~ 0.2 - 0.3. Cells were then cross-linked at an OD_{600} ~ 0.6 - 0.8 with 33.2 % Formaldehyd (37 % solution in water with 10 - 15% Methanol, Acros Organics) in NaCl 100 mM and 1 × PBS.

For cells harvested in saturated growth, 50 ml of culture were inoculated at an OD_{600} ~ 0.5 and grown to saturation (OD ~ 1.2 - 1.5). Cultures were cross-linked with 14.4 % formaldehyde (16% solution in methanol-free water, Ultra Pure EM Grade, Polysciences Inc.) in 1 × PBS containing 100 mM NaCl. Cells were cross-linked by incubation for 20 min at room temperature. Then, the reaction was stopped by adding 50 mM glycine (stock: 2.5 M in 1 × PBS, Sigma Aldrich). The culture was then centrifuged in a Beckman Coulter (Avanti J25, rotor JLA - 16.250, USA) and washed twice with 50 ml of 1 × PBS. The cell pelett was frozen and stored at -80°C.

To perform the ChIP assay, the cell pellet was resuspended in 800 µl of pre-cooled lysis buffer (50 mM HEPES/KOH, pH 7.5, 500 mM NaCl, 1 mM EDTA, 1 % Triton X-100, 0.1% DOC, 0.1 % SDS, 1 tablet protease inhibitor cocktail per 25 ml buffer (Complete protease inhibitor cocktail, Roche Diagnostics GmbH)) and 500 mg of glass beads (acid-washed, 425-600 µm in diameter, Sigma-Aldrich). The sample was vortexed (Vortex Genie 2, Bender & Hobein AG) 3 times for 90 sec on ice. Then, the sample was centrifuged (Centrifuge 5424, Eppendorf) at 10000 g for 4 min and placed on ice. Afterwards, the supernatant containing the soluble protein-DNA fraction was sonicated continuously for 10 sec (Branson Sonifier W250). The sample was then incubated on ice for 2 min and the procedure was repeated two more times.

For the immunoprecipitation, the lysate was centrifuged again at 10000 g for 2 min and transferred to a new micro tubes containing 50 µl of pre-cooled Protein A/G agarose mix in 1 × PBS (50% mix of Protein A/G agarose, immobilzed protein, Roche). Subsequently, the sample was incubated under rotation at 4°C for 2 h and centrifuged at 5000 g for 2 min. The supernatant was transferred to a new tube and 50 µl of the lysate were removed (input sample). The remaining amount was mixed with 5 µg of the appropriate antibody (see Table 2-7 for details) and incubated at 4

°C for 4 h. To immobilize the immune complex, 50 µl of Protein A/G agarose beads were added to the lysate and incubated at 4°C for 4 h. The beads were washed twice with 1 ml of pre-cooled lysis buffer and centrifugation at 100 g for 1 min. Then, the sample was washed again with 1 ml of DOC buffer (10 mM Tris-Cl, pH 8, 250 mM LiCl, 0.5 % NP-40, 0.5 % DOC, 1 mM EDTA, pH 8) and 1 ml of 1 × TE (Tris-Cl 10 mM, EDTA 1 mM, pH 8). Finally, washed beads were resuspended in 200 µl of 1 × TE and centrifuged at 100 g for 1 min. The residual buffer was removed with a filter tip (Greiner bio-one, filter tip Gel 20) and immunoprecipitated complexes eluted by adding 100 µl of TES buffer (Tris-Cl 50 mM, EDTA 10 mM, 1 % SDS pH 8). The sample was then incubated in a thermomixer (Thermomixer komfort, Eppendorf) at 65°C for 15 min. Beads were centrifuged at 10000 g for 1 min and the supernatant transferred to a new micro tube. Again, 100 µl of TES buffer was added to the beads and elution step was repeated resulting in 200 µl of eluted ChIP sample. In parallel, the input sample was mixed with 150 µl of TES buffer and both Input and ChIP samples were incubated over night (10 -14 h) at 65°C to reverse the cross-link by formaldehyde. Afterwards, samples were centrifuged at 12000 g for 30 sec and mixed with 200 µl of 1 × TE. RNase digestion was performed by adding 0.2 µg/ml RNase A (stock: 10 mg/ml in nuclease-free water, Sigma-Aldrich, Germany) and incubation at 37 °C for 2 h. Then, proteins of Input and ChIP samples were digested by adding 0.2 µg/ml Proteinase K (stock: 20 mg/ml in sterile water, Sigma-Aldrich, Germany) and incubation at 55°C for 2 h.

To extract the DNA, 400 µl of phenol:chloroform:isoamyl alcohol (25:24:1, Sigma-Aldrich, Germany) were added to the samples followed by centrifugation at 16000 g for 5 min. The upper aqueous layer was transferred to a new tube containing 16 µl of 5 M NaCl and 1 µl of LPA (Linear PolyAcrylamide, GenElute-LPA, stock: 25 mg/ml, Sigma-Aldrich, Germany). 1 ml of 100 % ethanol was added to the samples, which were then incubated at -20°C for 1 h and centrifuged at 20000 g for 30 min at 4°C. The supernatant fractions were removed and the DNA pellets washed with 500 µl of pre-cooled 80 % ethanol. After centrifugation at 20000 g for 15 min at 4°C, the supernatant fractions were removed and the pellet dried at room temperature for 15 min. Finally, pellets were resuspended in 20 µl of nuclease-free water (Ambion, USA) and stored for further analysis at -20°C.

Potential transcription factor binding sites for Fkh1 and Fkh2 at promoters of cyclin genes *CLB1-4* were localized by using the YEASTRACT database (http://www.yeastract.com/) (Figure 2-1). Oligonucleotides that have been used for the amplification of respective DNA fragments are indicated in Figure 2-1 (red lines) and listed in Table 2-6. In addition to the Forkhead transcription factors Fkh1 and Fkh2, the consensus binding site of Mcm1 is presented in Figure 2-1 [234].

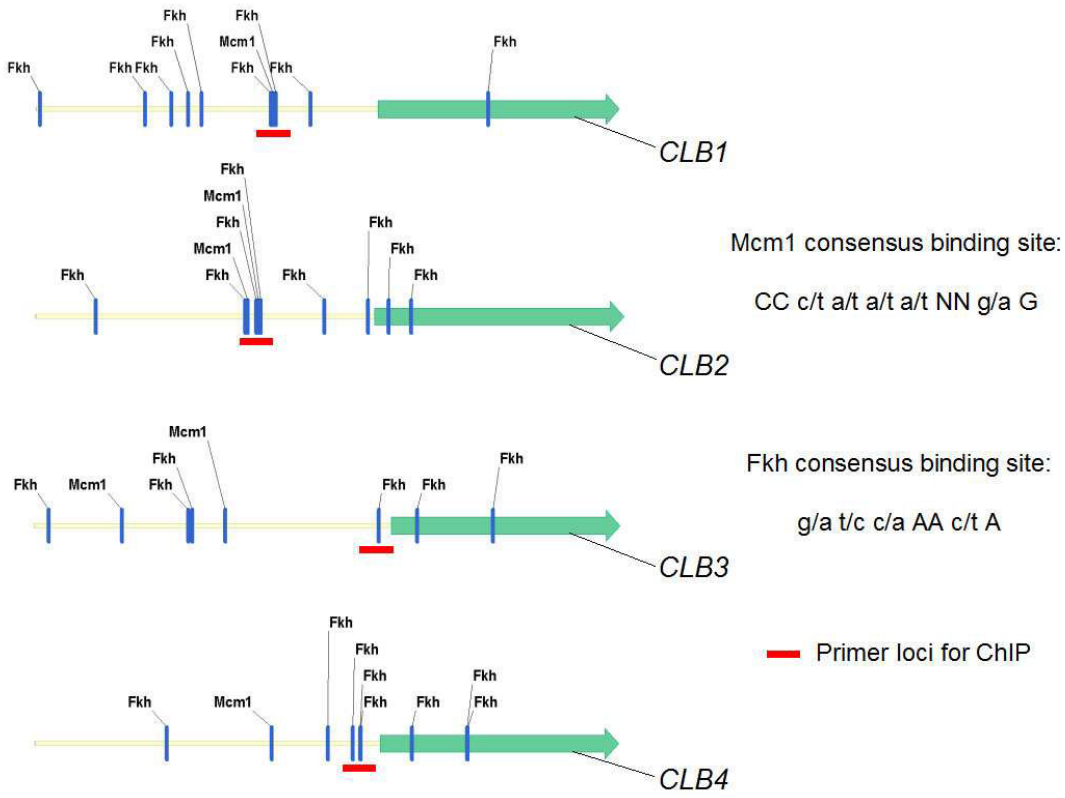

Figure 2-1. Binding sites of Forkhead proteins Fkh1 and Fkh2. Localization of consensus sites in the cyclin gene ORFs (indicated by the cyan colored arrows) and the promoter regions 2000 bp upstream of the gene (5' UTR, orange lines) were performed using the YEASTRACT database (http://www.yeastract.com/). The target loci for the binding of respective oligonucleotides are indicated by a red line.

2.2.20 Recombinant protein expression and protein solubility determination in *E. coli*

Yeast *ORF*s were cloned into the pGEX6p2 expression plasmid, generating N-terminal-tagged Glutathione S-transferase (GST) fusion proteins. The GST tag is under control of the *lac* promoter, and expression of recombinant proteins occurs after addition of isopropylbeta-D-thiogalactopyranoside (IPTG) to the media. *E. coli* cells derived from XL1-Blue or BL21(DE3) strains were used (genotypes are reported in Table 2-1).

A single bacterial colony transformed with a respective pGEX6p2-*ORF* construct was inoculated in 10 ml of LB medium and incubated over night at 37 °C. Afterwards, 0.5 ml of the over night culture were centrifuged at 10000 g for 3 min and resuspended in 10 µl of SDS sample buffer (94 mM Tris-Cl pH 6.8, 30 % glycerol, 3 % SDS, 0.02 % bromphenol blue, 100 mM DTT) (referred to as non-induced sample, IN). Then, 2.5 ml of the over night culture were inoculated in 50 ml LB medium and the culture was incubated until an OD_{600} ~ 0.5. Protein expression was induced by addition of Isopropyl-β-D-thiogalactopyranosid (IPTG, Fermentas, EU) (final concentration of 1 mM). The culture was incubated for additional 3 h at 37 °C and then centrifuged at 4000 g for 5 min. 1 ml of the culture was then centrifuged at 10000 g for 3 min and pellet resuspended in 10 µl of 5 × SDS sample buffer (referred to as induced sample, IN). The remaining culture was centrifuged at 4000 g for 10 min and mixed with 2 ml of resuspension buffer (20 mM Tris-Cl, pH 7.5) supplemented with protease inhibitor (Complete Proteinase Inhibitor-Cocktail Tablets, Roche, Germany). *E. coli* cells wall was disrupted through addition of lysozyme (Fermentas, EU) (final concentration of 100 µg/ml) and the lysate incubated for 15 min on ice. Then, the lysate was sonicated for 6 times for 10 sec (Branson Sonifier W250, USA). Centrifugation at 10000 g for 2 min separated the supernatant, or soluble cytoplasmatic fraction (SCF), from the pellet, or insoluble cytoplasmatic fraction (ICF). Then, 50 µl of SCF was mixed with 6 µl of protein sample buffer and the residual lysate discarded. ICF was instead resuspended in 50 µl of 1% SDS and mixed with 6 µl of protein sample buffer. Protein samples were stored at -20 °C or directly used for SDS-PAGE.

2.2.21 Protein quantification

Protein concentration was determined by using the Bradford method, which is based on a shift in the absorbance of an acidic solution of Coomassie Brilliant Blue G-250 from 465 nm to 595 nm in the presence of proteins.

A standard curve was designed using variable amounts of bovine serum albumin (BSA), and 1 mg/ml BSA solution was diluted 1:10, 1:20, 1:50, 1:100, 1:200 and 1:500. 5 µl of these dilutions were added to 800 µl of distilled water and transferred into plastic cuvettes (Sarstedt, Germany) containing 200 µl of staining dye (BioRad,

UK). The absorbance at 595 nm relative to a control without proteins was measured (Jenway 6700 Vis. Spectral photometer, UK).

2.2.22 GST pull-down assay

E. coli XL1blue or BL21 strains carrying the pGEX2T-6p2 plasmid were inoculated in 10 ml LB selection media and incubated over night at 37 °C. Then, 5-10 ml from this over night culture were transferred to 50 - 200 ml of fresh LB selection media to adjust an OD ~ 0.2. Afterwards, the culture was incubated until an OD ~ 0.5 - 0.7, supplemented with 100 mM isopropylbeta-D-thiogalactopyranoside (IPTG, Fermentas, final concentration of 1 mM) and additionally incubated for 3 h at 37 °C. Cells were then centrifuged at 4000 g for 7 min and pellets dissolved in 2 ml GST-binding buffer (20 mM TrisHCl pH 7.9, 125 mM NaCl, 5 mM $MgCl_2$, 0.5 mM DTT) and incubated for 30 min with 10 mg/ml of lysozyme (Sigma, Germany). Then, the cell suspension was mixed with Glycerol (10 % final concentration) and NP-40 (0.1 % final concentration), sonicated 6 times for 10 sec at 300 W and centrifuged at 10000 g for 25 min. The supernatant containing the expressed GST-tagged fusion proteins was transferred to a new tube and incubated with 100 µl of a 1:1 mix of 1 × PBS (137 mM NaCl, 2.7 mM KCl, 10 mM Na_2HPO_4, pH 7.4) and Glutathione Sepharose 4B beads (GE Healthcare) for 8 h at 4 °C. Then, the beads were washed twice by adding 1 ml of 1 × PBS and centrifugation at 500 g for 30 sec.

In parallel, yeast protein lysates were prepared: 4 ml of an appropriate yeast over night culture was inoculated in 200 ml of 1 × YPD medium and incubated at 30 °C to reach an OD_{600} ~ 0.6 - 0.8. Cells were centrifuged at 3000 g for 3 min and pellets washed with 1 × PBS. The suspension was centrifuged again and the cell pellet was dissolved in 2 ml of pre-cooled 1 × PBS. Lysis was performed through incubation in liquid nitrogen for few seconds. Subsequently, glass beads (acid washed, Sigma-Aldrich, Germany) were added to the protein lysate. The sample was vortexed 3 times for 2 min and centrifuged at 10000 g for 2 min. The superternant conatining the soluble protein fraction was further used for the binding analysis with GST-tagged proteins.

Therefore, 1 ml of yeast protein lysate (5 µg/µl of total proteins) were added to the washed beads complexed with Gluthatione Sepharose beads-coupled GST fusion

proteins. The sample was then incubated over night at 4 °C. Then, the sample was washed 2 times with 2 ml of pre-cooled GST-binding buffer and the bounded proteins eluted with SDS sample buffer and loaded on SDS gel. Precipitated proteins, blotted on nitrocellulose Protran membrane (PerkinElmer, USA), were detected with epitope-specific antibodies.

2.2.23 Denaturing polyacrylamide gel electrophoresis (SDS-PAGE)

Separation of proteins was performed in a Mini Protean III electrophoresis cell (BioRad). Protein samples were mixed with 5 × SDS page sample buffer (Tris-Cl 94 mM pH 6.8, 30 % glycerol, 3 % SDS, 0.02 % bromphenol blue, 100 mM DTT). The detergent SDS applies a negative charge to each protein in proportion to their mass and denatures secondary and tertiary structures, whereas DTT reduces disulfide bonds. Additional denaturation of proteins was achieved by heating the samples at 95 °C for 5 min.

SDS gels were prepared with separation buffer (375 mM Tris-Cl pH 8.8, 7.5 - 15 % acrylamide/bisacrylamide (Rotiophorese Gel 30, Roth, Germany), 0.05 % tetra-methylethylendiamine (Temed, Invitrogen, USA), 0.05 % ammonium persulfate (APS, Sigma Aldrich, Germany)). After polymerization, stacking gels (Tris-Cl 125 mM pH 6.8, 5 % acrylamide/bisacrylamide, 0.1 % APS, 0.2 % Temed) were prepared. Then, the gel was plased in an electrophoresis cell that was filled with running buffer (Tris-Cl 250 mM pH 8.3, glycine 250 mM, 1 % SDS). Protein samples were loaded onto gel. As protein marker, PageRuler Plus (Prestained Protein Ladder, Thermo Scientific, USA) was used. Protein separation was performed by applying a power of 50 mA for 90 min.

2.2.24 Coomassie staining of polyacrylamide gels

After electrophoresis, polyacrylamide gels were incubated for at least 2 h in a 20 ml staining solution (40 % Methanol, 7 % Acetic acid, 0.1 % Coomassie Brilliant Blue R250). Gels were then transferred in 15 ml of destaining solution (40 % Methanol, 10 % acetic acid) and incubated for 15 min at room temperature. New destaining solution was added until protein bands were clearly distinguishable from the background of the gels.

2.2.25 Western blotting

Separated proteins were transferred onto nitrocellulose membranes (Protran Nitrocellulose Transfer Membrane, Whatman AG) according to their SDS-dependent negative charge. The transfer was performed by a Mini Trans-blot electrophoretic cell (BioRad) provided with a Semi-Dry-Blot system. 3 Whatman papers pre-incubated with Transfer buffer (Tris-Base 25 mM, Glycin 192 mM, 20 % Methanol) were then placed on the positively charged side of the device, followed by the nitrocellulose membrane, the gel and 3 additional Whatman papers pre-incubated with Transfer buffer. The protein transfer was performed with a power of 200 mA for 42 min.

After transfer, membranes were incubated in a blocking solution (3 % milk powder in 1 × PBS) for 1 h at room temperature or over night at 4°C. Then, membranes were washed with 0.05 % Tween-20 in 1 × PBS for 5 min at room temperature. The wash step was repeated twice and membranes were incubated with a primary antibody diluted in 1 % BSA (Albumin from bovine serum in 1 × PBS, Sigma-Aldrich, Germany) for 4 h at room temperature or over night at 4 °C. The dilutions of primary antibodies used in this study are listed in Table 2-7. Subsequently, membranes were washed 3 times in 1 × PBS supplemented with 0.05 % Tween-20. A secondary antibody (POD-coupled secondary antibody, diluted 1:10000 in 1 × PBS and 0.5 % milk powder) was added and membranes were incubated for 2 h at room temperature or over night at 4 °C. Finally, membranes were washed 3 times in 1 × PBS and 0.05 % Tween-20. Proteins were visualized using ECL mixture (Western Lightning-ECL, Perkin Elmer). Then, membranes were exposed with photo films (Amersham, USA) for 30 min before to be developed in a Developer solution (Curix 60, Developer G153 A/B, Fixer G354, AGFA).

2.2.26 Microscopy

Yeast cells were analyzed in 1 × PBS or sterile water by transferring 5 µl of cell suspension onto an object slide (Roth, Germany) with a cover slip (Menzel-Gläser, Germany). Analysis was performed on a Zeiss AxioImager Z1 microscope (Carl Zeiss AG, Germany) with a Plan-NeoFluar 60 × / 1.3 NA oil immersion objective. Images were recorded on a Zeiss Axiocam Mrm (Carl Zeiss AG) with 2 × 2 binning.

Fluorescence images for BiFC were taken using a standard fluorescein isothiocyanate filter set (excitation band pass filter, 450-490 nm; beam splitter, 510 nm; emission band pass filter, 515-565 nm).

The nucleus of yeast cells was stained with DAPI. Therefore, yeast cells were grown to reach the exponential phase and samples collected in 1.5 ml micro tubes. DAPI (4',6-Diamidin-2-phenylindol, Sigma-Aldrich, Germany) was added to a final concentration of 2.5 µg/ml and cells were incubated for 30 min at 30 °C. Stained cells were harvested by centrifugation at 3000 g for 3 min, washed with 1 ml of 1 × PBS and incubated at room temperature for 2 min. Cells were centrifuged at 3000 g for 3 min, resuspended in 20 µl of 1 x PBS and subsequently analyzed at the microscope.

2.2.27 FACS analysis

Flow cytometry was used to measure the DNA content of various strains stained with the fluorescent dye propidium iodide (Invitrogen, USA) and as well for detecting other fluorescent markers expressed in yeast cells.

Analyses were performed with a flow cytometer FACSCalibur (Becton Dickinson Immunocytometry Systems, USA) that illuminates cells with an argon-ion laser. Scattered light and fluorescence signals are created simultaneously, and cell size and composition influences light reflection and absorption that are detected. Collected light is spectrally splitted, directed into a series of optical filters, converted to electronic signals and translated in digital values.

Approximately 10^7 cells were centrifuged at 3000 g for 3 min. Cell pellets were resuspended in 300 µl of sterile water and fixed with 700 µl of 95 % ethanol. Cell suspension was mixed by short vortexing and incubation over night at 4 °C. Cells were centrifuged at 10000 g for 1 min and the supernatant discarded. Cell pellets were resuspended in 1 ml of 50 mM citrate buffer (stock solution: 1 M sodium citrat, pH 7.4 adjusted with citric acid) and sonicated 10 times for 1 sec with intervals of 1 sec at 30 % output. Again, samples were centrifuged again at 10000 g for 1 min and the supernatant discarded. Cell pellets were resuspended in 1 ml of citrate buffer supplemented with 0.25 mg RNase A and incubated at 37 °C for 2 h. 25 µl of proteinase K (stock: 20 mg/ml) were added and samples additionally incubated for 2

h at 50 °C. Cell suspension was centrifuged, the supernatant discarded and pellets resuspended in 1 ml of 50 mM citrate buffer supplemented with 16 µg propidium iodide (Invitrogen). Samples were incubated in the dark for 30 min at room temperature and subsequently measured by FACS or stored at 4 °C. FACS measurements were performed with the CELLQuest software (BDIS) designed specifically for BDIS flow cytometers.

3. Results

3.1 Regulation of B-type cyclins

One of the main aims of this thesis was to address the role of the Cdc28-Clb stoichiometric inhibitor Sic1 and the transcription factors Fkh1 and Fkh2 in triggering the oscillatory behavior of the B-type cyclins Clb1-6. The rationale for this is based on a mathematical model, which predicted a role for Sic1 and both Fkh transcription factors in the regulation of mitotic Clb cyclins (Figure 3-1). In particular, it was proposed that Cdc28-Clb5, 6 complexes ideally activate *CLB3, 4* transcription by phosphorylation of a yet unknown transcription factor. Cdc28-Clb5 is known to phosphorylate Fkh2 for activating *CLB2* cluster genes, which in turn contribute to Fkh2 activation generating a positive feedback [21-23]. However, a potential role for Cdc28-Clb3, 4 in activating the Fkh2 transcription factor has also been predicted and activation of the coactivator Ndd1 was suggested [19, 22, 78, 235].

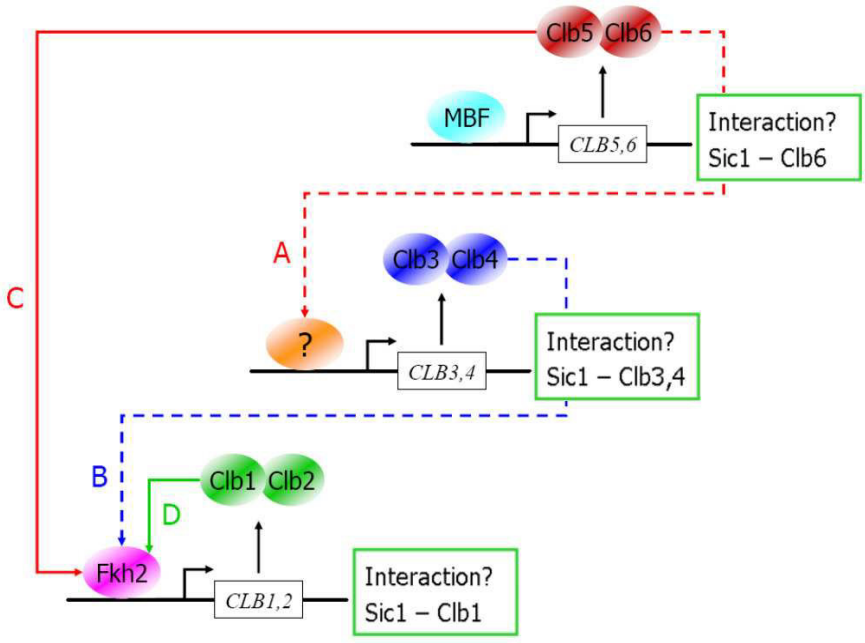

Figure 3-1. Regulation of B-type cyclin activities. The heterodimeric transcription factor MBF (Mbp1, Swi6) activates *CLB5, 6* transcription. Clb5, 6-dependent kinase activity promotes *CLB3, 4* transcription by phosphorylation of an unknown transcription factor (A). Afterwards, Clb3,4-dependent kinase activity promotes *CLB1, 2* transcription (B) with the help of Clb5, 6-dependent kinase activity, possibly phosphorylating Fkh2 (C). After production of Clb1, 2, Cdc28-dependent kinase activity promotes *CLB1, 2* transcription by phosphorylation of Fkh2, thus stimulating its own production (D). For simplicity, Cdc28 subunit has been omitted [236].

Since experimental validation of these predictions was missing, it was first aimed to perform protein-protein interaction studies between the key regulators in this model.

3.1.2 Binding studies between Sic1 and B-type cyclins

High throughput genome-wide screenings revealed a potential association of Sic1, the stoichiometric inhibitor of Cdc28-Clb activity, with Clb3 and Clb5 [237-241], and further analysis established the interaction with Clb2 and Clb5. However, interactions of Sic1 with Clb1, Clb3, Clb4 and Clb6 have been considered in the model (Figure 3-1), but lack a precise experimental validation. In order to verify this prediction, yeast-two-hybrid (Y2H) experiments were performed to analyze protein-protein interactions (PPI's) between Sic1 and B-type cyclins Clb1-6. To this purpose, the *SIC1* gene was cloned into the Y2H bait plasmid pBTM117c and *CLB1-6* genes were cloned into the Y2H prey vector pACT41b. Then, the Y2H strain L40ccua was transformed with the plasmid pBTM117c-Sic1 encoding the fusion protein LexA-Sic1 and prey vectors pACT41b-Clb1-6 encoding the respective fusion proteins AD-Clb1-6. Cotransformation of empty Y2H plasmids alone or in combination with all used bait and prey constructs was used as control in the analysis. The known interactions between Sic1 and Clb2 or Clb5 as well as the association between the C-terminal fragment 4 (F4) of ataxin-2 and the poly(A)-binding protein 1 (PABPC1) have been used as positive controls [227]. After transformation, cells were selected and four independent clones spotted onto SDII medium and for analysis of the reporter gene activity to SDIV selective medium or on a membrane for detection of β-galactosidase activity.

As shown in Figure 3-2A, yeast cells expressing the fusion protein LexA-Sic1 alone showed a weak blue color shift on the membrane, indicating moderate ß-Galactosidase activity. However, no growth was monitored on SDIV medium, demonstrating that the fusion protein LexA-Sic1 is still suitable for this approach. Compared to the controls, yeast cells expressing LexA-Sic1 and AD-Clb1-6 were able to grow on SDIV medium and showed a significant blue color shift, indicating an interaction between these proteins. Moreover, cells expressing LexA-Sic1 and AD-Clb2 showed weak growth compared to cells expressing LexA-Sic1 and AD-Clb1, 3, 4, 5 and 6 suggesting that the relative strength of this interaction might be lower.

In a second step, it was aimed to confirm the association between Sic1 and the Clbs *in vitro* by using glutathione S-transferase (GST) pull-down assays. For this, a strain carrying a Myc-tagged Sic1 fusion protein was generated by transforming a specific integration cassette in the BY4741 strain (see chapter 2.2.14 for details). Next, B-type cyclins were cloned into the pGEX2T-6p2 plasmid generating N-terminal tagged GST-Clb fusion proteins.

First, recombinant *E. coli* clones were tested for protein expression, using a GST-specific antibody (Figure 3-2C) as described in chapter 2.2.20. After validation of expression, GST-tagged Clb cyclins were immobilized onto Glutathione-covered Sepharose beads and incubated with yeast lysate prepared from BY4741/Sic1-Myc. Pull-down experiments were performed in triplicates and for immunodetection of Sic1-Myc an epitope-specific antibody was used. Sepharose alone (Figure 3-2B lane 2) and GST-coupled beads (lane 3) were used as negative controls. Sic1-Myc (~ 46 kDa, lane 1) coprecipitated with all GST-Clb fusion proteins (lanes 4 and 5) but not with Sepharose beads alone (lane 2) or with GST-coupled resins (lane 3), demonstrating an interaction between Sic1 and all B-type cyclins.

A

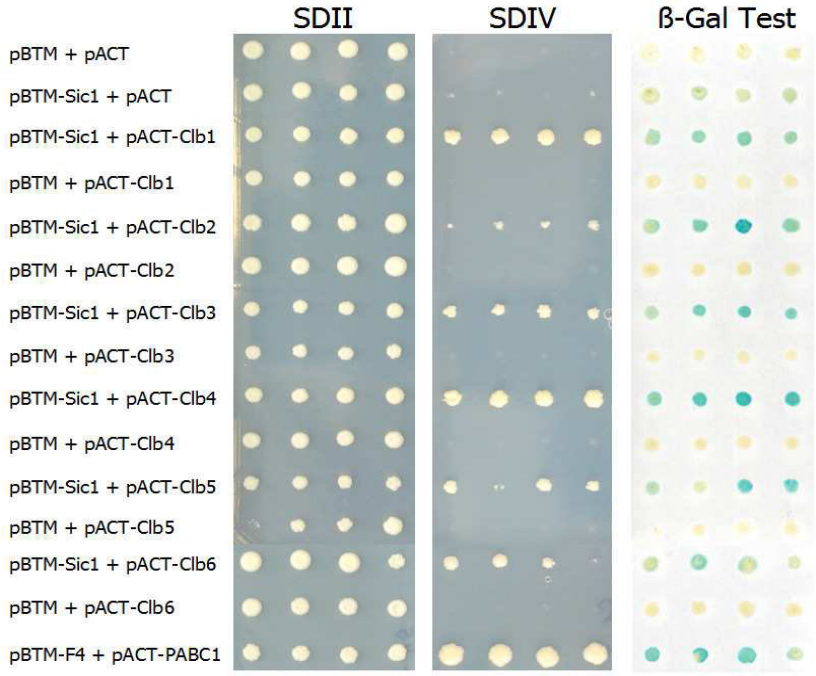

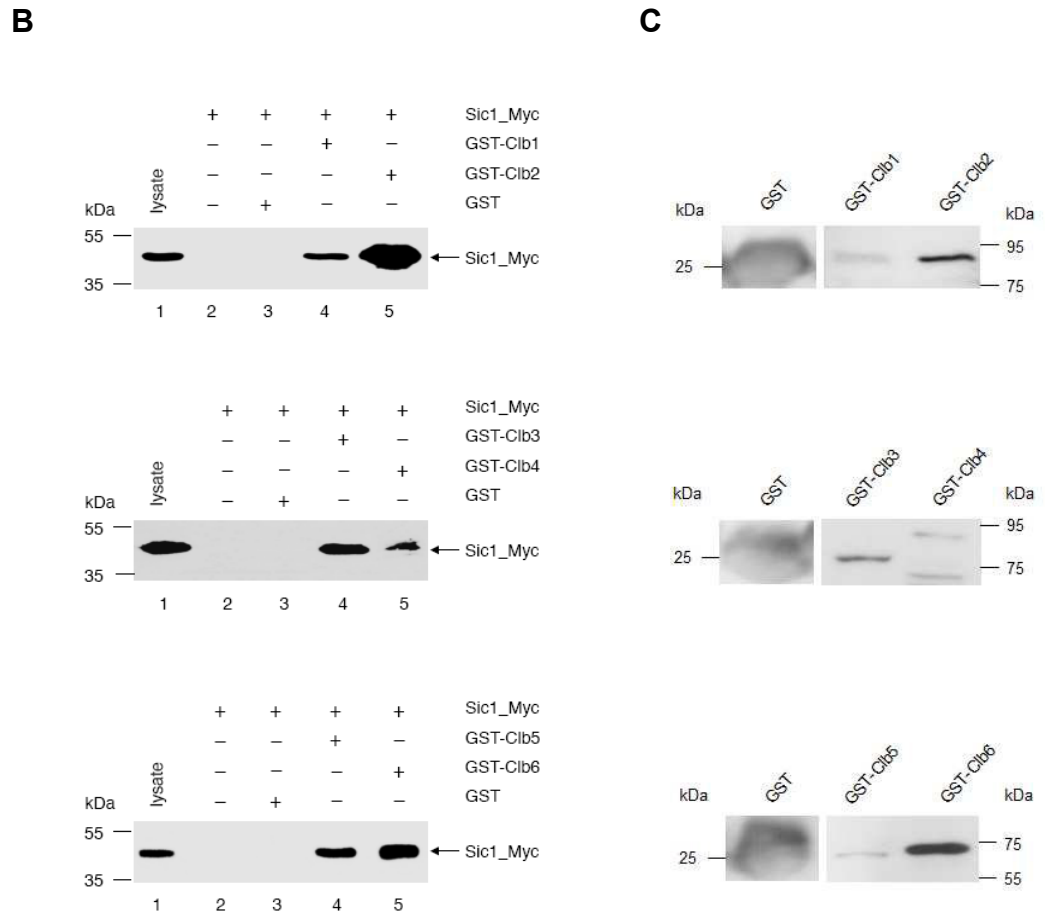

Figure 3-2. Interaction of Sic1 and B-type cyclins Clb1-6. (A) Y2H analysis: Growth of yeast colonies on SDII medium lacking leucine and tryptophane (-LEU, -TRP) indicated a successful transformation of bait pBTM117c and prey pACT41b constructs. Growth on SDIV medium lacking leucine, tryptophane, histidine, uracil and adenine (-LEU, -TRP, -HIS, -URA, -ADE) and blue color associated to the ß-Galactosidase activity indicated an interaction. Empty bait and prey plasmids in combination with corresponding constructs were used as negative controls. The interaction between the bait plasmid expressing binding domain of LexA fused to the C-terminal fragment 4 of ataxin-2 (F4) and the prey plasmid encoding poly(A)-binding protein 1 (PABPC1) fused to an activation domain (AD) was used as a positive control. **(B)** GST-pulldown: GST and GST-Clb1-6 proteins expressed in *E. coli* were immobilized on Glutathione Sepharose beads and incubated with lysate from yeast cells expressing Sic1-Myc from its endogenous promoter. Concentrated Sic1-Myc lysate were used as a loading control, whereas Sepharose beads and GST-coupled resins were used as negative controls. Precipitation of Sic1-Myc was detected with rabbit α-Myc antibody. **(C)** Western blot analysis: Bacterial expressed GST and GST-tagged cyclins used in the pulldown assays were detected using a GST-specific antibody.

Taken together, Y2H tests and GST pull-down studies showed that Sic1 interacts with all Clbs suggesting that the wave-like cyclins pattern might contribute to the binding of Sic1 to all three Clb pairs to inhibit Cdc28-Clb activity as predicted by the mathematical model.

3.1.3 Protein-protein interaction study between Clb1-6 and Fkh1 and Fkh2

In the budding yeast *Saccharomyces cerevisiae* a significant fraction of genes (~10 %) are transcribed with cell cycle periodicity. In most cases, periodic transcription is achieved by repressive and activating mechanisms. Differential expression of genes required for S/G2 and G2/M transitions of the cell cycle is driven by Cdc28-Clb-dependent phosphorylation of transcription factors Fkh1, Fkh2 and the coactivator Ndd1 [21, 22, 23].

According to the model (Figure 3-1), Cdc28-Clb5, 6 complexes potentially activate an unknown transcription factor to drive expression of *CLB3, 4* genes. Since it is known that Cdc28-Clb5 phosphorylates Fkh2 [23] and a genetic interaction of Fkh1 with Clb5 has been demonstrated [242], the involvement of Fkh1 and Fkh2 in the expression of *CLB3, 4* was further predicted. Moreover, a potential role for Cdc28-Clb3, 4 in activating the transcription factors Fkh1 and Fkh2 has been suggested as well. A mayor role for the expression of *CLB2* cluster genes, which includes *CLB1* and *CLB2*, has been reported for both Fkh1 and Fkh2 [74, 78, 83]. However, a direct association of Fkh1 and Fkh2 to all B-type cyclins have not been examined before.

3.1.3.1 Interaction studies between Fkh1 and the B-type cyclins

Next to Sic1, the specificity of all B-type cyclins to interact with Fkh1 was further analyzed using Y2H and pulldown assays. For this analysis, the respective gene ORF cloned into the bait plasmid generating a LexA-Fkh1 fusion construct. In a first assay, yeast cells were cotransformed with the bait plasmid pBTM-Fkh1 and the empty prey vector. Then, transformants were selected and spotted onto SDII and SDIV media.

This analysis revealed that cells expressing LexA-Fkh1 alone showed a relative strong autoactivation of reporter genes (Figure 3-3A). However, it was possible to reduce this autoactivation by adding 3-Amino-1,2,4-triazole (3-AT) to the SDIV medium. As a competitive inhibitor of the *HIS3* gene product, 3-AT allows additional selection for histidine auxotrophy of L40ccua cells, thereby reducing cell growth on the selection medium (see section 2.2.15 for details).

Then, the Y2H approach was analyzed for a potential interaction between Fkh1 and the B-type cyclins by transforming the plasmid pBTM-Fkh1 and the vector pACT-Clb1-6. In this analysis, cotransformation of empty Y2H plasmids alone or in combination with all used bait and prey constructs was used as a negative control and the interaction between the Ataxin-2-F4 and PABPC1 was used as positive control as described. The transformants were selected and spotted either onto SDII and SDIV media, SDIV medium supplemented with 1.2 mM 3-AT and on nylon membrane.

Yeast cells expressing LexA-Fkh1 and AD-Clb2, 3 and 5 showed a selective growth on SDIV medium supplemented with 3-AT indicating a potential association of bait and prey proteins (Figure 3-3A). However, yeast clones grown on SDII medium coexpressing LexA-Fkh1 and AD-Clb1 or AD-Clb4 showed a reduced colony size compared to other yeast clones. This observation suggests a decreased cell fitness due to the expression of the fusion proteins potentially effecting the growth on SDIV medium as well.

To further validate the observed PPI's independently and since the Y2H analysis for Clb1 and Clb2 was not conclusive, GST pull-down experiments were performed. To this aim, a Myc-tagged Fkh1 fusion protein was generated by integrating the respective DNA-cassete via homologues recombination (chapter 2.2.14). Again, GST-Clb1-6 fusion constructs were expressed in *E. coli*, immobilized on Glutathione Sepharose beads and incubated with yeast lysate prepared from strain BY4741/*FKH1-MYC9*. For immunodetection of Fkh1-Myc (~65 kDa) an epitope-specific antibody was used. As illustrated in Figure 3-3B, Fkh1-Myc protein coprecipitated with all GST-Clb fusion proteins (lanes 3-9) compared to the controls in which Sepharose beads alone (lane 2) or immobilized GST-complexed resins (lane 3) was used.

A

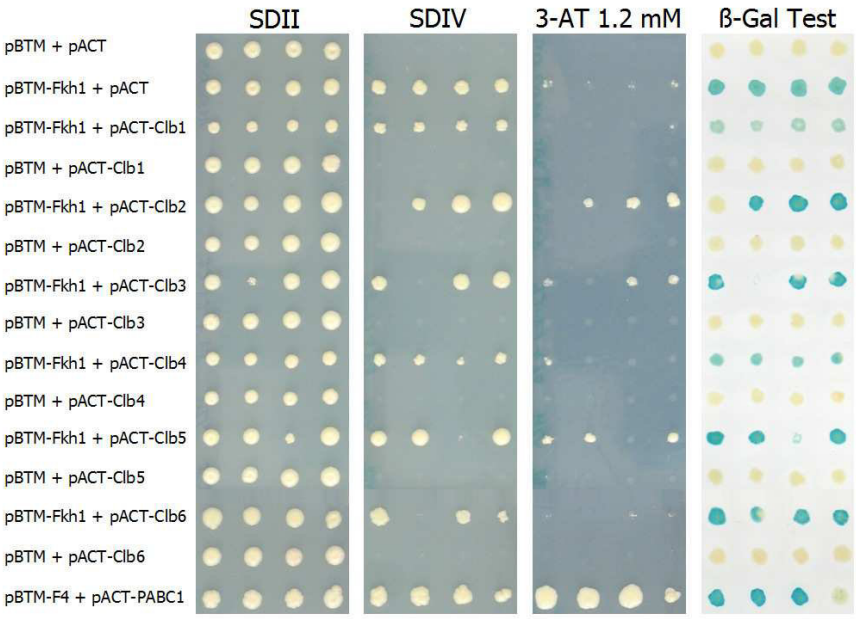

B

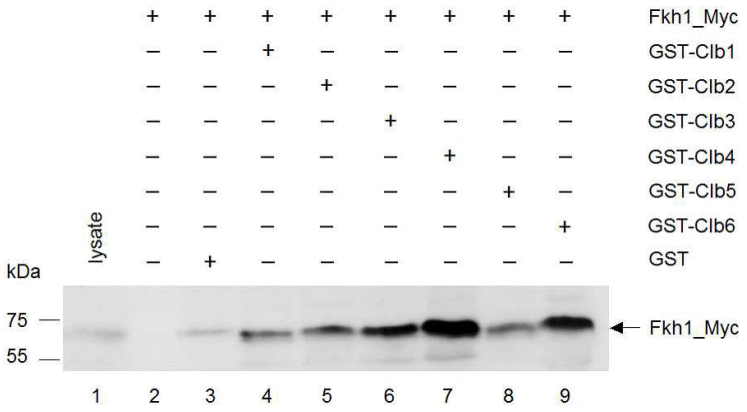

Figure 3-3. Interaction between Fkh1 and B-type cyclins Clb1-6. (A) As a control of yeast cell growth, clones were selected and spotted on SDII medium lacking leucine and tryptophane (-LEU, -TRP). Growth on SDIV medium lacking leucine, tryptophane, histidine, uracil and adenine (-LEU, -TRP, -HIS, -URA, -ADE) indicated reporter gene expression. Empty bait and prey plasmids in combination with corresponding Clb constructs were used as negative controls. The interaction between pBTM-F4 and pACT-PABPC1 was used as a positive control. 3-Amino-1,2,4-triazole (3-AT) was added to the SDIV medium to a final concentration of 1.2 mM to reduce autoactivation of reporter gene *HIS3*. **(B)** Bacterial expressed GST and GST-Clb1-6 were immobilized on Glutathione Sepharose beads and incubated with lysate from yeast cells expressing Fkh1-Myc from its endogenous promoter. Concentrated Fkh1-Myc lysate were used as a loading control, whereas Sepharose beads and GST-coupled resins were used as negative controls. Detection of Fkh1-Myc was performed by using a rabbit α-Myc antibody.

In conclusion, these results indicate that Fkh1 interacts with all B-type cyclins suggesting the forkhead protein as a potential substrate for Cdc28-Clb1-6 complex activities.

3.1.3.2 Interaction studies between Fkh2 and the B-type cyclins

In the next step, the potential association of B-type cyclins with Fkh2 was analyzed as well. Phosphorylation of Fkh2 by Cdk1-Clb5 and Cdk1-Clb2 has been demonstrated previously [23, 76], however interaction with all B-type cyclins was never shown. For this, yeast cells were first cotransformed with the pBTM-Fkh2 bait plasmid as well as empty prey vector and the selected transformants were analyzed for autoactivation of reporter genes as described.

As shown in Figure 3-4A, yeast cells expressing LexA-Fkh2 alone showed significant reporter gene activity and a concentration of 5 mM of 3-AT was necessary to strongly reduce this autoactivation. To follow the experimental design performed for LexA-Fkh1, L40ccua strain was transformed with plasmids pBTM-Fkh2 and pACT-Clb1-6 or in combination with empty plasmids as a negative control. Again, cotransformation of plasmids encoding ataxin-2-F4 and PABPC1 was used as a positive control. Selected clones were spotted either onto SDII and SDIV media, SDIV medium supplemented with 2.5 and 5 mM 3-AT as well as on nylon membrane.

As shown in Figure 3-4A, expression of LexA-Fkh2 and AD-Clb1-6 resulted in a stronger growth of yeast cells on SDIV medium treated with 3-AT compared to cells expressing LexA-Fkh1 alone. In addition, a reduced growth on SDII plate compared to other cyclin fusion proteins was observed for yeast cells coexpressing LexA-Fkh2 and AD-Clb1 and 4, as detected for LexA-Fkh1 (please see Figure 3-3A). These findings suggested that all B-type cyclins potentially bind to Fkh2, with an exception for Clb1.

As for Fkh1, the Y2H analysis was also not conclusive. To further validate the results, GST pull-down experiments were performed using GST-Clb1-6 and a Myc-tagged Fkh2 fusion protein. Recombinant expressed GST-tagged cyclins bound to

Glutathione Sepharose beads were incubated with yeast lysate obtained from strain BY4741/Fkh2-Myc and immunodetection was performed using an epitope-specific antibody.

As shown in Figure Figure 3-4B, Fkh2-Myc (~ 110 kDa) coprecipitated with all GST-Clb1-6 fusion proteins (lanes 4-9). No signal was detected using Sepharose beads alone (lane 2) or immobilized GST (lane 3) as negative controls.

In sum, Y2H and pulldown assays indicated an association between all B-type cyclins and Fkh2.

A

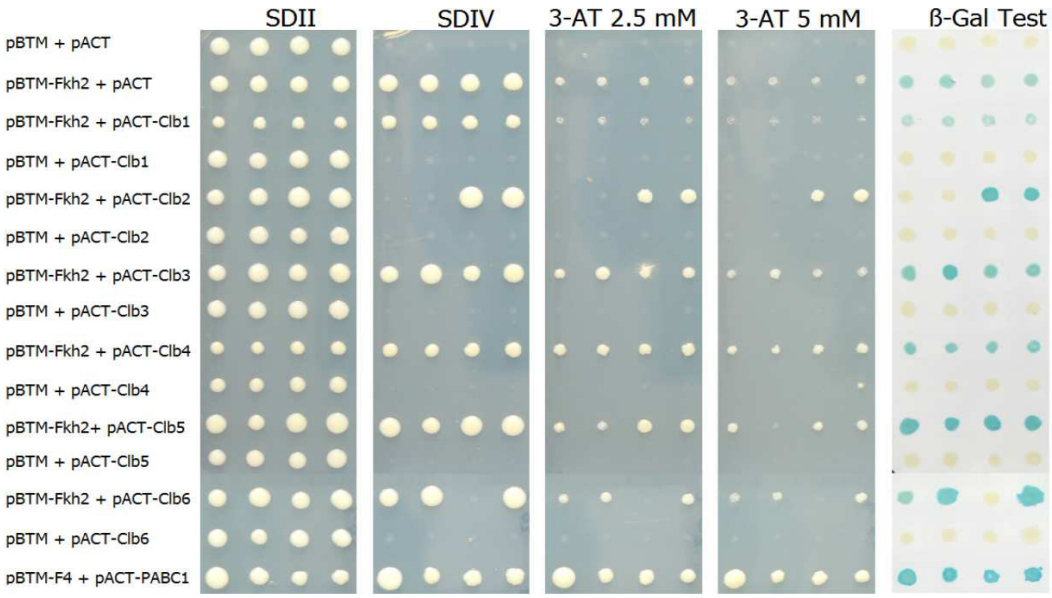

B

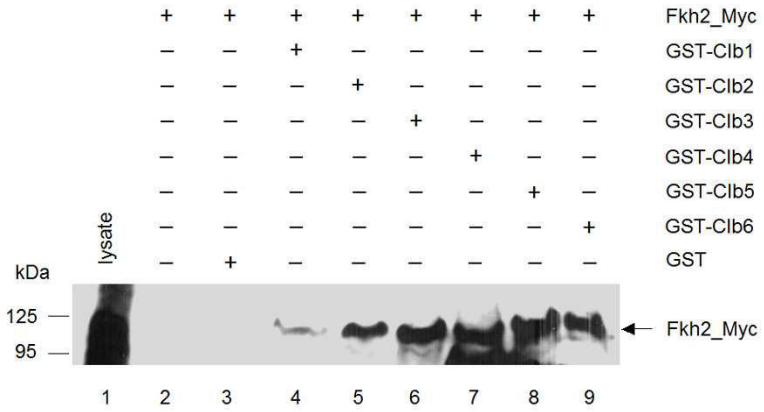

Figure 3-4. Interaction studies between Fkh2 and B-type cyclins Clb1-6. (A) Selection of yeast colonies on SDII medium lacking leucine and tryptophane (-LEU, -TRP) indicated cell viability after transformation. Growth on SDIV medium lacking leucine, tryptophane, histidine, uracil and adenine (-LEU, -TRP, -HIS, -URA, -ADE) corresponds to reporter gene activity and blue color shift indicates ß-Galactosidase expression. Empty bait (pBTM) and prey (pACT) plasmids cotransformed in combination with remaining constructs were used as negative controls. The known interaction between pBTM-F4 and pACT-PABPC1 served as a positive control. 3-Amino-1,2,4-triazole (3-AT) was added to the SDIV medium to a final concentration of 2.5 or 5 mM to reduce autoactivity of reporter genes induced by LexA-Fkh2 expression. **(B)** Recombinant expressed proteins GST and GST-Clb1-6 were immobilized on Glutathione Sepharose beads and incubated with protein lysate from yeast cells expressing Myc-tagged Fkh2 from its native promoter. Concentrated Fkh2-Myc lysate were used as a loading control (lane 1), whereas Sepharose beads (lane 2) and GST-coupled resins (lane 3) were used as negative controls. Precipitation of Fkh2-Myc was detected with a rabbit α-Myc antibody.

3.1.3.3 Binding study using truncated Forkhead proteins

Y2H assays using the full length fusion proteins LexA-Fkh1 and LexA-Fkh2 were complicated due to the autoactivity of the full-length fusion proteins. In this context, binding studies using truncated versions of Fkh2 revealed that transactivating properties of this transcription factor depends on the ForkHead Associated (FHA) domain in its N-terminus [79]. Since both proteins Fkh1 and Fkh2 posses a FHA domain, it was likely that the observed autoactivation is based on this domain. Therefore, binding analysis between Clb cyclins and the C-terminal region of both transcription factors was performed.

Fkh1 and Fkh2 transcription factors differ substantially in their C-terminal region, being Fkh2 extended of approximately 340 amino acids after the FKH domain (see

Figure 1-2 for details). However, various phosphorylation sites have been identified at serine and threonine residues within this region indicating potential binding of Cdc28-Clb complexes [21].

With the aim to further analyse the interaction between Clb1-6 and the C-terminal region of both transcription factors Fkh1 and Fkh2 Y2H experiments were performed. For this reason, bait plasmids carrying truncated versions of Fkh1 and Fkh2 were cloned. First, analyses were carried out considering a C-terminal region of Fkh2 ranging from 387 to 862 amino acids. L40ccua strain were transformed with plasmid pBTM-Fkh2$_{387}$ and prey constructs pACT-Clb1-6 to test an interaction, as well as all used plasmids in combination with empty vectors as a negative control. Again, cotransformation of plasmids encoding ataxin-2-F4 and PABPC1 was used as positive control. Transformants were selected and spotted either onto SDII and SDIV media or on nylon membrane.

Yeast cells coexpressing the LexA-Fkh2$_{387}$ and AD-Clb1-6 fusion proteins showed growth on SDIV medium and a blue color shift indicating reporter gene activity (Figure 3-5A), whereas mo growth of controls was observed, demonstrating an interaction between the C-terminus of Fkh2 and all B-type cyclins.

In a second step, Y2H analysis were performed to examine the interaction between Clb1-6 and the C-terminus of Fkh1 which encodes amino acids 360-485 of the full length protein. Yeast cells were transformed with plasmid pBTM-Fkh1$_{360}$ and vectors pACT-Clb1-6 and control plasmids as described before. Then, selected clones were spotted either onto SDII and SDIV media or on nylon membrane.

Both, growth on SDIV medium as well as ß-Galactosidase activity of cells coexpressing LexA-Fkh1$_{360}$ and AD-Clb2 plasmids indicated an interaction between these fusion proteins (Figure 3-5B). However, some clones expressing LexA-Fkh1$_{360}$ and AD-Clb3 and 6 showed a blue color shift, demonstrating moderate ß-Galactosidase activity. Since these cells displayed weak growth on SDIV that was found to be comparable with cells expressing LexA-Fkh1$_{360}$ alone this activation of repoter genes was not considered to be significant for an interaction.

Taken together, these data suggest that the association between Clb cyclins and Fkh2 occur in the C-terminus of the protein. Potentially this region could stabilize the binding of Clb cyclins, thus promoting Cdc28-Clb-dependent phosphorylation. Moreover, the C-terminal region of Fkh1 is potentially relevant for the binding with Cdc28-Clb2 complexes during cell cycle progression. However, it is worth mentioning that these findings does not exclude an association of cyclins with full-length Forkhead transcription factors as shown before.

A

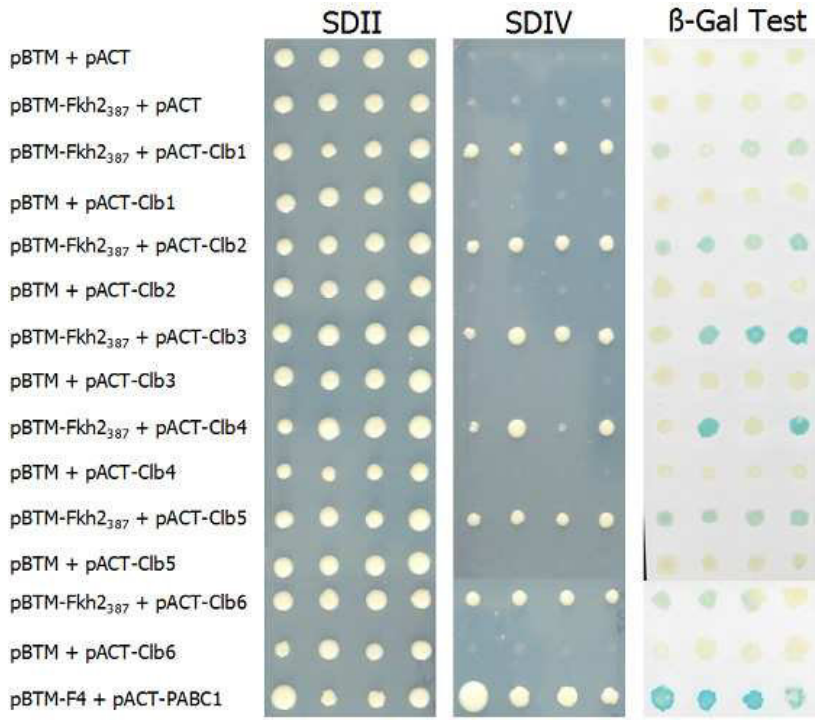

B

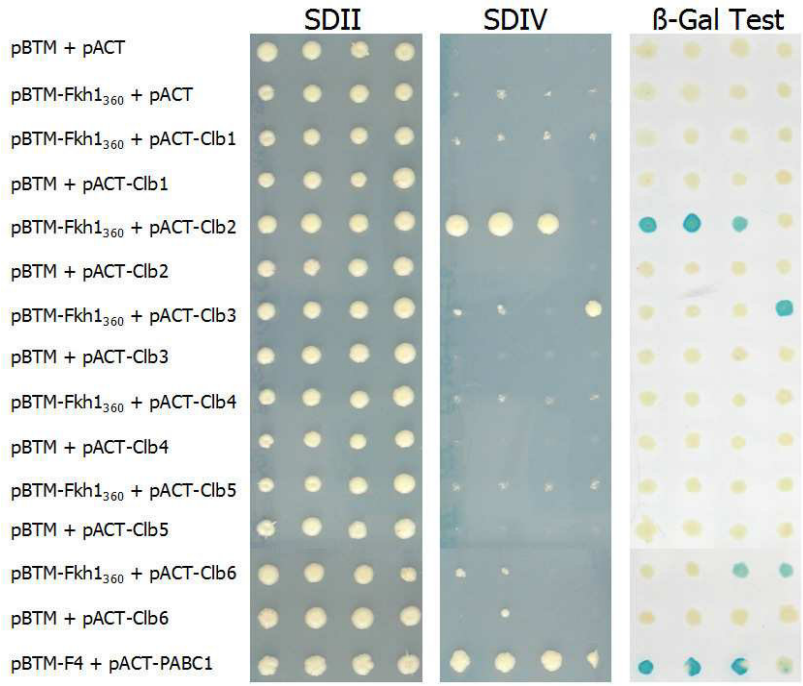

Figure 3-5. Y2H assay with C-terminal fragments of Fkh1 and Fkh2 and B-type cyclins Clb1-6. Growth of yeast colonies on SDII medium lacking leucine and tryptophane (-LEU, -TRP) indicated a successful transformation of bait (pBTM) and prey (pACT) constructs. Coexpression of LexA-Fkh2$_{387}$ **(A)** or LexA-Fkh1$_{360}$ **(B)** bait constructs and AD-Clb1-6 prey constructs were analyzed. A blue color shift associated to the ß-Galactosidase activity and growth on SDIV medium lacking leucine, tryptophane, histidine, uracil and adenine (-LEU, -TRP, -HIS, -URA, -ADE) indicated an interaction. Empty bait and prey plasmids in combination with corresponding constructs were used as negative controls. The interaction between LexA-F4 and AD-PABPC1 was used as a positive control.

3.1.4 Interaction studies between the coactivator Ndd1 and the B-type cyclins

To further gain insight into the regulatory mechanisms by which Cdc28-Clb activity promote cell cycle-dependent gene expression, the specificity of B-type cyclins to associate with Ndd1, the coactivator of Fkh2, was analyzed next. Cdc28-Clb-dependent phosphorylation of Fkh2 is required for the interaction with this coactivator [21, 22, 23]. Moreover, association of Fkh2 and Ndd1 correlates with Clb2 expression and is primed by Cdc28-Clb2 activity [21]. Despite the lack of data about the temporal binding of these factors, the involvement of other Clb cyclins has been suggested as indicated in the model (Figure 3-1) [78].

To investigate wether the B-type cyclins bind to Ndd1, Y2H analyses were performed. In a first step, LexA-Ndd1 fusion construct was generated, transformed into yeast cells and selected clones were tested for autoactivation of reporter genes.

Unfortunately, this analysis revealed that yeast cells expressing LexA-Ndd1 alone showed a strong autoactivation indicated by cell growth on SDIV selection medium supplemented with 20 mM 3-AT.

According to this finding, the *NDD1* gene was subcloned into the prey vector generating the fusion protein AD-Ndd1 and corresponding constructs of Clb1-6 were subcloned into the bait vector encoding the respective fusion proteins LexA-Clb1-6. First, the bait constructs were analyzed for autoactivity and yeast cells were cotransformed with the bait plasmids pBTM-Clb1-6 and the empty prey vector. Then, transformants were selected and spotted onto SDII and SDIV media.

This analysis revealed that cells expressing LexA-Clb1-4 alone showed a weak growth on SDIV and a moderate blue color shift, indicating weak autoactivation of reporter genes (Figure 3-6A). However, this autoactivation was reduced by adding 2.5 mM 3-AT to the SDIV medium as described before.

After these control experiments, L40ccua strain was cotransformed with the plasmids pBTM-Clb1-6 and the vector pACT-Ndd1 as well as empty plasmids alone or in combination with used bait and prey constructs as negative controls. The known interactions between Ndd1 and Clb2 as well as the association between the Ataxin-2-F4 and the PABPC1 was used as positive controls in this analysis. Transformants were selected, spotted onto SDII medium and for detection of the reporter gene activity onto SDIV medium or on a membrane for analysis of β-galactosidase activity.

As shown in Figure 3-6A, a growth on SDIV medium supplemented with 2.5 mM 3-AT was observed for cells coexpressing the fusion proteins LexA-Clb2 and AD-Ndd1 or LexA-Clb3 and AD-Ndd1, indicating an interaction between Ndd1 and both cyclins. Although, cells coexpressing LexA-Clb4 and AD-Ndd1 showed growth on 3-AT containing SDIV medium an interaction between Clb4 and Ndd1 was not considered due to the growth of cells expressing LexA-Clb4 alone. However, yeast cells coexpressing LexA-Clb1-6 and AD-Ndd1 showed a reduced colony size on

SDII medium, suggesting a decreased cell fitness due to the expression of these fusion proteins.

As result, a new interaction between Ndd1 and Clb3 was identified and the known association between Ndd1 and Clb2 confirmed.

To further validate the Ndd1-Clb interactions, GST pull-down experiments were carried on. GST-tagged B-type cyclins expressed in *E. coli* were immobilized on Sepharose beads and incubated with a yeast protein lysate prepared from a strain in which Myc-tagged Ndd1 is endogenously expressed (Figure 3-6B). The assay demonstrates an association of Ndd1 (~ 65 kDa) with Clb2 (lane 5) and Clb3 (lane 6)) but not with Sepharose beads alone (lane 2) or with GST-coupled resins (lane 3), confirming the results obtained from the Y2H analysis.

In conclusion, both Clb2 and Clb3 associate with Ndd1 and might be able to promote the Cdc28-dependent phosphorylation of Ndd1 for the activation of *CLB2* cluster genes.

A

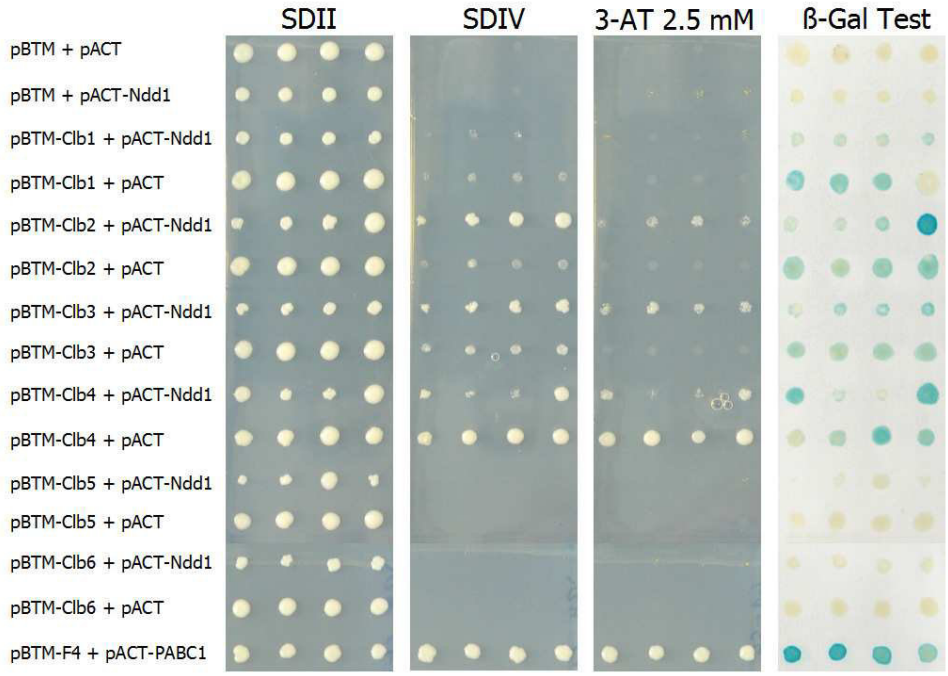

B

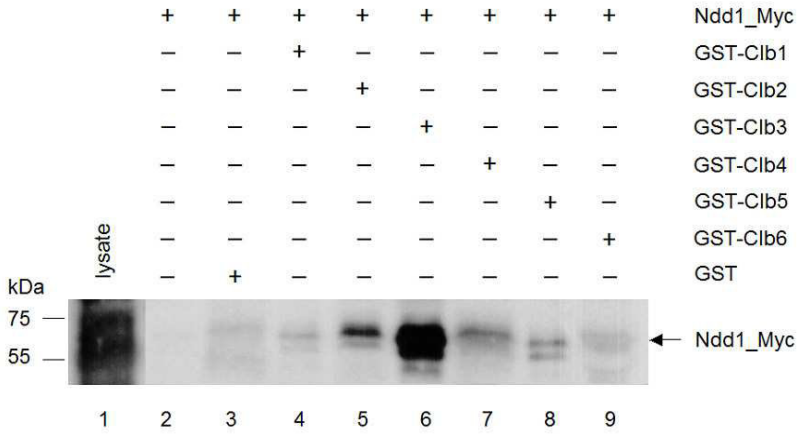

Figure 3-6. Interaction studies between Ndd1 and B-type cyclins Clb1-6. (A) Yeast clones were selected and spotted onto SDII medium lacking leucine and tryptophane (-LEU, -TRP) or on SDIV medium lacking leucine, tryptophane, histidine, uracil and adenine (-LEU, -TRP, -HIS, -URA, -ADE). Empty bait and prey plasmids in combination with corresponding constructs pBTM-Clb1-6 and pACT-Ndd1were used as negative controls. The interaction between pBTM-F4 and pACT-PABPC1 was used as a positive control. 3-Amino-1,2,4-triazole (3-AT) was added to the SDIV medium to a final concentration of 2.5 mM to reduce autoactivity. **(B)** GST and GST-Clb1-6 proteins expressed in *E. coli* were immobilized on Glutathione Sepharose beads and incubated with lysate from yeast cells expressing Ndd1-Myc from its endogenous promoter. Concentrated Ndd1-Myc lysate were used as a loading control (lane 1), whereas Sepharose beads (lane 2) and GST-coupled resins (lane 3) were used as negative controls. Precipitation of Ndd1-Myc bound to immobilized GST-Clb1-6 (lanes 3-9) was detected with rabbit α-Myc antibody.

3.1.5 Binding analysis between Forkhead proteins and Ndd1

Next to the binding analysis between B-type cyclines and the transcription factors Fkh1, Fkh2 and Ndd1, a potential interaction between Fkh1 and Ndd1 was examined. Ndd1 alone is not capable to bind DNA, thus activation of *CLB2* gene cluster depends on binding of Ndd1 to the FHA domain of Fkh2 [79]. Both transcription factors Fkh1 and Fkh2 contain a N-terminal FHA domain (please see Figure 1-2 for details), which recognizes phosphothreonine epitopes on proteins and promotes assembly of protein complexes, thus suggesting that Fkh1 could recruit Ndd1 to the promoter of target genes.

To further analyze whether Ndd1 interacts with Fkh1, Y2H experiments were performed cotransforming yeast cells with pBTM-Fkh1 and pACT-Ndd1 as well as the respective control plasmids as described before. In addition, cells were transformed with pBTM-Fkh2 and pACT-Ndd1 as a positive control. Transformants

were selected, spotted onto SDII and SDIV media or on a nylon membrane and analyzed for growth on selection media and blue color shift. Since both LexA-Fkh1 and LexA-Fkh2 are known to autoactivate reporter genes 3-AT was added to the SDIV selection medium to a final concentration of 10 mM.

Yeast cells coexpressing the fusion constructs LexA-Fkh1 and AD-Ndd1 or LexA-Fkh2 and AD-Ndd1 showed a significant growth on SDIV medium after treatment with 3-AT, indicating an interaction between both Forkhead transcription factors and Ndd1 (Figure 3-7A), whereas control did not.

Again, GST pull-down experiments were carried out to confirm this Y2H result. ORFs of *FKH1* and *FKH2* were subcloned, generating GST-tagged fusion proteins. Immobilization of proteins and incubation with yeast protein lysate containing Ndd1-Myc was performed as described previously. As positive control, the interaction between Fkh2 and Ndd1 was used in this analysis.

As shown in Figure 3-7B, Ndd1-Myc coprecipitates with both Fkh1 (Figure, lane 4) and Fkh2 (lane 5), suggesting that in addition to Fkh2 Ndd1 interact also with Fkh1.

In sum, the result of the GST pull-down assay confirmed the Y2H analysis, demonstrating that both Forkhead transcription factors interact with Ndd1 and can activate cell cycle-regulated gene transcription.

A

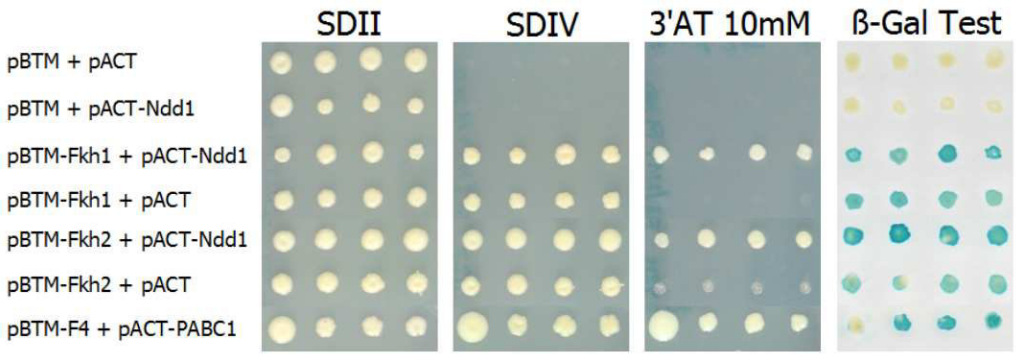

B

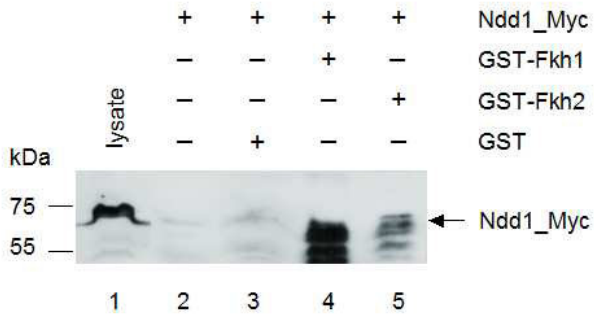

Figure 3-7. Interaction studies between Ndd1 and Forkhead proteins Fkh1 and Fkh2. (A) Coexpression of bait and prey constructs resulted in the growth of yeast colonies on SDII medium lacking leucine and tryptophane (-LEU, -TRP). Growth on SDIV medium lacking leucine, tryptophane, histidine, uracil and adenine (-LEU, -TRP, -HIS, -URA, -ADE) and blue color shift associated to the ß-Galactosidase activity indicated activation of reporter genes. Empty bait and prey plasmids in combination with corresponding constructs were used as negative controls. The interaction between pBTM-Fkh2 and pACT-Ndd1 was used as a positive control. Treatment with 3-Amino-1,2,4-triazole (3-AT) to a final concentration of 10 mM was performed to decrease autoactivation of reporter genes **(B)** Bacterial expressed proteins GST, GST-Fkh1 and GST-Fkh2 were immobilized on Glutathione Sepharose beads and incubated with lysate from yeast cells endogenously expressing Ndd1-Myc. Concentrated Ndd1-Myc lysate were used as a loading control (lane 1), whereas Sepharose beads (lane 2) and GST-coupled resins (lane 3) were used as negative controls. Precipitation of Ndd1-Myc bound to immobilized GST-Fkh1 (lane 4) or GST-Fkh2 (lane 5) was detected with rabbit α-Myc antibody.

3.1.6 Functional analysis of interactions between Fkh proteins and Ndd1

After validating the PPI's predicted in the mathematical model, the focus was on functional analysis of selected interaction partners. First, it was aimed to investigate the timing of the association between Ndd1 and the Forkhead transcription factors Fkh1 and Fkh2. A cell cycle regulated coactivation of Fkh1 has been suggested, but not demonstrated so far [78]. Since occupancy of *CLB2* cluster gene promoters by Fkh2 is not cell cycle regulated, periodic expression of these genes depends on the timing of the interaction between the coactivator Ndd1 and Fkh2 [79, 81]. However, Fkh1 and Fkh2 have been demonstrated to occupy the promoter of the same genes in a cell cycle independent manner [78, 81, 83]. These findings and the results obtained from the Y2H and GST pull-down analysis in this work strongly support the involvement of Fkh1 as a direct target for Ndd1. To further validate this prediction and to analyze the cell cycle-dependent timing of these interactions a fluorescence-based approach called Bimolecular Fluorescence Complementation (BiFC) was

established. The method is based on the reconstitution of a fluorescent complex from two separate, not fluorescent fragments carrying genes coding for potential interaction partners [232]. Furthermore, it can be used to study the interaction of two proteins expressed from their native promoter [232].

In a first step, the functionality of the BiFC method was investigated. On the one hand, a specific integration cassette was amplified, using the plasmid pFA6a-VC-His3MX6 as a template, and transformed into yeast strain BY4741. This cassette encoding the C-terminal part of a variant of the yellow fluorescent protein called Venus (VC) integrated into the genome of yeast cells by homologues recombination to allow for endogenous expression of C-terminal tagged Ndd1 (Ndd1-VC) (see chapter 2.2.14 for details). Clones were selected for histidine auxotrophy and intergration was validated by PCR. On the other hand, Fkh1 and Fkh2 were tagged at their N-terminal region with the N-terminal fragment of Venus (VN) using the plasmid pFA6a-VN-KanMX6. A constitutive expression of VN-tagged Fkh1 and Fkh2 was ensured by cloning the constructs *FKH1-VN* and *FKH2-VN* into the expression plasmid p426GPD. Then, yeast cells carrying the Ndd1-VC integration were transformed with vectors p426GPD-VN-Fkh1 or p426GPD-VN-Fkh2 and as a negative control with the plasmid p426GPD-VN. Selected transformants coexpressing the constructs Fkh1-VN and Ndd1-VC or Fkh2-VN and Ndd1-VC were analyzed for the so called “BiFC signal” that occurs in case proteins interact. In addition, the nucleus of yeast cells was stained with DAPI.

This analysis revealed that yeast cells expressing both Ndd1-VC and VN-Fkh2 as well as Ndd1-VC and VN-Fkh1 showed BiFC signals that localized to the nucleus of yeast cells (Figure 3-8 middle and bottom panels). As expected, no signal was observed in cells expressing Ndd1-VC and VN alone (top panels), demonstrating the validity of this method for the proposed functional analysis.

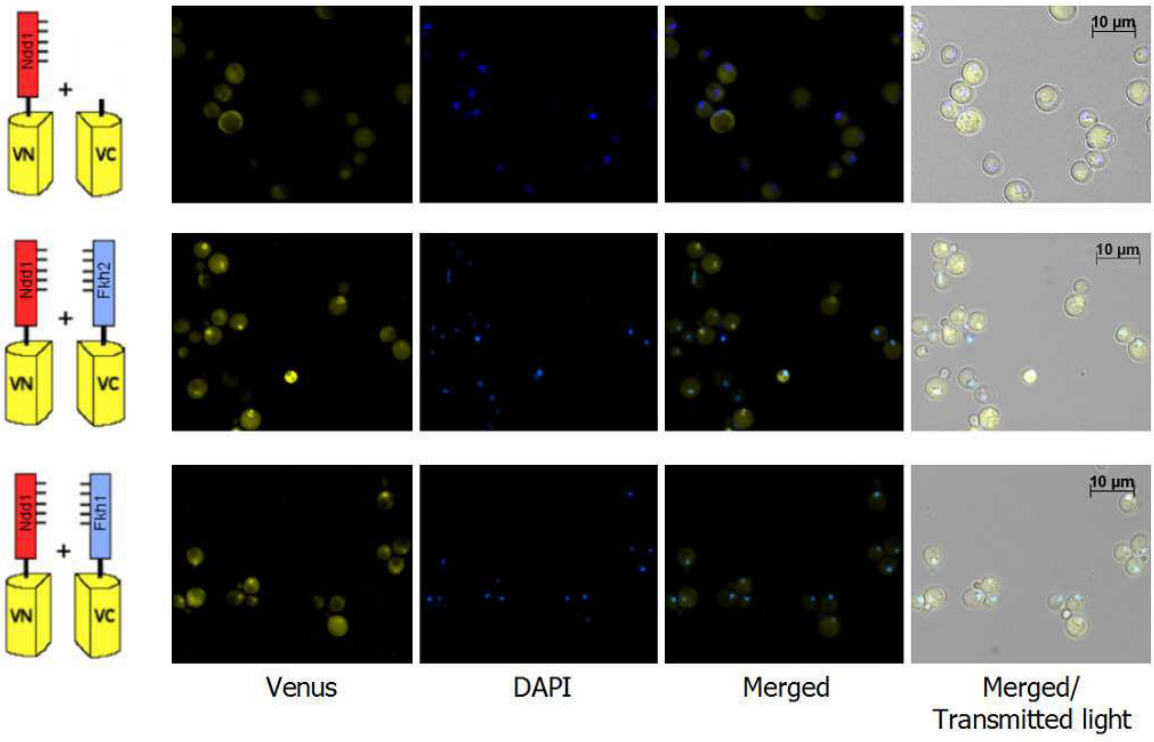

Figure 4-8. Visualization of the interaction between Ndd1 and Fkh1 or Fkh2 by BiFC. Top panels: Haploid cells endogenously expressing the C-terminal part of the Venus protein fused to the C-terminal region of Ndd1 (Ndd1-VC) and the N-terminal part of Venus (VN) constitutively expressed from the plasmid p426GPD. Middle panels: Haploid cells expressing Ndd1-VC and the N-terminal part of Venus fused to the N-terminal region of Fkh2 (VN-Fkh2) from the plasmid p426GPD. Bottom panels: Haploid cells expressing Ndd1-VC and VN-Fkh1 from the plasmid p426GPD.

In the next step, cell cycle-dependent binding of Ndd1-VC to VN-Fkh1 and VN-Fkh2 was analyzed. To this purpose, cells expressing Ndd1-VC/VN-Fkh2 and Ndd1-VC/VN-Fkh1 were synchronized in G1 phase by α-factor and arrested growth released by adding fresh medium (chapter 2.2.18). Subsequenly, yeast cells were collected every 10 min, analyzed for the BiFC signal and DNA content was measured by FACS analysis.

Yeast cells coexpressing the fusion proteins Ndd1-VC and VN-Fkh2 showed no distinct fluorescent signals at 0 min, indicating that binding does not occur in G1 phase (Figure 6-1A). Interestingly, the BiFC signal was observed after 10 min, demonstrating an association between Ndd1 and Fkh2 in early S phase. An increase in the intensity of the signal over time was observed with a peak at 30-40 min (the beginning of mitosis), and a decrease was then observed between 60 and 90 min, which contributes to the mitotic exit and the G1 phase of the next cell cycle.

Therefore, it can be concluded that oscillations in Ndd1 levels drive S and M phase-specific gene expression to mediate progression through the cell cycle.

In the second step, the cell cycle-dependent interaction between Ndd1-VC and VN-Fkh1 was analyzed. For this, a release of α-factor arrested cells were performed and Venus signals as well as DNA content of the culture followed over time (Figure 6-1B).

A lack of Venus signals in yeast cells coexpressing Ndd1-VC and VN-Fkh1 was observed bewteen 0 and 20 min, indicating no interaction between Ndd1 and Fkh1 at this time interval. Weak distinct fluorescent signals were first detected at 30 min (early S phase), whereby signal intensity peaked at 50-60 min (M phase). Yeast cells analyzed between 70 and 90 min showed a less strong intensity of the BiFC signal compared to the time intervals of 50 and 60 min, indicating that the interaction between Ndd1 and Fkh1 might not occur in late mitosis.

In conclusion, these findings demonstrate that in addition to Fkh2 Fkh1 can periodically associate with Ndd1 to promote expression of cell cycle-regulated genes. Moreover, this binding revealed a similar temporal pattern compared to the interaction between Fkh2 and Ndd1. Although, appearance and intensity maximum of the BiFC signals were different for both interactions, a strong overlapp in their timing was observed after comparing the time intervals in both experiments that showed a similar DNA content.

Figure 3-9. Time course analysis of BiFC signals after α-factor release of cells coexpressing Ndd1-VC and VN-Fkh1, 2. Haploid cells endogenously expressing the C-terminal part of Venus fused to the C-terminal region of Ndd1 (Ndd1-VC) and constitutively expressing the N-terminal part of Venus fused to the N-terminal region of **(A)** Fkh2 (VN-Fkh2) or **(B)** Fkh1 (VN-Fkh1) from plasmid p426GPD. Cells were synchronized in G1 phase by addition of α-factor and a release of growth arrest performed. Samples were collected in time intervals of 10 min and analyzed for the BiFC signal. DNA content was measured by FACS analysis.

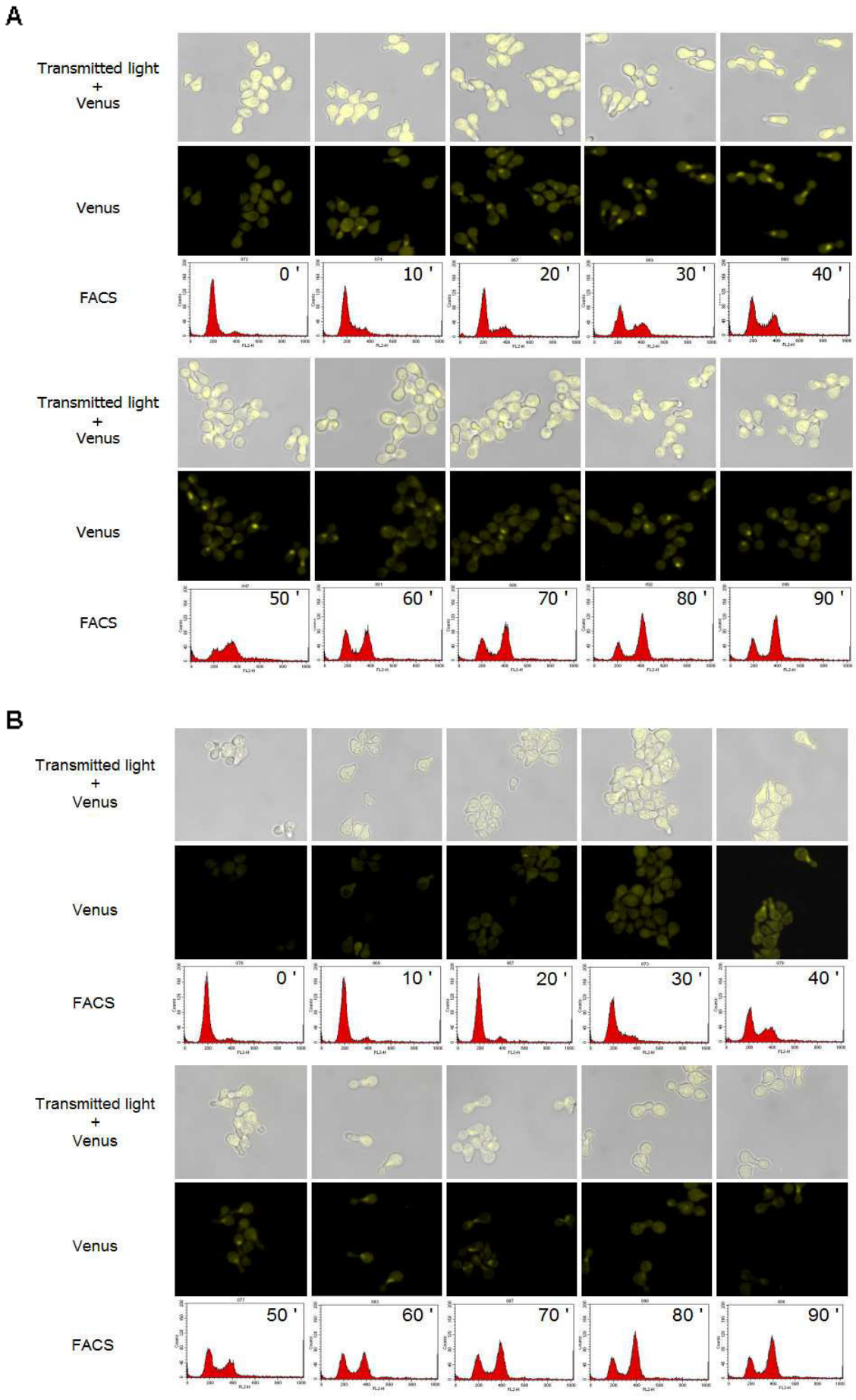
A
Transmitted light + Venus
Venus
FACS
0 '
10 '
20 '
30 '
40 '
Transmitted light + Venus
Venus
FACS
50 '
60 '
70 '
80 '
90 '
B
Transmitted light + Venus
Venus
FACS
0 '
10 '
20 '
30 '
40 '
Transmitted light + Venus
Venus
FACS
50 '
60 '
70 '
80 '
90 '

3.1.7 Role of Clb3 in the regulation of Forkhead-dependent genes

The interaction studies performed in this work demonstrated a potential association between all B-type cyclins and the Forkhead proteins suggesting their involvement in Cdc28-Clb-dependent phosphorylation. As proposed in the model (Figure 3-1), Cdc28-Clb5, 6 complexes might be involved in transcription of *CLB3, 4* genes. Cdc28-Clb3, 4 complexes are required for *CLB1, 2* expression, since it has been shown that Clb3, 4 can functionally compensate for deletion of *CLB1* and *CLB2* [6].

To address the potential role of Clb3 in priming Ndd1-dependent *CLB2* cluster transcription, the timing of the interaction between Fkh2 and Ndd1 was determined and compared with the temporal expression of the B-type cyclins Clb2 and Clb3.

Therefore, both cyclin genes were tagged with a gene encoding the cyan fluorescent protein (CFP) by homologues recombination, thus allowing expression of Clb2-CFP and Clb3-CFP on endogenous level. To generate the fusion proteins Ndd1-VC and VN-Fkh2, integration cassettes were amplified from plasmid pYM30-ECFP-His3MX6 and transformed into strain BY4741. Then, cells were grown until exponential phase and treated with hydroxyurea or nocodazole, which arrest cells in S phase or in M phase, respectively (see chapter 2.2.18 for more details). Samples were collected for microscopic analysis and DNA content was determined as previously described (Figure 3-10).

Yeast cells coexpressing the fusion proteins Ndd1-VC and VN-Fkh2 showed a BiFC signal as well as a distinct Clb3-CFP fluorescent signal when arrested in S phase (Figure 3-10, left panels). This was not observed in cells synchronized in M phase showing Venus signals but no Clb3-CFP-specific fluorescence (right panels). Interestingly, nocodazole-arrested cells coexpressing the fusion proteins Ndd1-VC, VN-Fkh2 and Clb2-CFP showed BiFC signals and Clb2-CFP fluorescent signals (right panels). Compared to cells expressing Clb3-CFP, Clb2-CFP-dependent fluorescence was not detected upon synchronization with hydroxyurea (left panels), indicating an expression of Clb3 in S phase and Clb2 in M phase.

Taken together, the results support a model in which Clb3-dependent kinase activity can prime association of Ndd1 to Fkh2 in S phase.

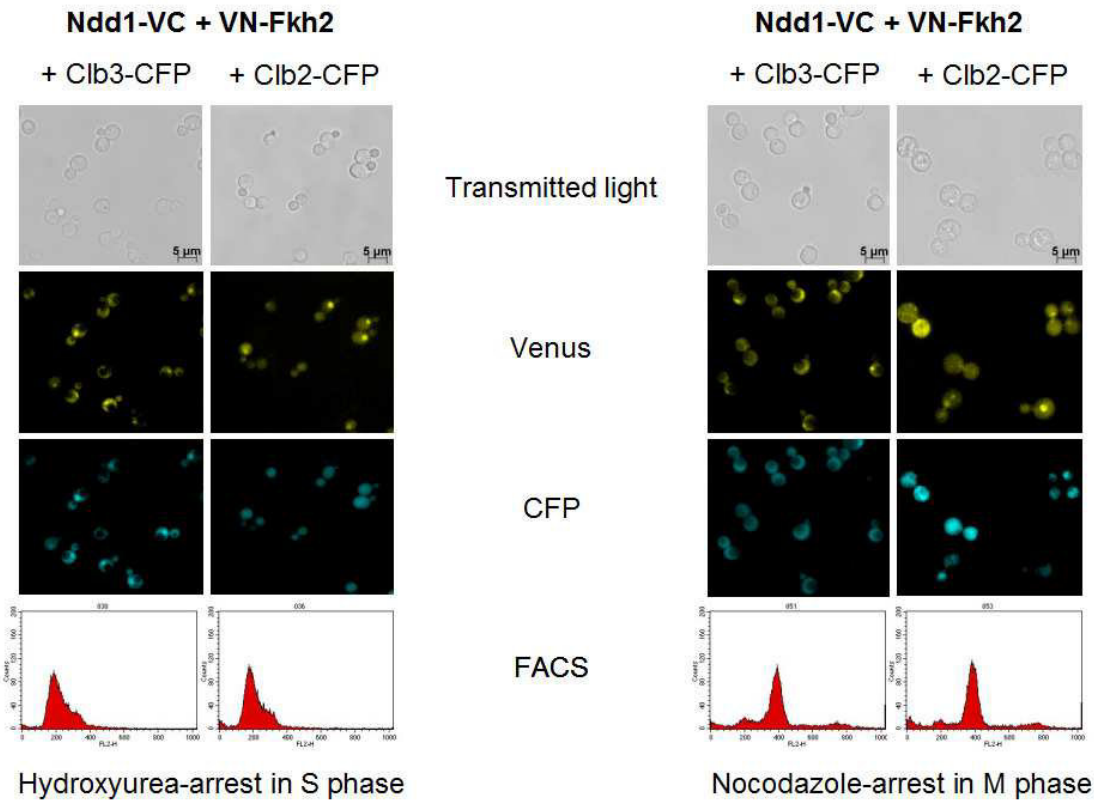

Figure 3-10. Cell cycle-dependent expression of Ndd1-VC/VN-Fkh2 and Clb2-CFP or Clb3-CFP. Haploid cells endogenously expressing chromosomal tagged Ndd1-VC and constitutively expressing VN-Fkh2 from the p426GPD plasmid were modified to express Clb2-CFP or Clb3-CFP from their endogenous promoters. Cells were arrested with hydroxyurea in S phase (left panels) or nocodazole in M phase (right panels) and DNA content determined by FACS analysis.

The primary cyclin responible for Cdc28-dependent phosphorylation of Ndd1 to activate the *CLB2* gene cluster expression in G2/M phase was reported to be Clb2 itself [21]. However, the data presented in this work indicate an involvement of Clb3, which peaked earlier in cell cycle presumably in S phase compared to Clb2. Nevertheless, this does not exclude that a basal protein level of Clb1 and Clb2 is sufficient to promote Ndd1/Fkh2 complex formation as previously suggested. To further support a role of Clb3 in Ndd1 activation, potential associations between the B-type cyclins Clb1-4 and the coactivator were investigated with the BiFC method. In addition, it was aimed to analyze whether a constitutive expression of either Clb1, 2, 3 or 4 promote expression of Clb3-CFP.

To this purpose, coding sequences of genes *CLB1-4* were subcloned into expression plasmid p426GPD-VN to allow for constitutive expression of VN-tagged Clb1-4. After validation of the fusion constructs, yeast cells endogenously coexpressing Ndd1-VC and Clb3-CFP were either transformed with plasmid

p426GPD-VN-Clb1, VN-Clb2 , VN-Clb3 or VN-Clb4. Cells were collected and subjected to fluorescence microscopy as mentioned before (Figure 3-11).

Yeast cells coexpressing the fusion proteins Ndd1-VC, VN-Clb1 and Clb3-CFP showed neither a BiFC signal nor a Clb3-specific fluorescence. Venus signals specific for an interaction between Ndd1 and Clb2 were detected in cells expressing Ndd1-VC, VN-Clb2 and Clb3-CFP. However, cyan fluorescent signals indicating expression of Clb3-CFP were not detected in these cells. Interstingly, cells constitutively expressing VN-Clb3 and endogenously expressing Ndd1-VC and Clb3-CFP showed both a Venus signal indicating interaction between Ndd1 and Clb3 as well as Clb3-CFP-dependent fluorescence. Expression of Ndd1-VC, VN-Clb4 and Clb3-CFP in yeast cells did not result in a detectable BiFC signal as well as fluorescence specific for Clb3-CFP expression.

In conclusion, the analysis confirmed the known interaction between Ndd1 and Clb2 as well as the predicted association between Ndd1 and Clb3. Interestingly, Clb3-CFP fluorescent signals were clearly detected in cells constitutively expressing VN-tagged Clb3 from the GPD promoter, suggesting a positive feedback mechanism where Clb3 promotes its own transcription.

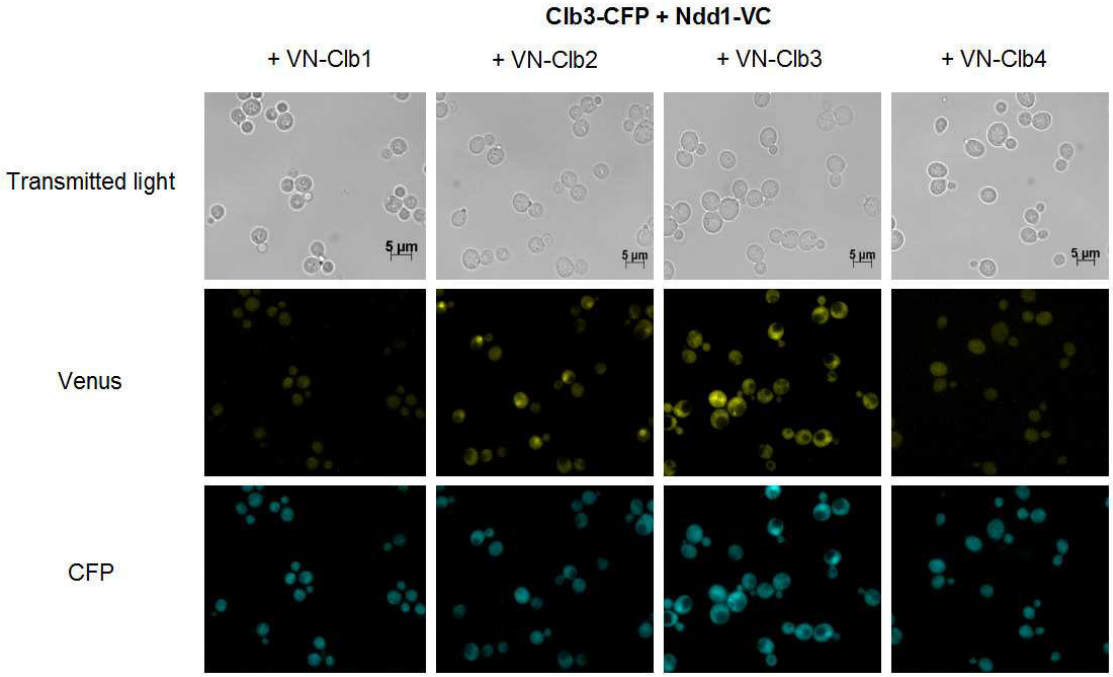

Figure 3-11. Visualization of the interaction between Ndd1-VC and VN-Clb1-4, and expression of Clb3-CFP. Haploid cells coexpressing Ndd1-VC and Clb3-CFP on endogenous level were transformed with plasmids p426GPD-VN-Clb1, p426GPD-VN-Clb2, p426GPD-VN-Clb3 and p426GPD-VN-Clb4 to allow constitutive expression of the VN-tagged cyclins. Exponentially growing transformants were analyzed for BiFC signals as well as expression of Clb3-CFP by microscopy.

3.1.8 Forkhead proteins and Ndd1 bind to the *CLB* promoters and drive Clb expression

The data presented so far in this work suggest an involvement of Clb cyclins in the regulation of Fkh1, Fkh2 and Ndd1. However, these transcription factors could also play a role in the activation of *CLB3, 4* genes, as indicated by expression analysis of Clb3-CFP and the assumptions presented in the network (Figure 3-1).

To analyse wether Fkh1, Fkh2 and Ndd1 occupy promoters of B-type cyclin genes *CLB1-4*, chromatin immunoprecipitation (ChIP) analyses were performed. Potential binding sites for the FKH domain were identified in both the upstream untranslated sequence (5' UTS) and the coding sequence (CDS) of each *CLB* gene (chapter 2.2.19). Therefore, different yeast strains were generated which endogenously expressed a C-terminal Myc-tagged protein of Fkh1, Fkh2 or Ndd1. Then, these strains were cultured to the mid logarithmic stage (OD_{600} ~ 0.6 - 0.8) and cells treated with formaldehyde to purify protein-DNA complexes as described in chapter 2.2.19. Immuno-precipitation was performed using an epitope-specific antibody and enrichment at the gene promoters of *CLB1-4* was quantified by real-time PCR (chapter 2.2.12). As controls, *TSA1* and *ACT1* genes were used, since they are not involved in cell cycle-related processes so far. As positive control, the binding of Fkh2 and Ndd1 at *CLB1* and *CLB2* promoters was used as described [83].

Yeast cells expressing Fkh1-Myc showed an enrichment of promoter DNA specific for *CLB1-4* (Figure 3-12A lane 3-6) and no enrichment of *TSA1* (lane 1) and *ACT1* (lane 2). Interestingly, the amount of immunoprecipitated DNA was higher for *CLB1-3* compared to *CLB4*. In cells expressing Fkh2-Myc increased levels of precipitated DNA was detected for *CLB1-3* (Figure 3-12B lane 3-5), whereas an enrichment of genomic DNA for *TSA1*, *ACT1* and *CLB4* was not detected (lane 1,2 and 6).

Immunoprecipitation of Ndd1-Myc-specific protein-DNA complexes (Figure 3-12C), similar to cells expressing Fkh2-Myc, revealed increased levels of *CLB1-3* DNA fragments (lane 3-5) and a weak enrichment of *CLB4*-specific DNA compared to control genes *TSA1* and *ACT1* (lane 1,2).

In sum, these data demonstrate binding of Fkh1, Fkh2 and Ndd1 at the promoters of

CLB1-3, whereas Fkh1 and Ndd1 associate with *CLB4* promoter. Furthermore, these results suggest that Fkh transcription factors could play a role in promoting the expression of mitotic cyclins for a timely cell cycle progression.

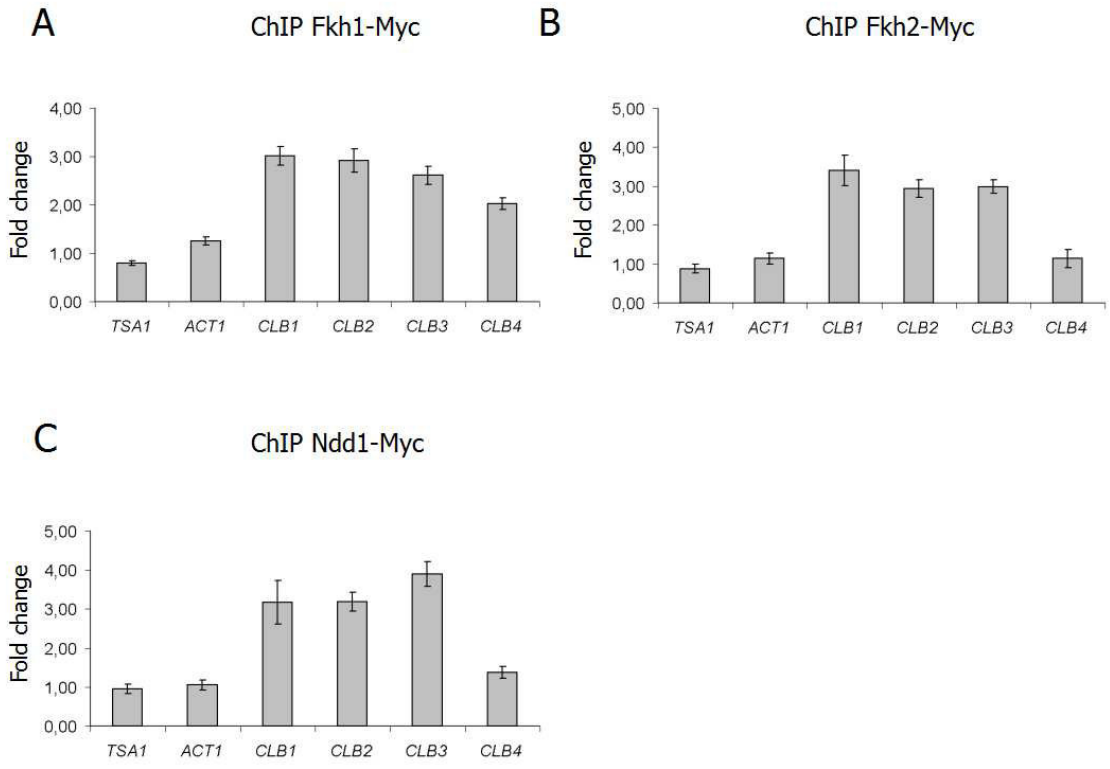

Figure 3-12. Promoter occupancy of Myc-tagged proteins Fkh1, Fkh2 and Ndd1 at promoters of *CLB1-4* genes. ChiP experiments were performed with exponentially growing cells using yeast protein extracts containing **(A)** Fkh1-Myc, **(B)** Fkh2-Myc and **(C)** Ndd1-Myc using epitope-specific antibodies. Immunoprecipitated DNA was quantified by real-time PCR. As controls, unrelated *TSA1* (lane 1) and *ACT1* (lane 2) genes were used. As positive control, known Fkh2 and Ndd1 promoter occupancy at *CLB1* (lane 3) and *CLB2* (lane 4) was used. Each lane represents the average of data from three independent experiments.

In a next step, it was aimed to validate whether Forkhead transcription factors Fkh1 and Fkh2 are able to recruit RNA Polymerase II (RNA Pol II) to promoters of *CLB1-4*. It is known that both transcription factors play important roles in the transcription of a broad spectrum of genes, in addition to their cruicial function in activation of *CLB2* gene cluster [243]. However, in *fkh1*Δ and *fkh2*Δ mutants active compexes consisting of Fkh proteins and RNA Pol II subunits should not be presented at both *CLB1, 2* and *CLB3, 4*.

To generate strains lacking *FKH1* and *FKH2* genes, specific integration cassettes were amplified using plasmid pUG6 as template and cassettes were transformed into wild type strain BY4741. Excision of selection marker cassette was performed

using the Cre/loxP (Causes Recombination/locus of X over P1) recombination system (see chapter 2.2.14 for details) and deletion of *FKH1* and *FKH2* was verified by PCR. Both wild type and mutant cells were then incubated until exponential growth and ChIP experiments were carried out. For immobilization of RNA Pol II to Protein A/G agarose beads, a protein-specific antibody was used. As controls, *TSA1* and *ACT1* genes were used as they have not been decribed as targets of Fkh1 and Fkh2. As positive control, the binding of Fkh2 to promoters of *CLB1*,*2* was used. Data obtained from quantitative real-time analysis of precipitated DNA in *fkh1*Δ and *fkh2*Δ mutants was normalized to wild type.

As shown in Figure 3-13, enrichment of DNA specific for the genes *CLB1-4* (lane 3-6) was moderately reduced in *fkh1*Δ mutants compared to wild type cells (please see Figure legend), whereas no significant changes were observed for control genes *TSA1* and *ACT1* (lane1,2). Interestingly, the binding of RNA Pol II to all *CLB* promoters was severely decreased in *fkh2*Δ cells compared to control genes and wild type cells, indicating a more specific role of Fkh2 in recruiting RNA Pol II to promoters of *CLB1-4*.

Taken together, these results demonstrate that Fkh1 and Fkh2 are able to recruit RNA Pol II to activate transcription of *CLB3, 4*. Moreover, these data are consistent with previous findings showing that Fkh transcription factors not only have regulatory functions in activation of *CLB2* cluster genes but also in expression of other gene clusters [243].

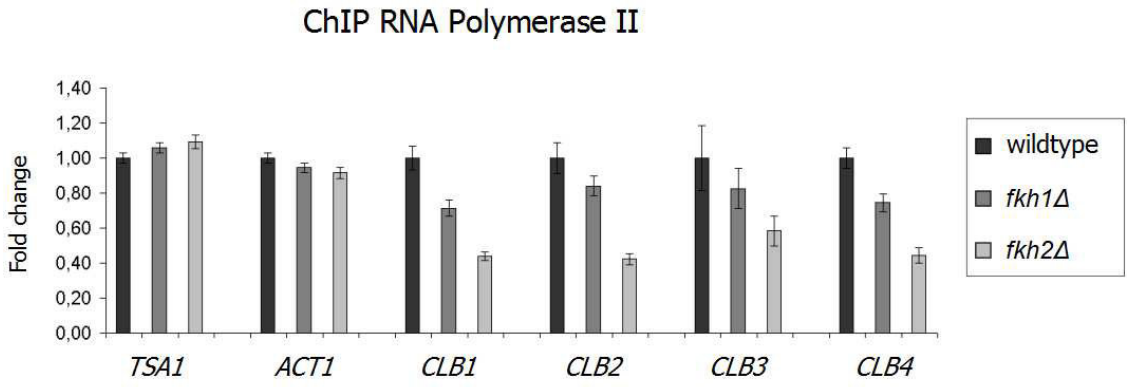

Figure 3-13. Promoter occupancy of RNA Pol II at promoters of *CLB1-4* genes in *fkh1*Δ and *fkh2*Δ strains. ChIP experiments were performed with exponentially growing cells. Yeast protein extracts were treated with RNA Pol II-specific antibodies. Immunoprecipitated DNA was quantified by real-time PCR. Data obtained from quantitative real-time analysis of precipitated DNA in *fkh1*Δ and *fkh2*Δ mutants was normalized to wild type. As control *TSA1* and *ACT1* was used. Each lane represents the average of three independent experiments.

3.1.9 Forkhead proteins drive expression of *CLB1-4*

Next, it was aimed to analyze whether deletion of *FKH1* and *FKH2* alters cell cycle-regulated expression of *CLB3, 4.* To this purpose, transcript levels of *CLB3, 4* in different cell cycle phases were analyzed. Since it is known that simultaneous disruption of *FKH1* and *FKH2* severely disrupt cell cycle-dependent expression of *CLB2* cluster [74, 83], a strain should be generated lacking both genes.

For the generation of the *fkh1*Δ*fkh2*Δ double deletion strain a *FKH1* disruption casette was integrated into the *fkh2*Δ strain. Excision of the loxP-flanked cassette was performed as mentioned in chapter 2.2.14. After validation of strain, synchronization of yeast cells in different cell cycle stages was ensured adding α-factor (G1 phase) or nocodazole (M phase) to the medium (see chapter 2.2.18 for details). The DNA content was determined by FACS analysis. Then, mRNA was isolated, transcribed into cDNA and quantified by real-time PCR. As controls the unrelated genes *TSA1* and *ACT1* were used; *CLB2* served as a positive control.

Wild type cells and single *FKH* mutants grown to exponential phase did not show a remarkable difference in *CLB3, 4* transcript levels compared to control genes *TSA1* and *ACT1* (Figure 3-14A, please see Figure legend). A significant reduction in transcript levels of *CLB1-4* was observed for the *fkh1*Δ*fkh2*Δ strain, indicating that disruption of both Fkh1 and Fkh2 leads to reduced *CLB* transcription. Interestingly, a comparable reduction of *CLB2* and *CLB3* transcripts in *fkh1*Δ*fkh2*Δ mutants was observed (~ 50 %), indicating an equal relevance of Forkhead-dependent expression of these genes. Moreover, *fkh1*Δ*fkh2*Δ mutants showed a strong reduction in *CLB1* transcription and a moderate decrease of *CLB4* compared to *CLB2,3* as well as *TSA1* and *ACT1.*

The quantification of mRNA levels of *fkh1*Δ, *fkh2*Δ and *fkh1*Δ*fkh2*Δ mutants arrested in metaphase revealed various changes for all mutants compared to wild type (Figure 3-14B): Interestingly, *CLB2* transcript level in *fkh1*Δ cells was moderately decreased, whereas transcription of *CLB4* significantly increased. These findings indicate an activatory role of Fkh1 for *CLB2* and a putative repressive one for *CLB4*. Moreover, a strong reduction of *CLB1-4* transcripts was observed in both *fkh2*Δ and *fkh1*Δ*fkh2*Δ mutants compared to wild type. In *fkh2*Δ mutants this effect was

stronger for *CLB1* and especially *CLB2*, suggesting that the Fkh2-dependent activation of *CLB1,2* expression is more relevant during this stage. However, *CLB1-3* transcript levels of nocodazole-arrested cells were strongly reduced in the *fkh1*Δ*fkh2*Δ mutant, indicating redundant functionality of Fkh1 and Fkh2 in transcriptional regulation of these genes. The reduction of *CLB4* mRNA level was comparable to the *fkh2*Δ mutant.

To complete the analysis, *CLB* transcript levels were also measured in G1 phase (Figure 3-14C). No significant effect on transcription was detected in *fkh1*Δ mutants. Furthermore, increased levels of *CLB1* and *CLB2* were detected in *fkh2*Δ cells, strongly supporting activating and repressive functions of Fkh2 [21, 78]. A strong enrichment of all *CLB* transcript was observed in *fkh1*Δ*fkh2*Δ cells, with the highest mRNA level for *CLB1* and *CLB2*, and less enrichment for *CLB3* and *CLB4*.

Considering that Fkh transcription factors bind at *CLB1, 2* promoters and that mitotic cyclins are transcribed from late S phase until G2/M phase [6], a change in mRNA levels of *CLB1, 2* was expected when synchronizing *fkh2*Δ and *fkh1*Δ*fkh2*Δ deletion mutants in metaphase. However, *CLB3, 4* transcription was impaired as well in *fkh2*Δ and *fkh1*Δ*fkh2*Δ mutants in M phase, also suggesting an important regulatory role for Fkh1 and Fkh2 in transcription of *CLB3* and *CLB4*. In support of this, increased levels for *CLB1-4* transcripts was detected in G1 phase, where repression of mitotic genes is required for cell division. This important observation further suggests that both transcription factors Fkh1 and Fkh2 act also as repressors to regulate target genes in a cell cycle-dependent manner.

Taken together, these data indicate that Clb cyclin transcription could be promoted mainly by Fkh2; however, a role for Fkh1 cannot be ruled out.

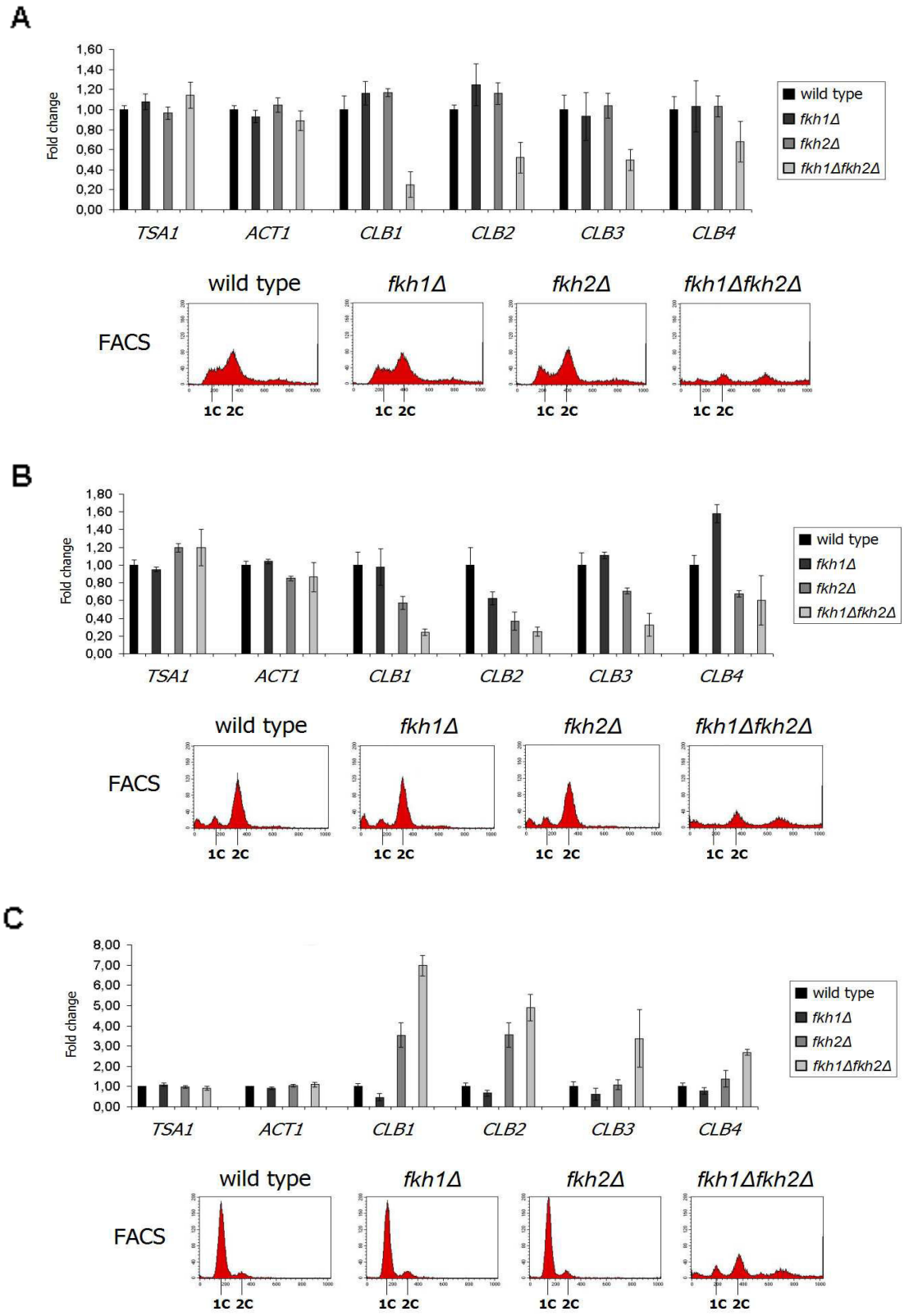

Figure 3-14. Real-time PCR for quantification of *CLB1-4* transcript levels in *fkh1*Δ, *fkh2*Δ and *fkh1*Δ*fkh2*Δ strains. Total RNA was isolated from exponentially growing cells **(A)**, nocodazole-arrested cells **(B)** and α-factor-arrested cells **(C)**. cDNA was obtained and quantified by real-time PCR. The average of values obtained from four independent experiments was normalized to wild type. *TSA1* and *ACT1* were used as negative controls and DNA content was determined by FACS analysis.

3.2 Role of Forkhead transcription factors and the histone deacetylase Sir2 in cell cycle regulation

The previous transcriptional analysis strongly suggested that Fkh transcription factors might be regulated not exclusively via a positive feedback loop involving B-type cyclins. Recently, Sir2 was found to interact with the S phase-specific Forkhead transcription factor Hcm1 [114], thus suggesting a potential involvement of Sir2 in the transcriptional silencing of G2/M-specific genes via the Forkhead transcription factors Fkh1 and Fkh2. In support to this, Fkh2 has been proposed to act as a repressor of *CLB2* cluster genes. Consistently, recent analyses revealed an enhanced *CLB2* transcription in G1 phase for cells lacking both Fkh2 and Ndd1 [21, 83]. In addition, Fkh1 was found to play a role in the silencing at mating-type locus HMR dependent on the histone deacetylase Sir2 [242].

3.2.1 Analysis of genetic interactions between Sir2 and Fkh1 and Fkh2

In a first step, it was aimed to reveal a functional relationship between Sir2 and the Forkhead proteins Fkh1 and Fkh2. For this reason, deletion strains *sir2*Δ, *fkh1*Δ*sir2*Δ and *fkh2*Δ*sir2*Δ were generated and viability tests should be performed using wild type cells, *fkh1*Δ and *fkh2*Δ, *sir2*Δ, *fkh1*Δ*sir2*Δ and *fkh2*Δ*sir2*Δ deletion strains. For deletion of *SIR2* gene in the BY4741 strain as well as in *fkh1*Δ and *fkh2*Δ mutants, specific integration cassette was generated using the plasmid pUG6 as template. Then, the cassette was transformed into yeast cells and resulting clones grown on selection medium were validated by PCR. In addition, wild type and deletion strains were transformed with an expression plasmid p426GALL encoding *SIR2* under control of galactose inducible promotor. Therefore, the *SIR2* gene was cloned into the expression plasmid generating vector p426GALL-Sir2. The construct was validated and wild type and deletion strains *fkh1*Δ, *fkh2*Δ, *sir2*Δ, *fkh1*Δ*sir2*Δ and *fkh2*Δ*sir2*Δ were transformed with either empty vector (control) or p426GALL-Sir2. Selected cells were grown to mid logarithmic phase and subsequently spotted in serial dilutions (1:5) on medium supplemented with glucose (control) or galactose to induce expression of Sir2. After three days of incubation, viability of cells was monitored comparing number and size of yeast colonies.

As illustrated in Figure 3-15, a reduced cell growth was observed in wild type strain BY4741 expressing Sir2 compared to cells transformed with the empty vector. As expected, no growth defects of BY4741 cells was observed on glucose plate. Interestingly, a Sir2-dependent reduction of cell growth was observed for *fkh1*Δ and *fkh2*Δ mutants compared to wild type strain expressing Sir2, indicating a genetic interaction between both Forkhead proteins and Sir2. Since, *fkh1*Δ and *fkh2*Δ mutants transformed with the empty vector showed no growth deffects on galactose medium compared to wild type cells, this finding suggests a Sir2-specific effect. Interestingly, a slight increase in viability of *sir2*Δ mutant cells expressing Sir2 was observed in comparison to wild type strain, indicating that a Sir2-dependent decrease in growth might partially be compensated by removing endogenous Sir2. Importantly, this rescue of cell viability was detected in *fkh1*Δ*sir2*Δ and *fkh2*Δ*sir2*Δ mutants expressing Sir2 as well, demonstrating that the deletion of Sir2 rescues the growth defects of cells lacking *FKH1* or *FKH2*.

Taken together, the data suggests a repressive role of Sir2 in the growth of yeast cells as well as its functional relationship to Forkhead proteins Fkh1 and Fkh2.

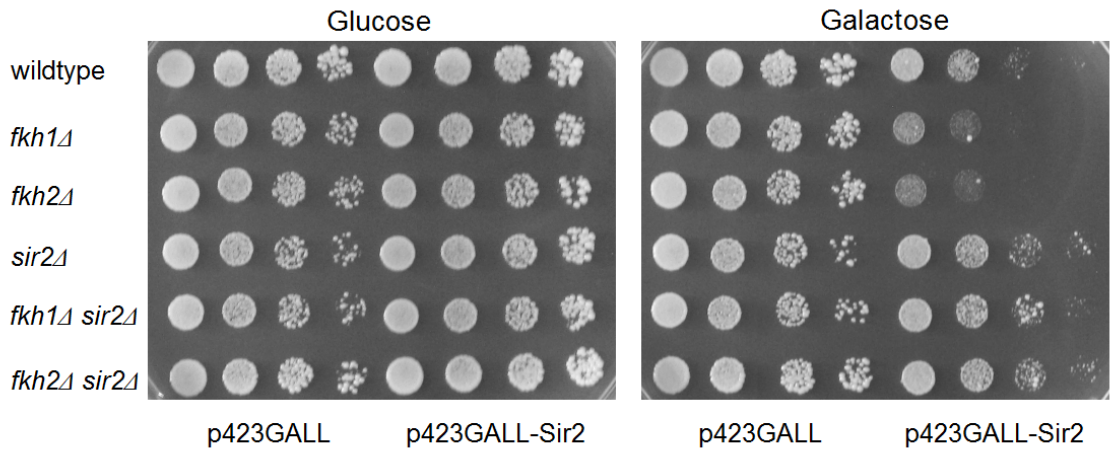

Figure 3-15. Genetic interaction between the Forkhead transcription factors Fkh1 and Fkh2 and Sir2. Wild type and deletion strains *fkh1*Δ, *fkh2*Δ, *sir2*Δ, *fkh1*Δ*sir2*Δ and *fkh2*Δ*sir2*Δ were transformed with empty vector or p423GALL-Sir2. Yeast strains were grown to mid exponential phase and spotted in serial dilutions (1:5) on glucose and galactose plates to compare viability after 3 days of incubation at 30°C under non-induced and induced conditions. The assay has been validated independently for three times.

3.2.2 Studies on physical interactions between Fkh1, Fkh2 and Sir2

Besides this genetic interaction, it was investigated next whether Sir2 physically interacts with Fkh1 and Fkh2 by performing GST pull-down experiments. For this, the ORF of *SIR2* was cloned into the plasmid pGEX6p2 and expression of GST-Sir2 was analyzed in *E. coli* as described in chapter 2.2.20. Next, bacterial expressed GST-Sir2 was immobilized on Glutathione Sepharose beads and incubated with yeast lysates generated from strains, in which Fkh1 and Fkh2 were endogenously tagged with the Myc epitope. As control, a strain was used expressing a C-terminal Myc-tagged fusion of Hcm1.

As shown in Figure 3-16, immunodetection of Fkh1-Myc (Figure 3-16A), Fkh2-Myc (Figure 3-16B) and Hcm1-Myc (Figure 3-16C) indicated their coprecipitation with GST-Sir2 (lane 4), but not with Sepharose beads alone (lane 2) or with GST-coupled resins (lane 3). Since input lysates with equal amounts of endogenously expressed proteins were loaded onto the gel and immunodetection of proteins was perfomed simultaneously, the assay could suggest higher protein levels *in vivo* for Fkh1 and Fkh2 and lower ones for Hcm1. Consistent with this observation, Fkh2 protein levels have been shown to be about 30 % of Fkh1 levels, whereas Hcm1 was found to represent only 10 % [114].

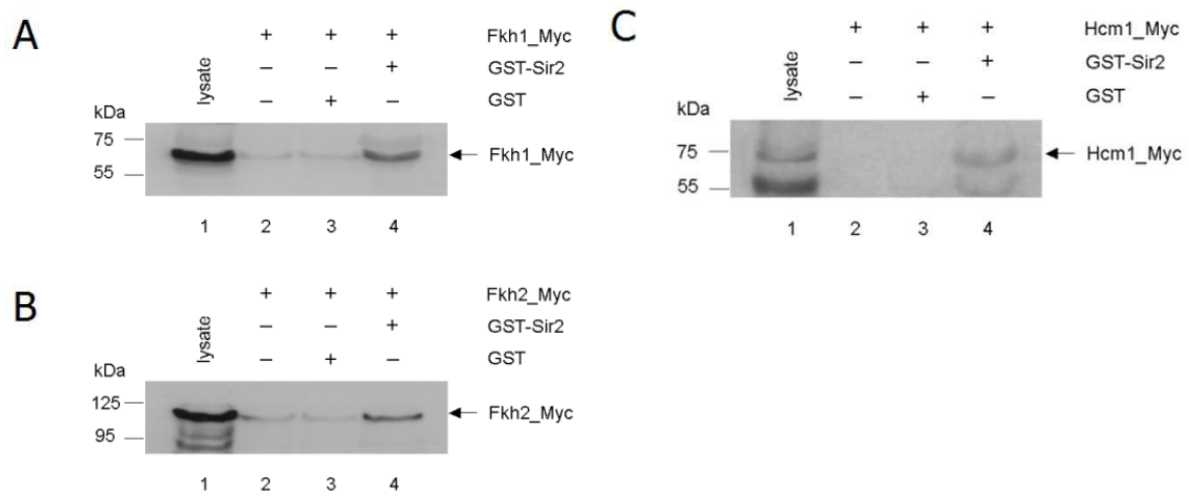

Figure 3-16. Pull-down assay between GST-Sir2 and Myc-tagged Forkhead transcription factors. GST and GST-Sir2 proteins expressed in *E. coli* were immobilized on Glutathione Sepharose beads and incubated with lysates from yeast cells endogenously expressing Myc-tagged Fkh1, Fkh2 and Hcm1. Concentrated lysates were used as a loading control (lane 1). Sepharose beads alone (lane 2) and GST-coupled resins (lane 3) were used as negative controls. Immunodetection of Fkh1-Myc **(A)**, Fkh2-Myc **(B)** and Hcm1-Myc **(C)** was performed with mouse α-Myc antibody.

To further validate the interaction between Sir2 and the Forkhead proteins Fkh1 and Fkh2, BiFC experiments were performed. To this purpose, DNA encoding the C-terminal fragment of Venus (VC) was fused to chromosomal *SIR2* by using the pFA6a-VC-KanMX6 plasmid as a template, thus generating a C-terminal tagged fusion protein Sir2-VC. In addition, the genes *HCM1* and *NDD1* were cloned into plasmid p426GPD-VN and resulting constructs p426GPD-VN-Hcm1 and p426GPD-VN-Ndd1 as well as the chromosomal integration of VC to the Sir2 locus were validated. Then, Sir2-VC expressing cells were either transformed with the plasmids p426GPD-VN-Fkh1, p426GPD-VN-Fkh2 or p426GPD-VN-Hcm1. As control, the vector p426GPD-VN-Ndd1 was transformed as well. Then, transformants were selected on appropriate medium and single clones cultured until mid logarithmic growth. Cells were fixed with ethanol, stained with DAPI and subjected to microscopy to detect fluorescent signals.

As shown in Figure 3-17, yeast cells either expressing Sir2-VC/VN-Fkh1 (upper panels), Sir2-VC/VN-Fkh2 (upper middle panels) and Sir2-VC/VN-Hcm1 (bottom middle panels) were positive for BiFC signals, which localized near to the nucleus. No signal was observed in cells coexpressing Sir2-VC/VN-Ndd1 (bottom panels), suggesting that Sir2 specifically interacts with Fkh1 and Fkh2. Moreover, BiFC signal intensity that was observed in cells expressing either Sir2-VC/VN-Fkh1, Sir2-VC/VN-Fkh2 and Sir2-VC/VN-Hcm1 differs compared to the fluorescent background of yeast cells. In particular, cells coexpressing Sir2-VC/VN-Fkh1 (upper panels) showed a strong fluorescence signal, which was slightly reduced for Sir2-VC/VN-Fkh2 (middle upper panels) and strongly decreased for the Sir2-VC/VN-Hcm1 association (middle bottom panels). Since the expression of Forkhead fusion proteins is under the control of the constitutive GPD promoter, it can be assumed that the variability in the fluorescence intensity might be due to variations in protein degradation. Specifically, Hcm1 is known to be periodically expressed between the late G1 phase and the early S phase and to undergo proteolysis in the subsequent cell cycle stages [75], whereas Fkh1 and Fkh2 are constantly bound to promoters of genes throughout cell cycle progression.

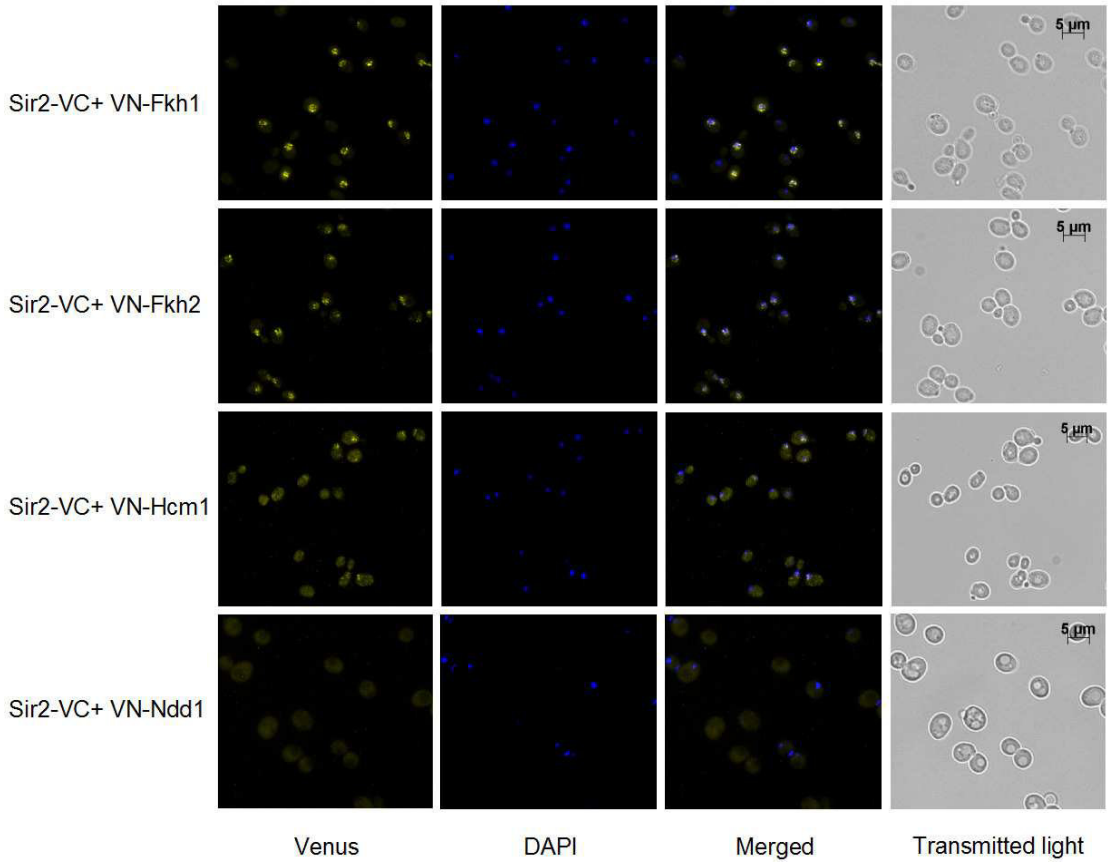

Figure 3-17. BiFC analysis of cells expressing Sir2-VC and VN-tagged transcription factors. Haploid cells expressing Sir2-VC from its endogenous promoter and VN-Fkh1 (upper panels), VN-Fkh2 (middle upper panels), VN-Hcm1 (middle bottom panels) or VN-Ndd1 (bottom panels) expressed constitutively from the p426GPD plasmid.

3.2.3 Functional analysis of the association between Sir2 and Fkh1 and Fkh2

In order to proof whether Sir2 can repress Fkh-specific gene targets, analyses based on the Y2H system were performed. Therefore, the fact that expression of LexA-tagged Forkhead proteins led to autoactivation of reporter genes was exploited. As control, the coding sequence of *HCM1* was cloned into the pBTM117c bait plasmid to generate a LexA-Hcm1 fusion protein as well. Subsequently, L40ccua yeast cells were either cotransformed with plasmids pBTM-Fkh1 and pACT-Sir2, pBTM-Fkh2 and pACT-Sir2, or pBTM-Hcm1 and pACT-Sir2. Cotransformation of empty Y2H plasmids alone or in combination with all used bait and prey constructs was used as a control in the assay. Transformants were selected and spotted in serial dilutions (1:5) on SDII and SDIV selection media to compare cell viability after five days of incubation (Figure 3-18).

Yeast cells either coexpressing LexA-Fkh1 and AD-Sir2, LexA-Fkh2 and AD-Sir2, or LexA-Hcm1 and AD-Sir2 showed a slightly reduced growth on SDII medium, indicated by the smaller colony size of respective cells compared to transformants expressing LexA-tagged Forkhead proteins alone. Interestingly, the reduction in colony size was not observed in cells expressing AD-Sir2 alone, suggesting that a genetic interaction occurs between Sir2 and Forkhead proteins as demonstrated in Figure 3-15. As expected, a strong growth on SDIV medium was detected for yeast cells expressing LexA-Fkh1 or LexA-Fkh2, indicating autoactivation of reporter genes as reported earlier. In addition, cotransformation of the plasmid pBTM-Hcm1 and the empty prey vector resulted in strong growth on SDIV medium, demonstrating that reporter gene activity is induced by expression of LexA-Hcm1 as well.

Interestingly, as compared to the respective control cells expressing LexA-tagged proteins alone, yeast cells coexpressing LexA-Fkh1 and AD-Sir2 or LexA-Fkh2 and AD-Sir2 showed reduced growth on SDIV, indicating lower reporter gene activity. In addition, this reduction was found to be more severe for cells expressing LexA-Fkh1 and AD-Sir2, suggesting that the Sir2-dependent alteration in Fkh1-promoted autoactivation of reporter genes might be stronger. However, cells coexpressing LexA-Hcm1 and AD-Sir2 showed only a slight decrease in cell growth on SDIV, suggesting a less strong repression of reporter genes.

These results demonstrated that Sir2 expression impairs cell growth on SDIV medium by repressing autoactivity of reporter genes due to an association with Fkh1 and Fkh2. Moreover, alterations in cell growth on SDIV medium caused by coexpression of LexA-Fkh1 and AD-Sir2, LexA-Fkh2 and AD-Sir2, or LexA-Hcm1 and AD-Sir2 correlate with the differences in the BiFC signal intensities observed in the microscopic analyses (Figure 3-17).

In conclusion, these findings supported a role for Fkh1 and Fkh2 in repression of target genes by recruiting the histone deacetylase Sir2.

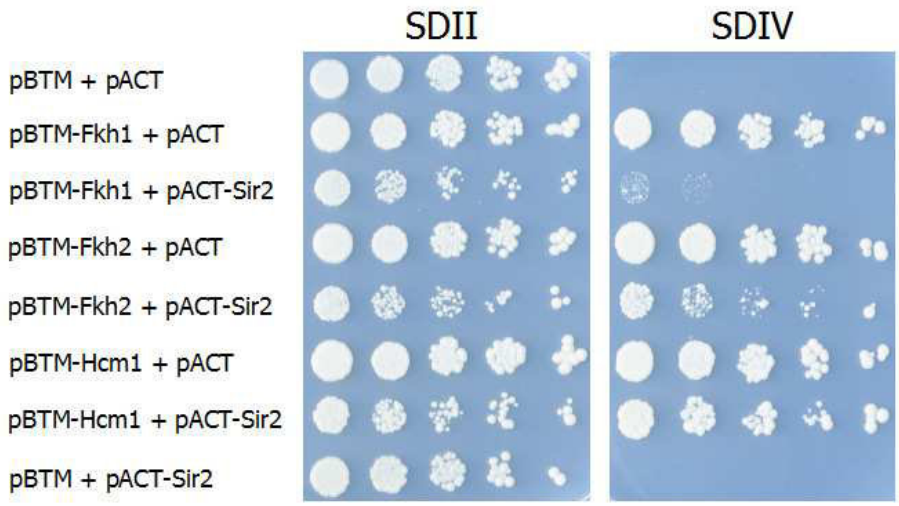

Figure 3-18. Functional analysis of the association between Sir2 and Fkh proteins using the Y2H system. Reporter gene activity of yeast cells was determined by spotting serial dilutions (1:5) onto SDIV medium lacking leucine, tryptophane, histidine, uracil and adenine (-LEU, -TRP, -HIS, -URA, -ADE). Cells grown on SDII medium lacking leucine and tryptophane (-LEU, -TRP) indicated a successful transformation of bait pBTM117c and prey pACT41b constructs. Growth of yeast cells was analyzed after 5 days of incubation at 30°C. Autoactivation of reporter genes upon expression of bait constructs alone, represented by growth of yeast colonies on SDIV medium, was used as a control. As negative controls, cells were cotransformed with either empty bait and prey plasmids as well as empty bait and pACT-Sir2.

In order to further analyze Sir2-mediated repression of Forkhead-dependent reporter gene activity, disruption of *SIR2* gene in the L40ccua strain was performed (chapter 2.2.14). Then, wild type strain and cells lacking *SIR2* were transformed with bait plasmids encoding LexA-tagged transcription factors. As a negative control, the empty bait vector was transformed into wild type strain and *sir2*Δ mutant. Transformants were selected, cultured to mid logarithmic growth in liquid SDII medium and liquid ß-galactosidase assays were carried out as detailed in chapter 2.2.15.

As shown in Figure 3-19, ß-galactosidase expression was significantly enhanced in *sir2*Δ mutants expressing LexA-Fkh1 and Lex-Fkh2 compared to wild type, suggesting a Sir2-mediated repression of the lacZ gene. Moreover, the ß-galactosidase activity was found to be increased by more than 50 % in *sir2*Δ mutants expressing LexA-Fkh2 as compared to an increase of roughly 25 % of those expressing LexA-Fkh1. As expected, wild type cells and *sir2*Δ mutants expressing LexA-Hcm1 showed almost the same ß-galactosidase activity, suggesting a less strong Hcm1/Sir2-dependent repression of the lacZ gene.

In sum, the data provide further evidence that Sir2 represses genes that are occupied by Fkh1 and Fkh2 proteins, supporting previous findings that both transcription factors have activating and repressing functions to regulate cell cycle-dependent genes as demonstrated in Figure 3-14.

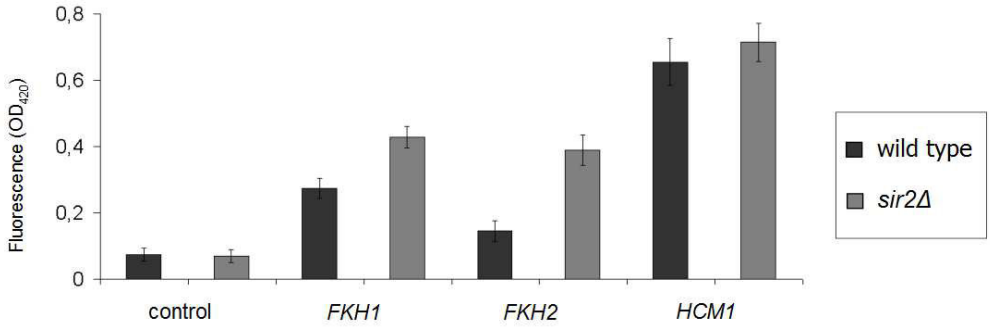

Figure 3-19. Liquid ß-galactosidase assay in wild type and *sir2*Δ cells. Protein lysates were prepared from exponentially growing cells expressing the fusion proteins LexA-Fkh1, LexA-Fkh2 or LexA-Hcm1 and absorbance at OD_{420} determined after addition of X-Gal. Cells transformed with the empty bait plasmid was used as negative controls. Each lane represents the average of data from three independent experiments.

3.2.4 *CLB2* promoter binding studies on Sir2

A Sir2-dependent role in the regulation of cell cycle-specific genes was previously discovered, demonstrating that the yeast Forkhead transcription factor Hcm1 interacts with Sir2 [114]. Furthermore, other histone deacetylases have been reported to repress *CLB2* cluster genes during G1 phase in association with Fkh2 [115]. In this light, it is quite likely that Sir2 in concert with Fkh1 and Fkh2 might play a repressive role in the cell cycle-dependent regulation of *CLB2* cluster genes.

In order to investigate this hypothesis, ChIP experiments were performed in different stages of the cell cycle to analyze the binding of Sir2 to *CLB2* promoter. To this aim, a Myc-tag at the 3' end of *SIR2* was introduced into the genome via homologues recombination. Resulting transformants were selected and verified by amplification of thte integration cassette using genomic DNA as template. Then, yeast cells endogenously expressing Sir2-Myc were cultured until mid exponential phase and growth arrest was performed by addition of α-factor (G1 phase), hydroxyurea (S phase) or nocodazole (M phase) (see chapter 2.2.18 for details). For immuno-

precipitation of Sir2-Myc, an epitope-specific antibody was used (table 2-8). Detection of coprecipitated DNA fragments was performed with quantitative real-time PCR using *CLB2* promoter-specific oligonucleotides, whereas *TSA1* and *ACT1* genes were used as controls in the assay.

As shown in Figure 3-20, a weak enrichment of *CLB2* promoter-specific DNA was observed in exponentially growing cells expressing Sir2-Myc as compared to control genes, indicating that the binding of Sir2 might be low under this condition. Interestingly, a significantly increased amplification of *CLB2* DNA relative to control genes was detected upon cell cycle arrest in G1 and M phases, strongly suggesting the binding of Sir2-Myc to the *CLB2* promoter at this stages of the cell cycle. No enrichment of *CLB2* was observed in cells synchronized in S phase, an observation that might contribute to Sir2 inactivity during intitiation of *CLB2* transcription by Fkh-dependent recruitment of coactivator Ndd1.

In conclusion, differential *CLB2* promoter occupancy of Sir2 suggests that association of histone deacetylase to Fkh proteins might be specific for G1 and M phases of the cell cycle.

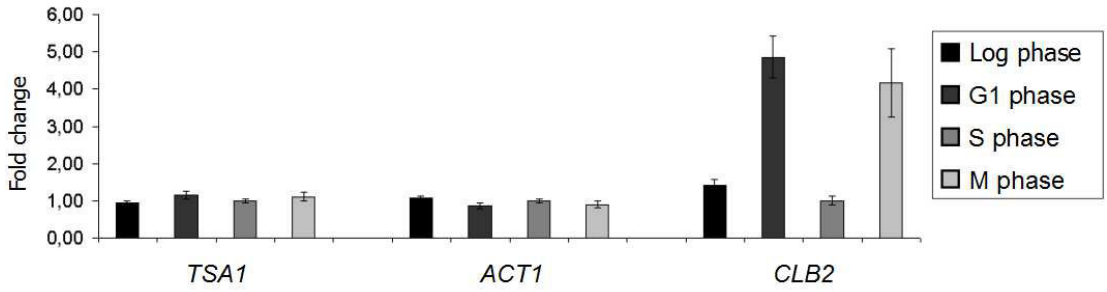

Figure 3-20. *CLB2* promoter occupancy of Sir2-Myc at different cell cycle stages. ChIP experiments were performed using anti-Myc antibodies. Protein/DNA complexes were purified from either exponential growing yeast cells or cells synchronized with α-factor (G1 phase), hydroxyurea (S phase) or nocodazole (M phase) to analyze promoter occupancy of Sir2-Myc. ChIP data representing the average of at three independent experiments were shown relative to the control genes *TSA* and *ACT1*.

3.2.5 Transcriptional analysis of *CLB2* in *sir2*Δ mutants

In the next step, the proposed influence of Sir2 in repressing *CLB2* activation was addressed on transcriptional level. If the silencing by the histone deacetylase would occur in a Fkh-dependent manner, then *CLB2* transcripts might be enhanced in cells lacking *SIR2* or altered in *sir2*Δ*fkh1*Δ and *sir2*Δ*fkh2*Δ mutants. To this purpose, wild type cells and *fkh1*Δ*, fkh2*Δ*, fkh1*Δ*fkh2*Δ*, sir2*Δ*, fkh1*Δ*sir2*Δ and *fkh2*Δ*sir2*Δ strains were grown to mid logarithmic phase and growth arrest in M phase was performed by addition of nocodazole. The DNA content of samples was determined by FACS analysis. Then, total RNA was isolated and mRNA converted to cDNA by reverse transcription and quantified by real-time PCR as described in chapter 2.2.12. For analysis of *CLB2* transcripts gene-specific oligonucleotides was used and unrelated genes *TSA1* and *ACT1* served as negative controls.

Compared to wild type, enhanced *CLB2* mRNA levels (4-fold) were detected for exponentially growing cells lacking *SIR2* (Figure 3-21A). Moreover, *CLB2* transcription was found to be increased (3-fold) in the *fkh1*Δ*sir2*Δ mutant as well. A slight increased *CLB2* mRNA level (1.5-fold) was observed in the *fkh2*Δ*sir2*Δ mutant. A decrease of *CLB2* transcription in the *fkh2*Δ*sir2*Δ mutant relative to the *sir2*Δ mutant was not expected, since exponentially grown *fkh2*Δ cells did not show an effect (please see also Figure 3-14A for details). However, differences were observed comparing the DNA content of the strains. Whereas wild type cells showed a DNA content with a higher proportion of cells in G2/M phase, the DNA profiles of *sir2*Δ*, fkh1*Δ*sir2*Δ and *fkh2*Δ*sir2*Δ strains revealed a significant increase of cells remaining in G1 phase (Figure 3-21A), indicating a delay in mitotic cell growth.

For further validation of Sir2-dependent effects on *CLB2* transcription, mRNA levels in *sir2*Δ, *fkh1*Δ*sir2*Δ and *fkh1*Δ*sir2*Δ mutants was analyzed upon synchronization with nocodazole. Metaphase-arrested cells lacking *SIR2* showed an increased *CLB2* transcription (3-fold) comparable to the increase of exponentially growing cells (Figure 3-21B). Moreover, *fkh1*Δ*sir2*Δ mutant cells showed a 3-fold higher level of *CLB2* gene-specific cDNA compared to wild type. This enrichment was observed to be approximately as high as for *sir2*Δ single deletion mutants. However, an enrichment of *CLB2* mRNA (1.5-fold) was almost absent in the *fkh2*Δ*sir2*Δ mutant as

detected for this strain in logarithmic growth phase. Of note, the DNA content of synchronized wild type cells and *sir2*Δ, *fkh1*Δ*sir2*Δ and *fkh2*Δ*sir2*Δ mutants did not show significant differences in their profiles (Figure 3-21B).

Taken together, these data indicated that *CLB2* repression could be promoted by Sir2 via a mechanism involving a direct recruitment on Fkh transcription factors. In particular Fkh1 could be more relevant for Sir2-mediated repression, whereas Fkh2 might be associated to a higher degree to Ndd1-dependent transactivation of *CLB2*. Consistent with this assumtion, a decrease in the transcription of *CLB2* upon metaphase arrest was detected in the *fkh2*Δ mutant compared to wild type (Figure 3-14B) as well as in *fkh2*Δ*sir2*Δ mutants relative to the single deletion strain *sir2*Δ (Figure 3-21B).

To further verify the proposed repressive function of Sir2 in G1 phase, which is indicated by the *CLB2* promoter occupancy of Sir2-Myc at this phase, wild type cells and deletion strains should be synchronized by addition of α-factor. Unfortunately, multiple efforts to synchronize *sir2*Δ cells failed (data not shown). However, consistent with this finding, a complete absence of pheromone-induced arrest in *sir2*Δ mutants was reported previously [244].

A

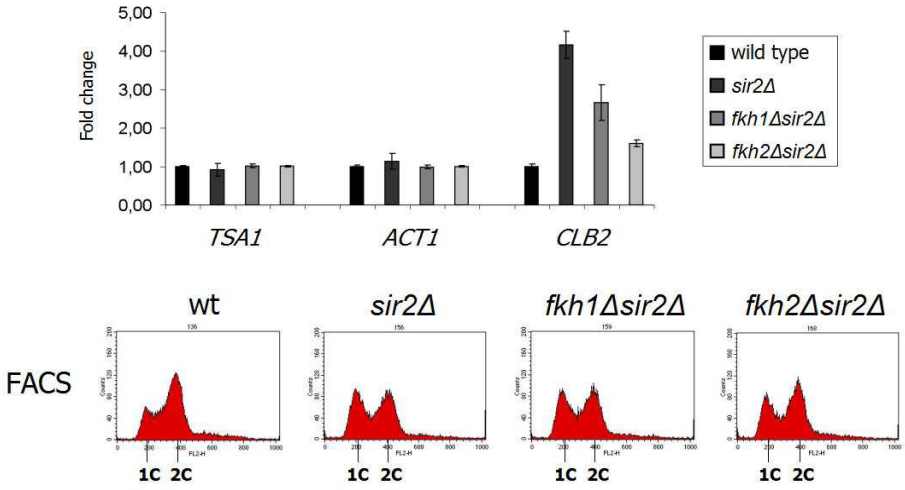

B

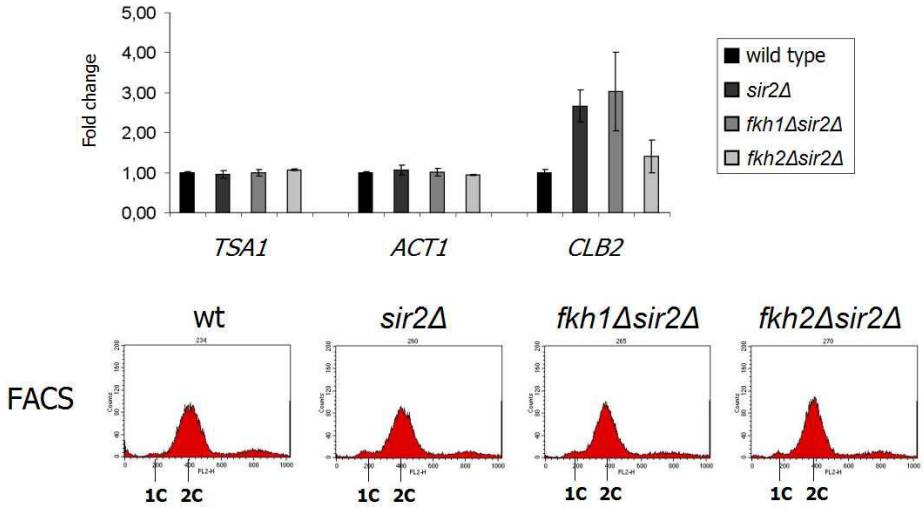

Figure 3-21. Real-time PCR for quantification of *CLB2* transcript levels in *sir2*Δ, *fkh1sir2*Δ and *fkh2sir2*Δ strains. Total RNA was isolated from exponentially growing cells **(A)** and nocodazole-arrested cells **(B)**. cDNA was obtained and analyzed by quantitative real-time PCR. The average of values obtained from three independent experiments was normalized to wild type and *TSA1* and *ACT1* genes were used as negative controls. DNA content was determined by FACS analysis.

3.2.6 Comparison of cell cycle-dependent interaction between Fkh proteins and putative coregulators Ndd1 and Sir2

The timing of the Ndd1-Fkh2 association from S until early M phase correlates with transcription of *CLB2* cluster [21]. Interestingly, the histone deacetylase Sin3 is directly recruited to the *CLB2* promoter region through association with the FHA domain of Fkh2 during late M and G1 phases of the cell cycle [115]. Since the activation of Fkh-controlled genes depends on the association between the coactivator Ndd1 and Fkh1/Fkh2, the results in this study suggests that the repression of these genes in turn depends on the interaction between Sir2 and Fkh1/Fkh2, suggesting that both interactions might counteract each other.

To investigate this, the interaction between Fkh2 and Ndd1 and between Fkh1 and Sir2 was monitored in different cell cycle stages by using the BiFC technique. Strains carrying genomic integrations of Ndd1-VC or Sir2-VC were transformed with p426GPD-VN-Fkh2 or p426GPD-VN-Fkh1 plasmids, respectively. Then, cells were cultured until mid logarithmic phase and growth arrest was performed by addition of

α-factor (G1 phase), hydroxyurea (S phase) or nocodazole (M phase) to the medium. Yeast strains were subsequently analyzed at the microscope for the BiFC signal.

As shown in Figure 3-22, α-factor-arrested cells coexpressing Sir2-VC and VN-Fkh1 showed a BiFC signal in G1 phase, whereas no fluorescent signal was observed in cells expressing Ndd1-VC and VN-Fkh2. Interestingly, distinct BiFC signals appeared for Ndd1-VC/VN-Fkh2 in cells synchronized in S phase, but not in cells coexpressing Sir2-VC and VN-Fkh1. These findings suggest a mutual exclusive binding of Ndd1 and Sir2 to Forkhead proteins Fkh1 and Fkh2 during these cell cycle stages. However, the coexistence of both interactions in M phase-arrested cells, as indicated by the BiFC signal for both Ndd1-VC/VN-Fkh2 and Sir2-VC/VN-Fkh1, suggested a time window where Ndd1 and Sir2 might displace each other or simultaneously occupy the promoter of target genes.

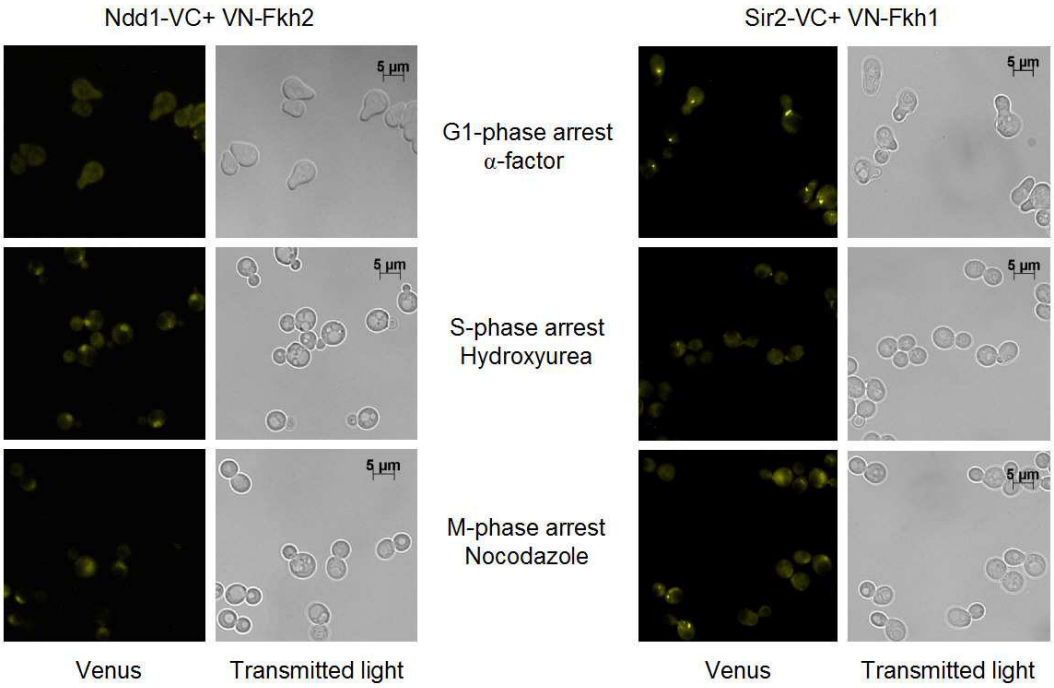

Figure 3-22. Visualization of the interactions Ndd1-VC/VN-Fkh2 and Sir2-VC/VN-Fkh1 in different cell cycle stages. Haploid cells endogenously expressing Ndd1-VC were transformed with plasmid p426GPD-VN-Fkh2 (left panels) or cells endogenously expressing Sir2-VC was transformed with the plasmid p426GPD-VN-Fkh1 (right panels). BiFC signals indicating association between Ndd1-VC and VN-Fkh2 or Sir2-VC and VN-Fkh1 was analyzed in cells arrested in G1 phase (upper panels), S phase (middle panels) and M phase (bottom left panels).

In conclusion, the analysis of BiFC-dependent interactions between Fkh2 and its coactivator Ndd1 and between Fkh1 and Sir2 confirmed the assumption that Forkhead transcription factors might act as a platform to recruit both the coactivator Ndd1 and the histone deacetylase Sir2 in an timely independent manner.

Based on these findings, the cell cycle-dependent recruitment of Ndd1 and Sir2 to the Forkhead proteins Fkh1 and Fkh2 was analyzed in more detail. For this, both interactions were visualized in time throughout the cell cycle using the BiFC method. Yeast cells coexpressing BiFC constructs Ndd1-VC/VN-Fkh2 and Sir2-VC/VN-Fkh1 were inoculated in liquid CSM selection media and synchronized in G1 phase with α-factor. Then, cells were transferred to fresh selection medium and samples were collected every 10 min and analyzed for the presence of BiFC signal by fluorescence microscopy. Cell growth of both strains was monitored for 2 hours and DNA content of samples determined by FACS analysis. Pictures illustrating the Fkh-dependent recruitment of Ndd1 and Sir2 in time are shown in Figure 3-23.

Yeast cells coexpressing Ndd1-VC and VN-Fkh2 showed no BiFC signal until S phase (~ 30 min), whereas a BiFC signal associated with Sir2/Fkh1 was clearly detectable during this time window, which disappeared after 30 min. Moreover, the Sir2/Fkh1 signals was almost absent until 70 min. However, a peak was observed in late M phase and especially during the next G1 phase (80-100 min), whereas the Ndd1/Fkh2 signal raised after 30 min and disappeared at 70-100 min. Therefore, the association between Ndd1/Fkh2 and Sir2/Fkh1 are complementary throughout cell cycle phases. However, consistent with the analysis reported for M phase arrest, an overlap of both interactions was observed at the end of the cell cycle.

Taken together, the observed BiFC signals peaked at different time points during a complete cell cycle highlighting the mutual exclusive binding of coregulator Ndd1 and the putative corepressor Sir2 to Forkhead proteins.

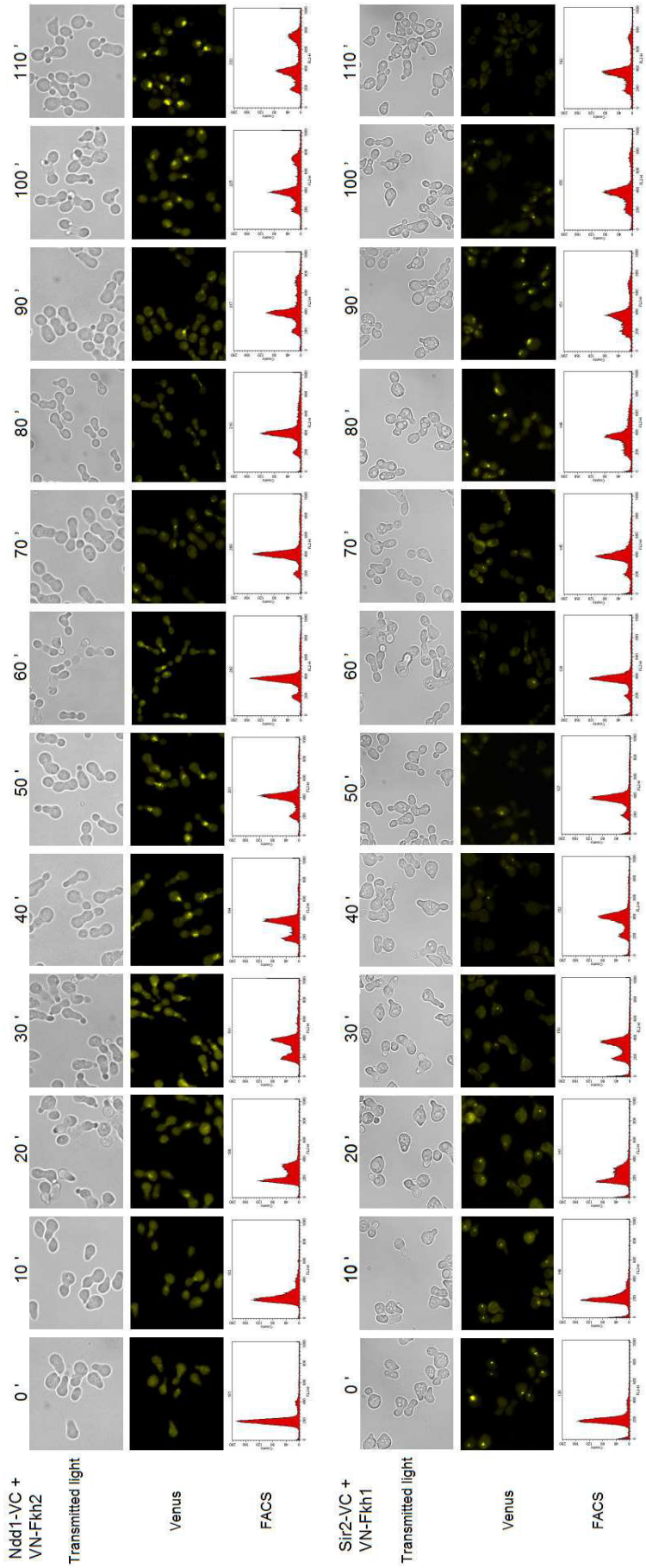

Figure 4-23. Time course analysis of the interaction between Ndd1-VC/VN-Fkh2 or Sir2- VC/VN-Fkh1. Haploid cells endogenousley expressing either Ndd1-VC or Sir2-VC were transformed with plasmids p426GPD-VN-Fkh2 or p426GPD-VN-Fkh1, respectively and synchronized with α-factor. Samples were collected every 10 min and analyzed at the microscope for the BiFC signals. DNA content of samples was determined by propidium iodide staining and FACS analysis.

3.2.7 Fkh1, Fkh2 and Sir2 mediate stress resistance in yeast

The S phase-specific Forkhead transcription factor Hcm1 was reported to be involved in the activation of genes that regulate oxidative stress resistance, and nuclear localization of Hcm1 has been shown to be dependent on Sir2 activity [114]. Furthermore, it has been previously reported that induction of oxidative stress in yeast by exposing cells to hydrogen peroxide (H_2O_2) and menadione (MD) resulted in a Fkh-dependent cell cycle arrest [245]. In particular, H_2O_2 treatment delays mitotic cell growth in S phase followed by G2/M arrest, whereas MD arrests cells in G1 phase [245, 246, 247]. Strikingly, oxidative stress treatment was shown to increase Sir2 protein levels [224].

Due to the findings that Sir2 overexpression resulted in a reduction of cell growth (Figure 3-15) and Sir2 was found to be involved in the repression of the main mitotic cyclin gene *CLB2* especially in late M and G1 phases (Figure 20-21), a potential relationship between Sir2 and Forkhead transcription factors to mediate stress response in yeast was suggested. Therefore, it was first aimed to investigate whether Forkhead proteins and Sir2 potentially share common pathways that effect the growth of yeast cells in exposure to oxidants that cause the intracellular accumulation of reactive oxygen species (ROS). To this purpose, wild type cells and *fkh1*Δ, *fkh2*Δ, *fkh1*Δ*fkh2*Δ, *sir2*Δ, *fkh1*Δ*sir2*Δ and *fkh2*Δ*sir2*Δ mutants were grown over night until saturation and spotted in serial dilutions (1:5) on solid CSM medium with 2 mM H_2O_2 or 40 µM menadione (MD). After three days of incubation, viability of cells was monitored comparing number and size of yeast colonies grown under normal or under stress conditions.

A reduced growth of all yeast strains was observed in the presence of oxidants compared to control plates (Figure 3-24). However, reduction of the colony size was less obvious in the *fkh1*Δ*fkh2*Δ mutant treated with H_2O_2 and MD. Interestingly, a reduction in the number of yeast colonies on medium containing H_2O_2 was observed for *fkh2*Δ, *sir2*Δ, *fkh1*Δ*sir2*Δ and *fkh2*Δ*sir2*Δ mutants compared to wild type cells. Moreover, this reduction was found to be stronger in the *sir2*Δ deletion strain, whereas the colony number of *fkh2*Δ*sir2*Δ and especially *fkh1*Δ*sir2*Δ cells was higher compared to *sir2*Δ cells. This observation demonstrates that both Fkh1 and

Fkh2 are functional related to Sir2 in response to oxidative stress. Nevertheless, only slight differences in cell growth was observed in the presence of MD. Interestingly, a slight reduction in the number of colonies was detected in *fkh2*Δ, *sir2*Δ and *fkh2*Δ*sir2*Δ mutants, whereas *fkh1*Δ*sir2*Δ cells showed a growth rescue compared to *sir2*Δ cells.

In sum, oxidative stress reduces mitotic cell growth of yeast cells. This effect seemed to be less for *fkh1*Δ*fkh2*Δ cells, indicating a relevance for both Forkhead proteins in mediating growth arrest in response to oxidative stress. In addition, Sir2 was oserved to be relevant for stress resistance, in agreement with its known antioxidant properties [114, 224], since deletion of *SIR2* significantly reduces number of yeast colonies. Importantly, the lethality of *sir2*Δ cells in the presence of oxidants was rescued in a *fkh1*Δ*sir2*Δ strain, suggesting their functional connection in mediating oxidative stress response.

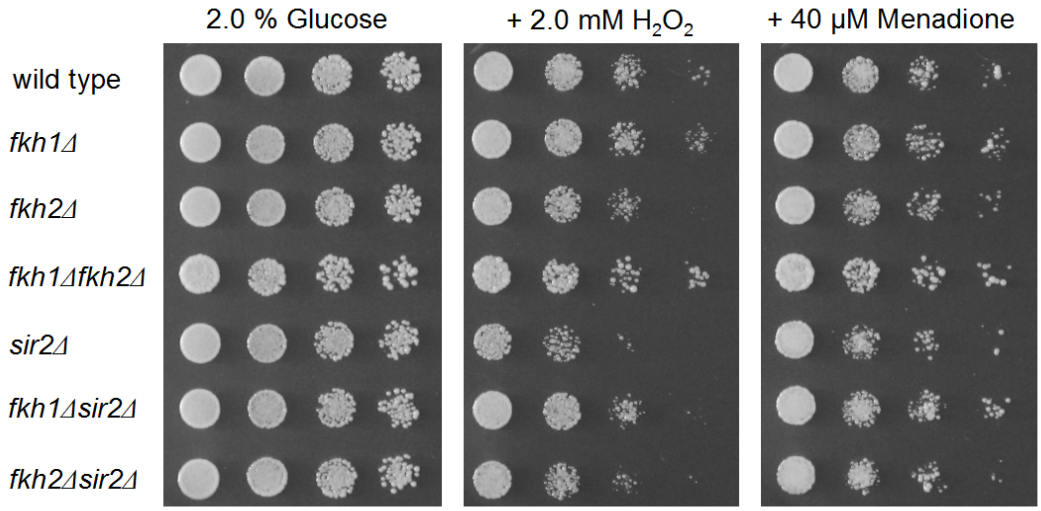

Figure 3-24. Growth of *fkh1*Δ, *fkh2*Δ, *fkh1*Δ*fkh2*Δ, *sir2*Δ, *fkh1*Δ*sir2*Δ and *fkh2*Δ*sir2*Δ strains upon oxidative stress. Yeast clones were pre-grown to saturation in YPD and spotted in serial dilutions (1:5) on CSM medium containing 2 % glucose (control) as well as 2 mM H_2O_2 or 40 µM menadione (MD). Cell growth was analyzed after 3 days of incubation at 30°C. The assay has been validated independently for three times.

3.2.8 Analysis of the association between Fkh proteins and the coregulators Ndd1 and Sir2 in response to stress

Growth analysis of deletion strains upon oxidative stress revealed a strong genetic interaction between the Forkhead proteins Fkh1, Fkh2 and Sir2. In this light, it was

aimed to examine the influence of oxidative stress on the physical interaction between Fkh proteins and Ndd1 or Sir2, respectively. Since the deletion of both *FKH1* and *FKH2* has been shown to impede normal lifespan and stress resistance of yeast cells, particularly in stationary phase [248], these interactions were analyzed under H_2O_2 or MD treatment as well as in stationary phase. As an important characteristic of stationary phase, cells undergo a metabolic switch from fermentation to respiration, thus creating a mild oxidative stress situation due to nutrient depletion [249-251].

In order to visualize the association between Fkh proteins and Ndd1 or Sir2 under stress conditions, BiFC signals for cells coexpressing the fusion proteins Ndd1-VC and VN-Fkh2 as well as Sir2-VC and VN-Fkh1 were monitored upon treatment with either 2 mM H_2O_2 or 40 µM MD and at stationary phase (OD_{600} = 1.5). As a control, both interaction pairs were analyzed in mid logarithmic growth (OD_{600} = 0.6).

As shown in Figure 3-25, exponentially growing cells coexpressing Sir2-VC and VN-Fkh1 (upper left panels) or Ndd1-VC and VN-Fkh2 (upper right panels) showed BiFC signals, indicating an interaction. However, the number of cells showing fluorescent signals for the interaction between Fkh1 and Sir2 was significantly lower compared to the number of cells indicating BiFC signals for the interaction between Fkh2 and Ndd1. Compared to logarithmic cell growth, BiFC signals appeared in almost all stationary cells coexpressing Sir2-VC and VN-Fkh1, whereas distinct Venus fluorescence indicating an association between Ndd1 and Fkh2 was not detected under this condition.

Moreover, a BiFC signal associated with the Sir2-VC/VN-Fkh1 interaction appeared in the majority of cells treated with H_2O_2 or MD. Although BiFC signals indicating the Ndd1-VC/VN-Fkh2 interaction were detectable especially in cells treated with H_2O_2, the fluorescence was less strong and more diffuse compared to untreated cells. A decrease in the BiFC signal associated with the Ndd1-VC/VN-Fkh2 interaction was observed in particular after treatment with menadione.

In conclusion, a comparison of BiFC signals showed a strong association between Sir2 and Fkh1, but no interaction between Ndd1 and Fkh2 in stationary cells. This result is in agreement with the fact that stationary cells are known to remain in a

postmitotic nondividing phase, thus explaining the dispensability of Ndd1-mediated cell cycle progression. Moreover, a significantly higher proportion of cells showed an association between Fkh1 and Sir2 in the presence of oxidants. A decrease in the BiFC signal associated to the Ndd1-VC/VN-Fkh2 interaction was observed in particular after treatment with menadione. Consistently, it has been reported that menadione-treated yeast cells arrest in G1 phase [245-247]. In this light, the impairment of the Ndd1/Fkh2 interaction in response to oxidative stress suggested that progression throughout the cell cycle might be slower compared to untreated cells. Indeed, a reduced growth of cells was observed on medium containing either H_2O_2 or MD (Figure 3-25).

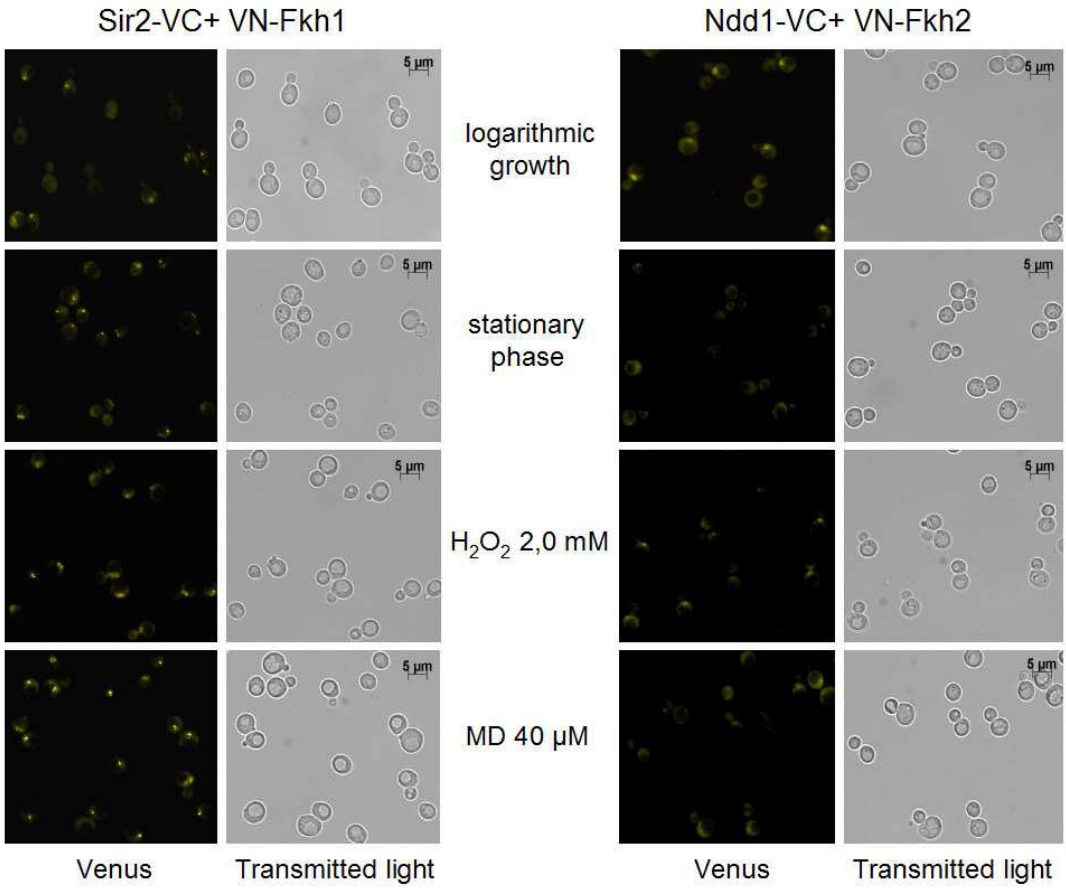

Figure 3-25. Visualization of BiFC signals in cells coexpressing Ndd1-VC/VN-Fkh2 or Sir2-VC/VN-Fkh1 in exponential, stationary growth or under oxidative stress. Haploid cells edogenously expressing Ndd1-VC or Sir2-VC were transformed with p426GPD-VN-Fkh2 or p426GPD-VN-Fkh1 plasmids, respectively. Yeast cells were analyzed for BiFC signals in exponential (OD_{600} = 0.6), stationary growth (OD_{600} = 1.5) or in presence of 2 mM H_2O_2 or 40 µM menadione (MD).

3.2.9 Studies on stress-dependent *CLB2* promoter occupancy by Sir2

Considering that the association between Fkh1 and Sir2 might be stronger under stress conditions, it is likely to hypothesize that Sir2 occupancy at promoters of Fkh-controlled genes might be enhanced in stationary cells or in presence of oxidants like H_2O_2. To address this question, ChIP experiments were performed. Yeast cells endogenously expressing Myc-tagged Sir2 were grown until exponential phase (OD_{600} = 0.6). Then, H_2O_2 was added to a final concentration of 2 mM. In addition, the Sir2-Myc expressing strain was incubated over night until saturation (OD_{600} = 1.5). Immunoprecipitation was performed using an epitope-specific antibody and enrichment at the gene promoter of *CLB2* quantified by real-time PCR as described previously. *TSA1* and *ACT1* were used as negative controls.

An enrichment of *CLB2* promoter-specific DNA was observed in stationary cells and in cells treated with H_2O_2, compared to exponentially growing cells (Figure 3-27). Surprisingly, this enrichment was found to be slightly higher for cells exposed to oxidant. This observation was not expected since the BiFC analysis of cells expressing Ndd1-VC and VN-Fkh2 showed fluorescent signals, whereas this signal was absent in cells grown to stationary phase. However, this observation indicates a binding of the histone deacetylase Sir2 to the promoter of *CLB2* and is consistent with the interaction analysis between Sir2 and Fkh1 obtained by using the BiFC technique. Distinct fluorescent signal was observed in the majority of yeast cells expressing Sir2-VC and VN-Fkh1 (Figure 3-25), and this result potentially correlates with *CLB2* promoter occupancy of Sir2.

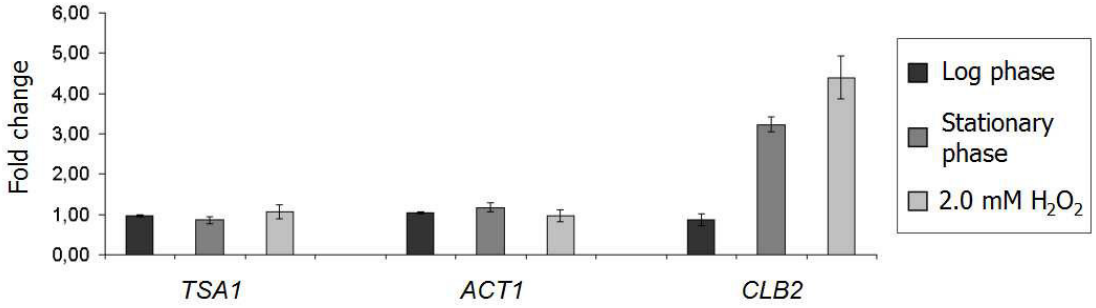

Figure 3-27. *CLB2* promoter occupancy of Sir2-Myc in exponential, stationary phase or after H_2O_2 treatment. Haploid cells were grown to exponential (OD_{600} = 0.6), stationary phase (OD_{600} = 1.5) or treated with 2 mM H_2O_2. Experiments were performed using protein extracts containing a C-terminal Myc-tagged Sir2 expressed from its native promoter. ChIP was carried out using anti-Myc antibodies and the average of three independent experiments is shown. *TSA1* and *ACT1* were used as negative controls.

Based on these findings, Sir2-dependent silencing of *CLB2* expression in response to stress conditions might be a potential mechanism to regulate mitotic growth of yeast cells.

In the next step, it was aimed to investigate whether the binding of Sir2 to the *CLB2* promoter under stress conditions was based on Fkh1 and Fkh2. To this purpose, genomic Myc-tagged Sir2 was generated in *fkh1*Δ and *fkh2*Δ mutants by transforming the respective integration cassette. Transformants were selected and analyzed for the expression of Sir2-Myc. Verified strains were grown until stationary phase (OD_{600} = 1.5) and ChIP experiments performed using anti-Myc antibodies. Immunoprecipitation of *CLB2* promoter DNA was quantified by real-time PCR and genes *TSA1* and *ACT1* were used as controls.

As shown in Figure 3-28, a decrease in the enrichment of *CLB2* promoter DNA was observed in cells lacking either *FKH1* or *FKH2* compared to the control strain.

In sum, this result indicates that both Forkhead proteins Fkh1 and Fkh2 might be involved in the recruitment of Sir2 to the *CLB2* promoter.

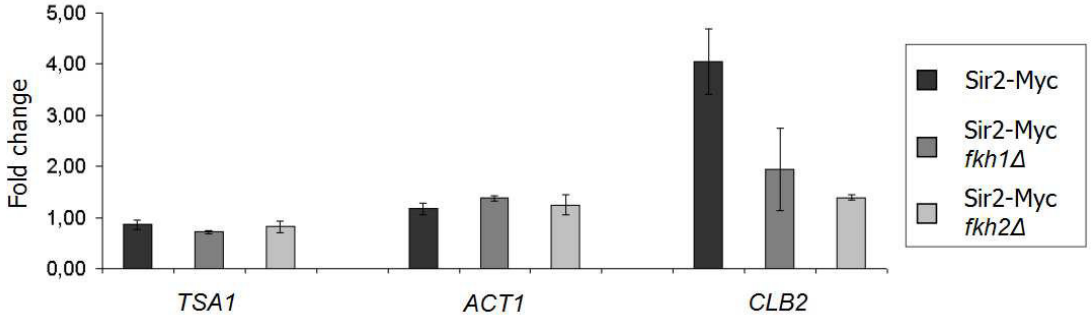

Figure 3-28. *CLB2* promoter occupancy of Sir2-Myc in *fkh1*Δ and *fkh2*Δ cells. Haploid cells containing a C-terminal tagged Sir2-Myc in wild type and *fkh1*Δ or *fkh2*Δ mutant background were grown to stationary phase (OD_{600} = 1.5) and ChIP experiments performed using anti-Myc antibodies. Data representing the average of three independent experiments were normalized to control genes *TSA1* and *ACT1*.

3.2.10 Role of Fkh1, Fkh2 and Sir2 in expression of *CLB2* under stress

To provide further evidence for a role of Sir2 in the Fkh-mediated regulation of cell cycle under stress conditions, alterations in the expression level of *CLB2* in the absence of *FKH1*, *FKH2* and *SIR2* as well as their corresponding double deletion

mutants were investigated. For this aim, wild type and *fkh1*Δ*, fkh2*Δ*, fkh1*Δ*fkh2*Δ*, sir2*Δ*, fkh1*Δ*sir2*Δ and *fkh2*Δ*sir2*Δ strains were grown until mid exponential phase (OD_{600} = 0.6) or until stationary phase (OD = 1.5). Cells in exponential growth were treated with H_2O_2. Total RNA was extracted from wild type and deletion strains, transcribed to cDNA and quantified by real-time PCR as described previously. In parallel, the DNA content was determined by FACS analysis. For analysis of *CLB2* transcripts, gene-specific oligonucleotides were used and genes *TSA1* and *ACT1* as controls.

Interstingly, an increase in *CLB2* transcript levels was observed for the *fkh1*Δ*fkh2*Δ mutant treated with H_2O_2 in comparison to wild type cells (Figure 3-28A). Moreover, the deletion of *SIR2* causes a slight increase in *CLB2* transcripts comparable with the *CLB2* level of *fkh1*Δ and *fkh2*Δ deletion mutants. No significant alteration in *CLB2* mRNA was observed in *fkh1*Δ*sir2*Δ and *fkh2*Δ*sir2*Δ cells. However, differences were observed comparing the DNA content of all strains. In fact, whereas wild type, *fkh1*Δ and *fkh2*Δ cells showed a DNA content of cells arrested in M phase (Figure 3-14B), DNA profiles of *sir2*Δ*, fkh1*Δ*sir2*Δ and *fkh2*Δ*sir2*Δ mutants resembled characteristics of exponentially growing cells (Figure 3-14A). This observation suggests mitotic cell divisions in the absence of H_2O_2-mediated growth arrest.

Higher *CLB2* mRNA levels in stationary *fkh2*Δ, *fkh1*Δ*fkh2*Δ and *sir2*Δ cells were detected compared to the wild type strain (Figure 3-28B). Interestingly, the increase in *CLB2* mRNA levels detected in the *fkh1*Δ*fkh2*Δ mutant was more significant and comparable with the one observed after H_2O_2 treatment. Moreover, a slight enrichment in transcript levels was detected in the *fkh1*Δ*sir2*Δ mutant. Interestingly, an increased C*LB2* transcription in *fkh2*Δ cells was not detected in the *fkh2*Δ*sir2*Δ mutant. A comparison of the FACS profiles of wild type and deletion strains revealed a slight reduction in the G1 phase-specific DNA content for *sir2*Δ, *fkh1*Δ*sir2*Δ and *fkh2*Δ*sir2*Δ.

In conclusion, a strong increase in *CLB2* transcription in *fkh1*Δ*fkh2*Δ mutants supports the assumption that both Forkhead proteins are involved in the transcriptional repression of *CLB2* as previously suggested for cells arrested in G1 phase. Furthermore, *fkh2*Δ and *sir2*Δ mutants showed only a slight increase in *CLB2* transcripts, indicating the involvement of other coregulators.

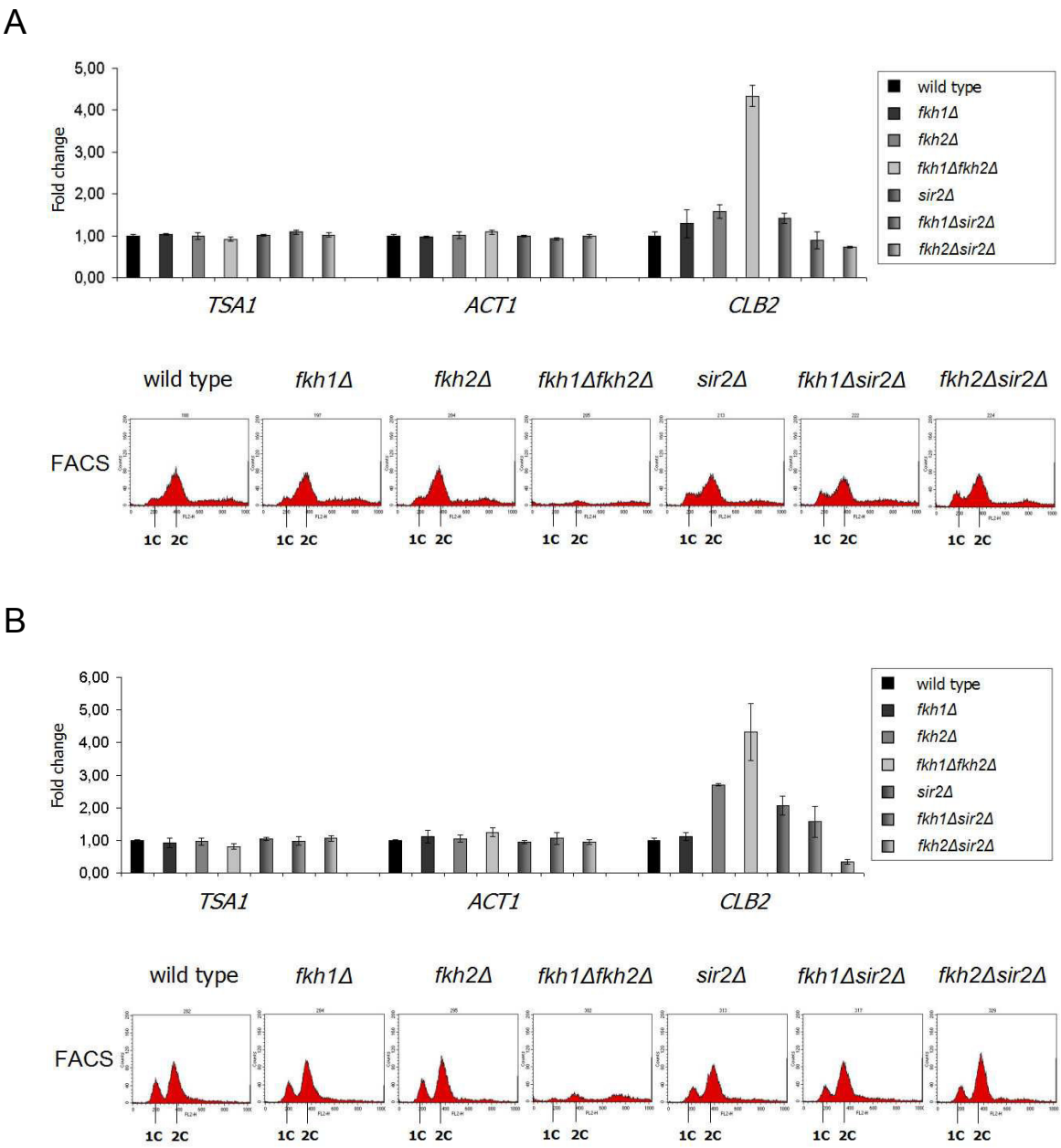

Figure 3-28. Real-time PCR analysis of *CLB2* transcript levels upon H_2O_2 treatment or stationary phase in wild type and *fkh1*Δ, *fkh2*Δ, *fkh1*Δ*fkh2*Δ, *sir2*Δ, *fkh1*Δ*sir2*Δ and *fkh2*Δ*sir2*Δ strains. (A) Total RNA was prepared from exponentially growing cells (OD = 0.5) incubated with 2 mM H_2O_2 for 90 min. **(B)** Total RNA was prepared from cells grown to stationary phase (OD_{600} = 1.5). In all experiments, cDNA was generated and analyzed by quantitative real-time PCR. The average of two independent experiments was normalized to wild type. *TSA1* and *ACT1* were used as negative controls. DNA content was determined by propidium iodide staining followed by FACS analysis.

In a second step, it was aimed to investigate whether alterations in *CLB2* transcription under stress conditions can be detected on the protein level as well. Therefore, protein extracts of wild type cells, *fkh1*Δ, *fkh2*Δ, *fkh1*Δ*fkh2*Δ, *sir2*Δ, *fkh1*Δ*sir2*Δ and *fkh2*Δ*sir2*Δ mutants were analyzed by western blot. Cells were

grown either to exponential phase (OD = 0.6) and treated with 2 mM H_2O_2 or incubated until stationary phase (OD = 1.5). Protein extracts were isolated, separated by SDS-PAGE, transferred to nitrocellulose membranes and Clb2 protein was detected using a protein-specific antibody as described in more detail in chapter 2.2.23-25.

As shown in Figure 3-29 (upper panel), exponentially grown *fkh1*Δ*fkh2*Δ cells showed a strong reduction of the Clb2 protein level compared to wild type cells. Interestingly, the level of Clb2 in *sir2*Δ*,* *fkh1*Δ*sir2*Δ and *fkh2*Δ*sir2*Δ mutants was slightly higher compared to wild type strain. Moreover, Clb2 protein level was weakly enhanced in lysates prepared from *fkh1*Δ cells. No differences in Clb2 levels was observed comparing wild type and *fkh2*Δ cells, highlighting the fact that Fkh1 can mediate expression of genes in the absence of *FKH2*.

Interestingly, analysis of protein level in *fkh1*Δ*fkh2*Δ cells treated with H_2O_2 revealed a strong enrichment of Clb2 compared to wild type cells (Figure 3-29 middle panel). A moderate increase of Clb2 levels relative to wild type cells was observed in *fkh2*Δ and *sir2*Δ mutants. No differences in the amount of Clb2 was detected between wild type and *fkh1*Δ. The Clb2 protein level of *fkh1*Δ*sir2*Δ and *fkh2*Δ*sir2*Δ cells was slightly lower compared to wild type, indicating their functional interconnection.

As shown in Figure 3-29 (bottom panel), a strong epitope-specific stain was observed in *fkh1*Δ*fkh2*Δ mutants compared to wild type. However, an increased amount of Clb2 was detected in *fkh2*Δ and *sir2*Δ mutants as well that was comparable with the Clb2 level of *fkh1*Δ*fkh2*Δ cells. Compared to wild type, a slight increase in Clb2 protein level was observed in *fkh1*Δ cells. No significant alterations in Clb2 level was observed in wild type, *fkh1*Δ*sir2*Δ and *fkh2*Δ*sir2*Δ cells.

Taken together, the results obtained from the protein analyses in exponential phase is consistent with the transcriptional analysis of *CLB2*. In particular, a strong reduction in *CLB2* transcripts in *fkh1*Δ*fkh2*Δ cells (Figure 3-14A) was detected on the Clb2 protein level as well. Furthermore, a higher amount of *CLB2* transcripts in exponentially grown *sir2*Δ*,* *fkh1*Δ*sir2*Δ and *fkh2*Δ*sir2*Δ mutants (Figure 3-21A) correspond to the analysis of Clb2 protein levels.

In addition, the detection of *CLB2* protein levels in wild type cells and deletion

mutants grown to stationary phase partially displayed similarities with the results obtained for cells treated with H_2O_2. In agreement with the analysis of *CLB2* transcripts indicated in Figure 3-28, a higher Clb2 level in *fkh2*Δ, *fkh1*Δ*fkh2*Δ and *sir2*Δ mutants under both stress conditions further validates the proposed function of Fkh1, Fkh2 and Sir2 to repress *CLB2* transcription not only during G1 phase but also under stress conditions. However, increased Clb2 mRNA levels that was observed in stationary *fkh2*Δ and *sir2*Δ cells as indicated in Figure 3-28B was not as high as in the *fkh1*Δ*fkh2*Δ.

In sum, these findings strongly suggest a direct involvement of Sir2 in the cell cycle regulation mediated by Fkh1 and Fkh2 transcription factors.

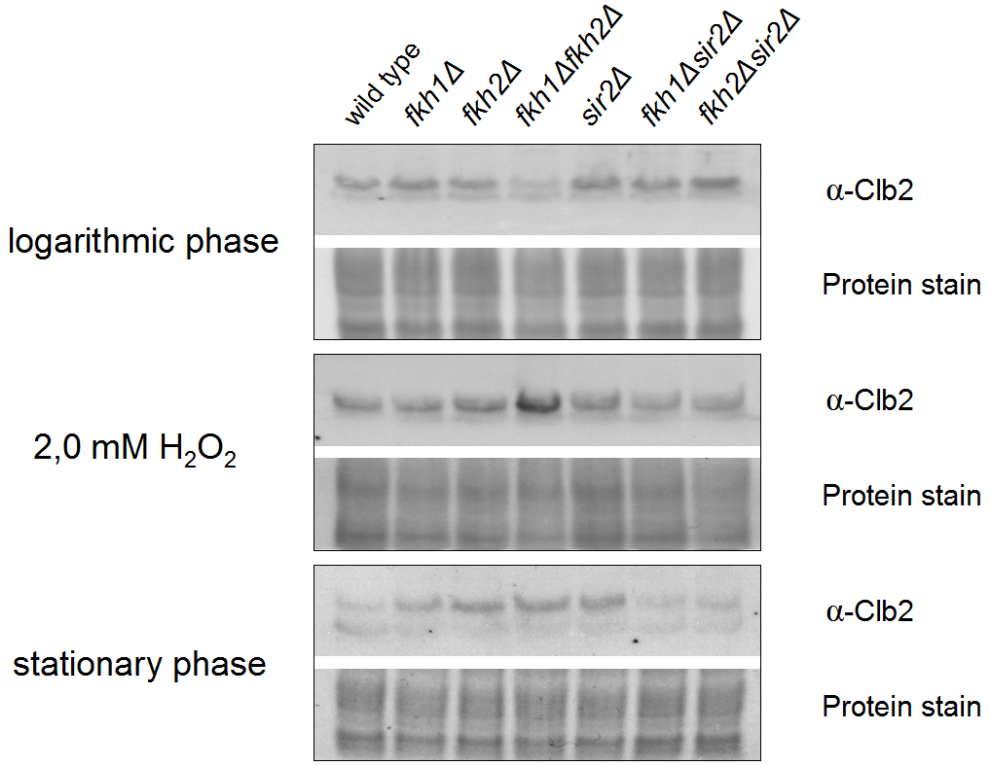

Figure 3-29. Clb2 levels in wild type and *fkh1*Δ, *fkh2*Δ, *fkh1*Δ*fkh2*Δ, *sir2*Δ, *fkh1*Δ*sir2*Δ and *fkh2*Δ*sir2*Δ strains grown to exponential phase, stationary phase or arrested upon H_2O_2 treatment. Protein extracts were isolated from exponential growing cells (OD_{600} = 0.5) (upper panels) or cells incubated with 2 mM H_2O_2 for 90 min (middle panels) as well as cells grown to stationary phase (OD_{600} = 1.5) (bottom panels), and Clb2 levels were determined by western blot using α-Clb2 specific antibody. Coomassie Brilliant Blue protein staining was used as a loading control.

3.3 Role of Forkhead proteins and Sir2 in a yeast Huntington's disease model

The understanding of molecular mechanisms contributing to neuronal degeneration in Huntington's disease (HD) has been advanced over the last decades, but remains far from being complete. In this light, *Saccharomyces cerevisiae* has become an important model organism to study huntingtin-induced toxicity and aggregation of polyglutamine proteins [252-254]. Global genetic approaches performed in yeast led to the identification of genes modifying mutant huntingtin (HTT) toxicity, thereby presenting promising targets for therapeutic intervention. Importantly, the mechanisms of polyQ-aggregation in yeast and higher organisms was shown to be similar [255].

In a yeast model of HD, it has been reported that expression of mutant HTT induces oxidative stress at late exponential phase, thereby reducing the stress resistance of cells [209]. Considering the involvement of forkhead proteins Fkh1 and Fkh2 in mediating cell cycle arrest and stress response in yeast as a result of the data presented in this work, a potential influence of forkhead transcription factors Fkh1 and Fkh2 on mutant HTT-dependent aggregation, is plausible.

3.3.1 Effects of Fkh1, Fkh2 and Sir2 on HTT-induced aggregation

To investigate whether Fkh1 and Fkh2 play a role in HTT aggregation, it was aimed to analyze protein aggregation induced by mutant HTT in deletion mutants of *FKH1* and *FKH2*. Therefore, wild type, *fkh1*Δ, *fkh2*Δ, and *fkh1*Δ*fkh2*Δ cells were either transformed with plasmids expressing the N-terminal fragment of HTT encoding 25 (pYES-25Q-RFP) or 103 glutamines (pYES-103Q-RFP) fused to a red fluorescence protein (RFP). Then, transformants were selected and cultured to mid exponential phase (OD_{600} = 0.6). Subsequently, yeast cells were fixed with ethanol and expression of HTT was visualized by fluorescence microscopy (see chapter 2.2.26 for details) as well as quantified by fluorescence flow cytometry (chapter 2.2.37). Data obtained from FACS analysis are plotted in histograms indicating the number of fluorescent cells (y-axes) in correlation to fluorescence intensity as well as density plots (right panels) showing inner complexity of cells (SSC, y-axis) in proportion to

fluorescence intensity (x-axis).

All strains expressing HTT-25Q-RFP showed a uniform cytoplasmatic fluorescence signal (Figure 3-30, left panels). A distinct localization of fluorescence signals indicating the formation of polyQ-dependent protein aggregates was observed in wild type yeast cells as well as *fkh1*Δ and *fkh2*Δ mutants expressing HTT-103Q-RFP (Figure 3-30, right panels). Consistently, flow cytometrical quantification of HTT-103Q-RFP signals in all strains revealed an increase in the fluorescence intensity as indicated by a shift on y-axis in histograms and density plots. Interestingly, in comparison to wild type a slight increasing number of fluorescent cells was observed for *fkh1*Δ cells expressing HTT-103Q-RFP, a result especially displayed by the corresponding histogram. In addition, *fkh2*Δ and *fkh1*Δ*fkh2*Δ mutants expressing HTT-103Q-RFP showed a reduced aggregation compared to wild type cells in agreement with the respective FACS plots. This reduction was more significant in *fkh1*Δ*fkh2*Δ mutant cells, as indicated by the FACS histogram as well that show a decrease in the number of fluorescent cells (second peak on y-axes is abscent). In addition, cell shape of *fkh1*Δ*fkh2*Δ mutants expressing HTT-103Q-RFP was elongated compared to wild type control, indicating mitotic defects that are potentially caused by the absence of macromolecular aggregates. Unfortunately, fluorescence quantification of the *fkh1Δfkh2Δ* mutant expressing HTT-25Q-RFP and HTT-103Q-RFP revealed an increase of inner cell complexity (density plot, y-axis) suggesting additional effects caused by this pseudohyphal phenotype.

Taken together, the data suggests that Fkh1 and Fkh2 alter protein aggregation of HTT-103Q, highlighting a putative role for both proteins in response to mutant HTT-specific stress. Importantly, the reduced aggregation that was observed in *fkh1*Δ*fkh2*Δ mutants correlates with an increased elongated cell morphology, suggesting an abnormal cell growth.

Figure 3-30. Analysis of HTT aggregation in *fkh1*Δ, *fkh2*Δ and *fkh1*Δ*fkh2*Δ deletion strains. Mid exponential growing cells (OD_{600} = 0.6) of wild type and *fkh1*Δ, *fkh2*Δ and *fkh1*Δ*fkh2*Δ strains were either transformed with plasmids pYES-25Q-RFP (left panels) and pYES-103Q-RFP (right panels). Fluorescence of cells were visualized by fluorescence microscopy or quantified by flow cytometry. Histograms (left panels) shows the number of fluorescent cells (y-axes) in correlation to fluorescence intensity (x-axes). Density plots (right panels) indicate inner complexity of cells (SSC, y-axis) against fluorescence intensity (x-axis).

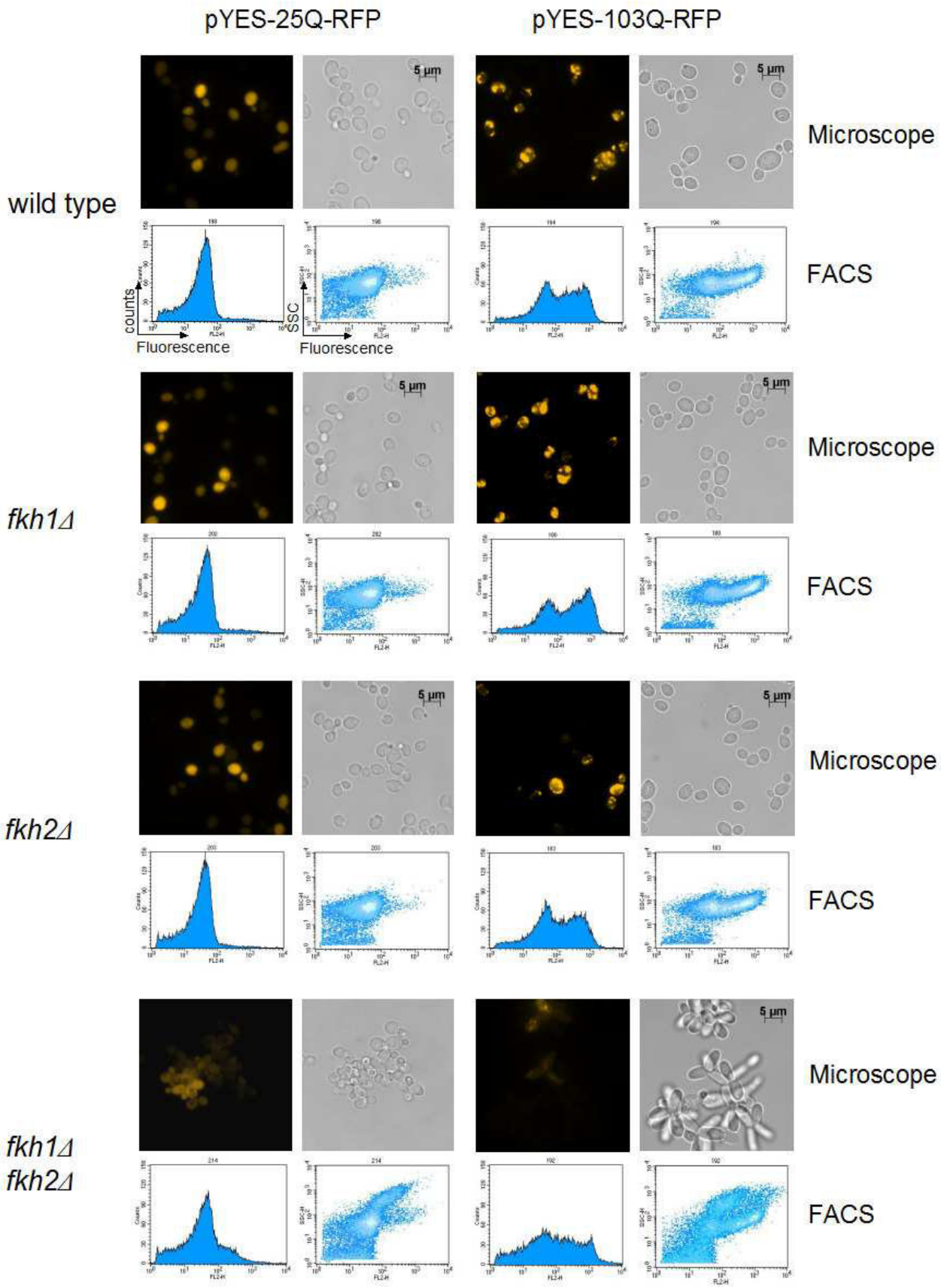
pYES-25Q-RFP
pYES-103Q-RFP
wild type
fkh1Δ
fkh2Δ
fkh1Δ
fkh2Δ
5 µm
Microscope
FACS
counts
Fluorescence
SSC
Fluorescence

3.3.2 HTT-induced cytotoxicity in yeast

The expression of the N-terminal region of HTT with a stretch of 103 glutamines is toxic in yeast [256]. In this light, it was aimed to adress next whether deletion of *FKH1* or *FKH2* in addition to polyQ-dependent aggregation also affects the toxicity observed for HTT-103Q-RFP. Since, hydrogen peroxide treatment of yeast cells expressing the N-terminal part of HTT with a 103Q stretch fused to GFP was shown to enhance mutant HTT-induced cytotoxicity [209], it was further aimed to investigate H_2O_2 conditions as well. Therefore, wild type, *fkh1*Δ, *fkh2*Δ and *fkh1*Δ*fkh2*Δ strains, expressing 25Q-RFP or 103Q-RFP under control of the galactose inducible promoter, were grown to mid logarithmic phase (OD_{600} = 0.6) and spotted in serial dilutions (1:5) on medium supplemented with either glucose or galactose as carbon source. In addition, the viability of these strains was analyzed under oxidative stress. For this, dilution series (1:5) of wild type and deletion strains were spotted in parallel on medium containing 1.5 mM H_2O_2 as well.

As shown in Figure 3-31, wild type strain and *fkh1*Δ, *fkh2*Δ and *fkh1*Δ*fkh2*Δ mutants expressing HTT-103Q-RFP showed a clear reduction of colony size on galactose containing plates, indicating HTT-103Q-specific cytotoxicity. As expected, cell viability was almost unaffected in strains expressing HTT-25Q-RFP. However, no differences between wild type cells and *fkh1*Δ and *fkh2*Δ mutants was oserved on galactose plate. Interestingly, a strong decrease in growth of *fkh1*Δ*fkh2*Δ mutant cells expressing HTT-103Q-RFP was detected on galactose plate, indicating increased lethality relative to wild type cells.

Obviously, wild type cells and deletion strains of *fkh1*Δ and *fkh2*Δ showed a reduction in cell growth on glucose containing plates that are supplemented with H_2O_2. Consistent with previous results (Figure 3-24), viability of *fkh1*Δ*fkh2*Δ mutant was less affected under these conditions. Moreover, *fkh2*Δ mutant cells transformed with plasmid pYES-HTT-25Q-RFP showed a reduced cell viability on glucose medium supplemented with H_2O_2 compared to wild type strain. In agreement with this result, growth of *fkh2*Δ mutant was effected as well in the presence of 2.0 mM H_2O_2 (Figure 3-24).

The viability of *fkh1*Δ*fkh2*Δ mutants expressing HTT-103Q-RFP on galactose medium was strongly reduced in exposure to oxidative stress. However, a decrease in colony size on galactose medium containing H_2O_2 was observed as well in the double deletion strain upon expression of HTT-25Q-RFP. Interestingly, the growth reduction of *fkh2*Δ mutants incubated on glucose medium containing H_2O_2 was almost absent when expressing HTT-103Q-RFP on galactose medium, whereas a reduced growth in *fkh2*Δ cells expressing HTT-25Q-RFP was still detectable, indicating a functional relationship between Fkh2-mediated oxidative stress response and aggregation of mutant HTT.

In sum, the expression of HTT-103Q-RFP reduces cell growth of yeast cells, indicating polyQ-dependent cytotoxic effects in agreement with previous findings [209, 254, 256]. Importantly, this lethality was enhanced in the *fkh1*Δ*fkh2*Δ mutants, highlighting a putative important role of Fkh1 and Fkh2 in mediating pro-survival effects. Based on these results, a potential correlation between mutant HTT-specific toxicity and Forkhead protein-dependent control of cell cycle progression in response to stress was suggested.

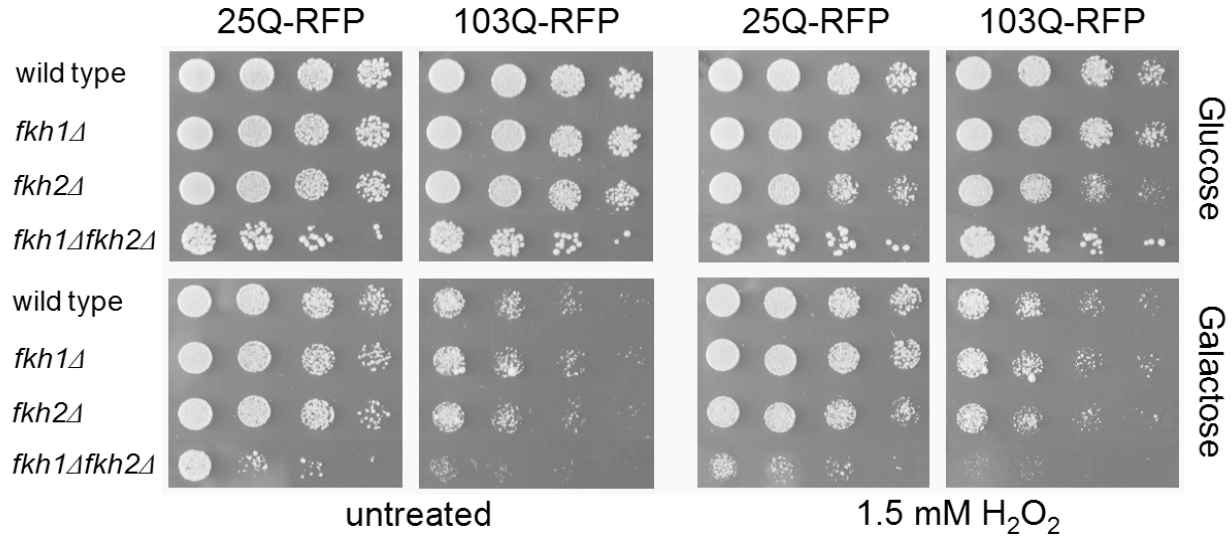

Figure 3-31. Growth of wild type cells and *fkh1*Δ, *fkh2*Δ and *fkh1*Δ*fkh2*Δ mutants upon expression of RFP-tagged 25Q and 103Q. Yeast cells were either transformed with pYES-25Q-RFP or pYES-103Q-RFP, pregrown over night (OD_{600} ~ 1.5) and spotted in parallel on media containing either 2 % of glucose or 2 % of galactose in serial dilutions (1:5, starting with OD_{600} = 0.3). In addition, transformants were spotted on media supplemented with 1.5 mM H_2O_2. Cell growth was analyzed after 3 days of incubation at 30°C.

3.3.3 Influence of mutant HTT on the interaction between Fkh2 and Sir2

The results presented in this work indicate an important role for Fkh1, Fkh2 and Sir2 in mediating cell cycle arrest in response to stress. In particular, a mechanism has been proposed by which Fkh proteins interact with Sir2 to repress the expression of the main mitotic cyclin Clb2. Considering the induction of oxidative stress upon mutant HTT-dependent protein aggregation in yeast cells [209], it was further aimed to examine whether the expression of mutant HTT influences the interaction between Fkh2 and Sir2. Interestingly, increased levels of SIRT1, the mammalian homolog of yeast Sir2, in response to stresses including oxidative stress, DNA damage and caloric restriction have been demonstrated. This increase is proposed to cause favorable changes in stress tolerance [257]. Moreover, it has been demonstrated that an increased level of Sir2 reduces aggregation of mutant HTT and the stress generated by expanded polyQ [209].

To further visualize a putative effect of mutant HTT on the association between forkhead protein Fkh2 and Sir2, fluorescence microscopy of respective BiFC strain was performed. Yeast cells carrying a chromosomal integration of Sir2-VC were cotransformed with plasmid p423GALL-VN-Fkh2 and pYES-25Q-RFP or pYES-103-RFP. Subsequently, transformants were selected, cultured to mid exponential phase (OD_{600} = 0.6) and incubated in medium with galactose for 6 hours to induce protein expression. Cells were fixed with ethanol, stained with DAPI and subjected to fluorescence microscopy in order to visualize BiFC signals as well as RFP-tagged proteins.

As shown in Figure 3-31, yeast cells expressing HTT-25Q-RFP showed a uniform cytoplasmatic RFP signal (upper panel). Almost no BiFC signals were observed in cells that displayed HTT-25Q-RFP-specific fluorescence. As expected, cells expressing HTT-103Q-RFP showed distinct localization of RFP signals indicating the formation of polyQ-dependent protein aggregates (bottom panel). Interestingly, all cells comprising mutant HTT-dependent aggregates showed distinct BiFC signals, indicating an interaction between Fkh2 and Sir2. Moreover, these signals appeared to be larger and more intensive compared to control cells. In addition, yeast cells

expressing HTT-103Q-RFP showed nuclear fragmentation as highlighted by white arrows (bottom left panel), whereas cells transformed with pYES-25Q-RFP did not.

In conlusion, these results indicate that the formation of mutant HTT-dependent aggregates enhances the interaction between forkhead proteins and Sir2. Since an increased Fkh1-Sir2 association was observed in cells exposed to oxidative stress, this finding could suggest a common mechanism whereby Forkhead proteins and Sir2 control mitotic cell growth in response to stress stimuli. In agreement with this assumption, a reduction in cell growth was observed in wild type cells expressing HTT-103Q-RFP compared to cells expressing HTT-25Q-RFP. Furthermore, mutant HTT expression caused a fragmentation of the nucleus, which is a marker characteristic for old grown yeast cells [258, 259]. Interestingly, previous work uncovered that mutant HTT interacts with Sirt1, the mammalian homolog of yeast Sir2, resulting in hyperacetylation of forkhead box O3 (FoxO3), thereby inhibiting its pro-survival function [260].

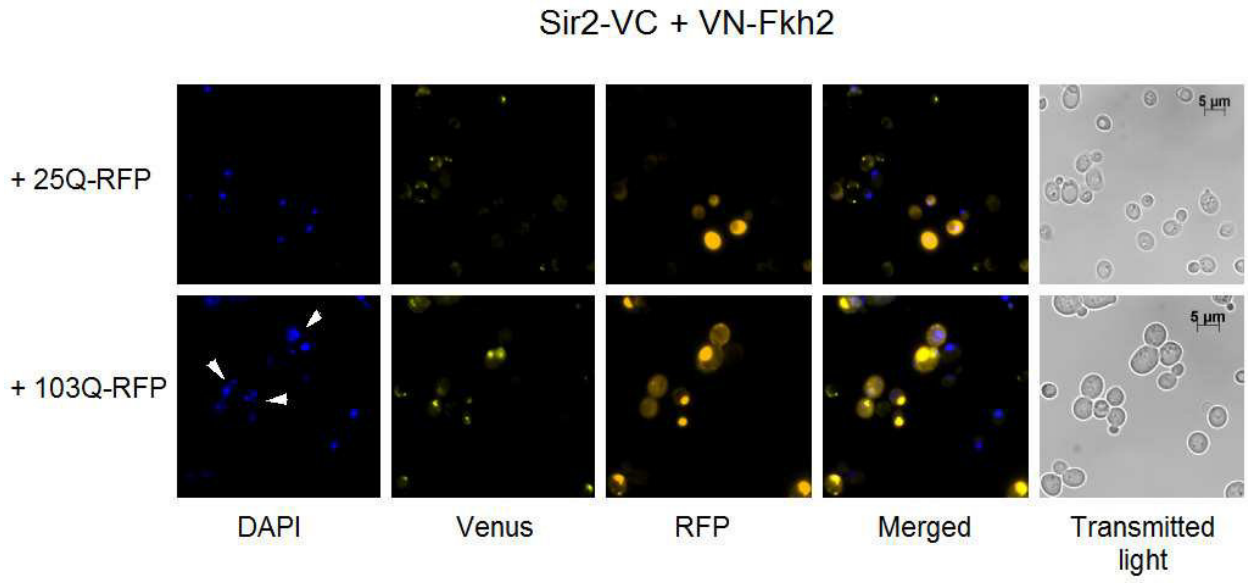

Figure 3-35. Visualization of 25Q-RFP and 103Q-RFP as well as Sir2-VC/VN-Fkh2 BiFC signals. Haploid cells endogenously expressing Sir2-VC were cotransformed with p423GALL-VN-Fkh2 and pYES-25Q-RFP (upper panels) or pYES-103Q-RFP (bottom panels). Mid exponentially growing cells (OD_{600} = 0.6) were fixed with ethanol and staining with DAPI.

Taken together, the data presented in this work emphazise a cell cycle dysregulation caused by heterologues expression of mutant HTT in a yeast model of HD. Since, polyQ-dependent aggregation is altered in deletion mutants of *FKH1* and *FKH2* and

the interaction between Fkh2 and Sir2 is enhanced in cells expressing HTT-103Q-RFP, the results provide further evidence for a role of Fkh proteins and Sir2 in mediating cell cycle control in response to stress caused by mutant HTT aggregation.

Moreover, equal mechanisms can be assumed in mammalian cells including neurons as well. In this light, the FoxO pathway is important to decrease proteotoxicity induced by a variety of stresses, thus possibly preventing the onset of neurodegenerative diseases [109]. It is possible that the reported interaction between mutant HTT and Sirt1, which inhibited the FoxO pathway, could be a reason for cytotoxic effects mediated by dysfunction of mitotic gene repression. Interestingly, elevated cyclin B levels were reported also for HD neurons [261]. Obviously, a tight control of cell cycle is important for differentiated cells in higher eukaryots to remain in a post mitotic phase known as G0.

4. Discussion

In this study, the mechanisms coordinating cell cycle-dependent gene expression in *Sacharomyces cerevisiae* during S/G and G2/M phases were investigated. In a first part, a mathematical model (Figure 4-1), which proposes a role for Sic1 and both Fkh transcription factors in the regulation of mitotic Clb cyclins, were validated by yeast-two-hybrid and GST pull-down studies demonstrating that Sic1 and both Forkhead proteins interact with all Clbs. In the second part of this thesis, it was shown that Fkh1, Fkh2 are involved in the regulation of *CLB1-4* by recruiting the coactivator Ndd1 from S until M phase or histone deacetylase Sir2 at the end of M phase until the end of G1 phase.

4.1 Sic1 plays a role in timing and oscillatory behaviour of B-type cyclins

The biochemical regulation that controls cell cycle has been recognized to be cyclic waves of Cdc28 activity, where Clbs bind to Cdc28 with the characteristic oscillatory behavior known as “waves of cyclins” [6, 262, 263]. However, the mechanism of this coordinated regulation remains elusive.

The results presented in this thesis support a role for Sic1 in the regulation of Cdc28-Clb complexes, acting as a timer in their regulation. A computational model suggested that the wave-like cyclins pattern is derived from the binding of Sic1 to all three Clb pairs rather than from the degradation of Clbs [236]. These predictions were validated in this thesis by yeast-two-hybrid and GST pull-down studies showing that Sic1 indeed interacts with all Clbs. Moreover, it was shown that Sic1 coexists in time with all Clbs and drives the staggering of the Clbs during cell cycle progression [236].

In *sic1*Δ cells, which show a high frequency of chromosome loss and breakage [264], all Clbs accumulate prematurely losing timing and periodicity of their appearance [236]. This finding is also supported by recent data indicating that in *sic1*Δ cells Clb5 accumulates earlier compared to the wild type and generates a higher Cdc28-Clb5, 6 activity in G1, promoting early DNA replication from few origins [265].

The data proposes a specific role for Sic1 in coordinating the appearance of Cdc28-Clb complexes to regulate cell cycle events. Besides Sic1 degradation via Cdc28-Cln and Cdc28-Clb phosphorylations, additional mechanisms that temporally drive Cdc28-Clb activities has been proposed in this thesis. These mechanisms include the phosphorylation of forkhead transcription factors Fkh1 and Fkh2 promoted by Cdc28-Clb activities. As a consequence of these phosphorylations, the Fkh-driven periodic expression of genes required for S/G2 and G2/M transitions of the cell cycle depends on the association between Fkh2 and the coactivator Ndd1 [21-23].

4.2 Forkhead transcription factors Fkh1 and Fkh2 regulates B-type cyclins Clb1-4

Evidence available in literature predicted a potential cascade of Cdc28-Clb regulation, suggesting a role of Fkh1 and Fkh2 to trigger the oscillatory behaviour of B-type cyclins Clb1-6 [236]. Protein-protein interaction data presented in this thesis suggest that Fkh1 directly interacts with Ndd1 *in vitro* and *in vivo* in a cell cycle-regulated manner. This observation interfers with previous data, where only the FHA domain of Fkh2 was reported to associate with the coactivator Ndd1 [79]. Because Fkh1 and Fkh2 share 47 % identity and 82 % similarity across the peptide sequence of Fkh1 [83], data presented in this thesis support a model, in which Ndd1 binds also to Fkh1 to activate transcription of *CLB2* cluster genes. Of particular relevance for this assumption, Fkh1 and Fkh2 contain DNA-binding domains that were found to be interchangeable for promoter occupancy of many *CLB2* cluster genes including for example *CLB2*, *SWI5*, *BUD3*, *BUD4, CDC5*, *CDC20*, *ALK1*, *HST3* and *ASE1* [76]. These genes are reported to be transcribed in late S and G2/M phase of the cell cycle and encode proteins necessary for normal cell cycle progression in yeast [7, 262]. Interestingly, it has been shown that Fkh1 occupies the *BUD3* or *FKH2* promoter more efficiently *in vivo* compared to Fkh2 [83]. Nevertheless, the interaction between Ndd1 and Fkh1 seemed to be less strong as compared to the interaction between Ndd1 and Fkh2, due to reduced fluorescence intensity after reconstitution of the Venus protein.

The timing of Ndd1-Fkh2 association correlates with the transcription of *CLB2* cluster genes and it is mediated by Cdk1-dependent phosphorylation of Ndd1 [21]. As observed for Fkh2, Fkh1 binds to Ndd1 at early S phase until late M phase,

emphasizing its capability to activate G2/M specific genes. This assumption was further supported in this thesis by protein-protein interaction data, DNA binding studies and analysis of transcript levels. Moreover, simultaneous deletion of *FKH1* and *FKH2* reduced expression of these genes. Consistently, disruption of both *FKH1* and *FKH2* was reported to reduce cell cycle-regulated transcription of *CLB2*-cluster genes, slowing progression through the G2/M phase [44, 76, 266]. This novel interaction might explain previous findings showing that in the absence of Fkh2 and Ndd1, Fkh1 mediates periodic expression of *CLB2* cluster genes [78].

The results further provided in this thesis demonstrate that both forkhead proteins are involved in the regulation of B-type cyclin genes *CLB3* and *CLB4*. Importantly, transcript levels of *CLB3* and *CLB4* seemed to be affected in the *fkh1*Δ *fkh2*Δ mutant, indicating regulatory roles for both forkhead proteins. Presumably, Clb3 seemed to be a suitable candidate for priming transcription of *CLB2* cluster genes as previously suggested [78]. Despite the observation that Clb1-4 interact with Fkh1 and Fkh2, a cell cycle-dependent association between Ndd1 and Clb3 was further demonstrated by using Clb2 as positive control. Constitutive expression of Venus-tagged Clb3, but not Clb2, enhanced Clb3-CFP level in S phase, which peaks earlier than G2/M phase-specific Clb2-CFP. Moreover, it was shown that overexpression of *CLB3* partially rescued pseudohyphal phenotype of *fkh1*Δ *fkh2*Δ mutants, sharing a property previously shown for Clb2 [76].

Furthermore, Cdc28-Clb3 directly phosphorylates Fkh2 and deletion of *FKH2* delayed abundance of Clb3 protein level, indicating its predicted relevance in fine tuning the transcriptional activation of G2/M genes. Interestingly, it has been shown that Clb3 and Clb4 can functionally compensate for deletion of *CLB1* and *CLB2* [6]. Cdc28-Clb3, 4 complexes are required for *CLB1, 2* expression, in fact cells lacking Clb3, Clb4 and Clb5 show a drastic reduction of *CLB2* transcription and Fkh2 phosphorylation, whereas deletion of Clb5 has only a moderate effect [4].

Taken together, the data reported in this thesis emphasize an involvement of multiple positive feedback loops regulating *CLB*2 cluster gene expression implying not only Clb2-Cdc28 but also Clb3-Cdc28 activity. In addition, a protein kinase-independent function of the Cdc28-Clb complexes has been proposed, which might include a structural role in the recruitment of protein complexes important for transcriptional events [115, 236].

4.3 Forkhead protein-mediated repression of G2/M genes requires histone deacetylase Sir2

One important observation made in this thesis was the identification of the histone deacetylase Sir2 as a potential negative regulator of *CLB2* transcription. Binding assays together with several genetic and biochemical analysis suggested that both Fkh1 and Fkh2 directly interact with Sir2 *in vitro* and *in vivo* unraveling a novel function of Sir2 in the regulation of G2/M genes in the cell cycle of budding yeast. However, a Sir2-dependent role in the regulation of S phase-specific yeast genes was previously discovered, demonstrating that the yeast forkhead transcription factor Hcm1 interacts with Sir2 [114]. Specifically, it has been reported that nuclear localization of Hcm1 during G1/S phase is dependent on Sir2 activity, in agreement with the known function of Hcm1 in the activation of these genes [114]. Moreover, Fkh1 was found to play a role in Sir2-dependent silencing at the mating-type locus HMR [242].

Importantly, another histone deacetylase complex named Sin3/Rdp3 was shown to be involved in the negative regulation of *CLB2* cluster genes in association with Fkh2 [115]. Sin3 is directly recruited to the *CLB2* promoter through association with the FHA domain of Fkh2 to remove acetylation of Histone 4 during G1/S transition. Moreover, it was postulated that Rdp3 acts as a boundary element for Sir2-dependent chromatin silencing at mating loci *HMR* and *HML* [123]. Deletion of *RPD3* leads to decreased levels of Sir2 at telomeres and HM but to increased levels at adjacent regions, resulting in Sir-dependent local propagation of transcriptional repression [123]. In addition to histone deacetylases, remodeling ATPases Isw1 and Isw2 have also been shown to repress *CLB2* expression in collaboration with Fkh1 and Fkh2 [267].

Altogether, these indications suggest an involvement of chromatin remodeling factors as crucial targets for Fkh-mediated gene silencing. Based on the findings presented in this thesis, it is possible to extend the knowledge suggesting that a direct recruitment of histone deacetylase Sir2 by Fkh proteins may, at least in part, help to terminate transcription of G2/M gene expression.

Another interesting aspect addressed in this thesis was to compare the timing of interaction between Fkh transcription factors and their coactivator Ndd1 with that of

the putative corepressor Sir2. The results clearly showed that both interactions mutual exclude each other in G1 and S/G2 phases, but partially overlap in G1/S and late M phases, in agreement with the known inactivation of *CLB2* gene cluster during M/G1 and its subsequent activation in S/G2 phase. Consistently, the results presented here showed that the deletion of both *FKH1* and *FKH2* leads to a strong increase of *CLB2* transcription in G1 phase, highlighting their repressive function in regulating G2/M genes.

Furthermore, the data helped to shed new light into previously uncharacterized differences between Fkh1 and Fkh2 in the negative regulation of *CLB2* cluster genes by Sir2. According to yeast two hybrid experiments, genetic data and BiFC assays, the association between Fkh1 and Sir2 might be more relevant for silencing target genes. In line with this assumption, the expanded C-terminal domain of Fkh2, which is absent in Fkh1, was not considered to be essential to recruit the histone deacetylase Sin3 [115]. Moreover, a putative association between Sin3 and Fkh1 was not excluded [115]. Transcriptional analysis of cells lacking *FKH1* revealed a slight upregulation of *CLB* mRNA levels, consistent with previous data reporting that the deletion of *FKH1* enhances *CLB2* transcription and overexpression of *FKH1* or deletion of *FKH2* reduces it [78, 83].

However, the data presented in this thesis provide evidence that Fkh2 is also strongly associated with Sir2 and a clear enrichment of *CLB2* transcription was observed in *fkh1*Δ *fkh2*Δ mutant in G1 phase. In agreement, promoter occupancy of Sir2 was shown to be reduced in both *fkh1*Δ and *fkh2*Δ mutants. Although both transcription factors were shown to bind the *CLB2* cluster promoters *in vivo* [24, 79], Fkh2, but not Fkh1, was reported to bind cooperatively with the MADS-box transcription factor Mcm1 at *CLB2* cluster promoters [24, 68, 74, 79, 83, 234]. In addition, previous studies suggested that Fkh1 protein compete with a stable Fkh2/Mcm1 complex for occupancy at target promoters. In fact, it has been proposed that Fkh1 limits transcriptional activation of target genes while Fkh2 plays an additional role in stabilizing Mcm1 at Fkh-controlled promoters [83].

The Mcm1/Fkh2 complex formation is not cell cycle regulated, while the key for periodic gene expression was demonstrated to be depend on recruitment of Ndd1 [78, 79, 81, 83]. Following the interaction between Sir2 and Fkh1 with the BiFC method, a cell cycle regulated recruitment of coregulators such as histone

deacetylases to Fkh proteins may provide an additional mechanism for the proper timing of *CLB2* cluster regulation. Consistently, the complex Sin3/Rpd3 was reported to periodically bind *CLB2* promoter in G1 phase [115] and deletion of *SIR2* in a BiFC strain coexpressing Ndd1-VC/VN-Fkh2 led to a reconstitution of Venus uncoupled from the cell cycle. In this context, a reduction in the relative fluorescence intensity of the Sir2-VC/VN-Fkh2 signal was observed by expressing *NDD1* and *CLB2* ectopically. In conclusion, the data presented in this thesis indicate that Fkh1 can play a more important role as compared to Fkh2 in repressing *CLB2* cluster genes to coordinate proper cell cycle transitions. The results of *CLB2* transcript analysis further confirmed this assumption because the deletion of *FKH2* as well as the simultaneous disruption of both *FKH2* and *SIR2* led to a decrease in mRNA levels in contrast to *fkh1*Δ and *fkh1*Δ *sir2*Δ mutants.

Previous findings showed that hypersensitive chromatin at *CLB2* promoter undergoes several cell cycle-specific structural modifications due to the remodeling of nucleosomes [115]. In particular, Fkh2 was shown to associate with the chromatin-remodeling ATPase Isw2. During transcriptional repression of *CLB2* in late M and G1 phases, Isw2-dependent 3' movement of nucleosomes occurs adjacent to the TATA box. In addition, Fkh1 remodels chromatin in association with Isw1 at the early coding region to negatively regulate *CLB2* transcription in M phase [267]. It has been proposed that both forkhead transcription factors might function to stabilize chromatin-mediated repression or promote other repressing activities, such as the recruitment of histone deacetylases to promoters of target genes [115].

In summary, the results here presented favor a scenario where G2/M-specific transcriptional regulators recruit chromatin remodeling factors to coordinate cell cycle events independently from Clb-Cdc28 complex activities. Recent studies on the latter subject focused on positive-feedback loops involving polo kinase Cdc5, Clb5-Cdc28 and/or Clb2-Cdc28 to phosphorylate the forkhead transcription factor Fkh2 and its coactivator Ndd1 [19, 21, 23, 268]. These studies did not explain neither a G1/S phase-specific transcriptional initiation, nor repression of G2/M genes during G1 phase. However, our findings agree with the idea that histone modifications silence transcriptional active chromatin including cell cycle genes with a peak in late M and early G1 phases [269].

4.4 Repression of G2/M genes in response to oxidative stress

The data reported in this thesis provide evidence to support an evolutionary conserved role for the yeast forkhead transcription factors Fkh1 and Fkh2 in lifespan determination and in response to oxidative stress. A microarray analysis of *fkh1*Δ *fkh2*Δ cells initially identified such a role, identifying alterations in stress response genes [82]. Importantly, an additional role for yeast Sir2 in mediating oxidative stress resistance and mitochondrial metabolism has been previously reported [114, 209]. Moreover, localization of the yeast forkhead transcription factor Hcm1 was shown to be Sir2-dependent, resulting in the activation of genes involved in stress resistance [114]. Nevertheless, the functional relevance for nuclear sirtuins in this context still remains poorly explored. Since Fkh1 and Fkh2 are known to localize into the nucleus a recruitment of Sir2 to these proteins might have an important biological role.

The results shown in this work indicate that Sir2 interacts with Fkh transcription factors under normal and stress conditions, and genetic and biochemical studies highlighted a dual function of Fkh1 and Fkh2 in the regulation of cell cycle progression in response to oxidative stress.

Oxidative stress has been studied in yeast by exposing cells to agents such as H_2O_2, or drugs that cause intracellular accumulation of reactive oxygen species (ROS) [270-272]. Menadione (MD) is such a drug, generating reactive superoxide ions, which can be further oxidized to H_2O_2 [273, 274].

Interestingly, the induction of oxidative stress in yeast by exposure to H_2O_2 and MD results in a Fkh-dependent cell cycle arrest [246, 247]. Specifically, MD was reported to arrest cells at the G1 phase, whereas H_2O_2 caused a delay in S phase but ultimately led to a G2/M arrest [245-247]. In particular, H_2O_2 treatment encompasses almost a complete loss of the periodic transcription patterns [7, 275]. Two small gene clusters, which are essential for cell cycle progression through G2/M phase showed abnormal transcription patterns under H_2O_2 treatment [6, 276], and inactivation of the Mcm1p–Fkh2p–Ndd1p complex was suggested to be responsible in mediating these effects [245]. In addition, deletion of both *FKH1* and *FKH2* has been shown to block normal lifespan and stress resistance of cells, particularly in stationary phase,

whereas overexpression of both genes extended chronological and replicative lifespan and stress resistance [248]. In the same way, the yeast forkhead transcription factor Hcm1 plays an important role in oxidative stress resistance [114]. Deletion of *HCM1* showed a reduced viability upon H_2O_2 and MD treatment, whereas its overexpression led to an increased stress resistance. In addition, Hcm1 was observed to shift from the cytoplasma to the nucleus during G1/S phase under normal conditions but nuclear translocation was found to be enhanced under conditions of oxidative stress [114].

The results of this work provide evidence that Fkh1 and Fkh2 may also act in controlling stress response because cell viability is altered in single and double deletion mutants of Fkh1, Fkh2 and Sir2. Furthermore, *CLB2* promoter occupancy by Sir2 was found to be enhanced when cells were treated with H_2O_2 and, consistent with this observation, transcript and protein levels of *CLB2* were altered comparing *fkh1*Δ and *fkh2*Δ single mutants with *fkh1*Δ *fkh2*Δ, *fkh1*Δ *sir2*Δ and *fkh2*Δ *sir2*Δ double mutants. However, most severe effects were observed in cells lacking both *FKH1* and *FKH2* genes supporting previous assumptions where both proteins might be primary responsible for inhibition of cell cycle-regulated transcription resulting in growth arrest [44, 76, 266].

The present study highlighted similarities in the experimental results comparing cells treated with H_2O_2 and grown to early stationary phase. Yeast cells entering in early stationary phase undergo a metabolic switch from fermentative to respiratory metabolism known as diauxic shift. As a consequence, genes involved in gluconeogenesis, respiration, stress response and mitochondria synthesis become activated, including *SIR2* [142, 277, 278]. It is also worth to mention that ROS generation, as a product of aerobic metabolism, mainly occurs in the mitochondrial electron transport chain, leading to damage of DNA, membrane lipids and proteins [279, 280].

In cultures with increased cell density, glucose levels becomes limited similar to calorie restricted cultures (applying glucose concentrations less than 0.5 %), thus leading to a metabolic switch from fermentation to respiration. Signaling pathways ultimately promote an increased electron transport in mitochondria to obtain energy more efficiently [144]. These metabolic changes in yeast cells generates a well-

described mild stress situation that induces antioxidant defenses [249-251]. In addition to the free radical damage protection mediated for example by mitochondrial enzymes Sod1 and Sod2 [142, 143], it was reported that Sir2 might have a protective role through activation of mitochondrial metabolism and stress resistance [114, 209, 281]. The results of this work and those previously described suggest that Fkh transcription factors act in concert with Sir2 to induce cell cycle arrest upon oxidative stress as well as under calorie restriction when cells reach stationary phase to maintain genome stability and increase stress resistance. Consistently, it has been demonstrated that yeast cells grown on media with low glucose concentration (0.2 %) show a three-fold higher rate of respiration. An increase in oxidation of NADH to NAD^+ in TCA cycle may result in a higher chromatin silencing activity of Sir2, due to the increased availability of cofactor [145].

Interestingly, it was previously reported that ionizing radiation was shown to cause a G2/M arrest accompanied by repression of forkhead-associated transcription in wild-type cells [272]. Consistently, the DNA damage checkpoint protein Rad9 was shown to contribute to a G2/M arrest in response to H_2O_2 treatment [246].

4.5 Sir2 is involved in gene silencing and APC-mediated cell cycle control

Another important function of Sir2 is its involvement in rDNA silencing as a component of the nucleolar RENT complex. This complex promotes exit from mitosis and includes a core subunit called Net1 and the phosphatase Cdc14 that promotes the phosphorylation and degradation of B-type cyclins and the accumulation of Sic1 in G1 phase. Net1 is localized to rDNA via interaction with unknown DNA-bound factors and it is believed to recruit subunits of RENT including Sir2 and Cdc14. During late mitosis, Sir2 and Cdc14 are released from RENT resulting in desilencing of rDNA at the anaphase-telophase transition of the cell cycle. Interestingly, such changes in the structure of rDNA at late M phase have been suggested as well for telomeric silencing, which is known to be dependent on Sir2 [281]. As a consequence of the release of Sir2 and Cdc14, the nucleolus segregates to the nuclear periphery, where Cdc14 dephoshorylates Cdh1 to activate (i) anaphase promoting complex, APC^{Cdh1}, for the degradation of mitotic B-type cyclins and (ii) Sic1 to prevent the recognition of Sic1 by ubiquitin ligases [51, 52]. Increased Sir2

levels may lead to a delay in Cdc14 release causing an accumulation of Clb2 due to lower APC^{Cdh1} activity, ultimately resulting in cell cycle delay/arrest in late M phase.

As aforementioned, Fkh transcription factors regulate *CLB2* cluster encoding genes required for APC activity including *APC1* (APC subunit), *CDC5*, *CLB2* and *CDC20* (APC activators/targets). APC mutants were observed to exhibit reduced mitotic and post-mitotic lifespan, while increased *APC10* expression extended replicative (mitotic) longevity [283, 284]. Moreover, APC mutants are sensitive to DNA damaging agents, and showed chromatin assembly and histone modification defects [284-288]. The APC has been demonstrated to be critical for regulating genomic stability, stress response, and longevity in yeast and higher eukaryotic organisms [283, 285, 289, 290, 291]. It may be possible that the repression of Fkh-dependent APC-activating genes by Sir2 in response to stress impairs APC function during late mitosis, thus leading to cell cycle arrest at M/G1 phase.

4.6 Involvement of Fkh1 and Fkh2 and Sir2 in Huntington's Disease

Huntington's disease (HD) is an inherited neurodegenerative disorder caused by a glutamine repeat expansion (polyQ) in the huntingtin (Htt) protein. It has been shown that Htt interacts with various proteins including kinases, phosphatases, proteases and transcription factors amongst others [292, 293]. In agreement with this, mutant Htt is believed to interfere with transcriptional networks that are essential to maintain neuronal functions [294, 295]. Recent findings showed that calorie restriction ameliorates disease pathogenesis and slows down disease progression in a murine model of HD [296]. Furthermore, it was reported that overexpression of Sirt1, the closest mammalian homologue of yeast Sir2, protects neurons against the mutant Htt toxicity, improves motor function, reducing brain atrophy and attenuates mutant Htt-mediated metabolic abnormalities in HD mice [297]. The mutant Htt directly interacts with Sirt1 inhibiting its deacetylase activity, which results in hyperacetylation of Sirt1 substrates such as FoxO3. Overexpression of Sirt1 counteracts this deacetylase deficit by enhancing a pro-survival function of the forkhead transcription factor FoxO3 [226].

Another aim of this thesis was to identify yeast genes involved in cell cycle regulation for their ability to alter protein aggregation and cell viability upon expression of exon1

of the gene *IT15* with an expanded stretch of CAG repeats. Interestingly, *fkh1*Δ and especially *fkh2*Δ mutants were observed to rescue the lethality of yeast cells expressing RFP-tagged Htt with 103 polyglutamines (polyQ). Unfortunately, the rescue in cell viability was not robust when testing different yeast deletion strains and transformants. However, fluorescence microscopy and flow cytometry of yeast cells lacking *FKH2* revealed a significant decrease in formation of aggregates, an effect that was found to be even more drastic in *fkh1*Δ *fkh2*Δ mutant. In addition, overexpression of Sir2 drastically reduced polyQ aggregation, consistent with previous reports in which the use of isonicotinamide, a selective Sir2 activator, decreased aggregation in yeast [209].

How could Fkh1 and Fkh2 play a role in the aggregation of mutant polyQ proteins in yeast? First yeast-based studies showed that expression of the N-terminal fragment of Htt carrying an expanded polyQ stretch slows yeast cell growth, affecting cell cycle progression [298]. It has been assumed that aggregation overloads the proteasome, thus slowing down cyclin proteolysis and delaying cell division [294]. Consistent with this assumption it has been demonstrated that deletion of genes encoding substrates of APC, for example *ASE1* and *CLB2*, rescues Htt-103Q-induced toxicity [254]. Consequently, a removal of APC substrates alleviates its overload, resulting in an enhanced degradation of cyclins.

Based on these findings, a simple explanation for Fkh-mediated rescue of lethality might be due to their transcriptional properties; in fact, both Fkh1 and Fkh2 activate transcription of mitotic cyclins as well as other APC effectors. In particular, deletion of *FKH2* and especially the double deletion of *FKH1* and *FKH2* lead to a decrease in expression of B-type cyclins Clb1-4. In agreement with this, it has been shown that overexpression of *CDH1* reduces cytotoxic effects caused by mutant Htt-103Q in yeast [254]. It was speculated that hyperactive APC^{Cdh1}, which promotes mitotic exit directing Clb2 for degradation, reduces the toxicity of expanded polyQ fragments [254].

However, it might be reasonable that accumulation of APC substrates is related to neurodegenerative diseases. In Alzheimer's disease (AD), affected neurons frequently attempt abortive mitosis, initiation of DNA duplication followed by cell death. Importantly, it has been shown that this is caused by cyclin B accumulation, arguing that protein aggregates in AD inhibit APC function [261]. Although elevated

cyclin B levels were reported also for HD neurons, affected cells did not undergo abortive mitosis [299]. Nevertheless, other substrates of APC such as the neuronal differentiation factors Id2 and SnoN might be affected [300, 301]. Consistently, increased neuronal differentiation in murine model of HD has been reported [302]. Interestingly, neither *ase1* and *clb2* mutants nor *CDH1* overexpression were observed to alter aggregation of Htt-103Q as shown for *fkh2*Δ and *fkh1*Δ *fkh2*Δ mutants. Cell lethality was not found to be rescued in *fkh1*Δ *fkh2*Δ mutant, indicating the involvement of additional mechanisms that might explain mutant Htt-induced toxicity and/or perturbation of yeast cell growth as consequence of cell cycle misregulation.

The results presented in this thesis provided evidence that forkhead transcription factors act in concert with Sir2 to slow down progression through the cell cycle, resulting in a slow growth of yeast cells. In particular, Fkh1 and Fkh2 were shown to interact with Sir2 upon oxidative stress as well as following nutrient depletion in early stationary phase. Importantly, a strong association of these proteins was also observed when cells expressed Htt-103Q-RFP but not Htt-25Q-RFP. How can polyQ-dependent aggregation lead to an increased interaction between Sir2 and forkhead transcription factors?

Recent studies demonstrated that expanded polyQ expression at late exponential phase in yeast generates oxidative stress, as evidenced by an increased protein oxidation [209]. Consistently, an important role for oxidative stress in HD has been demonstrated in mouse and mammalian cells [303-306], thus suggesting that antioxidants slow down disease progression as shown in a mouse model of HD [307]. Additionally, it has been reported that expression of expanded polyQ in yeast and mammals oxidizes mitochondrial proteins, leading to mitochondrial dysfunction [201, 213, 308]. Similar results were obtained in human HD plasma [306] and brain tissue [207, 305, 309].

As a consequence of mutant polyQ-mediated stress induction, it was shown that transcription of *SIR2* becomes activated [114]. Increased Sir2 levels may enhance mitochondrial biogenesis and trigger stress tolerance in yeast in cooperation with the forkhead transcription factor Hcm1 [114]. In fact, *de novo* biogenesis of mitochondria suppresses polyQ-induced toxicity in both budding yeast [211] and mammalian cells

[222]. In this context, it is of interest that cells lacking *FKH2* as well as *fkh1*Δ *fkh2*Δ mutants were found to have increased levels of mitochondria. This observation could be one explanation for the reduced number of aggregates observed in both strains. However, it remains unclear whether there is a direct connection between Fkh1 and Fkh2 and mitochondrial metabolism, considering that the transcriptional profile of *fkh1*Δ *fkh2*Δ mutant reveals stress response genes [82]. One possibility might be that Sir2 could interact with Hcm1 to a much higher extent when both proteins Fkh1 and Fkh2 are missing, thus stimulating its nuclear localization and activation of mitochondrial metabolism. On the one hand, this observation may explain the less altered viability of *fkh1*Δ *fkh2*Δ mutant in response to oxidative stress, and on the other hand it might be a consequence of the fact that cells are unable to perform a cell cycle arrest as indicated by higher Clb2 levels. However, Htt-polyQ-induced lethality is not rescued in *fkh1*Δ *fkh2*Δ mutant, suggesting the involvement of additional features. Time-laps microscopy of mammalian cells expressing toxic 103Q proteins revealed a condensation of nuclei and apoptotic cell morphology as well as nuclear translocation of large aggregates in later stages of cell death processes [310]. Consistently, a fragmented nucleus was observed in yeast cells expressing comprise mutant polyQ aggregates. Moreover, the *fkh1*Δ *fkh2*Δ mutant showed nuclear fragmentation, although to a less strong extend, also under normal growth conditions. The results raise the possibility that deletion of both forkhead genes may result in a Sir2-dependent decrease in genome stability and to an increased mutation frequency, thus potentially activating genes mediating oxidative stress resistance. Expression of mutant polyQ as well as external stress exposure at the same time may lead to an overcharge of this antioxidant defense, enhancing the cytotoxic effects. Indeed, lethality of *fkh1*Δ *fkh2*Δ mutant was found to increase under these conditions as compared to wild type cells and *fkh1*Δ or *fkh2*Δ mutants. These findings are in agreement with previous data, where expression of 103Q in *sir2*Δ mutant increases protein oxidation in exponential phase and activates genes involved in stress resistance as compared to wild type cells [281].

Since it is known that a dysregulation of cell cycle components is involved in age-related human diseases such as HD, my work shed light onto molecular determants that are effected in this disease, thereby presenting promising targets for therapeutic intervention.

4.7 Pathways including Fkhs and sirtuins are conserved from yeast to humans

Up to now, four forkhead transcription factors have been identified in budding yeast and three of them have been demonstrated to be essential for cell cycle control, stress resistance and longevity (Hcm1, Fkh1 and Fkh2). In contrast, at least 34 forkhead transcription factors are known to be involved in cell proliferation and differentiation, cell cycle progression, glucose sensing, immunity, apoptosis, stress response and longevity in mammalian cells. Many of them have been shown to play important roles in tissue specific cancer and other human diseases [60, 61]. The closest functional homologue of yeast Hcm1 and Fkh seems to be represented by human subfamilies FOXO and FOXM1.

In dividing cells, the expression of FoxO proteins can promote cell cycle checkpoint-mediated arrest at G1/S and G2/M transitions in response to stress. This is partially mediated by upregulation of cell cycle inhibitors such as p21/p27, the mammalian homologue of Sic1, or repression of cyclin D1/D2 activity, human homologues of Cln3 [311, 312]. In addition, FoxO proteins have been shown to activate genes involved in DNA repair [313, 314] and oxidative stress response [315], but also to trigger cell death especially in lymphocytes and neurons [316-318]. The FoxO pathway is activated by a variety of stresses including oxidative stress, heat shock and UV radiation [319], DNA damage, nutrient deprivation, cytokinesis and hypoxia [320-326]. In this regard, mammalian Sirt1 associates and deacetylates FoxO1, 3 and 4 in response to stress stimuli by changing their promoter occupancy to differentially regulate target genes [110, 111, 112, 319]. SIR-2.1, the homologue of yeast Sir2 in *C. elegans*, is thought to activate DAF-16, the homolog of human FOXO, to promote longevity as well as stress resistance [185, 189, 327]. Overexpression of Sir2 homologues in worms, yeast and flies extend lifspan [173, 185, 189, 190], underlying the evolutionary conserved role of this protein in longevity pathways.

4.8 Conclusions and outlook

Combining computational and experimental analyses [236] suggested that the cyclin-dependent kinase inhibitor Sic1 may function as a timer in coordinating the oscillatory behavior of the phase-specific B-type cyclin levels. Future studies will have to concentrate on identifying by which additional mechanisms, besides Sic1 degradation via Cdc28-Cln and Cdc28-Clb phosphorylations, Sic1 can be regulated throughout the cell cycle. This could be possibly investigated from one side by experimentally testing the involvement of kinases and phosphatases known to play a role in Sic1 regulation.

Another focus of this study was to investigate the role of Forkhead transcription factors Fkh1 and Fkh2 in the regulation of G2/M transition of the cell cycle in budding yeast. In *vitro* and *in vivo* data suggested that transcriptional activation of genes controlled by Fkh proteins depends not only on recruitment of the coactivator Ndd1 to Fkh2 but also to Fkh1. In addition, expression of B-type cyclins Clb3 and Clb4 was shown to be dependent on forkhead-associated regulation, suggesting the involvement of Fkh1 and Fkh2 in initiation of transcriptional activation of G2/M genes.

As a consequence of these findings, the activation of Forkhead transcription factors Fkh1 and Fkh2 promoted by Cdc28-Clb5, 6 activities in early S phase may induce transcription of both *CLB3, 4* and *CLB 1, 2*. Since the interaction of Clb2, 3 and Ndd1 was shown in this thesis as well, the expression of Clb3, 4 in turn may result in the activation of its own transcription by Cdc28-dependent phosphorylation of Fkh1, 2 and Ndd1. Moreover, it is possible that Clb3 play a role in the priming of *CLB 1, 2* gene expression in S/G2 phase. However, Clb1, 2-dependent kinase activity promotes *CLB1, 2* transcription by phosphorylation of Fkh1, 2 and Ndd1, thus stimulating its own production in G2/M phase as previously reported [21].

At the end of mitosis until the onset of S phase, the activity of Cdc28-Clb1-6 complexes are negatively regulated by the association with Sic1. In addition, Cdc28-Clb1-6 complexes may phosphorylate Sic1 to mark it for degradation.

As an important result of this thesis, the histone deacteylase Sir2 was shown to bind the promoter of *CLB2* by the association with Fkh1, 2. This association was shown to be important for the repression of *CLB2* gene and demonstrated to counteract on the

binding between Fkh1, 2 and Ndd1. Since a binding of these transcription factors to the promoter of *CLB1-4* was varified, an involvement of Sir2 in repression of *CLB1, 3* and *4* was suggested in an extended model as well (Figure 4-1).

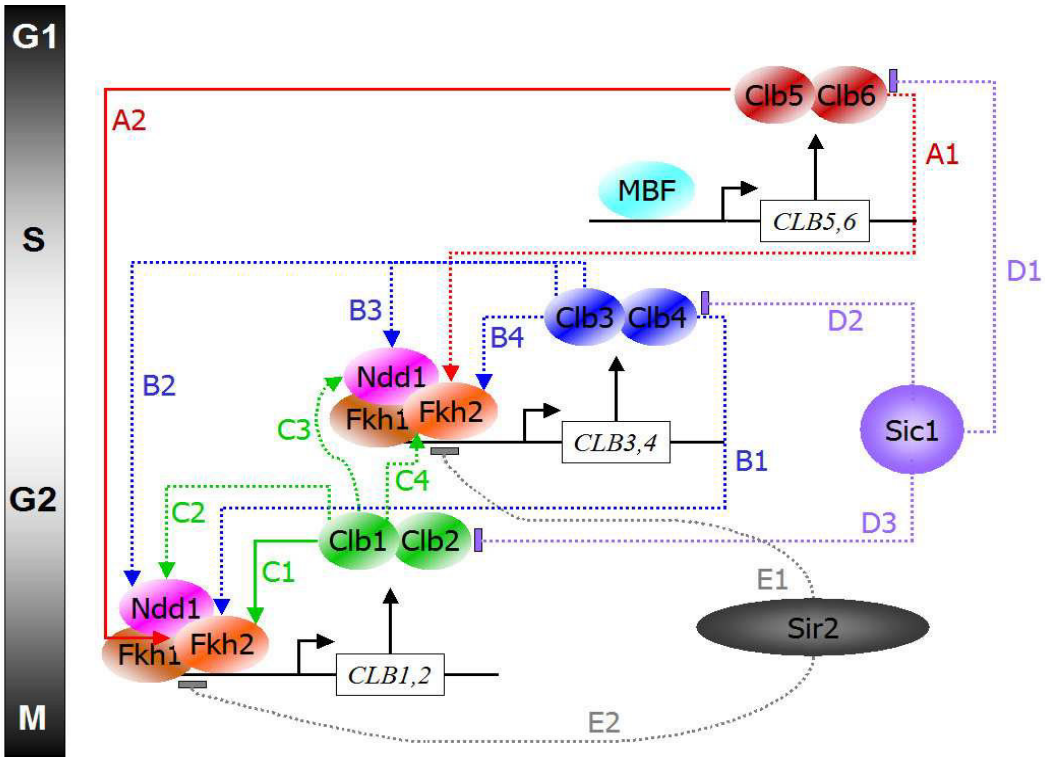

Figure 4-1. Mechanisms controlling cell cycle-regulated gene expression. The heterodimeric transcription factor MBF (Mbp1, Swi6) activates *CLB5, 6* transcription at early S phase. During S/G2 phase, Clb5, 6-dependent kinase activity promotes *CLB3, 4* (A1) and *CLB1, 2* (A2) transcription by phosphorylation of Fkh1, 2. Afterwards, Clb3,4-dependent kinase activity promotes *CLB1, 2* transcription by phosphorylating Fkh1, 2 (B1) and Ndd1 (B2). Moreover Cdc28-Clb3 complex activity stimulate its own expression by activating Ndd1 (B3) and Fkh1, 2 (B4). After production of Clb1, 2 in G2/M phase, Cdc28-dependent kinase activity promotes *CLB1, 2* transcription by phosphorylation of Fkh1, 2 (C1) and Ndd1 (C2), thus generating a positive feedbackloop to fully activates its own production. In addition, it is possible that Cdc28-Clb1, 2 complexes stimulate expression of *CLB3, 4* by phosphorylation of Ndd1 (C3) and Fkh1, 2 (C4). At the end of mitosis and during G1 phase Cdc28-Clb activity is inhibited by the binding of Sic1 to cyclins 5, 6 (D1), 3, 4 (D2) and 1, 2 (D3), thereby preventing phosphorylation of Fkh1, 2 and Ndd1. An additional silencing of B type cyclin genes *CLB3, 4* (E1) and *CLB1, 2* (E2) during these phases can be achieved by the association of histone deacetylase Sir2 with the proteins Fkh1, 2. For simplicity, Cdc28 subunit has been omitted.

The focus of the last part of my work was to investigate how the mechanism controlling the progression through the cell cycle can act in response to environmental stimuli such as oxidative stress, nutrient depletion or protein aggregation in a yeast Huntington's disease (HD) model.

When grown at early stationary phase, in exposure to oxidative stress or upon expression of Htt with an expanded polyQ stretch in exponential growing phase, yeast cells showed a reduced growth that might contribute at least in part to an

increased interaction observed between forkhead proteins and negative regulator Sir2, supporting a model in which Fkh1 and Fkh2 trigger progression through the cell cycle by a progressive activation or inactivation of G2/M genes.

To identify the molecular mechanisms by which forkhead transcription factors act in response to environmental stimuli is intriguing, since they are involved in a variety of cellular pathways. Of special interest might be to understand in more detail how related proteins induce cell cycle arrest via checkpoint proteins in order to activate detoxification mechanisms, thus preventing malfunctions that can lead to neurodegenerative disorders or cancer. Little is known about the interplay between forkhead transcription factors and their association with transcriptional regulators in response to different environmental stimuli to increase stress resistance, alter metabolic and developmental responses, improve immunity and extend lifespan in different species among the animal kingdom. The results presented in this thesis improved this knowledge by showing that yeast Fkh transcription factors directly interact with the histone deacetylase Sir2 to control cell cycle progression through G2/M phase, in addition to its known function in chromatin silencing. This association might suppress cell proliferation in response to oxidative stress as well as other stress stimuli to ensure proper function of pathways modulating oxidative stress response and longevity. Interestingly, overexpression of Sir2 leads to a reduction of cell growth, underlying its potential role in suppressing genes controlling cell cycle progression. In this context, it is assumed that reducing the number of divisions of a single mitotic cell in a specific time period leads to an extension of its lifespan. In yeast, old mother cells have an average replicative lifespan of 22 divisions in glucose rich medium [133]. Growth of cells in calorie restriction may lead to an extended lifespan even if the number of divisions is not altered, arguing that progression through each cell cycle round is slow down. However, for post-diauxic survival of yeast cells, known as chronological lifespan, Fkh proteins may help to anchor Sir2 and other histone deacetylases to maintain genome stability, consistent with previous studies where Sir2 silences heterochromatin structures like telomeres, nucleolar rDNA and mating type loci.

Interestingly, nuclear fragmentation was observed in *fkh1*Δ *fkh2*Δ mutant and sterility of old cells indicated by fragmentation of nucleoulus, as a reliable marker of aging in yeast [170, 258]. In this context, independent studies showed that relocalization of

Sir complexes from silent loci to DNA breaks also results in sterility [161, 162, 328]. Additionally, overexpression of Sir2 has been reported to enhance silencing at both telomeres and rDNA, implying Sir2 as a limiting component of the silencing apparatus [173, 175].

Importantly, reduction of mutant polyQ aggregation in *fkh2*Δ and especially *fkh1*Δ *fkh2*Δ mutant might be due to elevated unbound Sir2 as a consequence of missing chromatin-restricted anchor proteins, thus resulting in an extended Sir2-dependent acetylation and ubiquitinylation of polyQ fragments. However, in case of *fkh1*Δ *fkh2*Δ mutant as well as cells expressing toxic polyQ, genome instability might be a consequence of Sir2-dependent localization. Decreased genome stability may lead to accelerated aging phenotypes like fragmentation of nucleus as it is well known for old mother yeast cells [170, 258]. Consistently, aged budding yeast mother cells have been reported as well to show markers of oxidative stress and apoptosis [187].

5. Summary

Understanding the complex interplay between cell cycle regulators in functional contexts poses a great challenge, since an involvement of these proteins in multiple pathways, driving expression of genes according to environmental conditions, effected growth of mitotic and maintenance of postmitotic cells. The dysregulation of cell cycle components can result in a decline of cellular function eventually leading to senescence, apoptosis, cancer, aging and age-related diseases such as neurodegenerative disorders.

To gain insight into the function of proteins driving cell cycle progression, and to identify regulatory networks potentially relevant for these diseases, interaction studies have been performed. Specifically, associations between the regulatory subunits of heterodimeric cyclin-dependent kinases complexes called B-type cyclins (Clbs) and Sic1, a specific stoichiometric inhibitor of the Cdc28-Clb complexes were investigated. The experimental analyses combined with recent computational studies highlighted an additional role for Sic1 in the regulation of Cdc28-Clb complexes, acting as a timer in their regulation [236].

In addition, the role of Forkhead (Fkh) transcription factors Fkh1, Fkh2 and the coactivator Ndd1 in the coordination of Cdc28-Clb activities required for S/G2 and G2/M transitions of the cell cycle was analyzed. Therefore, the specificity of B-type cyclins to interact with Fkh1 and Ndd1 as well as a potential association between Fkh1 and Ndd1 was tested. Importantly, all B-type cyclins Clb1-6 was found to bind Ndd1 and both Fkh transcription factors including Clb2 and Clb5 which have been previously implicated to target Fkh2 for Cdc28-dependent phosphorylation. Moreover, the results validated an involvement of Fkh1 in the periodic activation of B-type cyclin genes due to the association with Ndd1. In addition, a potential role of Clb3 in priming Ndd1-dependent *CLB2* cluster transcription was identified. Considering that Fkh transcription factors bind at *CLB1-4* promoters, this result further demonstrates that the Fkh transcription factors could also play a role in promoting the expression of early mitotic cyclins to timely regulate cell cycle progression.

Furthermore, the data presented in this study indicated that Fkh1 and Fkh2 might act as a platform to recruit both the coactivator Ndd1 in S phase and the histone deacetylase Sir2 in late M phase in a mutual exclusive manner. Sir2, a histone deacetylase known to promote stress response and longevity pathways might be involved in repression of *CLB2* to control mitotic growth of yeast cells. Consistently, the Fkh-Sir2 interplay was further demonstrated to be relavant for stress resistance including exposure to oxidants, calorie restriction and protein aggregation caused by the polyglutamine protein Huntingtin.

The results in the course of this thesis further demonstrate that Sir2-dependent chromatin silencing in response to stress represses Fkh-controled cell cycle genes such as *CLB2.* Importantly, a direct link between Sir2-dependent chromatin silencing in response to stress and Fkh-mediated regulation of cell cycle components such as *CLB2* has not been considered before.

6. Zusammenfassung

Die Vertiefung des Verständnisses komplexer Zusammenhänge von Zellzyklusregulatoren stellt eine große Herausforderung dar, da Komponenten dieses Regulationsapparats an der Koordination zahlreicher zellulärer Vorgänge beteiligt sind, die in Abhängigkeit von Umwelteinflüssen die Zellteilung steuern und so das Wachstum und die Entwicklung vielzelliger Organismen maßgeblich beeinflussen. Das Versagen dieser Kontrollmechanismen kann schließlich zu Krebs, Seneszenz, Apoptose und alters-abhängigen Erkrankungen, z.B. neurodegenerative Erkrankungen, führen.

Ziel dieser Arbeit war es, Einsichten in die Proteinfunktion von Zellzyklusregulatoren zu erlangen, um regulatorische Netzwerke zu identifizieren, die für die Entstehung dieser Erkrankungen relevant sein könnten. Hierzu wurden Protein-kodierende Sequenzen bekannter Zellzyklusregulatoren kloniert und Protein-Interaktionsstudien *in vivo* und *in vitro* vorgenommen. Dazu erfolgte zunächst eine Untersuchung der Assoziation von regulatorischen Untereinheiten heterodimerischer Kinasekomplexe, den B-Typ Cyclinen (Clbs) und Sic1, einem spezifischen stoichiometrischen Inhibitor dieser Cdc28-Clb Komplexe. Die experimentellen Interaktionsdaten sowie bestehende mathematische Modellierungen führten so zu neuen Erkenntnissen über die Funktion von Sic1 in der Zellzyklus-abhängigen Steuerung von Cdc28-Clb1-6 [236].

Des weiteren wurde ein Einfluss der Forkhead (Fkh) Transkriptionsfaktoren Fkh1, Fkh2 und des Koaktivators Ndd1 auf die Koordination der Cdc28-Clb Aktivität, welche für den Übergang der Zellzyklusphasen S/G2 und G2/M verantwortlich sind, untersucht. Hierzu wurde die Interaktion der B-Typ Cycline mit Fkh1, Fkh2 und Ndd1 getestet, sowie eine potentielle Bindung zwischen Fkh1 und Ndd1 analysiert. Diese Untersuchung ergab, dass Clb1-6 mit Ndd1 und beiden Transkriptionsfaktoren Fkh1 und Fkh2 interagiert, welche die bereits bekannte Bindung von Fkh2 mit Clb2 und Clb5 einschließt. Zudem konnte in dieser Arbeit die Bindung des bisher als Fkh2-spezifisch beschriebenen Koaktivators Ndd1 mit Fkh1 gezeigt werden. Eine sich daraus ableitende Beteiligung beider Forkhead Transkriptionsfaktoren an der transkriptionellen Aktivierung von frühen mitotischen Cyclinen wie Clb3 und Clb4

konnte mittels genetischer und biochemischer Untersuchungen bestätigt werden. Darüber hinaus konnte eine potentielle Rolle von Cdc28-Clb3 bei der Initiation der Expression von G2/M-Genen, einschließlich *CLB2*, identifiziert werden.

Schließlich wurde eine funktionelle Rolle der Histondeacetylase Sir2 bei der Forkhead-vermittelten transkriptionellen Repression von *CLB2* ermittelt. Frühere Studien zeigten, dass die Regulation der Fkh-abhängigen Transkription mitotischer Zellzyklusgene von der Aktivität spezifischer B-Typ Cyclin-Kinase Komplexe abhängt. Die in dieser Arbeit präsentierten Ergebnisse weisen daraufhin, dass Fkh1 und Fkh2 als Chromatin-bindende Gerüstproteine dienen, welche Koregulatoren wie Ndd1 in der S-Phase und Sir2 in der späten M-Phase des Zellzyklus rekrutieren.

Eine Interaktion zwischen Fkh Proteinen und Sir2 erscheint auch für Stressresistenz von Hefezellen von Bedeutung, welche oxidativen Stress, Kaloriebegrenzung und Proteinaggregation von zytotoxisch wirksamen Huntingtin mit verlängertem Glutaminstretch einschließt. Ein Zusammenhang zwischen der Sir2 abhängigen Stressantwort und wichtigen Zellzyklusregulation wie Fkh1 und Fkh2, welche die Repression der Expression von Genen mitotischer Cycline durch epigenetische Mechanismen einschließt, wurde bisher nicht in Betracht gezogen.

6. References

1. Simon I., Barnett J., Hannett N., Harbison C.T., Rinaldi N.J., Volkert T.L., et al. Serial regulation of transcriptional regulators in the yeast cell cycle. *Cell* **106**, 697-708 (2001).

2. Cross F. R. and Blake V. M. The yeast Cln3 protein is an unstable activator of Cdc28. *Mol. Cell Biol.* **13**, 3266-3271(1993).

3. Di Como C. J., Chang H. and Arndt K.T. Activation of CLN1 and CLN2 G1 cyclin gene expression by BCK2. *Mol. Cell Biol.* **15**, 1835-1846 (1995).

4. Richardson H., Lew D. J., Henze M., Sugimoto K., Reed S. I. Cyclin-B homologs in *Saccharomyces cerevisiae* function in S phase and in G2. *Genes Dev.* **6**, 2021-2034 (1992).

5. Schwob E. and Nasmyth K. CLB5 and CLB6, a new pair of B cyclins involved in DNA replication in *Saccharomyces cerevisiae*. *Genes Dev.* **7**, 1160-1175 (1993).

6. Fitch I., Dahmann C., Surana U., Amon A., Nasmyth K., Goetsch L., Byers B., Futcher B. Characterization of four B-type cyclin genes of the budding yeast *Saccharomyces cerevisiae*. *Mol. Biol. Cell* **3**, 805-818 (1992).

7. Spellman P. T., Sherlock G., Zhang M. Q., Iyer V. R., Anders K., Eisen M. B., Brown P. O., Botstein D., Futcher B. Comprehensive identification of cell cycleregulated genes of the yeast *Saccharomyces cerevisiae* by microarray hybridization. *Mol. Biol. Cell* **9**, 3273-3297 (1998).

8. Richardson H. E., Wittenberg C., Cross F. and Reed S. I. An essential G1 function for cyclin-like proteins in yeast. *Cell* **59**, 1127-1133 (1989).

9. Tyers M., Tokiwa G., Nash R. and Futcher B. The Cln3-Cdc28 kinase komplex of S. cerevisiae is regulated by proteolysis and phosphorylation. *EMBO J.* **11**, 1773-1784 (1992).

10. Tyers M., Tokiwa G. and Futcher B. Comparison of the *Saccharomyces cerevisiae* G1 cyclins: Cln3 may be an upstream activator of Cln1, Cln2 and other cyclins. *EMBO J.* **12**, 1955-1968 (1993).

11. Nasmyth K. & Dirick, L. The role of SWI4 and SWI6 in the activity of G1 cyclins in yeast. *Cell* **66**, 995-1013 (1991).

12. Ogas J., Andrews B. J. & Herskowitz, I. Transcriptional activation of *CLN1*, *CLN2* and a putative new G1 cyclin (HCS26) by SWI4, a positive regulator of G1-specific transcription. *Cell* **66**, 1015-1026 (1991).

13. Bean J. M., Siggia E.D.& Cross, F. R. High functional overlap between MluI cello-cycle box binding factor and Swi4/6 cello-cycle box binding factor in tue G1/S transcriptional program in *Saccharomyces cerevisiae*. *Genetics* **171**, 49-61 (2005).

14. de Bruin R.A., McDonald W. H., Kalashnikova T. I., Yates J. 3rd & Wittenberg, C. Cln3 activates G1-specific transcription in Yeast. *Cell* **117**, 899-913 (2004).

15. Costanzo M. *et al*. CDK activity anatgonizes Whi5, an inhibitor of G1/S transcription in yeast. *Cell* **117**, 899-913 (2004).

16. Cross F. R. and Tinkelenberg A.H. A potential positive Feedback loop Controlling *CLN1* and *CLN2* gene expression at the start of the yeast cell cycle. *Cell* **65**, 875-883 (1991).

17. Dirick L. and Nasmyth K. Positive feedback in the activation of G1 cyclins in yeast. *Nature* **351**, 754-757 (1991).

18. Geymonat M., Spanos A., Wells G. P., Smerdon, S. J. &Sedgwick, S. G. Clb6/Cdc28 and Cdc 14 regulate phophorylation Status and zellular localization of Swi6. *Mol. Cell. Biol*. **24**, 2277-2285 (2004).

19. Amon A., Teyers M., Futcher B. and Nasmyth K. Mechanisms that help tue yeast cell cycle clock tick: G2 cyclins transcriptionally activate G2 cyclins and repress G1 cyclins. *Cell* **74**, 993-1007 (1993).

20. Siegmund R.F. and Nasmyth K. A. The *Saccharomyces cerevisiae* Start-specific transcription factor Swi4 interacts through the ankyrin repeats with tue mitotic Clb2/Cdc28 kinase and through ist conserved carboxy terminus with Swi6. *Mol. Cell. Biol*. **16**, 2647-2655 (1996).

21. Reynolds D., Shi B. J., McLean C., Katsis F., Kemp B. and Dalton S. Recruitment of Thr319-phosphorylated Ndd1p to the FHA domain of Fkh2p requires Clb kinase activity: a mechanism for *CLB* Cluster gene activation. *Genes Dev*. **17**, 1789-1802 (2003).

22. Darieva Z., *et al*. Cell cycle-regulated transcription through the FHA domain of Fkh2p and the coactivator Ndd1p. *Curr. Biol*. **13**, 1740-1745 (2003).

23. Pic-Taylor A., Darieva Z., Morgan B. A. and Sharrocks A. D. Regulation of cell cycle-specific gene Expression through cyclin dependent kinase-mediated phosphorylation of the forkhead transcription Faktor Fkh2p. *Mol. Cell. Biol.* **24**, 10036-10046 (2004).

24. Kumar R., Reynolds D.M., Shevchenko A., Goldstone S.D. and Dalton S. Forkhead transcription factors, Fkh1p and Fkh2p, collaborate with Mcm1p to control transcription required for M-phase. *Curr. Biol*. **10**, 896-906 (2000).

25. Darieva Z., Clancy A., Bulmer R., Williams E., Pic-Taylor A., Morgan B. A. and Sharrocks A. D. A Competitive Transcription Factor Binding Mechanism Determines the Timing of Late Cell Cycle-Dependent Gene Expression. *Molecular Cell* **38**, 29-40 (2010).

26. Althoefer H., Schleiffer A., Wassermann K., Nordheim A. and Ammerer G. Mcm1 is required to coordinate G2-specific transcription in *Saccharomyces cerevisiae. Mol. Cell. Biol*. **15**, 5917-5928 (1995).

27. Pramila T., Miles S., GuhaThakurta D., Jemiolo D. and Breeden L. L. Conserved homedomain proteins interact with MADS box protein Mcm1 to restrict ECB-dependent transcription to the M/G1 phase of the cell cycle. *Genes Dev*. **16**, 3034-3045 (2002).

28. Mai B., Miles S. and Bereden L. L. Characterization of the ECB binding complex responsible for the M/G1-specific transcription of CLN3 and SWI4. Mol. Cell. Biol. **16**, 2135-2143 (1996).

29. Barral Y., Jentsch S. and Mann C. G1 cyclin turnover and nutrient uptake are controled by a common pathway in yeast. *Genes Dev*. **9**, 399-409 (1995).

30. Skowyra D., Craig K. L., Teyers M., Elledge S. J. and Harper J. W. F-box proteins are receptors that recruit phophorylated substrates to the SCF ubiquitin-ligase complex. *Cell* **91**, 209-219 (1997).

31. Jackson L. P., Reed S. I. and Haase S. B. Distinct mechanisms control the stability of the related S-phase cyclins Clb5 and Clb6. *Mol. Cell. Biol.* **26**, 2456-2466 (2006).

32. Shirayama M., Toth A., Galova M. and Nasmyth, K. APC^{Cdc20} promptes exit from Mitosis by destroying tue anaphase inhibitor Pds1 and cyclin Clb5. *Nature* **402**, 203-207 (1999).

33. Wasch R. and Cross F. R. APC-dependent proteolysis of the mitotic cyclin Clb2 is essential for mitotic exit. *Nature* **418**, 556-562 (2002).

34. Huang J. N., Park I., Ellingson E., Littlepage L. E. and Pellman D. Activity of the APC^{Cdh1} form of the anaphase-promoting complex persists until S phase and prevents the premature expression of Cdc20p. *J. Cell Biol.* **154**, 85-94 (2001).

35. Shwob E., Bohm T., Mendenhall M. D. and Nasmyth K. The B-type cyclin kinase inhibitor p40SIC1 controls the G1 to S transition in *S. cerevisae. Cell* **79**, 233-244 (1994).

36. Spellman P. T., Sherlock G., Zhang M. Q., Iyer V. R., Anders K., Eisen M. B., Brown P. O., Botstein D. and Futcher B. Comprehensive identification of cell cycleregulated genes of the yeast *Saccharomyces cerevisiae* by microarray hybridization. *Mol. Biol. Cell.* **9**, 3273-3297 (1998).

37. Feldmann R. M., Correl C. C., Kapplan K. B. and Deshaies R. J. A complex of Cdc4p, Skp1p, and Cdc53p/cullin catalyzes ubiquitination of tue phosphorylated CDK inhibitor Sic1p. *Cell* **91**, 221-230 (1997).

38. Verma R. *et al*. Phophorylation of Sic1p by G1 Cdk required for its degradation and entry into S phase. *Science* **278**, 455-460 (1997).

39. Breitkreutz A. and Teyers M. MAPK signaling specificity: it takes two to tango. *Trends Cell Biol*. **12**, 254-257 (2002).

40. Peter M. and Herskowitz I. Direct inhibition of the yeast cyclin-dependent kinase Cdc28-Cln by Far1. *Science* **265**, 1228-1231 (1994).

41. Jeoung D. I., Oehlen L. J. and Cross F. R. Cln3-associated kinase activity in *Saccharomyces cerevisiae* is regulated by the mating pathway. *Mol. Cell. Biol.* **18**, 433-441 (1998).

42. McKinney J. D., Chang F., Heintz N. and Cross F. R. Negative regulation of Far1 at the start of tue yeast cell cycle. *Genes Dev*. **7**, 833-843 (1993).

43. Henchoz S. *et al.* Phosphorylation- and ubiquitindependent degradation of the cyclin dependent kinase inhibitor Far1p in budding yeast. *Genes Dev.* **11**, 3046-3060 (1997).

44. Lew D. J. and Reed S. I. A cell cycle checkpoint monitors cell morphogenesis in budding yeast. *J. Cell Biol.* **129**, 739-749 (1995).

45. McMillan J. N., Sia R. A., Bardes E. S. and Lew D. J. Phosphorylation-independent inhibition of Cdc28p by the tyrosine kinase Swe1p in tue morphogenesis checkpoint. *Mol. Cell. Biol.* **19**, 5981-5990 (1999).

46. Harvey S. L., Charlet A., Haas W., Gygi, S. P. and Kellogg D. R. Cdk1-dependent regulation of the mitotic inhibitor Wee1. *Cell* **122**, 407-420 (2005).

47. Thornton B. R. and Toczyski D. P. Securin and B-cyclin/CDK are the only essential targets of the APC. *Nature Cell Biol.* **5**, 1090-1094 (2003).

48. Asano S. *et al.* Concerted mechanism of Swe1/Wee1 regulation by multiple kinases in budding yeast. *EMBO J.* **24**, 2194-2204 (2005).

49. Jaspersen S. L., Charles J. F. and Morgan D. O.Inhibitory phosphorylation of the APC regulator Hct1 is controlled by the kinase Cdc28 and the phosphatase Cdc14. *Curr. Biol.* **9**, 227-236 (1999).

50. Schwab M., Lutum A. S. and Seufert W. Yeast Hct1 is a regulator of Clb2 cyclin proteolysis. *Cell* **90**, 683-693 (1997).

51. Visintin R. *et al.* The phosphatase Cdc14 triggers mitotic exit by reversal of Cdk-dependent phosphorylation. *Mol. Cell* **2**, 709-718 (1998).

52. Jaspersen S. L., Charles J. F., Tinker-Kulberg R. L. and Morgan D. O. A late mitotic regulatory network controlling cyclin destruction in *Saccharomyces cerevisiae*. *Mol. Biol. Cell* **9**, 2803-2817 (1998).

53. Bardin A. J., Visintin R. and Amon A. A mechanism for coupling exit from mitosis to partitioning of the nucleus. *Cell* **102**, 21-31 (2000).

54. Alexandru G., Zachariae W., Schleiffer A. and Nasmyth K. Sister chromatid separation and chromosome re-duplication are regulated by different mechanisms in response to spindle damage. *EMBO J.* **18**, 2707-2721 (1999).

55. Azzam R. *et al.* Phosphorylation by cyclin B-Cdk underlies release of mitotic exit activator Cdc14 from the nucleolus. *Science* **305**, 516-519 (2004).

56. Jaspersen S. L. and Morgan D. O. Cdc14 activates Cdc15 to promote mitotic exit in budding yeast. *Curr. Biol.* **10**, 615-618 (2000).

57. Stegmeier F., Visintin R. and Amon A. Separase, polo kinase, the kinetochore protein Slk19, and Spo12 function in a network that controls Cdc14 localization during early anaphase. *Cell* **108**, 207-220 (2002).

58. Shou W., *et al.* Net1 stimulates RNA polymerase I transcription and regulates nucleolar structure independently of controlling mitotic exit. *Mol. Cell* **8**, 45-55 (2001).

59. Baldauf S. L. A Search for the origins of animals and fungi: Comparing and combining molecular data. *Am. Nat.* **154**, 178-88 (1999).

60. Tuteja G. and Kaestner K. H. SnapShot: forkhead transcription factors I. *Cell* **130**, 1160 (2007).

61. Tuteja G. and Kaestner K. H. Forkhead transcription factors II. *Cell* **131**, 192 (2007).

62. Partridge L. and Bruning J. C. Forkhead transcription factors and ageing. *Oncogene* **27**, 2351-63 (2008).

63. Cirillo L. A., McPherson C. E., Bossard P., Stevens K., Cherian S., Shim E.Y., *et al.* Binding of the winged-helix transcription factor HNF3 to a linker histone site on the nucleosome. *EMBO J.* **17**, 244-54 (1998).

64. Clark K. L., Halay E. D., Lai E. and Burley S. K. Co-crystal structure of the HNF-3/fork head DNA-recognition motif resembles histone H5. *Nature* **364**, 412-20 (1993).

65. Gajiwala K. S., Chen H., Cornille F., Roques B.P., Reith W., Mach B., *et al.* Structure of the winged-helix protein hRFX1 reveals a new mode of DNA binding. *Nature* **403**, 916-21 (2000).

66. Scott K. L. and Plon S. E. Loss of Sin3/Rpd3 histone deacetylase restores the DNA damage response in checkpoint-deficient strains of *Saccharomyces cerevisiae*. *Mol. Cell Biol.* **23**, 4522-31 (2003).

67. Major M. L , Lepe R. and Costa R. H. Forkhead box M1B transcriptional activity requires binding of Cdk-cyclin complexes for phosphorylation-dependent recruitment of p300/CBP coactivators. *Mol. Cell Biol*. **24**, 2649-61 (2004).

68. Pic A., Lim F. L., Ross S. J., Veal E. A., Johnson A. L. , Sultan M. R., *et al.* The forkhead protein Fkh2 is a component of the yeast cell cycle transcription factor *SFF. EMBO J.* **19**, 3750-61 (2000).

69. Jorgensen P., Rupes I., Sharom J.R., Schneper L., Broach J.R., Tyers M. A dynamic transcriptional network communicates growth potential to ribosome synthesis and critical cell size. *Genes Dev.* **18**, 2491-505 (2004).

70. Rudra D., Zhao Y., Warner J.R. Central role of Ifh1p-Fhl1p interaction in the synthesis of yeast ribosomal proteins. *EMBO J.* **24**, 533-42 (2005).

71. Schawalder S.B., Kabani M., Howald I., Choudhury U., Werner M., Shore D. Growth-regulated recruitment of the essential yeast ribosomal protein gene activator Ifh1. *Nature* **432**, 1058-61 (2004).

72. Wade J.T., Hall D.B., Struhl K. The transcription factor Ifh1 is a key regulator of yeast ribosomal protein genes. *Nature* **432**, 1054-8 (2004).

73. Schmelzle T., Beck T., Martin D.E., Hall M.N. Activation of the RAS/cyclic AMP pathway suppresses a TOR deficiency in yeast. *Mol. Cell Biol.* **24**, 338-51 (2004).

74. Zhu G., Muller E. G., Amacher S. L., Northrop J. L., Davis T. N. A dosage-dependent suppressor of a temperaturesensitive calmodulin mutant encodes a protein related to the fork head family of DNA-binding proteins. *Mol. Cell Biol.* **13**, 1779-87 (1993).

75. Pramila T., Wu W., Miles S., Noble W.S. and Breeden L.L. The Forkhead transcription factor Hcm1 regulates chromosome segregation genes and fills the S-phase gap in the transcriptional circuitry of the cell cycle. *Genes Dev*. **20**, 2266-78 (2006).

76. Hollenhorst P.C., Bose M.E., Mielke M.R., Muller U. and Fox C.A. Forkhead genes in transcriptional silencing, cell morphology and the cell cycle: Overlapping and distinct functions for FKH1 and FKH2 in *Saccharomyces cerevisiae*. *Genetics* **154**, 1533–1548 (2000).

77. Breeden L.L. Cyclin transcription: Timing is everything. *Curr. Biol.* **10**, 586–588 (2000).

78. Wittenberg C. and Reed S. I. Cell cycle-dependent transcription in yeast: promotors, transcription Faktors, and transcriptomes. *Oncogene* **24**, 46-2755 (2005).

79. Koranda M., Schleiffer A., Endler L. and Ammerer G. Forkhead-like transcription factors recruit Ndd1 to the chromatin of G2/M-specific promoters. *Nature* **406**, 94-8 (2000).

80. Shore P. and Sharrocks A.D. The MADS-box family of transcription factors. *Eur. J. Biochem*. **229**, 1-13 (1995).

81. Loy C.J., Lydall D. and Surana U. NDD1, a high-dosage suppressor of cdc28-1N, is essential for expression of a subset of late-S-phase-specific genes in *Saccharomyces cerevisiae*. *Mol. Cell Biol.* **19**, 3312-27 (1999).

82. Zhu G., Spellman P.T., Volpe T., Brown P.O., Botstein D., Davis T.N., *et al.* Two yeast forkhead genes regulate the cell cycle and pseudohyphal growth. *Nature* **406**, 90-4 (2000).

83. Hollenhorst P.C., Pietz G. and Fox C.A. Mechanisms controlling differential promoter-occupancy by the yeast forkhead proteins Fkh1p and Fkh2p: implications for regulating the cell cycle and differentiation. *Genes Dev.* **15**, 2445-56 (2001).

84. Darieva Z., Bulmer R., Pic-Taylor A., Doris K.S., Geymonat M, Sedgwick S.G., *et al.* Polo kinase controls cell cycle-dependent transcription by targeting a coactivator protein. *Nature* **444**, 494-8 (2006).

85. Lin K., Dorman J.B., Rodan A., Kenyon C. daf-16: An HNF-3/forkhead family member that can function to double the life-span of *Caenorhabditis elegans*. *Science* **278**, 1319–1322 (1997).

86. Giannakou M.E., Goss M., Junger M.A., Hafen E., Leevers S.J., et al. Longlived Drosophila with overexpressed dFOXO in adult fat body. *Science* **305**, 361 (2004).

87. Hwangbo D.S., Gershman B., Tu M.P., Palmer M., Tatar M. Drosophila dFOXO controls lifespan and regulates insulin signalling in brain and fat body. *Nature* **429**, 562–566 (2004).

88. Kappeler L., De Magalhaes Filho C., Dupont J., Leneuve P., Cervera P., et al. Brain IGF-1 receptors control mammalian growth and lifespan through a neuroendocrine mechanism. *PLoS Biol*. **6**, e254. doi:10.1371/journal. pbio.0060254 (2008).

89. Yuan R., Tsaih S.W., Petkova S.B., Marin de Evsikova C., Xing S., et al. Aging in inbred strains of mice: study design and interim report on median lifespans and circulating IGF1 levels. *Aging Cell* **8**, 277-287 (2009).

90. Li Y., Wang W.J., Cao H., Lu J., Wu C., et al. Genetic association of FOXO1A and FOXO3A with longevity trait in Han Chinese populations. *Hum. Mol. Genet*. **18**, 4897-4904 (2009).

91. Willcox B.J., Donlon T.A., He Q., Chen R., Grove J.S., et al. FOXO3A genotype is strongly associated with human longevity. *Proc Natl. Acad. Sci. USA* **105**, 13987-13992 (2008).

92. Arden K.C., et al. FOXO animal models reveal a variety of diverse roles for FOXO transcription factors. *Oncogene* **27**, 2345-2350 (2008).

93. Murakami H., Aiba H., Nakanishi M. and Murakami-Tonami Y. Regulation of yeast forkhead transcription factors and FoxM1 by cyclin-dependent and polo-like kinases. *Cell Cycle* **16**, 3233-3242 (2010).

94. Laoukili J., Kooistra M.R., Bras A., Kauw J., Kerkhoven R.M., Morrison A., et al. FoxM1 is required for execution of the mitotic programme and chromosome stability. *Nat. Cell Biol*. **7**, 126-36 (2005).

95. Wang Z., Ahmad A., Li Y., Banerjee S., Kong D., Sarkar F.H. Forkhead box M1 transcription factor: A novel target for cancer therapy. *Cancer Treat. Rev.* (2009).

96. Laoukili J., Stahl M., Medema R.H. FoxM1: at the crossroads of ageing and cancer. *Biochem. Biophys. Acta* **1775**, 92-102 (2007).

97. Pandit B., Halasi M., Gartel A.L. p53 negatively regulates expression of FoxM1. *Cell Cycle* **8**, 3425-3427 (2009).

98. Petrovic V., Costa R.H., Lau L.F., Raychaudhuri P., Tyner A.L. Negative regulation of the oncogenic transcription factor FoxM1 by thiazolidinediones and mithramycin. *Cancer Biol. Ther.* **9**, 1008-1016 (2010).

99. Tang S.Y., Jiao Y., Li L.Q. [Significance of Forkhead Box m1b (Foxm1b) gene in cell proliferation and carcinogenesis]. *Ai Zheng* **27**, 894-896 (2008).

100. Major, M. L , Lepe, R., Costa, R. H. Forkhead box M1B transcriptional activity requires binding of Cdk-cyclin complexes for phosphorylation-dependent recruitment of p300/CBP coactivators. *Mol. Cell Biol*. **24**, 2649-61 (2004).

101. Laoukili J., Kooistra M.R., Bras A., Kauw J., Kerkhoven R.M., Morrison A., et al. FoxM1 is required for execution of the mitotic programme and chromosome stability. *Nat. Cell Biol*. **7**, 126-36 (2005).

102. Wang I.C., Chen Y.J., Hughes D.E., Ackerson T., Major M.L., Kalinichenko V.V., et al. FoxM1 regulates transcription of JNK1 to promote the G1/S transition and tumor cell invasiveness. *J. Biol. Chem.* **283**, 20770-8 (2008).

103. Wang I.C., Chen Y.J., Hughes D., Petrovic V., Major M.L., Park H.J., et al. Forkhead box M1 regulates the transcriptional network of genes essential for mitotic progression and genes encoding the SCF (Skp2-Cks1) ubiquitin ligase. *Mol. Cell Biol*. **25**, 10875-94 (2005).

104. Ustiyan V., Wang I.C., Ren X., Zhang Y., Snyder J., Xu Y., et al. Forkhead box M1 transcriptional factor is required for smooth muscle cells during embryonic development of blood vessels and esophagus. *Dev. Biol.* **336**, 266-79 (2009).

105. Korver W., Schilham M.W., Moerer P., van den Hoff M.J., Dam K., Lamers W.H., et al. Uncoupling of S phase and mitosis in cardiomyocytes and hepatocytes lacking the winged-helix transcription factor Trident. *Curr. Biol.* **8**, 1327-30 (1998).

106. Nurse P. Universal control mechanism regulating onset of M-phase. *Nature* **344**, 503-8 (1990).

107. Laoukili J., Alvarez M., Meijer L.A., Stahl M., Mohammed S., Kleij L., et al. Activation of FoxM1 during G2 requires cyclin A/Cdk-dependent relief of autorepression by the FoxM1 N-terminal domain. *Mol. Cell. Biol.* **28**, 3076-87 (2008).

108.Fu Z., Malureanu L., Huang J., Wang W., Li H., van Deursen J.M., et al. Plk1-dependent phosphorylation of FoxM1 regulates a transcriptional programme required for mitotic progression. *Nat. Cell Biol.* **10**, 1076-82 (2008).

109.Brunet A., Sweeney L.B., Sturgill J.F., Chua K.F., Greer P.L., et al. Stressdependent regulation of FOXO transcription factors by the SIRT1 deacetylase. *Science* **303**, 2011-2015 (2004).

110.Daitoku H., Hatta M., Matsuzaki H., Aratani S., Ohshima T., et al. Silent information regulator 2 potentiates Foxo1-mediated transcription through its deacetylase activity. Proc. Natl. Acad. Sci. USA **101**, 10042-10047. (2004).

111.Motta M. C., Divecha N., Lemieux M., Kamel C., Chen D., et al. Mammalian SIRT1 represses forkhead transcription factors. *Cell* **116**, 551-563 (2004).

112.Yang Y., Hou H., Haller E.M., Nicosia S.V., Bai W. Suppression of FOXO1 activity by FHL2 through SIRT1-mediated deacetylation. *EMBO J.* **24**, 1021-1032 (2005).

113.Van der Horst A., L.G. Tertoolen, L.M. de Vries-Smits, R.A. Frye, R.H. Medema, B.M. Burgering, *J. Biol. Chem.* **279**, 28873-28879 (2004).

114.Rodriguez-Colman M. J., Reverter-Branchat G., Sorolla M. A., Tamarit J., Ros J. and Cabiscol E. The Forkhead Transcription Factor Hcm1 Promotes Mitochondrial Biogenesis and Stress Resistance in Yeast. *J. Biol. Chem.* **285**, 37092-37101 (2010).

115.Veis J., Klug H., Koranda M. and Ammerer G. Activation of the G2/M-Specific Gene *CLB2* Requires Multiple Cell Cycle Signals *Mol. Cell Biol*. **27**, 8364-8373 (2007).

116.Rundlett S. E., Carmen A. A., Kobayashi R., Bavykin S., Turner B. M. and Grunstein M. HDA1 and RPD3 are members of distinct yeast histone deacetylase complexes that regulate silencing and transcription. *Proc. Natl. Acad. Sci.* USA **93**, 14503-14508 (1996).

117.Sandmeier J. J., French S., Osheim Y., Cheung W. L., Gallo C. M., Beyer A.L. and J. S. Smith. RPD3 is required for the inactivation of yeast ribosomal DNA genes in stationary phase. *EMBO J.* **21**, 4959-4968 (2002).

118.Vogelauer M., Rubbi L., Lucas I., Brewer B. J. and Grunstein M. Histone acetylation regulates the time of replication origin firing. *Mol. Cell* **10**, 1223-1233 (2002).

119.Chang K. T., and Min K. T. Regulation of lifespan by histone deacetylase. *Ageing Res. Rev.* **1**, 313-326 (2002).

120.Kim S., Benguria A., Lai C. Y. and Jazwinski S. M. Modulation of life-span by histone deacetylase genes in *Saccharomyces cerevisiae. Mol. Biol. Cell* **10**, 3125-3136 (1999).

121.Vannier D., Balderes D., and Shore D. Evidence that the transcriptional regulators SIN3 and RPD3, and a novel gene (SDS3) with similar functions, are involved in transcriptional silencing in *S. cerevisiae. Genetics* **144**, 1343-1353 (1996).

122.Sun, Z.W. and Hampsey, M. A general requirement for the Sin3-Rpd3 histone deacetylase complex in regulating silencing in *Saccharomyces cerevisiae*. *Genetics* **152**, 921-932 (1999).

123.Zhou J., Zhou B. O., Lenzmeier B. A. and Zhou J. Histone deacetylase Rpd3 antagonizes Sir2-dependent silent chromatin propagation *Nucleic Acids Res.* **37**, 3699-3713 (2009).

124.Bernstein B. E., Tong J. K., and Schreiber S. L. Genomewide studies of histone deacetylase function in yeast. *Proc. Natl. Acad. Sci*. USA **97**, 13708–13713 (2000).

125.Rogina B., Helfand S. L., and Frankel S. Longevity regulation by Drosophila Rpd3 deacetylase and caloric restriction. *Science* **298**, 1745 (2002).

126.Pletcher S. D., Macdonald S. J., Marguerie R., Certa U., Stearns S. C., Goldstein D. B., and Partridge L. Genome-wide transcript profiles in aging and calorically restricted *Drosophila melanogaster. Curr. Biol.* **12**, 712-723 (2002).

127.Imai S., Armstrong C. M., Kaeberlein M., and Guarente L. Transcriptional silencing and longevity protein Sir2 is an NAD-dependent histone deacetylase*. Nature* **403**:795-800 (2000).
128.Shore D., Squire M., Nasmyth K.A., Characterization of two genes required for the position-effect control of yeast mating-type genes. *EMBO J.* **3**, 2817-2823 (1984).

129.Kaeberlein M., McVey M., Guarente L., The SIR2/3/4 complex and SIR2 alone promote longevity in Saccharomyces cerevisiae by two different mechanisms. *Genes Dev.* **13**, 2570-2580 (1999).

130.Landry J., Sutton A., Tafrov S. T., Heller R. C., Stebbins J., Pillus L., and Sternglanz R. The silencing protein SIR2 and its homologs are NAD-dependent protein deacetylases. *Proc. Natl. Acad. Sci.* USA **97**, 5807-5811 (2000).

131.Smith J. S., Brachmann C. B., Celic I., Kenna M. A., Muhammad S., Starai V. J., Avalos J. L., Escalante-Semerena J. C., Grubmeyer C., Wolberger C., and Boeke J. D. A phylogenetically conserved NAD-dependent protein deacetylase activity in the Sir2 protein family. *Proc. Natl. Acad. Sci*. USA **97**, 6658-6663 (2000).

132.Froyd C. A., Rusche L. N. The duplicated deacetylases Sir2 and Hst1 subfunctionalized by acquiring complementary inactivating mutations. *Mol. Cell Biol.* **16**, 3351-65 (2011).

133.Bitterman K. J., Medvedik O., Sinclair D. A., Longevity regulation in *Saccharomyces cerevisiae* linking metabolism, genome stability, and heterochromatin. *Microbiol. Mol. Biol. Rev.* **67**, 376-399 (2003).

134.Sauve A. A., Celic I., Avalos J., Deng H., Boeke J. D., and Schramm V. L. Chemistry of gene silencing: the mechanism of NAD-dependent deacetylation reactions. *Biochemistry* **40**, 15456-15463 (2001).

135.Moazed D. Enzymatic activities of Sir2 and chromatin silencing. *Curr. Opin. Cell Biol.* **13**, 232-238 (2001).

136.Luo J., Nikolaev A. Y., Imai S., Chen D., Su F., Shiloh A., Guarente L., and Gu W. Negative control of p53 by Sir2alpha promotes cell survival under stress. *Cell* **107**, 137-148 (2001).

137.Bitterman K. J., Anderson R. M., Cohen H. Y., Latorre-Esteves M., and Sinclair D. A. Inhibition of silencing and accelerated aging by nicotinamide, a putative negative regulator of yeast sir2 and human SIRT1. *J. Biol. Chem.* **277**, 45099-45107 (2002).

138.Anderson, R. M., K. J. Bitterman, J. G. Wood, O. Medvedik, and D. A. Sinclair. Nicotinamide and PNC1 govern lifespan extension by calorie restriction in *Saccharomyces cerevisiae. Nature* **423**, 181-185 (2003).

139.Sandmeier J. J., Celic I., Boeke J. D., and Smith J. S. Telomeric and rDNA silencing in *Saccharomyces cerevisiae* are dependent on a nuclear NAD(+) salvage pathway. *Genetics* **160**, 877-889 (2002).

140.Shama S., Lai C. Y., Antoniazzi J. M., Jiang J. C., and Jazwinski S. M. Heat stress-induced life span extension in yeast. *Exp. Cell Res.* **245**, 379-388 (1998).

141.Swiecilo A., Krawiec Z., Wawryn J., Bartosz G., and T. Bilinski. Effect of stress on the life span of the yeast *Saccharomyces cerevisiae. Acta Biochim. Pol.* **47**, 355-364 (2000).

142.Longo V. D., and Fabrizio P. Regulation of longevity and stress resistance: a molecular strategy conserved from yeast to humans? *Cell. Mol. Life Sci.* **59**, 903-908 (2002).

143.Longo, V. D., E. B. Gralla, and J. S. Valentine. Superoxide dismutase activity is essential for stationary phase survival in *Saccharomyces cerevisiae.* Mitochondrial production of toxic oxygen species in vivo. *J. Biol. Chem.* **271**, 12275-12280 (1996).

144.Pronk J. T., Yde Steensma H., and Van Dijken J. P. Pyruvate metabolism in *Saccharomyces cerevisiae. Yeast* **12**, 1607-1633 (1996).

145.Lin S. J., Kaeberlein M., Andalis A. A., Sturtz L. A., Defossez P. A., Culotta V. C., Fink G. R., and Guarente L. Calorie restriction extends *Saccharomyces cerevisiae* lifespan by increasing respiration. *Nature* **418**, 344-348 (2002).

146.Werner-Washburne M., Braun E. L., Crawford M. E., and Peck V. M. Stationary phase in *Saccharomyces cerevisiae. Mol. Microbiol.* **19**, 1159-1166 (1996).

147.Werner-Washburne M., Braun E., Johnston G. C., and Singer R. A. Stationary phase in the yeast *Saccharomyces cerevisiae. Microbiol. Rev.* **57**, 383-401 (1993).

148.Stephen D. W., Rivers S. L., and Jamieson D. J. The role of the YAP1 and YAP2 genes in the regulation of the adaptive oxidative stress responses of *Saccharomyces cerevisiae. Mol. Microbiol.* **16**, 415-423 (1995).

149.Longo V. D., Liou L. L., Valentine J. S., and Gralla E. B. Mitochondrial superoxide decreases yeast survival in stationary phase. *Arch. Biochem. Biophys.* **365**, 131-142 (1999).

150.Harman D. A theory based on free radical and radiation chemistry. *J. Gerontol.* **11**, 298-304 (1956).

151.Fabrizio P., Liou L. L., Moy V. N., Diaspro A., SelverstoneValentine J., Gralla E. B., and Longo V. D. SOD2 functions downstream of Sch9 to extend longevity in yeast. *Genetics* **163**, 35-46 (2003).

152.Fabrizio P., Pozza F., Pletcher S. D., Gendron C. M., and Longo V. D. Regulation of longevity and stress resistance by Sch9 in yeast. *Science* **292**, 288-290 (2001).

153.Lillie S. H., and Pringle J. R. Reserve carbohydrate metabolism in *Saccharomyces cerevisiae*: responses to nutrient limitation. *J. Bacteriol.* **143**, 1384-1394 (1980).

154.Lin S. J., Defossez P. A. and Guarente L. Requirement of NAD and SIR2 for life-span extension by calorie restriction in *Saccharomyces cerevisiae Science* **289**, 2126‑2128 (2000).

155.Kennedy B. K., Austriaco N. R., Zhang J., and Guarente L. Mutation in the silencing gene *SIR4* can delay aging in *S. cerevisiae. Cell* **80**, 485-496 (1995).

156.Loo S., and Rine J. Silencing and heritable domains of gene expression. *Annu. Rev. Cell Dev. Biol.* **11**, 519-548 (1995).

157.Moazed, D. Common themes in mechanisms of gene silencing. *Mol. Cell* **8**, 489–498 (2001).

158.Martin S. G., Laroche T., Suka N., Grunstein M., and Gasser S. M. Relocalization of telomeric Ku and SIR proteins in response to DNA strand breaks in yeast. *Cell* **97**, 621–633 (1999).

159.Mills K.D., Sinclair D.A., and Guarente L. *MEC1*-dependent redistribution of the Sir3 silencing protein from telomeres to DNA double-strand breaks. *Cell* **97**, 609–620 (1999).

160.Smith J. S., and Boeke J. D. An unusual form of transcriptional silencing in yeast ribosomal DNA. *Genes Dev.* **11**, 241-254 (1997).

161.Lee S. E., Paques F., Sylvan J., and Haber J. E. Role of yeast SIR genes and mating type in directing DNA double-strand breaks to homologous and non-homologous repair paths. *Curr. Biol.* **9**, 767-770 (1999).

162.McAinsh A. D., Scott-Drew S., Murray J. A., and Jackson S. P. DNA damage triggers disruption of telomeric silencing and Mec1p-dependent relocation of Sir3p. *Curr. Biol.* **9**, 963-966 (1999).

163.Muller I. Parental age and the life-span of zygotes of *Saccharomyces cerevisiae. Antonie Leeuwenhoek* **51**, 1-10 (1985).

164.Smeal T., Claus J., Kennedy B., Cole F., and Guarente L. Loss of transcriptional silencing causes sterility in old mother cells of *S. cerevisiae*. *Cell* **84**, 633-642 (1996).

165.Kennedy B. K., Gotta M., Sinclair D. A., Mills K., McNabb D. S., Murthy M., Pak S. M., Laroche T., Gasser S. M., and Guarente L. Redistribution of silencing proteins from telomeres to the nucleolus is associated with extension of life span in *S. cerevisiae*. *Cell* **89**, 381-391 (1997).

166.Kim S., Villeponteau B., and Jazwinski S. M. Effect of replicative age on transcriptional silencing near telomeres in *Saccharomyces cerevisiae. Biochem. Biophys. Res. Commun.* **219**, 370-376 (1996).

167.Sinclair D. A., and Guarente L. Extrachromosomal rDNA circles-a cause of aging in yeast. *Cell* **91**, 1033-1042 (1997).

168.Cockell, M. M., and Gasser S. M. The nucleolus: nucleolar space for RENT. *Curr. Biol.* **9**, R575-R576 (1999).

169.Melese, T., and Xue Z. The nucleolus: an organelle formed by the act of building a ribosome. *Curr. Opin. Cell Biol.* **7**, 319-324 (1995).

170.Sinclair D. A., Mills K., and Guarente L. Accelerated aging and nucleolar fragmentation in yeast sgs1 mutants. *Science* **277**, 1313-1316 (1997).

171.Egilmez N. K., and Jazwinski S. M. Evidence for the involvement of a cytoplasmic factor in the aging of the yeast *Saccharomyces cerevisiae. J. Bacteriol.* **171**, 37-42 (1989).

172.Miller C. A., and Kowalski D. *cis*-acting components in the replication origin from ribosomal DNA of *Saccharomyces cerevisiae. Mol. Cell. Biol.* **13**, 5360-5369 (1993).

173.Kaeberlein M., McVey M., and Guarente L. The *SIR*2/3/4 complex and SIR2 alone promote longevity in *Saccharomyces cerevisiae* by two different mechanisms. *Genes Dev.* **13**, 2570-2580 (1999).

174.Lin S. J., Defossez P. A., and Guarente L. Requirement of NAD and *SIR2* for life-span extension by calorie restriction in *Saccharomyces cerevisiae. Science* **289**, 2126-2128 (2000).

175.Smith J. S., Brachmann C. B., Pillus L., and Boeke J. D. Distribution of a limited Sir2 protein pool regulates the strength of yeast rDNA silencing and is modulated by Sir4p. *Genetics* **149**, 1205-1219 (1998).

176.Masoro E. J. Caloric restriction and aging: an update. *Exp. Gerontol.* **35**, 299-305 (2000).

177.McCay C. M., Maynard L. A., Sperling G., and Barnes L. L. Retarded growth, life span, ultimate body size and age changes in the albino rat after feeding diets restricted in calories. *Nutr. Rev.* **33**, 241-243. (1975) [Reprint of *J. Nutr.* **18**, 1-13 (1939)].

178.Kenyon C., Chang J., Gensch E., Rudner A. and Tabtiang R. A *C. elegans* mutant that lives twice as long as wild type. *Nature* **366**, 461-464 (1993).

179.Kimura K. D., Tissenbaum H. A., Liu Y., and Ruvkun G. *daf-2*, an insulin receptor-like gene that regulates longevity and diapause in *Caenorhabditis elegans. Science* **277**, 942-946 (1997).

180.Morris J. Z., Tissenbaum H. A. and Ruvkun G. A phosphatidylinositol-3-OH kinase family member regulating longevity and diapause in *Caenorhabditis elegans. Nature* **382**, 536-539 (1996).

181Clancy D. J., Gems D., Harshman L. G., Oldham S., Stocker H., Hafen E., Leevers S. J. and Partridge L. Extension of life-span by loss of CHICO, a *Drosophila* insulin receptor substrate protein. *Science* **292**, 104-106 (2001).

182.Tatar M., Kopelman A., Epstein D., Tu M. P., Yin C. M. and Garofalo R. S. A mutant *Drosophila* insulin receptor homolog that extends life-span and impairs neuroendocrine function. *Science* **292**, 107-110 (2001).

183. Kenyon C. A conserved regulatory mechanism for aging. *Cell* **105**, 165-168 (2001).

184.Tsang A. W. and Escalante-Semerena J. C. CobB, a new member of the SIR2 family of eucaryotic regulatory proteins, is required to compensate for the lack of nicotinate mononucleotide:5,6-dimethylbenzimidazole phosphoribosyltransferase activity in cobT mutants during cobalamin biosynthesis in *Salmonella typhimurium* LT2. *J. Biol. Chem.* **273**, 31788-31794 (1998).

185.Tissenbaum H. A., and Guarente L. Increased dosage of a *sir-2* gene extends lifespan in *Caenorhabditis elegans. Nature* **410**, 227-230 (2001).

186.Vaziri H., Dessain S. K., Eaton E. N., Imai S. I., Frye R. A., Pandita T. K., Guarente L., and Weinberg R. A. hSIR2(SIRT1) functions as an NAD-dependent p53 deacetylase. *Cell* **107**, 149-159 (2001).

187.Laun P., Pichova A., Madeo F., Fuchs J., Ellinger A., Kohlwein S., Dawes I., Frohlich K. U., and Breitenbach M. Aged mother cells of *Saccharomyces cerevisiae* show markers of oxidative stress and apoptosis. *Mol. Microbiol.* **39**, 1166-1173 (2001).

188.Virag L., and Szabo C. The therapeutic potential of poly(ADPribose) polymerase inhibitors. *Pharmacol. Rev.* **54**, 375-429 (2002).

189.Berdichevsky A., Viswanathan M., Horvitz H. R., Guarente L. *C. elegans* SIR-2.1 interacts with 14-3-3 proteins to activate DAF-16 and extend life span. *Cell* **125**, 1165-1177 (2006).

190.Rogina B., Helfand S. L. Sir2 mediates longevity in the fly through a pathway related to calorie restriction. *Proc. Natl. Acad. Sci.* USA **101**, 15998-16003 (2004).

191.Reiner A., Albin R. L., Anderson K. D., D'Amato C. J., Penney J. B. Differential loss of striatal projection neurons in Huntington disease. *Proc. Natl. Acad. Sci.* USA **85**, 5733-5737 (1988).

192.Browne S. E., Ferrante R. J., Beal M. F. Oxidative stress in Huntington's disease. *Brain Pathol.* **9**, 147-163 (1999).

193.The Huntington's Disease Collaborative Research Group, A novel gene containing a trinucleotide repeat that is expanded and unstable on Huntington's disease chromosomes. *Cell* **72**, 971-983 (1993).

194.Benitez J., Fernandez E., Garcia-Ruiz P., Robledo M., Ramos C., Yébenes J., Trinucleotide (CAG) repeat expansion in chromosomes of Spanish patients with Huntington's disease. *Hum. Genet.* **94**, 563-564 (1994).

195.Andrew S.E., Goldberg Y.P., Kremer B., Telenius H., Theilmann J., Adam S., Starr E., Squitieri F., Lin B., Kalchman M.A., et al. *Nat. Genet.* **7**, 513-519 (1993).

196.Ross C.A. Intranuclear neuronal inclusions: a common pathogenic mechanism for glutamine-repeat neurodegenerative diseases? *Neuron* **19**, 1147-1150 (1997).

197.Nakamura K., Jeong S.Y., Uchihara T., Anno M., Nagashima K., Nagashima T., Ikeda S., Tsuji S., Kanazawa I. SCA17, a novel autosomal dominant cerebellar ataxia caused by an expanded polyglutamine in TATA-binding protein. *Hum. Mol. Genet.* **10**, 1441-1448 (2001).

198.Wyttenbach A., Sauvageot O., Carmichael J. Heat shock protein 27 prevents cellular polyglutamine toxicity and suppresses the increase of reactive oxygen species caused by huntingtin. *Hum. Mol. Genet.* **11**, 1137-1151 (2002).

199.Perutz M.F. Glutamine repeats and neurodegenerative diseases: molecular aspects. *Trends Biochem. Sci.* **24**, 58-63 (1999).

200.Nagai Y., Inui T., Popiel H. A., Fujikake N., Hasegawa K., Urade Y., Goto Y., Naiki H., Toda T. A toxic monomeric conformer of the polyglutamine protein. *Nat. Struct. Mol. Biol.* **14**, 332-340 (2007).

201.Wellington C. L., Ellerby L. M., Gutekunst C.A., Rogers D., Warby S., Graham R. K., Loubser O., van Raamsdonk J., Singaraja R., Yang Y. Z., Gafni J., Bredesen D., Hersch S. M., Leavitt B. R., Roy S., Nicholson D. W., Hayden M. R. Caspase cleavage of mutant huntingtin precedes neurodegeneration in Huntington's disease. *J. Neurosci.* **22**, 7862-7872 (2002).

202.Wang L. H., Qin Z. H. Animal models of Huntington's disease: implications in uncovering pathogenic mechanisms and developing therapies. *Acta Pharmacol. Sin.* **27**, 1287-1302 (2006).

203.Bence N. F., Sampat R. M., Kopito R. R. Impairment of the ubiquitin-proteasome system by protein aggregation. *Science* **292**, 1552-1555 (2001).

204.Trushina E., Dyer R. B., Badger J. D. 2nd, Ure D., Eide L., Tran D. D., Vrieze B. T., Legendre-Guillemin V., McPherson P. S., Mandavilli B. S., Van Houten B., Zeitlin S., McNiven M., Aebersold R., Hayden M., Parisi J. E., Seeberg E., Dragatsis I., Doyle K., Bender A., Chacko C., McMurray C.T. Mutant huntingtin impairs axonal trafficking in mammalian neurons in vivo and in vitro. *Mol. Cell. Biol.* **24**, 8195-8209 (2004).

205.Giorgini F., Guidetti P., Nguyen Q., Bennett S. C., Muchowski P. J. A genomic screen in yeast implicates kynurenine 3-monooxygenase as a therapeutic target for Huntington disease. *Nat. Genet.* **37**, 526-531 (2005).

206.Cha J. H. Transcriptional dysregulation in Huntington's disease. *Trends Neurosci.* **23**, 387-392 (2000).

207.Gu M., Gash M. T., Mann V. M., Javoy-Agid F., Cooper J. M., Schapira A. H. Mitochondrial defect in Huntington's disease caudate nucleus. *Ann. Neurol.* **39**, 385-389 (1996).

208.Jenkins B. G., Koroshetz W. J., Beal M. F., Rosen B. R. Evidence for impairment of energy metabolism *in vivo* in Huntington's disease using localized 1H NMR spectroscopy. *Neurology* **43**, 2689-2695 (1998).

209.Sorolla M. A., Nierga C., Rodríguez-Colman M. J., Reverter-Branchat G., Arenas A., Tamarit J., Ros J., Cabiscol E. Sir2 is induced by oxidative stress in a yeast model of Huntington disease and its activation reduces protein aggregation. *Arch. Biochem. Biophys.* **510**, 27-34 (2011).

210.Solans A., Zambrano A., Rodríguez M., Barrientos A. Cytotoxicity of a mutant huntingtin fragment in yeast involves early alterations in mitochondrial OXPHOS complexes II and III. *Hum. Mol. Genet.* **15**, 3063-3081 (2006).

211.Ocampo A., Zambrano A. , Barrientos A. Suppression of polyglutamine-induced cytotoxicity in *Saccharomyces cerevisiae* by enhancement of mitochondrial biogenesis. *FASEB J.* **24**, 1431-1441 (2010).

212.Sorolla M. A., Reverter-Branchat G., Tamarit J., Ferrer I., Ros J., Cabiscol E. Proteomic and oxidative stress analysis in human brain samples of Huntington disease. *Free Radic. Biol. Med.* **45**, 667-678 (2008).

213.Nakao N., Brundin P. Effects of alpha-phenyl-tert-butyl nitrone on neuronal survival and motor function following intrastriatal injections of quinolinate or 3-nitropropionic acid. *Neuroscience* **76**, 749-761 (1997).

214.Levine R. L., Williams J. A., Stadtman E.R., Shacter E. Carbonyl assays for determination of oxidatively modified proteins. *Methods Enzymol.* **233**, 346-357 (1994).

215.Cabiscol E., Piulats E., Echave P., Herrero E., Ros J. Oxidative stress promotes specific protein damage in *Saccharomyces cerevisiae*. *J. Biol. Chem.* **275**, 27393-27398 (2000).

216.Irazusta V., Moreno-Cermeño A., Cabiscol E., Ros J., Tamarit J. Major targets of iron-induced protein oxidative damage in frataxin-deficient yeasts are magnesium-binding proteins. *Free Radic. Biol. Med.* **44**, 1712-1723 (2008).

217.Perluigi M., Poon H. F., Maragos W., Pierce W. M., Klein J. B., Calabrese V., Cini C., de Marco C., Butterfield D. A. Proteomic analysis of protein expression and oxidative modification in r6/2 transgenic mice: a model of Huntington disease. *Mol. Cell. Proteomics* **4**, 1849-1861 (2005).

218.Outeiro T.F., Marques O., Kazantsev A. Therapeutic role of sirtuins in neurodegenerative disease. *Biochim. Biophys. Acta* **1782**, 363-369 (2008).

219.Parker J. A., Arango M., Abderrahmane S., Lambert E., Tourette C., Catoire H., Néri C. Resveratrol rescues mutant polyglutamine cytotoxicity in nematode and mammalian neurons. *Nat. Genet.* **37**, 349-350 (2005).

220.Ho D. J., Calingasan N. Y., Wille E., Dumont M., Beal M. F. Resveratrol protects against peripheral deficits in a mouse model of Huntington's disease. *Exp. Neurol.* **225**, 74-84 (2010).

221.Rodgers J. T., Lerin C., Haas W., Gygi S. P., Spiegelman B. M., Puigserver P. Nutrient control of glucose homeostasis through a complex of PGC-1alpha and SIRT1. *Nature* **434**, 113-118 (2005).

222.Lagouge M., Argmann C., Gerhart-Hines Z., Meziane H., Lerin C., Daussin F., Messadeq N., Milne J., Lambert P., Elliott P., Geny B., Laakso M., Puigserver P., Auwerx J. Resveratrol improves mitochondrial function and protects against metabolic disease by activating SIRT1 and PGC-1alpha. *Cell* **127**, 1109-1122 (2006).

223.Pervaiz S. Resveratrol: from grapevines to mammalian biology. *FASEB J.* **17**, 1975-1985 (2003).

224.Sorolla M. A. , Nierga C., Rodríguez-Colman M. J., Reverter-Branchat G., Arenas A., Tamarit J., Ros J., Cabiscol E. Sir2 is induced by oxidative stress in a yeast model of Huntington disease and its activation reduces protein aggregation. *Arch. Biochem. Biophys.* **510**, 27-34 (2011).

225.Olmos Y., Valle I., Borniquel S., Tierrez A., Soria E., Lamas S., Monsalve M. Mutual dependence of Foxo3a and PGC-1alpha in the induction of oxidative stress genes. *J. Biol. Chem.* **284**, 1476-1484 (2009).

226. Jiang M., Wang J., Fu J., Du L., Jeong H., West T., Xiang L., Peng Q., Hou Z., Cai H., Seredenina T., Arbez N., Zhu S., Sommers K., Qian J., Zhang J., Mori S., Yang X. W., Tamashiro K. L., Aja S., Moran T. H., Luthi-Carter R., Martin B., Maudsley S., Mattson M. P., Cichewicz R. H., Ross C. A., Holtzman D. M., Krainc D., Duan W. Neuroprotective role of Sirt1 in mammalian models of Huntington's disease through activation of multiple Sirt1 targets. *Nat. Med.* Dec **18**, 153-158 (2011).

227.Ralser M., Albrecht M., Nonhoff U., Lengauer T., Lehrach H., Krobitsch S. An integrative approach to gain insights into the cellular function of human ataxin-2. *J. Mol. Biol.* **346**, 203-214 (2005).

228.Ralser M., Nonhoff U., Albrecht M., Lengauer T., Wanker E. E., Lehrach H. Krobitsch S. Ataxin-2 and huntingtin interact with endophilin-A complexes to function in plastin-associated pathways. *Hum. Mol. Genet.* **14**, 2893-2909 (2005).

229.Stelzl U., Worm U., Lalowski M., Haenig C., Brembeck F. H., Goehler H., Stroedicke M., Zenkner M., Schoenherr A., Koeppen S., Timm J., Mintzlaff S., Abraham C., Bock N., Kietzmann S., Goedde A., Toksöz E., Droege A., Krobitsch S., Korn B., Birchmeier W., Lehrach H., Wanker E. E.

A human protein-protein interaction network: a resource for annotating the proteome. *Cell* **122**, 957-968 (2005).

230.Mumberg D., Muller R. and Funk M. Regulatable promoters of Saccharomyces cerevisiae: comparison of transcriptional activity and their use for heterologous expression. *Nucleic Acids Res.* **22**, 5767-5768 (1994).

231.Mumberg D., Muller R. and Funk M. Yeast vectors for the controlled expression of heterologous proteins in different genetic backgrounds. *Gene*. **156**, 119-122 (1995).

232.Sung M. and Huh W. Bimolecular fluorescence complementation analysis system for *in vivo* detection of protein-protein interaction in *Saccharomyces cerevisiae Yeast* **24**, 767-775 (2007).

233.Tauber E., Miller-Fleming L., Mason R. P., Kwan W., Clapp J., Butler N. J., Outeiro T. F., Muchowski P. J., Giorgini F. Functional gene expression profiling in yeast implicates translational dysfunction in mutant huntingtin toxicity. *J. Biol. Chem.* **286**, 410-419 (2010).

234.Boros J., Lim F. L., Darieva Z., Pic-Taylor A., Harman R., Morgan B. A., Sharrocks A. D. Molecular determinants of the cell-cycle regulated Mcm1p-Fkh2p transcription factor complex.*Nucleic Acids Res.* **31**, 2279-2288 (2003).

235.Barberis M., Klipp E. Insights into the network controlling the G(1)/S transition in budding yeast. *Genome Inform* **18**, 85-99 (2007).

236.Barberis M., Linke C., Adrover M. A., Lehrach H., Posas F., Krobitsch S., Klipp E. Sic1 plays a role in timing and oscillatory behaviour of B-type cyclins. *Biotechnol. Adv.* **30**, 108-30 (2012).

237.Archambault V., Chang E. J., Drapkin B. J., Cross F. R., Chait B. T., Rout M. P. Targeted proteomic study of the cyclin-Cdk module. *Mol. Cell* **14**, 699-711 (2004).

238.Honey S., Schneider B. L., Schieltz D. M., Yates J. R., Futcher B. A novel multiple affinity purification tag and its use in identification of proteins associated with a cyclin-CDK complex. *Nucleic Acids Res* **29**, E24 (2001).

239.Krogan N. J., Cagney G., Yu H., Zhong G., Guo X., Ignatchenko A., Li J., Pu S., Datta N, Tikuisis A. P., Punna T., Peregrín-Alvarez J. M., Shales M., Zhang X., Davey M., Robinson M. D., Paccanaro A., Bray J. E., Sheung A., Beattie B., Richards D. P., Canadien V., Lalev A., Mena F., Wong P., Starostine A., Canete M. M., Vlasblom J., Wu S., Orsi C., *et al.*: Global landscape of protein complexes in the yeast Saccharomyces cerevisiae. *Nature* **440**, 637-643 (2006).

240.Collins S. R., Kemmeren P., Zhao X. C., Greenblatt J. F., Spencer F., Holstege F. C., Weissman J. S., Krogan N. J. Toward a comprehensive atlas of the physical interactome of Saccharomyces cerevisiae. *Mol Cell Proteomics* **6**, 439-450 (2007).

241.Verma R., Feldman R. M., Deshaies R.J. SIC1 is ubiquitinated in vitro by a pathway that requires CDC4, CDC34, and cyclin/CDK activities. *Mol. Biol. Cell* **8**, 1427-1437 (1997).

242.Casey L., Patterson E. E., Muller U., Fox C. A. Conversion of a Replication Origin to a Silencer through a Pathway Shared by a Forkhead Transcription Factor and an S Phase Cyclin. *Mol. Biol. Cell* **19**, 608-22 (2008).

243.Morillon A., O'Sullivan J., Azad A., Proudfoot N., Mellor J. Regulation of elongating RNA polymerase II by forkhead transcription factors in yeast. *Science* **300**, 492-5 (2003).

244.Chasse S. A., *et al.* Genome-scale analysis reveals Sst2 as the principal regulator of mating pheromone signaling in the yeast *Saccharomyces cerevisiae*. *Eukaryot. Cell* **5**, 330-46 (2006).

245.Shapira M., Segal E. and Botstein D. Disruption of Yeast Forkhead-associated Cell Cycle Transcription by Oxidative Stress *Mol. Biol. Cell* **15**, 5659-5669 (2004).

246.Flattery-O'Brien J. A., Dawes I. W. Hydrogen peroxide causes RAD9-dependent cell cycle arrest in G2 in *Saccharomyces cerevisiae* whereas menadione causes G1 arrest independent of RAD9 function. *J. Biol. Chem.* **273**, 8564-71 (1998).

247.Leroy C., Mann C., and Marsolier M.C. Silent repair accounts for cell cycle specificity in the signaling of oxidative DNA lesions. *EMBO J.* **20**, 2896-2906. (2001).

248.Postnikoff S. D., Malo M. E., Wong B., Harkness T.A.The yeast forkhead transcription factors fkh1 and fkh2 regulate lifespan and stress response together with the anaphase-promoting complex. *PLoS Genet* **8**, e1002583 (2012).

249.Jakubowski W., Bilinski T., Bartosz G. Oxidative stress during aging of stationary cultures of the yeast *Saccharomyces cerevisiae*. *Free Radic. Biol. Med.* **28**, 659-664 (2000).

250.Zuin A., Castellano-Esteve D., Ayté J., Hidalgo E. Living on the edge: stress and activation of stress responses promote lifespan extension. *Aging* (Albany NY) **2**, 231‑237 (2010).

251.Cabiscol E., Belli G., Tamarit J., Echave P., Herrero E., Ros J. Mitochondrial Hsp60, resistance to oxidative stress, and the labile iron pool are closely connected in Saccharomyces cerevisiae. J. Biol. Chem. **277**, 44531-44538 (2002).

252.Gokhale K. C., Newnam G. P., Sherman M. Y., Chernoff Y. O. Modulation of prion-dependent polyglutamine aggregation and toxicity by chaperone proteins in the yeast model. *J. Biol. Chem.* **280**, 22809-18 (2005).

253.Meriin A. B., Zhang X., Alexandrov I. M., Salnikova A. B., Ter-Avanesian M. D., Chernoff Y. O., Sherman M. Y. Endocytosis machinery is involved in aggregation of proteins with expanded polyglutamine domains. *FASEB J.* **21**, 1915-25 (2007).

254.Bocharova N. A., Sokolov S. S., Knorre D. A., Skulachev V. P., Severin F. F. Unexpected link between anaphase promoting complex and the toxicity of expanded polyglutamines expressed in yeast. *Cell Cycle.* Dec **7**, 3943-6 (2008).

255.Wang L. H., Qin Z. H. Animal models of Huntington's disease: implications in uncovering pathogenic mechanisms and developing therapies.*Acta Pharmacol. Sin.* **27**, 1287‑1302 (2006).

256.Sokolov S., Pozniakovsky A., Bocharova N., Knorre D., Severin Expression of an expanded polyglutamine domain in yeast causes death with apoptotic markers. *F. Biochem. Biophys. Acta.* **1757**, 660-6 (2006).

257.Nisoli E., Tonello C., Cardile A., Cozzi V., Bracale R., Tedesco L., Falcone S., Valerio A., Cantoni O., Clementi E., Moncada S., Carruba M. O. Calorie restriction promotes mitochondrial biogenesis by inducing the expression of eNOS. *Science* **310**, 314-327 2005.

258.Sinclair D. A., Mills K., Guarente L. Accelerated Aging and Nucleolar Fragmentation in Yeast *sgs1* Mutants *Science* **277**, 1313-1316 (1997).

259.Guarente L. Link between aging and the nucleolus *Genes Dev.* 11, 2449-55 (1997).

260.Jiang M., Wang J., Fu J., Du L., Jeong H., West T., Xiang L., Peng Q., Hou Z., Cai H., Seredenina T., Arbez N., Zhu S., Sommers K., Qian J., Zhang J., Mori S., Yang X. W., Tamashiro K. L., Aja S., Moran T. H., Luthi-Carter R., Martin B., Maudsley S., Mattson M. P., Cichewicz R. H., Ross C. A., Holtzman D. M., Krainc D., Duan W. Neuroprotective role of Sirt1 in mammalian models of Huntington's disease through activation of multiple Sirt1 targets. *Nat. Med.* **18**, 153-8 (2011).

261.Aulia S., Tang B. L. Cdh1-APC/C, cyclin B-Cdc2, and Alzheimer's disease pathology. *Biochem. Biophys. Res. Commun.* **339**, 1-6 (2006).

262.Futcher B. Cyclins and the wiring of the yeast cell cycle. *Yeast* **12**, 1635-1646 (1996).

263.Koch C., Nasmyth K. Cell cycle regulated transcription in yeast. *Curr. Opin. Cell Biol.* **6**, 451-459 (1994).

264.Nugroho T. T., Mendenhall M. D. An inhibitor of yeast cyclin-dependent protein kinase plays an important role in ensuring the genomic integrity of daughter cells. *Mol. Cell Biol.* **14**, 3320-3328 (1994).

265.Lengronne A., Schwob E. The yeast CDK inhibitor Sic1 prevents genomic instability by promoting replication origin licensing in late G1. *Mol. Cell* **9**, 1067-1078 (2002).

266.Kron S. J., Styles C. A., Fink G. R.Symmetric cell division in pseudohyphae of the yeast *Saccharomyces cerevisiae*. *Mol. Biol. Cell* **5**, 1003-22 (1994).

267.Sherriff J. A., Kent N. A., Mellor J. The Isw2 chromatin-remodeling ATPase cooperates with the Fkh2 transcription factor to repress transcription of the B-type cyclin gene CLB2. *Mol. Cell Biol*. **27**, 2848-60 (2007).

268.Darieva Z., Bulmer R., Pic-Taylor A., Doris K. S., Geymonat M., Sedgwick S. G., Morgan B. A. and Sharrocks A. D. Polo kinase controls cell-cycle-dependent transcription by targeting a coactivator protein. *Nature* **444**, 494-498 (2006).

269.Altheim B. A. and Schulz M. C. Histone modification governs the cell cycle regulation of a replication-independent chromatin assembly pathway in *Saccharomyces cerevisiae Proc. Natl. Acad. Sci. USA* **96**, 1345-1350 (1999).

270.Godon C., Lagniel G., Lee J., Buhler J. M., Kieffer S., Perrot M., Boucherie H., Toledano M. B., Labarre J. The H2O2 stimulon in Saccharomyces cerevisiae. *J. Biol. Chem.* **273**, 22480-9 (1998).

271.Dumond H., Danielou N., Pinto M., Bolotin-Fukuhara M. A large-scale study of Yap1p-dependent genes in normal aerobic and H2O2-stress conditions: the role of Yap1p in cell proliferation control in yeast. *Mol. Microbiol.* **36**, 830-45 (2000).

272.Gasch A. P., Spellman P. T., Kao C. M., Carmel-Harel O., Eisen M. B., Storz G., Botstein D., Brown P. O. Genomic expression programs in the response of yeast cells to environmental changes. *Mol. Biol. Cell.* **11**, 4241-57 (2000).

273.Monks T. J., Hanzlik R. P., Cohen G. M., Ross D. and Graham, D. G. Quinone chemistry and toxicity. *Toxicol. Appl. Pharmacol.* **112**, 2-16 (1992).

274.Shackelford R. E., Kaufmann W. K. and Paules R. S. Oxidative stress and cell cycle checkpoint function. *Free. Radic. Biol. Med.* **28**, 1387-1404 (2000).

275.Cho R. J., *et al*. A genome-wide transcriptional analysis of the mitotic cell cycle. *Mol. Cell* **2**, 65-73 (1998).

276.Toyn J. H., Johnson A. L., Donovan J. D., Toone W. M., and Johnston L. H. The Swi5 transcription factor of *Saccharomyces cerevisiae* has a role in exit from mitosis through induction of the cdk-inhibitor Sic1 in telophase. *Genetics* **145**, 85-96 (1997).

277.Jiang R., and Carlson M. Glucose regulates protein interactions within the yeast SNF1 protein kinase complex. *Genes Dev.* **10**, 3105-3115 (1996).

278.Liao X. S., Small W. C., Srere P. A. and Butow R. A. Intramitochondrial functions regulate nonmitochondrial citrate synthase (CIT2) expression in *Saccharomyces cerevisiae. Mol. Cell. Biol.* **11**, 38-46 (1991).

279.Finkel T., Holbrook N. J. Oxidants, oxidative stress and the biology of ageing. *Nature* **408**, 239-247 (2000).

280.Neumann C. A., Krause D. S., Carman C. V., Das S., Dubey D. P., Abraham J. L., Bronson R. T., Fujiwara Y., Orkin S. H., and Van Etten R. A. Essential role for the peroxiredoxin Prdx1 in erythrocyte antioxidant defence and tumour suppression. *Nature* **424**, 561-565 (2003).

281.Fabrizio P., Gattazzo C., Battistella L., Wei M., Cheng C., McGrew K., Longo V. D. Sir2 blocks extreme life-span extension. *Cell* **123**, 655-667 (2005).

282.Andrulis E. D., Neiman A. M., Zappulla D. C., Sternglanz R. Perinuclear localization of chromatin facilitates transcriptional silencing. *Nature* **394**, 592-5 (1998).

283.Harkness T. A. A, Shea K. A. , Legrand C., Brahmania M., Davies G. F. A functional analysis reveals dependence on the anaphase-promoting complex for prolonged life span in yeast. *Genetics* **168**, 759-774 (2004).

284.Harkness T. A. A. The Anaphase Promoting Complex and aging: the APCs of longevity. *Curr. Genomics* **7**, 263-272 (2006).

285.Harkness T. A. A., Davies G. F., Ramaswamy V., Arnason T. G. The ubiquitindependent targeting pathway in Saccharomyces cerevisiae plays a critical role in multiple chromatin assembly regulatory steps. *Genetics* **162**, 615-632 (2002).

286.Turner E. L., Malo M. E., Pisclevich M. G., Dash M. D., Davies G. F., *et al.* The *Saccharomyces cerevisiae* Anaphase Promoting Complex interacts with multiple histone-modifying enzymes to regulate cell cycle progression. *Eukaryot. Cell* **9**, 1418-1431 (2010).

287.Harkness T. A. A Chromatin assembly from yeast to man: Conserved factors and conserved molecular mechanisms. *Current Genomics* **6**, 227-240 (2005).

288.Islam A., Turner E. L., Menzel J., Malo M. E., Harkness T. A. Antagonistic Gcn5-Hda1 interactions revealed by mutations to the Anaphase Promoting Complex in yeast. *Cell Div.* **6**, 13 (2011).

289.Hartwell L. H., Smith D. Altered fidelity of mitotic chromosome transmission in cell cycle mutants of S. cerevisiae. *Genetics* **110**, 381-395 (1985).

290.Palmer R. E., Hogan E., Koshland D. Mitotic transmission of artificial chromosomes in cdc mutants of the yeast, *Saccharomyces cerevisiae*. *Genetics* **125**, 763-774 (1990).

291.Baker D. J., Jeganathan K. B., Cameron J. D., Thompson M., Juneja S., *et al.* BubR1 insufficiency causes early onset of aging-associated phenotypes and infertility in mice. *Nat. Genet.* **36**, 744-749 (2004).

292.Harjes P. and Wanker E.E. The hunt for huntingtin function: interaction partners tell many different stories.*Trends Biochem. Sci.* **28**, 425-33 (2003).

293.Li S. H., Li X. J. Huntingtin-protein interactions and the pathogenesis of Huntington's disease.*Trends Genet.* **20**, 146-54 (2004).

294.Bocharova N., Chave-Cox R., Sokolov S., Knorre D., Severin F. Protein aggregation and neurodegeneration: clues from a yeast model of Huntington's disease. *Biochemistry* **74**, 231-4 (2009).

295.Stevanin G., Fujigasaki H., Lebre A. S., Camuzat A., Jeannequin C., Dode C., Takahashi J., San C., Bellance R., Brice A., Durr A. Huntington's disease-like phenotype due to trinucleotide repeat expansions in the TBP and JPH3 genes. *Brain* **126**, 1599-603 (2003).

296.Duan W., Guo Z., Jiang H., Ware M., Li X. J., Mattson M. P. Dietary restriction normalizes glucose metabolism and BDNF levels, slows disease progression, and increases survival in huntingtin mutant mice. *Proc. Natl. Acad. Sci.* USA Mar **100**, 2911-6 (2003).

297.Ho D. J., Calingasan N. Y., Wille E., Dumont M., Beal M. F., Resveratrol protects against peripheral deficits in a mouse model of Huntington's disease *Exp. Neurol.* **225**, 74-84 (2010).

298.Meriin A. B., Zhang X., He X., Newnam G. P., Chernoff Y. O., Sherman M. Y. Huntington toxicity in yeast model depends on polyglutamine aggregation mediated by a prion-like protein Rnq1. *J. Cell Biol.* **157**, 997-1004 (2002).

299.Bodner R. A., Outeiro T. F., Altmann S., Maxwell M. M., Cho S. H., Hyman B. T., McLean P. J., Young A. B., Housman D. E., Kazantsev A. G. Pharmacological promotion of inclusion formation: a therapeutic approach for Huntington's and Parkinson's diseases. *Proc. Natl. Acad. Sci.* USA. **103**, 4246-51 (2006).

300.Lasorella A., Stegmüller J., Guardavaccaro D., Liu G., Carro M. S., Rothschild G., de la Torre-Ubieta L., Pagano M., Bonni A., Iavarone A. Degradation of Id2 by the anaphase-promoting complex couples cell cycle exit and axonal growth. *Nature* **442**, 471-4 (2006).

301.Stegmüller J., Konishi Y., Huynh M. A., Yuan Z., Dibacco S., Bonni A. Cell-intrinsic regulation of axonal morphogenesis by the Cdh1-APC target SnoN. *Neuron* **50**, 389-400 (2006).

302.Lorincz M. T., Zawistowski V. A. Expanded CAG repeats in the murine Huntington's disease gene increases neuronal differentiation of embryonic and neural stem cells. *Mol. Cell Neurosci.* **40**, 1-13 (2009).

303.Browne S. E., Ferrante R. J., Beal M. F. Oxidative stress in Huntington's disease. *Brain Pathol.* **9**, 147-163 (1999).

304.Wyttenbach A., Sauvageot O., Carmichael J. Heat shock protein 27 prevents cellular polyglutamine toxicity and suppresses the increase of reactive oxygen species caused by huntingtin.*Hum. Mol. Genet.* **11**, 1137-1151 (2002).

305.Sorolla M. A., Rodríguez-Colman M. J., Tamarit J., Ortega Z., Lucas J. J., Ferrer I., Ros J., Cabiscol E. Protein oxidation in Huntington disease affects energy production and vitamin B6 metabolism. *Free Radic. Biol. Med.* **49** 612-621 (2010).

306.Chen C. M., Wu Y. R., Cheng M. L., Liu J. L., Lee Y. M., Lee P. W., Soong B. W., Chiu D. T. Increased oxidative damage and mitochondrial abnormalities in the peripheral blood of Huntington's disease patients. *Biochem. Biophys. Res. Commun.* **359**, 335-40 (2007).

307.Shilling G., Coonfield M. L., Ross C. A., Borchelt D. R. Coenzyme Q10 and remacemide hydrochloride ameliorate motor deficits in a Huntington's disease transgenic mouse model. *Neurosci Lett.* **315**, 149-53 (2001).

308.Panov A. V., Gutekunst C. A., Leavitt B. R., Hayden M. R., Burke J. R., Strittmatter W. J., Greenamyre J. T. Early mitochondrial calcium defects in Huntington's disease are a direct effect of polyglutamines. *Nat. Neurosci.* **5**, 731-736 (2002).

309.Schapira A. H. Mitochondrial involvement in Parkinson's disease, Huntington's disease, hereditary spastic paraplegia and Friedreich's ataxia. *Biochim. Biophys. Acta* **1410**, 159-170 (1999).

310.Herrera F., Tenreiro S., Miller-Fleming L., Outeiro T. F. Visualization of cell-to-cell transmission of mutant huntingtin oligomers. *PLoS Curr.* **3**, RRN1210 (2011).

311.Paik J. H., Kollipara R., Chu G., Ji H., Xiao Y., Ding Z*., et al.* FoxOs are lineage-restricted redundant tumor suppressors and regulate endothelial cell homeostasis. *Cell* **128**, 309-23 (2007).

312.Bouchard C., Lee S., Paulus-Hock V., Loddenkemper C., Eilers M., Schmitt C. A. FoxO transcription factors suppress Myc-driven lymphomagenesis via direct activation of Arf. *Genes Dev.* **21**, 2775-87 (2007).

313.Tran H., Brunet A., Grenier J. M., Datta S. R., Fornace A. J., DiStefano P. S.*, et al.* DNA repair pathway stimulated by the forkhead transcription factor FOXO3a through the Gadd45 protein. *Science* **296**, 530-4. 2002

314.Ramaswamy S., Nakamura N., Sansal I., Bergeron L., Sellers W. R. A novel mechanism of gene regulation and tumor suppression by the transcription factor FKHR. *Cancer Cell* **2**, 81-91 (2002).

315.Kops G. J., Dansen T. B., Polderman P. E., Saarloos I., Wirtz K. W., Coffer P. J.*, et al.* Forkhead transcription factor FOXO3a protects quiescent cells from oxidative stress. *Nature* **419**, 316-21 (2002).

316.Brunet A., Bonni A., Zigmond M. J., Lin M. Z., Juo P., Hu L. S.*, et al.* Akt promotes cell survival by phosphorylating and inhibiting a Forkhead transcription factor. *Cell* **96**, 857-68 (1999).

317.Zheng W. H, Kar S., Quirion R. Insulin-like growth factor-1-induced phosphorylation of the forkhead family transcription factor FKHRL1 is mediated by Akt kinase in PC12 cells. J. Biol. Chem. **275**, 39152-8 (2000).

318.Gilley J., Coffer P. J., Ham J. FOXO transcription factors directly activate bim gene expression and promote apoptosis in sympathetic neurons. J. Cell Biol. **162**, 613-22 (2003).

319.Brunet A., Sweeney L. B., Sturgill J. F., Chua K. F., Greer P. L., Lin Y.*, et al.* Stress-dependent regulation of FOXO transcription factors by the SIRT1 deacetylase. *Science* **303**, 2011-5 (2004).

320.Seoane J., Le H. V., Shen L., Anderson S. A., Massague J. Integration of Smad and forkhead pathways in the control of neuroepithelial and glioblastoma cell proliferation. *Cell* **117**, 211-23 (2004).

321.Gomis R. R., Alarcon C., Nadal C., Van Poznak C., Massague J. C/EBPbeta at the core of the TGFbeta cytostatic response and its evasion in metastatic breast cancer cells. *Cancer Cell* **10**, 203-14 (2006).

322.Gomis R. R., Alarcon C., He W., Wang Q., Seoane J., Lash A.*, et al.* A FoxO-Smad synexpression group in human keratinocytes. *Proc. Natl. Acad. Sci.* USA **103**, 12747-52 (2006).

323.Huang H., Regan K. M., Lou Z., Chen J., Tindall D. J. CDK2-dependent phosphorylation of FOXO1 as an apoptotic response to DNA damage. *Science* **314**, 294-7 (2006).

324.Greer E. L., Dowlatshahi D., Banko M. R., Villen J., Hoang K., Blanchard D.*, et al.* An AMPK-FOXO pathway mediates longevity induced by a novel method of dietary restriction in *C. elegans*. *Curr. Biol.* **17**, 1646-56 (2007).

325.Greer E. L., Oskoui P. R., Banko M. R., Maniar J. M., Gygi M. P., Gygi S. P.*, et al.* The energy sensor AMP-activated protein kinase directly regulates the mammalian FOXO3 transcription factor. *J. Biol. Chem.* **282**, 30107-19 (2007).

326.Bakker W. J., Harris I. S., Mak T. W. FOXO3a is activated in response to hypoxic stress and inhibits HIF1-induced apoptosis via regulation of CITED2. Mol. Cell **28**, 941-53 (2007).

327.Wang Y., Oh S. W., Deplancke B., Luo J., Walhout A. J., *et al. C. elegans* 14-3-3 proteins regulate life span and interact with SIR-2.1 and DAF-16/FOXO. *Mech. Ageing Dev.* **127**, 741-747 (2006).

328.Mills K. D., Sinclair D. A. and Guarente L. MEC1-dependent redistribution of the Sir3 silencing protein from telomeres to DNA doublestrand breaks. *Cell* **97**, 609-620 (1999).

Verzeichnis der Publikationen

Chung H. R., Dunkel I., Heise F., Linke C., Krobitsch S., Ehrenhofer-Murray A. E., Sperling S. R., Vingron M. The effect of micrococcal nuclease digestion on nucleosome positioning data. *PLoS One* **5**(12), e15754 (2010).

Barberis M., Linke C., Adrover M. À., González-Novo A., Lehrach H., Krobitsch S., Posas F., Klipp E. Sic1 plays a role in timing and oscillatory behaviour of B-type cyclins. *Biotechnol. Adv.* **30**(1), 108-30 (2012).

Eidesstattliche Versicherung

Hiermit versichere ich an Eides Statt, dass ich die vorliegende Arbeit selbständig verfasst und keine anderen als die hier angegebenen Quellen und Hilfsmittel verwendet habe.

Ich versichere, dass diese Arbeit in dieser oder ähnlicher Form keiner anderen Prüfungsbehörde vorgelegt wurde.

Berlin, den _____ Christian Linke

Danksagung

Mein erster Dank gebührt Dr. Sylvia Krobitsch für die Möglichkeit in ihrer Arbeitsgruppe an einem spannenden Thema zu forschen. Die Offenheit für konstruktive Diskussionen und die Freiheit neue Ideen ausprobieren zu können, habe ich sehr genossen.

Ich danke Prof. Dr. Hans Lehrach für die Möglichkeit an seinem Institut meine Doktorarbeit anfertigen zu dürfen. Weiterhin möchte ich Prof. Dr. Rupert Mutzel für die Übernahme des Zweitgutachtens danken.

Besonders herzlich möchte ich Dr. Matteo Barberis für seine stete Diskussionsbereitschaft und die wertvolle Unterstützung als Wissenschaftler zu wachsen danken. Er ist mir in dieser Zeit sowohl ein Mentor als auch ein teurer Freund gewesen.

Meinen aktuellen und ehemaligen Arbeitskollegen der AG Krobitsch Ute Nonhoff, Linda Hallen, Franziska Welzel, Anja Nowka, Gunnar Seidel, Artemis Fritsche, Marcel Schulze und Guifré Ruiz möchte ich für eine angenehme, diskussionsreiche und hilfsbereite Arbeitsatmosphäre danken. Ein besonders dickes Dankeschön geht an Silke Wehrmeyer, die mir immer wieder mit literweise Puffer und Medien, dem selbstloses Verleihen ihrer Pipetten und ihrer fröhlichen und lieben Art den Laboralltag erhellt hat. Bei Christian Kähler möchte ich mich für die Diskussions- und außergewöhnliche Hilfsbereitschaft bedanken. Eine große Hilfe waren außerdem meine Mitarbeitsstudenten Judith Hey und Eva Dittinger. Vielen Dank auch an Hans-Jörg Warnatz, Markus Ralser und Cornelia Lange, die mir arbeitsgruppen-übergreifend mit Rat und Tat beigestanden haben.

Zuletzt möchte ich mich noch bei meiner Familie und besonders meinen Eltern bedanken, die mich in diesen vier Jahren in jeglicher Hinsicht unterstützt haben. Auch danke ich Clara Schäfer für ihre Unterstützung und ihren Humor in den letzten Jahren. Außerdem danke ich auch all meinen Freunden, die mich in dieser Zeit immer wieder unterstützt und motiviert haben.